Doctoral theses at NTNU, 2021:241

Federico Ustolin

# Modelling of Accident Scenarios from Liquid Hydrogen Transport and Use

Doctoral thesis

NTNU
Norwegian University of Science and Technology
Thesis for the Degree of Philosophiae Doctor
Faculty of Engineering
Department of Mechanical and Industrial Engineering

NTNU
Norwegian University of Science and Technology

Federico Ustolin

# Modelling of Accident Scenarios from Liquid Hydrogen Transport and Use

Thesis for the Degree of Philosophiae Doctor

Trondheim, July 2021

Norwegian University of Science and Technology
Faculty of Engineering
Department of Mechanical and Industrial Engineering

NTNU
Norwegian University of
Science and Technology

**NTNU**
Norwegian University of Science and Technology

Thesis for the Degree of Philosophiae Doctor

Faculty of Engineering
Department of Mechanical and Industrial Engineering



ISBN 978-82-326-5575-5 (printed ver.)
ISBN 978-82-326-6523-5 (electronic ver.)
ISSN 1503-8181 (printed ver.)
ISSN 2703-8084 (online ver.)

Doctoral theses at NTNU, 2021:241

Printed by NTNU Grafisk senter

“All models are wrong, but some are useful.”

George E. P. Box

## Preface

This thesis is submitted to the Norwegian University of Science and Technology (NTNU) for partial fulfilment of the requirements for the degree of Philosophiae Doctor.

The work was carried out at the Department of Mechanical and Industrial Engineering at NTNU, in Trondheim, Norway. Professor Nicola Paltrinieri from the abovementioned Department at NTNU was the main supervisor while Gunhild Reigstad from Sintef Energy was the co-supervisor.

The Research Council of Norway funded the doctoral work through the project “Safe Hydrogen Fuel Handling and Use for Efficient Implementation ($SH_2IFT$)” under the ENERGIX programme (Grant No. 280964).

The target audience of this work include researchers and practitioners interested in the following areas: hydrogen safety, loss of integrity and containment of hydrogen technology, atypical accident scenarios, physical explosions (BLEVE and RPT), modelling of the accident scenario consequences.

This page is intentionally left blank

**Summary**

Hydrogen is one of the most suitable candidates to replace hydrocarbons and reduce the environmental pollution and $CO_2$ emissions. Hydrogen is valuable energy carrier, potentially clean and renewable thanks to its peculiar properties. However, hydrogen has a few characteristics, such as high flammability and low density that must be taken into account when stored or handled, especially in relation to the associated safety. For this reason, this PhD study aims to increase the knowledge on safety of hydrogen technologies.

Hydrogen safety is a broad topic which involves several disciplines. This PhD focusses on the modelling of atypical accident scenarios of liquid hydrogen ($LH_2$) technologies by adopting a multidisciplinary approach. This type of accident scenarios is called atypical because they have low probability to happen but high consequences. A few times, the neglection of these scenarios by conventional risk assessment techniques led to major accidents. For this reason, the atypical accident scenario cannot be omitted during a risk assessment and must be further analysed.

Firstly, through a comprehensive literature review, this PhD study investigates the causes of loss of integrity (LOI) and loss of containment (LOC) of hydrogen equipment since the atypical accident scenarios always occurred after these critical events. The consequences of an $LH_2$ release are then analysed. The focus is placed on the boiling liquid expanding vapour explosion (BLEVE) and the rapid phase transition (RPT) explosions for liquid hydrogen technologies because a significant dearth of knowledge is still present.

Secondly, the possibility for the BLEVE to occur after the catastrophic rupture of an $LH_2$ vessel is theoretically assessed by gathering information on previous accident and applying accepted thermodynamic theories for this event. The consequences of a potential BLEVE for $LH_2$ (pressure wave, missiles and fireball) are evaluated. Unique

experimental series on $LH_2$ bursting tank scenario and fire tests are simulated. Different approaches are employed for the BLEVE event: analytical models, empirical correlations and CFD analysis. Finally, the time to failure of an $LH_2$ tank exposed to a fire is estimated with a thermal node model.

Thirdly, the RPT event is analysed from a more theoretical approach since no records of $LH_2$ RPT are found in literature. The knowledge gained for other substances such as liquefied natural gas (LNG) and liquid nitrogen (LIN) is applied to $LH_2$. The consequences of a hypothetical $LH_2$ RPT are evaluated by means of an analytical model and compared to the LNG RPT aftermath.

The main contributions of this PhD study are the following:

- investigation on the causes of LOI of hydrogen technology;
- identification of the $LH_2$ release consequences;
- understanding of the BLEVE feasibility for $LH_2$ storage systems;
- determination of the $LH_2$ BLEVE consequences;
- estimation of the time to failure of $LH_2$ tanks exposed to a fire;
- analysis of the theories and mechanisms of RPT explosions;
- determination of the $LH_2$ RPT consequences.

This PhD study provides relevant safety indications on the causes of LOI of hydrogen technologies as well as on the BLEVE and RPT phenomena for $LH_2$ technologies. The knowledge gap in these topics is highlighted and partially fulfilled. The limitations of existing models for the simulation of these explosions are emphasised. The results of this thesis serve as a starting point for future studies.

## Acknowledgments

First of all, I would like to express my gratitude to my main supervisor, professor Nicola Paltrinieri. You have been a guide for me since we met the first time in Madrid. During these three years you became an older brother for me, always ready to support and trust me. My knowledge and expertise were enhanced thanks to the freedom and independency you gave me.

A special thanks to my co-supervisor, Dr. Gunhild Allard Reigstad to share your experience with me and provide me valuable insights during the research process. I would like to thank all the colleagues at Sintef Energy who have been collaborating with me on the $SH_2IFT$ project, especially Lars, Hans and Eskil. I would also like to thank my co-authors for the great collaboration and exchange of knowledge during this PhD journey.

I would like to express my gratitude to the $SH_2IFT$ project coordinator, Dr Anders Ødegård from Sintef Industry, and all the project partners. In this regard, I would like to acknowledge the Research Council of Norway for the funding of both my fellowship and the visiting period.

My gratitude goes to the research group of the Environmental Research Lab. of the National Centre of Scientific Research "Demokritos" in Athens, Greece. A huge thanks in particular to Alexandros Venetsanos, Ilias Tolias and Stella Giannissi. Despite all the difficulties related to the pandemic you made me feel at home since the first day. During the visiting period, I did not expect to meet new friends beyond extremely valuable colleagues.

Thanks to the colleagues and all co-workers I met at the Department of Mechanical and Industrial Engineering at NTNU. Petr and Renny, I always enjoyed our long chit-chat during the breaks. Michael, you have been the best co-worker I ever met. I enjoyed your

extravagant personality and your transparency. We spent together only 16 months, but I feel we have known each other for much longer.

A huge thanks to the support provided by all the friends that I left in Trieste and in the rest of Italy: my best man Diego, Lorenzo, Simone, Fabrizio and Jean. Andrea, we have not been living in the same city for almost four years, but I feel our friendship is as strong as before. Our long calls always helped us to steam off and find a solution to the difficulties we were facing along the road.

I could never be grateful enough to my family for believing in me when I was rowing or studying, and always providing me with everything I needed. Each one of you was a model to follow and taught me something that made me who I am today.

Finally, my wife, Hana, always here to encourage me. Thank you for understanding me and growing with me every day.

**Contents**

**Part I: Main Report**

This page is intentionally left blank

## List of figures



## List of tables

## Nomenclature

### Acronyms

AAS: atypical accident scenario

BLEVE: boiling liquid vapour explosion

CFD: computational fluid dynamics

CP: critical point

DyPASI: Dynamic Procedure for Atypical Scenario Identification

DRA: dynamic risk assessment

EoS: equation of state

FV: finite volume

$GH_2$: gaseous hydrogen

HAZID: hazard identification

HD: hydrogen damage

$LCO_2$: liquid carbon dioxide

$LH_2$: liquid hydrogen

LIN: liquid nitrogen

LNG: liquefied natural gas

LOC: loss of containment

LOI: loss of integrity

LOX: liquid oxygen

LPG: liquefied petroleum gas

LPI: loss of physical integrity

MFCI: molten fuel coolant interaction

MIMAH: methodology for the identification of major accident hazards

MIRAS: methodology for the identification of reference accident scenarios

NCSR: National Centre for Scientific Research

NBP: normal boiling point

PRESLHY: prenormative research for safe use of liquid hydrogen

PRV: pressure relief valve

PR: Peng Robinson

RPT: rapid phase transition

SC: supercritical

SEP: surface emissive power

$SH_2IFT$: safe hydrogen fuel handling and use for efficient implementation

$T_{SL}$: superheat limit temperature

$T_{SP}$: spinodal temperature

TTF: time to failure

VCE: vapour cloud explosion

VOF: volume of fluid

WP: work package

## Thesis structure

This doctoral thesis is a collection of articles and it is structured in two main parts:

- Part I, the main report which interrelates the articles and summarises the research performed during the entire PhD study;
- Part II, where the articles published in the PhD framework are collected.

It is suggested to read the two parts in the proposed order. However, two parts are stand-alone and can be read in any order.

This page is intentionally left blank

The scientific papers authored by the candidate during his PhD period are collected in Table 1. This table is divided in two parts containing: (i) the articles published within the $SH_2IFT$ project framework, and (ii) additional publications falling outside the scope of the $SH_2IFT$ project, thus not addressed by this thesis.

*Table 1: the scientific papers considered in this thesis are listed in the upper part of the table. Additional publications are listed in the lower part of the table. (Abbreviations: C: conference, J: journal publication, B: book chapter).*

| Article no. | Type | Title |
|---|---|---|
| Article I | J | Loss of integrity of hydrogen technologies: A critical review |
| Article II | J | An innovative and comprehensive approach for the consequence analysis of liquid hydrogen vessel explosions |
| Article III | J | A CFD Analysis of Liquefied Gas Vessel Explosions Using the ADREA-HF Code |
| Article IV | C | The influence of H2 safety research on relevant risk assessment |
| Article V | C | Modelling Liquid Hydrogen BLEVEs: A Comparative Assessment with Hydrocarbon Fuels |
| Article VI | C | Risk and Consequences of Rapid Phase Transition for Liquid Hydrogen |
| Article VII | C | Hydrogen Fireball Consequence Analysis |
| Article VIII | C | Theories and Mechanism of Rapid Phase Transition |
| Article IX | C | Time to Failure Estimation of Cryogenic Liquefied Tanks Exposed to a Fire |

*Table 1: the scientific papers considered in this thesis are listed in the upper part of the table. Additional publications are listed in the lower part of the table. (Abbreviations: C: conference, J: journal publication, B: book chapter) (continued).*

| Article no. | Type | Title |
|---|---|---|
| | | *Additional publications* |
| Article X | J | Digital Moka: Small-Scale Condition Monitoring in Process Engineering |
| Article XI | J | A new risk-based framework to integrate occupational and process safety |
| Article XII | B | Energy and Safety of Hydrogen Storage |
| Article XIII | B | Liquid Air Energy Storage: Analysis and Prospects |
| Article XIV | C | Risk-based inspection planning for hydrogen technologies: review of currents standards and suggestions for modification |
| Article XV | C | Computational Fluid Dynamics Modeling of Liquid Hydrogen Release and Dispersion in Gas Refuelling Stations |
| Article XVI | C | Development of Tools Enabling the Deployment and Management of a Multi-Energy Renewable Energy Community with Hybrid Storage |

Article I

Ustolin F, Paltrinieri N, Berto F. Loss of integrity of hydrogen technologies: A critical review. Int J Hydrogen Energy 2020;45:23809–40. https://doi.org/https://doi.org/10.1016/j.ijhydene.2020.06.021.

Contribution of authors:

The first and second authors conceptualised the research idea and methodology. The first author conducted the review and wrote the original draft. Both second and third authors reviewed and edited the paper, and supervised during the whole research process.

Article II

Ustolin F, Paltrinieri N, Landucci G. An innovative and comprehensive approach for the consequence analysis of liquid hydrogen vessel explosions. J Loss Prev Process Ind 2020;68:104323. https://doi.org/https://doi.org/10.1016/j.jlp.2020.104323.

Contribution of authors:

The first author conceptualised the research idea and methodology, implemented the analytical models, and wrote the original draft. The second author aided the methodology development, wrote part of the manuscript. Both second and third authors reviewed and edited the paper, and supervised during the whole research process.

Article III

Ustolin F, Tolias I, Giannissi S, Venetsanos A, Paltrinieri N. A CFD Analysis of Liquefied Gas Vessel Explosions Using the ADREA-HF Code. (submitted to the International Journal of Hydrogen Energy).

Contribution of authors:

The first, second and third authors conceptualised the research idea and methodology, and conducted the numerical analysis. The first author wrote the original draft. The fourth author suggested critical improvements of the numerical settings, and supervised during the entire research process. The article was iteratively reviewed and edited by all the authors.

Article IV

Ustolin F, Song G, Paltrinieri N. The influence of H2 safety research on relevant risk assessment. Chem Eng Trans 2019;74:1393–8. https://doi.org/10.3303/CET1974233.

Contribution of authors:

The first and second authors conceptualised the research idea and methodology. The first author conducted the review, applied the methodology and wrote the original draft. The

second author reviewed and edited the paper, and supervised during the whole research process. The third author reviewed the paper.

Article V

Ustolin F, Salzano E, Landucci G, Paltrinieri N. Modelling Liquid Hydrogen BLEVEs: A Comparative Assessment with Hydrocarbon Fuels. 30th Eur. Saf. Reliab. Conf. 15th Probabilistic Saf. Assess. Manag. Conf. (ESREL2020 PSAM15), 2020. https://doi.org/978-981-14-8593-0.

Contribution of authors:

The first author conceptualised the research idea and methodology, implemented the analytical models, and wrote the original draft. The second author reviewed and edited the paper, and supervised during the whole research process. The third and fourth authors reviewed the paper.

Article VI

Aursand E, Odsæter LH, Skarsvåg HL, Reigstad GA, Ustolin F, Paltrinieri N. Risk and Consequences of Rapid Phase Transition for Liquid Hydrogen. 30th Eur. Saf. Reliab. Conf. 15th Probabilistic Saf. Assess. Manag. Conf. (ESREL2020 PSAM15), 2020. https://doi.org/10.3850/978-981-14-8593-0.

Contribution of authors:

The first, second and third authors conceptualised the research idea and methodology, implemented the analytical models, and wrote the original draft. The fourth author reviewed and edited the paper, and supervised during the whole research process. The fifth and sixth authors reviewed the paper.

Article VII

Ustolin F, Paltrinieri N. Hydrogen Fireball Consequence Analysis. Chem Eng Trans 2020;82:211–6. https://doi.org/10.3303/CET2082036.

Contribution of authors:

The first author conceptualised the research idea and methodology, implemented the analytical and empirical models, and wrote the original draft. The second author reviewed and edited the paper, and supervised during the whole research process.

Article VIII

Ustolin F, Odsæter LH, Reigstad G, Skarsvåg HL, Paltrinieri N. Theories and Mechanism of Rapid Phase Transition. Chem Eng Trans 2020;82:253–8. https://doi.org/10.3303/CET2082043.

Contribution of authors:

The first author conceptualised the research idea and methodology, conducted the review, and wrote the original draft. All the authors reviewed and edited the paper. In addition, the fifth author supervised during the whole research process.

Article IX

Ustolin F, Iannaccone T, Cozzani V, Jafarzadeh S, Paltrinieri N. Time to Failure Estimation of Cryogenic Liquefied Tanks Exposed to a Fire, (Submitted to the 31st European Safety and Reliability Conference – ESREL2021)

Contribution of authors:

The first and second authors conceptualised the research idea and methodology, carried out the modelling activity. The first author wrote the original draft. All the authors reviewed and edited the paper. In addition, the fifth author supervised during the whole research process.

This page is intentionally left blank

# Part I

## Main report

This page is intentionally left blank

# 1. Introduction

Global warming, climate change and environmental pollution are issues that have been receiving attention and fostering awareness in the scientific community as well as in the public society during the first decades of the 21st century. In June 2019, the international energy agency (IEA) stated "the time is right to tap into hydrogen's potential to play a key role in a clean, secure and affordable energy future" in its report titled "The future of hydrogen" (IEA, 2019). After the COVID-19 pandemic outbreak, hydrogen gained even more interest and new plans for the energy transition were made in Europe and worldwide. Next generation EU is a new recovery instrument of €750 billion proposed by the European Community in the period 2021-2027 (European Commission, 2020). One of the strategy points of the plan is "rolling out renewable energy projects, especially wind, solar and kick-starting a clean hydrogen economy in Europe" (European Commission, 2020). Therefore, the implementation of renewable energy sources (RESs) such as wind and solar energies is among the most suitable options to abandon fossil fuels. One of the main RESs drawbacks is their intermittency. Hydrogen is one of the best candidates to solve this issue since it is an abundant, light energy carrier, and a potentially clean and renewable fuel (Kovač et al., 2021). In fact, hydrogen has a high gravimetric energy content (120 MJ $kg^{-1}$ (McAllister et al., 2011)) compared with hydrocarbons, it can be produced by different sources and it is not toxic.

However, a few limitations in the implementation of hydrogen can be identified. It is highly flammable (minimum ignition energy of 0.017 mJ (Ono et al., 2007)), and its molecule is the smallest in nature, meaning that, when gas, it can escape from microscopical holes making it difficult to contain. Furthermore, its flame is scarcely visible with daylight (Schefer et al., 2009) and its gas density is very low (0.0883 kg $m^{-3}$ at atmospheric conditions (NIST, 2019)), thus it must be compressed or liquefied to increase its storage capacity. Liquid hydrogen ($LH_2$) is a cryogenic fluid usually stored at

atmospheric pressure at 20.3 K (NIST, 2019). In this manner, its density is increased up to 70.9 kg $m^{-3}$ (NIST, 2019) which is still one order of magnitude lower than other cryogenic hydrocarbons. For example, liquefied natural gas (LNG) has a density between 431 and 453 kg $m^{-3}$ at its boiling point (approx. 112 K) depending on its composition (Woodward and Pitblado, 2010). Moreover, the energy required to liquefy hydrogen is between 10 and 13 kWh $kg_{H2}$ which corresponds to almost 30% of its lower heating value (33 kWh) (DOE, 2009). The required energy depends on the efficiency of the liquefaction plant and decreases for larger amount of $LH_2$ produced. For this reason, it is more convenient to employ $LH_2$ in fields such as aerospace, aeronautical and maritime, where a high energy density and large amount of fuel are necessary (NCE Maritime Cleantech, 2019) or increased storage of stationary applications are required (DNV-GL, 2020).

Appropriate and currently expensive cryogenic plants and equipment are needed to produce and store $LH_2$. For instance, $LH_2$ must be stored in highly insulated tanks (double walled type) to reduce the heat losses with the environment and consequent evaporation (Barthelemy et al., 2017). The quality of the tank depends mainly on the type of insulation. A vacuum jacket is created between the inner and outer tank where a highly insulating material (e.g. perlite) or a multilayer insulation (MLI) is installed to minimise the heat transfer with the surroundings (Barron and Nellis, 2016). The boil off gas (BOG) formation must be reduced or avoided for both economical and safety aspects. For instance, the BOG must be vented out to keep the pressure below a certain safety value. In case of safety device failure, the BOG might produce a pressure build up that may generate mechanical stress on the tank material, and lead to a loss of integrity and containment.

Hydrogen is also foreseen to be employed in new applications. As an example, the first $LH_2$ fuelled ferry will be deployed in Norway in 2023 (FuelCellsWork, 2020). Despite the fact that hydrogen was used in several industrial fields for more than one century, it becomes an emerging technology when applied in new fields, and emerging risks could arise (Jovanović and Baloš, 2013). Therefore, emerging risks such as atypical accident scenarios must always be considered during a risk analysis. These are accident scenarios with low probabilities, which may be neglected by conventional risk assessment techniques (Paltrinieri et al., 2015). The neglection of the atypical accident scenarios can

lead to major accidents. The accidents occurred in Toulouse (2001) and in Buncefield (2005) are unfortunate reminders (Paltrinieri et al., 2012a). The boiling liquid expanding vapour explosion (BLEVE) and rapid phase transition are two physical explosion that might occur after the loss of containment (LOC) of cryogenic equipment and may be considered as atypical. The BLEVE might occur after the catastrophic rupture of a liquefied gas vessel if its content is superheated (Casal et al., 2016). The expansion of the compressed gas and the flashing of the liquid due to the rapid depressurisation can generate this sever explosion. The RPT can happen when a fluid is released onto or into another liquid with a different temperature due to the sudden heat transfer and the violent boiling of the colder fluid. This is a very well-known phenomenon for LNG spills onto water (Woodward and Pitblado, 2010) as well as for molten metal and water interactions (Reid, 1983). Therefore, the possibility for these phenomena to occur after an LOC of $LH_2$ tanks or pipes must be investigated since limited knowledge is available.

The atypical accident scenarios for hydrogen technologies must be tackled in the early stages of its deployment in new applications. In this regard, several research projects are ongoing on hydrogen safety. In particular, the projects "Safe Hydrogen Fuel Handling and Use for Efficient Implementation ($SH_2IFT$)" and "Prenormative REsearch for Safe use of Liquid Hydrogen (PRESLHY)" are focussing on the consequences of $LH_2$ releases, fires, and explosions. During the Norwegian project $SH_2IFT$, both experimental and modelling activities on $LH_2$ BLEVE and RPT events are being carried out. The focus of this PhD study is on the loss of integrity and containments of $LH_2$ technologies and the modelling of the $LH_2$ BLEVE and RPT phenomena. In Part I, Sec. 2 describes the $SH_2IFT$ project and the abovementioned explosions while in Sec. 3 a research background on the topics investigated during the PhD is provided. The research questions, objectives, methodology and methods are explained in Sec. 4, 5, 6 and 7, respectively. The contributions of the PhD study are reported in Sec. 8 and then discussed in Sec. 9. Finally, conclusions and future works can be found in Sec. 10 and 11, respectively.

This page is intentionally left blank

## 2. $SH_2IFT$ project, BLEVE and RPT explosions

"Safe Hydrogen Fuel Handling and Use for Efficient Implementation ($SH_2IFT$)" is an ongoing Norwegian project which is focussing on hydrogen safety. The project consists of six partners: SINTEF Industry (coordinator), SINTEF Energy Research, Norwegian University of Science and Technology (NTNU), The Institute of Transport Economics, RISE Fire Research, and Christian Michelsen Research. $SH_2IFT$ is mainly funded by the Research Council of Norway under the ENERGIX programme. This programme provides funding for research on renewable energy, efficient use of energy, energy systems and energy policy. The programme is key instrument in the implementation of Norway's national RD&D strategy, Energi21, as well as achieving other energy policy objectives. The $SH_2IFT$ project addresses several thematic areas within the ENERGIX program:

- energy use and conversion: (i) transition from fossil to renewable energy carriers (industry), (ii) hydrogen infrastructure, vehicles and vessels (transport), (iii) export, safety and maritime use (hydrogen).
- New business opportunities for renewable energy (power to hydrogen).
- Energy policy, economics and sustainability: technology analysis, innovation and dissemination of knowledge that is vital to the implementation of new solutions (society and behaviour).

Additional funding is allocated by: Statens Vegvesen, Jernbanedirektoratet, Direktoratet for samfunnssikkerhet og beredskap, Fylkeskommunene, Viken, Vestland, Møre & Romsdal, Trøndelag, Finnmark. The project is also sponsored by several companies: Equinor, Shell, NASTA, Statkraft, Ariane, Air Liquide, Nye veier, Total and Safetech. The duration of the project is four years and it started in April 2018.

The primary objective of the $SH_2IFT$ project is to increase competence within safety of hydrogen technology, especially focussing on consequences of handling large amounts of this fuel within closed and semi-closed environments and in maritime transport. Relevant aspects from the whole value chain from industry and authorities to end users/general public are investigated, with special emphasis on the potential obstacles and bottlenecks for early implementation of hydrogen as fuel. The project is both developing new models, perform large-scale fire and explosion experiments, and providing guidelines for use of hydrogen in industry and transport. Thus, the project aims to contribute to the reduction of green-house gas emissions and growth in existing and new Norwegian hydrogen industry.

The secondary objective of the project is to evaluate the relevance and performance of currently available tools for estimating consequences and risks associated with hazardous events involving gaseous ($GH_2$) and liquid hydrogen ($LH_2$). The current knowledge gaps related to safe handling of hydrogen as a fuel are being filled. This is addressed by investigating the physical behaviour of hydrogen in mid- and large-scale experiments, as well as development and validation of numerical models. In particular, hydrogen jet fires are experimentally reproduced and numerically simulated. Moreover, boiling liquid expanding vapour explosion (BLEVE) and rapid phase transition (RPT) explosions are being generated in separate tests from $LH_2$ storage system releases. Concerns and potential barriers in the Norwegian society (industry/public/authorities) regarding implementation, handling and use of hydrogen technology and infrastructure are addressed and recommendations and guidelines for handling hydrogen are developed. The results and gained knowledge are expected to contribute significantly to the following areas:

- increased relevance and accuracy of consequence models and risk assessments, resulting from experimental investigations and state-of-the-art modelling;
- input to requirements, procedures and guidelines regarding $GH_2$ and $LH_2$ safety in road, rail and maritime applications (tunnels, parking facilities, ships and transport of hydrogen);

- increased acceptance and accelerated implementation of hydrogen technology in society, thus contributing to reduced carbon emissions and growth in the Norwegian hydrogen industry.

## 2.1. Involvement in the project

This PhD position is funded by the $SH_2IFT$ project, thus a full involvement in the project was required. The main task of the PhD is to model accident scenarios of liquid hydrogen during storage and transport, which coincides with one of the project tasks aiming to innovative models for estimating formation and consequences of the BLEVE and RPT explosions.

A series of experimental tests are also being carried out within the $SH_2IFT$ project: jet fires from pressurised bottles, fire tests on $LH_2$ vessels and release of $LH_2$ onto water. The fire tests aim to study the behaviour of the double walled tanks exposed to a fire and measure the consequences of a BLEVE explosion. The behaviour of $LH_2$ water interaction is investigated in the $LH_2$ release tests together with the probability to provoke an RPT as consequence of the spill. The PhD candidate is directly involved with the setting up of the fire tests and $LH_2$ release on water.

## 2.2. BLEVE and RPT explosions

In this section, the boiling liquid expanding vapour explosion (BLEVE) and the rapid phase transition (RPT) are described in detail. These two phenomena are introduced by focussing on the physics of the explosion and their consequences.

### 2.2.1. Boiling liquid expanding vapour explosion (BLEVE)

The term BLEVE was used for the first time in 1957 by J.B. Smith, W.S. Marsh, and W.A. Walls employees of the Factory Mutual Research Corporation (Abbasi and Abbasi, 2008). This trio coined the term BLEVE after observing and analysing an explosion of a cast iron vessel employed for the production of a phenolic resin (Walls, 1978). Several

definitions of BLEVE were proposed by different authors in the past (Abbasi and Abbasi, 2007a). One of the most recent definitions was stated by Casal et al. (2016): "a BLEVE is the explosion of a vessel containing a liquid (or liquid plus vapour) at a temperature significantly above its boiling point at atmospheric pressure". Therefore, a tank which contains a liquid (or a liquefied gas), regardless the type of substance, might undergo a BLEVE if its lading is superheated. In fact, this event occurred even for water, nitrogen and carbon dioxide several times in the past, which are not reactive nor flammable substances (Abbasi and Abbasi, 2007a; Heymes et al., 2020). In Table 2, the substances involved in one or more major BLEVE accidents in the period 1926-2004 are collected.

*Table 2: List of the substances which underwent a BLEVE in the period 1926-2004 (adapted from* (Abbasi and Abbasi, 2007a)*).*

| **Substance** | **Type** | **No. of accidents** | **Total no. of death** | **Total no. of injured** |
|---|---|---|---|---|
| Propane | Flammable | 24 | 821 | 7,761 |
| LPG | Flammable | 17 | 12 | 35,127 |
| Chlorine | Toxic | 7 | 139 | - |
| Ammonia | Toxic | 6 | 55 | 25 |
| Butane | Flammable | 5 | 394 | 7,510 |
| Gasoline | Flammable | 3 | 10 | 2 |
| Acrolein | Flammable | 2 | - | - |
| Carbon dioxide | Non-flammable, non-toxic | 2 | 9 | - |
| Ethylene oxide | Flammable | 2 | 1 | 5 |
| LNG | Flammable | 2 | 14 | 76 |
| Propylene | Flammable | 2 | 213 | - |
| Vinyl chloride | Flammable and toxic | 2 | 1 | 50 |
| Borane-tetrahydrofuran | Flammable and toxic | 1 | - | 2 |
| Butadiene | Flammable and toxic | 1 | 57 | - |

*Table 2: List of the substances which underwent a BLEVE in the period 1926-2004 (adapted from (Abbasi and Abbasi, 2007a)) (continued).*

| Substance | Type | No. of accidents | Total no. of death | Total no. of injured |
|---|---|---|---|---|
| Chlorobutadiene | Toxic | 1 | 3 | - |
| Ethyl ether | Flammable | 1 | 209 | - |
| Hydrogen | Flammable | 1 | 7 | - |
| Isobutene | Flammable | 1 | - | 1 |
| Maltodextrin and other chemicals | Toxic | 1 | - | - |
| Methyl bromide | Toxic | 1 | 2 | - |
| Nitrogen | Non-flammable, non-toxic | 1 | - | - |
| Phosgene | Toxic | 1 | 11 | 171 |
| Steam | Non-flammable, non-toxic | 1 | 4 | 7 |
| Water | Non-flammable, non-toxic | 1 | 7 | - |

Propane seems to be one of the most hazardous substances. The boiler explosions, which occur when holding superheated water, were not included in Table 2. This type of explosion is particularly difficult to interpret since three causes of explosion usually coexist: flammable gas, hot surfaces and superheated water (Heymes et al., 2020). If the boiler explosions that occurred in the past are considered as BLEVEs, water may be the substance most frequently involved in BLEVEs (Abbasi and Abbasi, 2007a).

A BLEVE might occur under certain circumstances after the catastrophic rupture of the vessel, which is the critical event, due to the sudden depressurisation of its content. The loss of integrity of the tank can be provoked by several phenomena: defects in the tank material (e.g. corrosion, embrittlement), degradation of the insulation (if any), accidental events (e.g. fire, tank puncture). If the BLEVE is thermally induced (e.g. due to fire

exposure) it is usually defined as “fired” or “hot BLEVE” (Paltrinieri et al., 2009). On the other hand, if the BLEVE is not thermally induced but provoked by several causes (e.g. violent impact or safety device failure), it is named “cold BLEVE”. Therefore, the BLEVE formation depends on several aspects: (i) the thermal insulation of the tank, (ii) the presence and effectiveness of the pressure relief valves (PRVs), (iii) the filling degree of the vessel, and (iv) the type of tank rupture. For instance, Birk et al. (2007) observed two types of BLEVE during the fire tests on propane tanks: single and two-step BLEVEs. The first one is generated if the container rupture is complete and virtually instantaneous, while the two-step BLEVE occurs if the vessel failure time is on the order of 2 s. Birk et al. (2007) concluded that a two-step BLEVE generates the largest blast overpressures when compared with the single-step one. When the tank is completely opened, the compressed gaseous phase abruptly expands generating the first shock wave, whilst a fraction of the superheated liquid flashes (change in phase) at a slower rate (Birk et al., 2007).

According to several authors, the primary requirement for an explosion to be categorised as a BLEVE is the superheated status of the liquid phase (Casal, 2008; Heymes et al., 2020; Pinhasi et al., 2005; Salla et al., 2006; van der Voort et al., 2012). Many authors refer to the theory of superheated liquids (or superheat limit theory) developed by Reid (1976) to determine under which operative conditions (mainly the tank pressure and liquid temperature) a BLEVE may be generated. If a liquid has a temperature above its expected boiling point, it is superheated and thus in a metastable status (Reid, 1976). The superheat limit temperature ($T_{SL}$) is the temperature above which the substance cannot exist in liquid phase, and it varies with pressure. Moreover, the $T_{SL}$ is a characteristic property of each substance. The liquid spinodal curve is the locus of all the $T_{SL}$ values (Reid, 1976). Therefore, if the liquid temperature exceeds the $T_{SL}$ at the given pressure, the substance is thermodynamically unstable. In this case, homogenous nucleation is initiated, and the liquid violently boils by provoking a physical explosion. However, a liquid may flash even in a metastable status through heterogeneous nucleation, especially if triggered (e.g. by a shock wave) (Reid, 1983). In this case, the yield of the explosion is lower since homogeneous nucleation is a more powerful process. Based on these considerations, Reid (1976) formulated the theory of superheated liquids by stating that

a liquid explosively flashes if its temperature reaches the $T_{SL}$ at the given pressure. This criterion can be exploited to estimate the minimum tank pressure required prior the vessel failure to achieve a BLEVE explosion.

The first direct consequence of the BLEVE explosion is the pressure wave generated by the expansion of the compressed gaseous phase and the flashing of the liquid. The debris of the vessel or other piece of equipment thrown away by the blast wave represents another BLEVE aftermath: the missiles. Finally, if the substance contained in the tank is flammable (e.g. fuels) and reaches an ignition source, a fire or fireball can be generated. For the reasons previously mentioned, , the BLEVE explosion is fortunately considered as an atypical scenario since it has a low frequency yet high yield consequences (Paltrinieri et al., 2015). However, this event continues to manifest, as in August 2018 when a BLEVE was generated after the collision of two trucks on a motorway bridge in Bologna, Italy (Eyssette et al., 2021). One of the trucks was transporting a load of liquefied petroleum gas (LPG) which was engulfed in a fire erupted after the traffic collision. This event led to the destruction of the tank and formation of the BLEVE.

### 2.2.2. Rapid phase transition (RPT)

An RPT between liquefied natural gas (LNG) and water was observed for the first time by Constock Liquid Methane Corporation at Bayou Long, Louisiana in 1956 (Reid, 1983). The rapid phase transition (RPT) is another physical explosion which usually is generated by the interaction of two liquids at different temperatures. In fact, it might occur for several fluid pairs (cold liquid in contact with the hot one) in different industrial fields or applications. In the following, some of the fluid pair which underwent an RPT more often are collected:

- water and molten metals (e.g. steel, aluminium, tin);
- water and molten fuel (e.g. uranium);
- water and smelt (molten inorganic salts);
- hydrocarbons (e.g. propane, ethane, isobutane) and water;
- liquefied refrigerants (e.g. R22 -$CHClF_2$-) and water (or oil);

- cryogenic fluids (e.g. liquefied natural gas -LNG-, liquid nitrogen -$LN_2$-) and water.

The fluid on the left-hand side of each pair is the cold one which explosively boils during the interaction. Water can act as the cold as well as the hot fluid in the pair, and it usually always involved in this phenomenon. For this reason, an RPT is often called vapour explosion. Moreover, many other names were assigned to the RPT explosion by several authors: water explosion, vapour explosion, steam explosion, explosive boiling, thermal explosion, thermal interaction, thermal detonation and molten fuel coolant interaction (MFCI). This represents a constrain when this accident scenario is sought in literature. Since RPT may be generated by the interaction of different fluid pairs, this phenomenon accidentally manifested in many types of industries as well as a natural phenomenon during volcanic activity (water-magma interaction) (Wohletz et al., 2012):

- metal foundry;
- nuclear field;
- paper industry;
- petrochemical industry;
- volcanic activity.

Among several definitions, Woodward and Pitblado (2010) described the RPT for the LNG and water pair as "an explosively fast evaporation of LNG to vapor when LNG is suddenly contacted with a warm fluid, usually water". Even though this might be seen as a simplistic definition of the phenomenon, the flashing of the LNG is primarily caused by the rapid heat transferred from water to the cryogenic mixture. The complexity is represented by the behaviour of the fluids during their interaction. Thus, it is arduous to determine under which conditions (mainly temperature of the fluids, flowrate or mass of the cold fluid) the explosion can manifest. As for the BLEVE, the superheat theory (Reid, 1976) is employed to determine if the cold fluid can violently boils when in contact with the hot liquid. The same properties are considered with a slightly different approach. Firstly, it is assumed that the two fluids are at atmospheric pressure. Secondly, the boiling curve of the cold liquid must be considered. In fact, if the temperature of the hot fluid is higher than the Leidenfrost temperature of the cold liquid, the film boiling regime is met

and the heat flux is strongly limited. In this latter case, a trigger is required to rupture the film boiling and allow direct contact between the two liquids. For this reason, two different types of RPT can develop during or after the spill of LNG onto water: early or delayed (Aursand and Hammer, 2018). An early RPT may be initiated if the cryogenic fluid is released as a jet into the water. The depth of penetration, momentum, high degree of mixing (large interface area), and the turbulences (trigger) in the mixing zone are the main factors that can influence the early RPT formation. On the other hand, a delayed RPT may happen after the LNG pool is spread on top of water (stratified geometry), if triggered by the evaporation of methane with consequent change of composition of the hydrocarbon mixture and film boiling collapse (Aursand and Hammer, 2018).

The main consequence of an RPT is the pressure wave. Fires can be ignited if the hot fluid is thrown by the explosion toward combustible materials. For instance, fires developed many times during an RPT in the metallurgical industry where molten metal was shattered and spread around the facility by the shock wave (Li and Ji, 2016). Moreover, a flammable cloud can be created after the evaporation of flammable substances (e.g. hydrocarbons). RPT is also considered as an atypical accident scenario due to the low probabilities to occur. Nevertheless, this event continues to manifest especially in the metallurgical industry. As an example, the accident occurred at the Tata steelworks plant in Port Talbot, UK, on April 2019, can be recognised as an RPT (BBC, 2019).

### 2.2.3. Analogies and differences between BLEVE and RPT

This subsection aims to summarise and compare the characteristics of the BLEVE and RPT explosions. These are two physical explosions which are generated by the violent boiling of a superheated liquid. They may occur for several substances as previously described, on a large temperature range (from cryogenics up to molten metals temperatures) depending on the properties of the involved substances.

One of the main differences is that only one substance is sufficient to provoke a BLEVE, while a fluid pairs is involved in an RPT. In addition, a BLEVE occurs after the depressurisation of the vessel content, whilst the liquid can be considered at atmospheric

pressure for an RPT event. Moreover, the cold volatile fluid of the pair flashes if their interface temperature is found in a certain range (nucleate or transition boiling regions of the cold fluid boiling curve). On the other hand, the probabilities for a BLEVE to be generated constantly increase with the raise in temperature and pressure inside the tank. The mechanisms and consequences of these explosions are treated in detail in the following sections.

# 3. Research background

BLEVE and RPT phenomena have been broadly investigated by several authors. However, it seems that only few researchers considered these events in the case of liquid hydrogen. On the other hand, accident scenarios involving $LH_2$ have been studied for many decades. In particular, the focus has been placed on the $LH_2$ releases on the ground. In this section, an overview of relevant studies conducted on the two physical explosions as well as the investigations of $LH_2$ accident scenarios are presented.

Firstly, a brief description and review of atypical accident scenarios, such as BLEVE and RPT, is presented. Secondly, the abovementioned superheated liquids theory used to characterise the type of explosion is described. Thirdly, past BLEVE and RPT experimental tests and modelling activities carried out by several authors are reported.

## 3.1. Atypical accident scenarios

Paltrinieri et al. (2012) defined an atypical accident scenario (AAS) as "a scenario deviating from normal expectations of unwanted events or worst case reference scenarios and, thus, not deemed credible by the common processes applied for risk assessment". Typically, an AAS is a major accident which has extremely severe consequences. Conventional hazard identification (HAZID) methodologies may not consider such events (Paltrinieri et al., 2013). Two major accidents which were categorised as atypical occurred in Europe in the last two decades: the vapour cloud explosion (VCE) at Buncefield oil depot in 2005 and the explosion in a fertilizer factory in Toulouse in 2001. In addition, it was demonstrated by Paltrinieri et al. (2015) that BLEVE and RPT may be two AASs for innovative LNG regassification technologies.

The issue of atypical accident scenarios was associated to emerging technologies by the FP7 EC project iNTeg-Risk (Jovanović and Baloš, 2013; Jovanović and Löscher, 2014). Even when a very well-known substance is employed in a new application, atypical accident scenarios might manifest. Hydrogen can be used as an example since it has been used for long time in several applications (Ausfelder and Bazzanella, 2016). Currently, it could be selected as fuel in the maritime field thanks to its favourable proprieties (high specific energy content, potentially renewable and clean) (Taccani et al., 2018). However, the hydrogen deployment in this sector can be seen as an emerging technology since barely few vessels were fuelled by hydrogen in the past (van Biert et al., 2016).

### 3.2. Superheated liquids theory

This section allows to determine under which operative conditions (temperature and pressure) the substance might undergo a homogeneous nucleation during its depressurisation, or when a large heat flux is received from another fluid. In the first case, a BLEVE is generated, whilst an RPT event may manifest from the interaction between the fluids. Reid (1976) proposed to estimate the superheat temperature ($T_{SL}$) of each fluid by considering the ratio between its critical temperature and the liquid spinodal temperature at atmospheric pressure. It must be remembered that the liquid spinodal curve is the locus of the maximum temperatures at which the liquid phase can exist at the given pressure. On the other hand, the vapour spinodal curve is the locus of the minimum temperatures at which the vapour phase can exist at the given pressure. The liquid spinodal curve can be determined experimentally (e.g. bubble column experiment) or through an equation of state (EoS). Reid (1976) obtained a good agreement by comparing the Redlich-Kwong EoS and the experimental results for different hydrocarbons (cyclohexane, n-pentane, n-hexane, n-heptane). Pinhasi et al. (2005) adopted a similar approach by comparing different equations of state: Van der Waals, Soave, Peng-Robinson. An EoS can be more suitable for a substance than another one. For this reason, the EoS must be chosen carefully depending on the analysed substance. For instance, the Redlich-Kwong-Mathias-Copeman EoS seems to be the most accurate and robust for hydrogen calculations (Nasrifar, 2010). The water $T_{SL}$ was calculated with this approach by Abbasi and Abbasi (2007b).

Several authors demonstrated the limitations of the superheat limit theory (Birk and Cunningham, 1994; McDevitt et al., 1990; Prugh, 1991; Yu and Venart, 1996). In fact, few BLEVEs occurred in the past when the substances were below their $T_{SL}$. As stated by Casal et al. (2016), this theory is applicable at a small-scale rather than at large-scale where different phenomena manifest: (i) non-homogeneous temperature, (ii) local heating and (iii) liquid stratification. Certainly, the yield of the explosion consequences increases when the substance is more superheated (higher temperature), and the probability to achieve a BLEVE raises as well. Therefore, it is suggested to adopt this theory during a consequence analysis to comprehend the possibility to achieve a BLEVE at the storage conditions or during an accident scenario. The different methods to estimate the $T_{SL}$ of a substance are explained in detail in Sec. 7.3.

### 3.3. BLEVE experimental investigation

Many BLEVE experiments on different substances were conducted by different authors in the past. Two main types of BLEVE experiments were performed and here are renamed as fire and bursting tank scenario tests. During a fire test, either a pool or a jet fire is ignited below the tank to engulfed it completely (worst-case scenario). Hydrocarbons such as kerosene or propane are commonly employed to feed the fire. The fire is kept burning until the tank fails generating a hot BLEVE. In this manner, it is possible to monitor the behaviour of the container and its lading and measure the time to failure of the vessel. The vessel can be weakened by reducing its wall thickness usually in specific areas on the top, to diminish its mechanical performance and assure its rupture. Instead, the rupture of the vessel is provoked by explosive charges during a bursting test. The advantage of this type of experiment is the possibility to set a precise pressure inside the tank and thus assess how this parameter affects the consequences of the explosion. The pressure is increased by warming up the tank lading by means of electric heaters or water heat exchangers. Incendiary devices such as roman candles or gerbs can be placed in the vicinity of the vessel to ensure the ignition of the flammable substance during the explosion, and to observe the consequent fire or fireball. In Table 3, some of the most significant BLEVE tests on different substances are collected.

*Table 3: List of BLEVE tests conducted on different substances (F: fire, B: bursting test).*

| **Reference** | **Substance** | **Test type** | **Tank weakened** | **Tank volume ($m^3$)** |
|---|---|---|---|---|
| (Moodie et al., 1988) | Propane | F | No | 10.250 |
| (Barták, 1990) | Water | B[a,b] | No[c] | 0.010 |
| (Johnson et al., 1991) | Butane, Propane | B[a] | No | 5.659, 10.796 |
| (Birk and Cunningham, 1994) | Propane | F | No | 0.400 |
| (Barbone et al., 1995) | R-22 ($CHClF_2$) | B[d] | No[c] | 0.26 L |
| (Pehr, 1996a) | Hydrogen | B | No | 0.120 |
| (Pehr, 1996b) | Hydrogen | F | No | 0.120 |
| (Balke et al., 1999) | LPG | F | No | 45.360 |
| (Roberts et al., 2000) | Propane | F | No | 4.057[b] |
| (Birk, 2002) | Propane | F | No | 1.800 |
| (Stawczyk, 2003) | LPG | F[b] | No | 0.022[e] |
| (Birk et al., 2007) | Propane | F | Yes | 0.4, 2.0 |
| (Chen et al., 2007) | Water | B[a] | No[c] | 0.039 |
| (Chen et al., 2008) | Water | B[a] | No[c] | 0.023 |
| (van der Voort et al., 2012) | $LCO_2$ | B | No | 0.040 |
| (Laboureur et al., 2014) | Propane | F[b] | Yes | 95 mL |
| (Betteridge and Phillips, 2015) | LNG | B | No | 5.055 |
| (Kamperveen et al., 2016) | LNG | F | No | 3.000 |
| (Tschirschwitz et al., 2018) | LPG | F | No | 0.064 |
| (Birk et al., 2018) | Water, propane | F | Yes | 0.6 L |
| (Heymes et al., 2020) | Water | F[b] | Yes | 0.014 |

Notes:

[a] the liquefied gas temperature was increased through electric resistances.

[b] supercritical BLEVE test.

[c] the opening of the container and consequent depressurisation was controlled with a rupture disc assembly.

[d] the liquefied gas temperature was increased through a water heat exchanger.

[e] tank volume was estimated from the propane mass declared in the experiments and the propane density at NBP.

It can be noticed that many tests were performed on propane and LPG which are the most affected substances by the BLEVE phenomenon, according to Table 2. The BLEVE consequences (blast wave, fragments and fireball) or the two-phase flow during the depressurisation were the main focuses of these tests. Both small and large-scale tests were conducted in the past. The purpose of small-scale experiments is to study closely the shock waves in the near field, and test a large number of samples (tanks) at a reduced cost. Non-flammable substances such as water, $CO_2$ and R-22 allow to avert the combustion effect and focus on the physical explosion. Supercritical BLEVE might manifest in small propane bottles as demonstrated by Stawczyk (2003) and Laboureur et al. (2014), as well as in small $LH_2$ tanks (Pehr, 1996b). This type of BLEVE may be more likely for substances with a low critical pressure such as hydrogen. The supercritical BLEVE consequences must be deeply assessed since these can have a different yield from the subcritical BLEVE ones. For instance, Pehr (1996b) observed that the $LH_2$ tanks ruptured into few pieces (typical for BLEVEs (CCPS, 2010)) when the internal pressure was below the critical one. On the other hand, the same type of vessel broke up into several fragments at supercritical conditions. Finally, it must be noted that only two mid-scale tests were conducted for liquid hydrogen in the past: one fire and one bursting tank scenario tests series. These tests were conducted by BMW car manufacturer as part of a safety programme where an automotive $LH_2$ tank was analysed. More details regarding these experiments are provided in Sec. 3.3.1.

### 3.3.1. BMW safety test programme

Two unique tests series on $LH_2$ double walled tanks were performed by BMW car manufacturer during a four years research programme (1992-1995) (Pehr, 1996b). In particular, the bursting tank scenario (Pehr, 1996b) and the fire tests were conducted (Pehr, 1996a). The technical specifications of the $LH_2$ vessel developed in collaboration with the tank manufacturer Messer Griesheim GmbH and Linde AG can be retrieved in

(Rüdiger, 1992). The $LH_2$ vessel was part of the storage system installed onboard of the BMW Hydrogen 7 customer car (Amaseder and Krainz, 2006). During the bursting tank scenario experiments, ten vessels were ruptured by means of explosive at different pressures and filling degrees (Pehr, 1996b). Instead, two vessels filled at 50% with $LH_2$ were completely engulfed in a propane fire during the fire tests. As result, the entire content evaporated and was vented through the PRV in only 15 minutes. Therefore, the tank did not rupture during the fire tests.

### 3.4. BLEVE modelling

Several researchers attempted to simulate the BLEVE consequences by developing new models or adapting existing explosion methods. The BLEVE consequences can be simulated by means of empirical or analytical models, or through computational fluid dynamics (CFD) tools. In the following, the most critical models for the simulation of the BLEVE consequences are presented.

#### 3.4.1. Empirical and analytical models

As previously mentioned, a BLEVE explosion has three main consequences: blast wave, missiles and fireball (for flammable substances). Most of the analytical models firstly estimate the mechanical energy generated by the explosion. Some of these models, such as the one proposed by Brode (1959), were initially developed for explosive charges and then adapted for BLEVE explosion. Originally, these methods take into account only the gaseous phase. Clancey (1974) and Prugh (1991) proposed a correlation to estimate the flashing fraction of the liquid. Hence, the volume of the flashing liquid can be estimated thanks to this fraction. The total volume of the flashing liquid and compressed vapour phase can be used as input of the models. Moreover, different models assume that the gas behaves as an ideal gas. For instance, Brode (1959) assumed an isochoric process during the expansion of the gas, instead Smith and Van Ness (1996) approximated it with an isothermal process. On the other hand, many models were developed specifically for the BLEVE explosion, thus the liquid phase is already implemented. An exception is the model proposed by Birk et al. (2007) which considers only the compressed gaseous phase.

Instead, few methods estimate barely the liquid phase effect (Casal and Salla, 2006; Genova et al., 2008), while other models estimate the mechanical energy from the expansion of both gaseous and liquid phases (Planas-Cuchi et al., 2004; van den Bosch and Weterings, 2005). The models developed for BLEVE explosion usually consider real gas behaviour. The blast wave overpressure and impulse are then estimated from the mechanical energy with the aid of the trinitrotoluene (TNT) equivalent mass method or the Sachs scaling law (Sachs, 1944). Only part of the mechanical energy generated by the explosion will be converted in pressure wave. In fact, the released energy generates the following phenomena: pressure wave, missiles (kinetic energy and plastic deformation energy absorbed by the fragments), heating of the environment (negligible) (Planas-Cuchi et al., 2004). A comparison of both ideal and real gas behaviour models was conducted by Laboureur et al. (2014) who simulated the large-scale (Balke et al., 1999; Johnson et al., 1991), mid-scale (Birk et al., 2007) and small-scale (Laboureur et al., 2012; Stawczyk, 2003) BLEVE tests. The aforementioned models where adopted by Salla et al. (2006) to estimate the mechanical energy generated by the BLEVE explosion of different substances: propane, butane, methane, water, vinyl chloride, chlorine, ethylene, ammonia, propylene and ethylene oxide. Finally, Hemmatian et al. (2017) compared different ideal and real gas behaviour models to simulate the pressure wave overpressure measured during the butane and propane BLEVE experiments carried out by Johnson et al. (1991) and (Birk et al., 2007).

The range reached by the flying fragments (missiles) is a critical parameter for the determination of the safety distance from the tank in case of explosion. This range can be estimated mainly with empirical correlations as proposed by (Birk, 1996), or by analytical models such as the one developed by Baum (1988). In the first case, only the mass of the substance contained in the tank must be known. Instead, an analytical model is influenced by many parameters: mechanical energy generated by the explosion, empty mass of the vessel, velocity of the fragment, and initial trajectory angle. If the fluid dynamic forces are considered by the analytical model, also the mass of the fragment, its cross-section area and drag coefficient are required. Obviously, it is almost impossible to foresee the exact rupture of the tank, thus the number, mass, and dimensions of the debris. Therefore, these models usually overpredict the fragments range, especially if conservative

assumptions are made. In particular, the initial trajectory angle as a great effect on the results. If the optimal angle (45°) is selected, very long ranges are calculated (CCPS, 2010). An extensive analysis of the fragments generated by the explosion of the S-IV All System Vehicle, which contained $LH_2$ and liquid oxygen (LOX) tanks, is published in (Gayle, 1964). Another fragments range estimation on $LH_2$ BLEVE explosion was carried out by Mires (1985).

The consequences of a potential fireball generated during a BLEVE of flammable substances are often more severe than those generated by the blast (Planas and Casal, 2016). The fireball consequences such as the thermal radiation can strongly vary depending on the type of substance. For these reasons, an accurate consequences analysis of the fireball must be always conducted by means of either empirical or theoretical methods. Both diameter and duration are important for the determination of the separation distance. In particular, the fireball duration is required to estimate the thermal dose received by a target at a certain distance. Different exposure times to the same radiation heat flux can result in different levels of burns. Thus, it is fundamental to estimate the correct value of radiation emitted by the fireball. The radiation depends on several parameters: fireball radius, surface emissive power, view factor, atmospheric attenuation factor (transmissivity), and distance of the target from the fireball. Again, different assumptions must be made to estimate the fireball thermal radiation. For instance, the value of surface emissive power (SEP) is chosen from experimental values of radiation for a specific substance. Otherwise, as suggested in (CCPS, 2010), theoretical models can be employed to estimate the SEP value when it is not measured before. Fireballs generated during a BLEVE were studied by several authors. During the 1960s, NASA and Sandia laboratories investigated the consequences of the fireballs generated by the explosion of different liquid rocket propellants and proposed different empirical correlations (Gayle, 1964; Gayle and Bransford, 1965; High, 1968; Kite et al., 1965), . Bader et al. (1971) and Prugh (1994) developed different models to simulate liquid propellants fireballs. Specific models for propane and LNG fireballs were proposed by Hardee and Lee (1973) and Hardee et al. (1978), respectively. Finally, the $LH_2$ BLEVE fireball consequences were modelled during the IDEALHY project (Lowesmith and Hankinson, 2013). In that case,

the radiation was estimated by means of a jet fire model. Additional models and details for the BLEVE consequence analysis are provided in Sec. 7.4.3.

### 3.4.2. Computational Fluid Dynamics simulations

Safety is one of fields in which the Computational Fluid Dynamics (CFD) analysis is employed. Fires and explosions are broadly studied by means of CFD codes. Many properties of the involved fluids and parameters can be estimated with a high degree of accuracy: pressure, temperatures, densities, velocities, concentrations, flammable mass and cloud volume. Several parameters can be selected during a CFD analysis: CFD code, turbulence model, numerical schemes for the discretisation of space and time, equation of state, and so on. If proper combustion models are selected even the radiation emitted by the fireball can be calculated. Transient simulations can provide these results for each time-step, hence the dynamic of the explosion and its related phenomena (e.g. boiling, condensation) can be investigated in the near-field as well as far away from the expanding source. However, CFD simulations are usually complex to set up and require high-qualified users, are computational and time demanding, and a validation process is always required. Moreover, the flying fragments cannot be simulated through a CFD analysis. Nevertheless, an accurate analysis of the BLEVE consequences can be achieved with a CFD tool. Most of the CFD analyses on BLEVE conducted in the past by several authors are collected in Table 4. Mostly hydrocarbons, liquid $CO_2$ ($LCO_2$) and water were previously simulated. Even though the same phenomenon was modelled a large variety of numerical settings was selected as can be noted in the "Model" column of Table 4. Several BLEVE experiments were simulated in past CFD studies to compare the experimental results with the numerical outcomes, and thus validate the selected models. It can be noticed that often the same research group conducted both the experimental study and the numerical simulation. A similar approach is being adopted within the $SH_2IFT$ project.

*Table 4: Literature review of BLEVE CFD analysis (abbreviations: EoS: equation of state; FV: finite volume; SC: supercritical VOF: volume of fluid; PR: Peng Robinson) (adapted from (Ustolin et al., 2021)).*

| Author(s) | Substance | Scale | Model | Simulated experiments |
|---|---|---|---|---|
| (Deaves et al., 2001) | Freon-11, butane | Small (1.0 L), large (5.7 $m^3$) | STAR-CD (vers. 3.05), unstructured FV solver. Standard buoyancy-extended k–ε. Ideal gas, incompressible liquid correlation. | (Pettitt, 1990), (Johnson et al., 1991) |
| (van der Voort et al., 2012) | $LCO_2$ | Medium (40.0 L) | Inertia limited model. Euler equations. Ideal gas. | (van der Voort et al., 2012) |
| (Zhao et al., 2015) | $CO_2$ (SC) | Small (3.6 L) | Ansys Fluent, VOF. Ideal gas. | - |
| (Tolias et al., 2016) | $LCO_2$, propane | Large (29, 46 $m^3$) | ADREA-HF, Navier-Stokes equations. k-ε turbulence model. Ideal gas, PR EoS. | - |
| (Hansen and Kjellander, 2016) | Butane, propane | Large (1.9 ÷ 10.8 $m^3$) | FLACS, Pseudo-source model. k-ε turbulence model. | (Johnson et al., 1991), (Birk et al., 2007) |
| (Yakush, 2016) | Propane, propylene | Small to large (4.2 L, 0.5 $m^3$, 33.5 $m^3$) | Two distinct zones model: Ghost Fluid Method for the interface – Euler equations for the ambient atmosphere | (Giesbrecht et al., 1981b, 1981a) |

*Table 4: Literature review of BLEVE CFD analysis (abbreviations: EoS: equation of state; FV: finite volume; SC: supercritical VOF: volume of fluid; PR: Peng Robinson) (adapted from (Ustolin et al., 2021)) (continued).*

| Author(s) | Substance | Scale | Model | Simulated experiments |
|---|---|---|---|---|
| (Eyssette et al., 2018) | Water | Small (0.6 L) | Density-based solver with explicit time stepping. | (Eyssette et al., 2018) |
| (Li and Hao, 2020) | Propane, LPG | Large (2, 45 $m^3$) | FLACS, liquid correction and shock tube methods. k-ε turbulence model. Ideal gas. | (Birk et al., 2007), (Balke et al., 1999) |
| (Abdel-Jawad, 2020) | Propane | Large (1.8 $m^3$) | exploCFD, hybrid (analytical-numerical) method | (Birk and VanderSteen, 2006) |
| (Li and Hao, 2021) | Propane | Small (1.0 L), large (5.7 $m^3$) | FLACS, Pseudo-source model. k-ε turbulence model. | Bologna accident (no experiments) |

### 3.5. Behaviour of a liquefied gas tank engulfed in a fire

The understanding of the behaviour of both the container and its lading when exposed to a fire is paramount for the determination of appropriate safety measures to avoid the BLEVE formation. The mechanical resistance of the tank can be evaluated by means of finite element model (FEM) (Paltrinieri et al., 2009). Appropriate passive fire protection can be designed to reduce the thermal stresses on the tank wall and supports, and extend the time to failure (TTF) of the vessel. The evaluation of the TTF in the worst-case scenario is a critical indication for the emergency responders intervention. Both analytical models and CFD analysis can be employed to simulate the behaviour of the substance inside the tank. The stresses on the tank wall caused by the pressure build-up inside the vessel due to the evaporation of the liquid can be assessed by means of conservative criteria (e.g. Von Mises). Scarponi et al. (2016) developed a lumped model to assess the thermal and mechanical response of LNG tanks exposed to fire, while Scarponi et al. (2018) conducted a CFD analysis on the LPG vessels content when engulfed in the fire. Therefore, these effective approaches can be applied to a variety of substances and can provide important information to the safety experts as well as to the tank manufacturer.

### 3.6. RPT experiments

As previously mentioned, an RPT explosion might manifest from the interaction of a fluids pair and the violent boiling of the colder fluid due to the large heat transferred by the hotter substance. It was shown that water is virtually always one of the two fluids of the pair. Despite the fact that RPT can occur in absence of water (e.g. liquid refrigerants-oil, LNG-hydrocarbons (Reid, 1983)), this latter is always considered because present in many industrial processes or in the vicinity of the facilities (e.g. ground water, rivers, lakes, sea). Therefore, the probabilities that water is involved in an RPT event are quite high.

*Table 5: List of relevant RPT tests conducted on different substances (adapted from (Woodward and Pitblado, 2010)).*

| Reference | Test name | Substance | Water source | Spill rate ($m^3$/min) |
|---|---|---|---|---|
| (Felbauer et al., 1972) | Esso | LNG | Sea | 18.9 |
| (Kneebone and Prew, 1974) | Shell | LNG | Ocean | 2.7 - 19.3 |
| (Koopman et al., 1980) | Avocet | LNG | Pond | 4 |
| (Koopman et al., 1982) | Burro | LNG | Pond | 11.3 - 18.4 |
| (Ermak et al., 1988) | Maplin Sands, Shell | LNG, LPG | River | 1.5 - 4 |
| (Goldwire et al., 1983) | Coyote | LNG, LIN | Pond | 14 - 19 |
| (Brown et al., 1990) | Falcon | LNG | Pond | 8.7 - 30.3 |
| (Verfondern and Dienhart, 1997) | BAM | $LH_2$ | Pool | 0.3 |

After the first RPT observation from the interaction between LNG and water in 1956, several experimental tests were conducted on hydrocarbons and liquid refrigerants. Most of these experiments were on small laboratory scale. A thorough review of these tests can be found in (Reid, 1983). Since 1972 different large scale LNG RPT experiments were conducted by several research groups and companies (Woodward and Pitblado, 2010). During the Coyote test series, beyond the analysis of the LNG RPT, the dispersed cloud was ignited to determine the characteristics of fire (Goldwire et al., 1983). To the author's knowledge, only one experiments of $LH_2$ spill onto water was conducted in the past by Verfondern and Dienhart (1997) at BAM facility in Germany. During these tests, an RPT was not observed. In fact, Pritchard and Rattigan (2010) stated that "no record of a RPT resulting from an $LH_2$ spill has been found". They also added that this does not mean that RPT from $LH_2$ can be excluded. In Table 5, some of the most relevant RPT tests on different substances are collected.

### 3.7. RPT modelling

The phenomena which might lead to an RPT explosion can be simulated with different approaches. First of all, the release of the fluid can be simulated as either analytical or numerical (e.g. CFD) models. This type of analysis can provide critical information regarding the momentum of the released fluid and its penetration into the other liquid. Thus, the behaviour of fluids during the interaction can be analysed. Two main zones can develop during the interaction of the fluids: a pool and a highly turbulent mixing zone. The pool spread and the evaporation of the cold fluid can be modelled again by analytical or numerical models. A thorough review of LNG pool analytical models can be found in (Woodward and Pitblado, 2010). Another interesting review of the models to simulate RPT caused by the interaction between water and molten metal was provided by Eckhoff (2016). This author defined this event as a water vapour explosion, and the term RPT was omitted. It must be mentioned that to simulate the spill of cryogenic fluids onto water through CFD, a complicated multiphase flow model must be employed. Moreover, heat transfer and phase change models must be implemented to simulate the related phenomena generated due to the large temperature difference. Furthermore, these models are usually not validated for different substances such as hydrogen, making their outcomes unreliable. However, a good agreement between the CFD analysis outcomes and the $LH_2$ spills onto water experiments (Verfondern and Dienhart, 1997) was found by Nazarpour et al. (2017).

The analytical models reported in (Woodward and Pitblado, 2010) or the method proposed by Aursand and Hammer (2018) can be employed for the consequence analysis of the RPT phenomenon. In this case, only the expansion of the liquid phase is considered since the vapour is not compressed, and the initial conditions will be different than for a BLEVE (initial pressure equal to the atmospheric one). A conservative assumption is that the entire volume of the cold, volatile fluid violently boils, otherwise it would be very arduous to establish the exact fraction of liquid which explodes. Furthermore, there is a high probability that the fraction of vaporising fluid will trigger the film boiling collapse and consequent flashing of the rest of the cold fluid. The RPT modelling is discussed again in Sec. 7.4.4.

# 4. Research questions

The knowledge gap in hydrogen safety, especially in the case of liquid hydrogen, and the numerous potential new applications from which emerging risks might arise, motivated the investigation of atypical accident scenarios for $LH_2$ technologies. The focus of this PhD is placed on two AASs for $LH_2$ technologies: BLEVE and RPT explosions. In the case of $LH_2$, there is little or no knowledge on these two phenomena, but they were extensively studied for other substances such as hydrocarbons (Abbasi and Abbasi, 2007a; Woodward and Pitbaldo, 2010). In a preliminary phase, the knowledge acquired for similar substances such as LNG as well as liquid nitrogen (LIN) should be exploited.

## 4.1. LOI and LOC: research questions I and II

It is well-known that the physical explosions such as BLEVE and RPT may occur as consequence of a loss of integrity (LOI) and consequent loss of containment (LOC) of the equipment (e.g. tanks, pipes). Thus, research question I is:

"*What are the causes of a loss of integrity of hydrogen technologies?"*

The investigation of the phenomena which provoke the LOI of hydrogen technologies can aid the risk assessment in term of prevention and provide paramount indications during the design of the equipment and its maintenance. On the other hand, the potential consequence of a LOC must be mitigated, thus research question II is:

*"What are the consequences of an $LH_2$ release?"*

### 4.2. BLEVE: research questions III-V

As previously mentioned, the AASs have a very low probability but severe consequences. Due to the small amount of information on the $LH_2$ BLEVE, research question III naturally arises:

*"Can a BLEVE explosion occur after a catastrophic rupture of an $LH_2$ vessel?"*

During the review on AASs and $LH_2$ BLEVE, it is confirmed that this accident scenario has an extremely low probability but severe consequences. For this reason, the idea is to focus on the consequence analysis of the BLEVE explosion. This is also one of the main interests of the partner of the $SH_2$IFT project consortium, and goal of the $SH_2$IFT experimental activity. Therefore, research question IV is:

*"What is the yield of the consequences of an $LH_2$ BLEVE explosion?"*

Once it is established that at least two BLEVEs have occurred in the past for $LH_2$ storage systems, and the consequences of the explosion are modelled by reproducing the BMW safety tests (Pehr, 1996b), the focus should be placed on the formation of the phenomenon, i.e. the behaviour of both the $LH_2$ vessel and its lading. This can provide critical information to the emergency responders intervention in case of fire and optimise their training. Therefore, research question V is:

*"What is the time to failure of an $LH_2$ tank exposed to a fire?"*

### 4.3. RPT: research questions VI and VII

Since an RPT is a AAS as well as a BLEVE is, a similar approach is adopted. Research question VI is:

*"Can an RPT explosion occur when $LH_2$ is spilled onto water?"*

Despite the fact that research questions III and VI are very similar, the latter is more challenging since no RPT record as consequence of an $LH_2$ spill is found in literature. This means that a large effort must be spent to comprehend the RPT theories and mechanisms. Other substances must be preliminarily investigated until the $LH_2$ spill

experiments will be performed. However, the focus must be placed again on the consequences since this event is disruptive for several substances, including LIN which has a few analogies with $LH_2$. Hence, the last research question (VII) is:

*"What is the yield of an RPT explosion of $LH_2$?"*

This page is intentionally left blank

## 5. Objectives

The main goal of this thesis is to increase the knowledge on safety of hydrogen technologies. The focus is placed on the consequences of the loss of containment of liquid hydrogen storage systems, in particular on the BLEVE and RPT explosions. Therefore, the following objectives derive from the research questions presented in Sec. 4.

- Objective 1: investigate the loss of integrity of hydrogen equipment:
  - Objective 1.1: comprehend the causes of loss of integrity of hydrogen technologies
  - Objective 1.2: identify the potential consequences of an $LH_2$ release
- Objective 2: investigate the BLEVE phenomenon for an $LH_2$ vessel
  - Objective 2.1: explore the possibility of BLEVE generation for an $LH_2$ tank
  - Objective 2.2: assess the yield of the BLEVE explosion for an $LH_2$ storage system
  - Objective 2.3: determine the time to failure of an $LH_2$ vessel during an accident scenario (e.g. exposed to a fire)
- Objective 3: investigate the RPT phenomenon for an $LH_2$ release
  - Objective 3.1: explore the possibility of the RPT generation after the release of $LH_2$ onto water
  - Objective 3.2: assess the yield of an RPT explosion caused by an $LH_2$ spill onto water

The focus on LOI of $LH_2$ technologies aims to prevent the LOC in several manners. Firstly, the study of the phenomena (e.g. hydrogen embrittlement), which may lead to the LOI of hydrogen technology, can aid the design phase of the equipment. Moreover, critical indications can be provided for the maintenance phase and the modifications of

risk-based inspection methodologies, fundamental part of the risk assessment, can be proposed. Secondly the consequences of an $LH_2$ LOC must be investigated. Therefore, several fields are touched by this investigation (e.g. material science, safety) making it a multidisciplinary analysis.

Probability and consequence of an accident scenario must be evaluated to assess and eventually reduce the associated risk (Kaplan and Garrick, 1981). There are mainly two ways to analyse the consequences of the physical explosions (BLEVE and RPT) as described in Sec. 3: through experiments or by modelling the phenomena. From the research background it is clear that the modelling strictly depends on the experimental activity. Once the consequences have been analysed, their effects can be mitigated by selecting appropriate and effective safety barriers. Even though several techniques are available for the safety barriers selection (e.g. MIRAS technique (Delvosalle et al., 2006)), it should be verified if these are effective for $LH_2$ technologies.

### 5.1. Overview of papers

The links between the objectives and the articles published in the PhD framework are illustrated in Figure 1. Article I aims to both comprehend what are the phenomena and fault events that provoke the LOI of hydrogen technologies (objective 1.1) together with the consequences of their LOC (objective 1.2). The first goal (objective 1.1) is shared by Article IV where a preliminary consequence analysis of $LH_2$ BLEVE is conducted as well. The approaches chosen in these two articles are explained in Sec. 7.1 and 7.2.

Objective 2.1 which address a fundamental research question about the possibility to achieve a BLEVE for $LH_2$ storage vessels, is the focus of Article I-Article V. In Article I and Article IV it is found that $LH_2$ BLEVEs occurred in the past, thus Article II, Article III and Article V attempt to understand which conditions (e.g. operative conditions, thermodynamic status of the substance) are necessary for this explosion to manifest by

employing mainly the superheat limit theory (Sec. 7.3). Article II-Article V and Article VII address the objective 2.2. In particular, Article II, Article IV, Article V and Article VII adopted the analytical models described in Sec. 7.4, whilst a parametric CFD analysis (Sec. 7.5) of the $LH_2$ BLEVE consequences is performed in Article III. Finally, objective 2.3 is addressed in Article IX which provided an estimation of the time to failure of liquefied gas vessels exposed to a fire. In this paper, the BMW fire test (Pehr, 1996a) is chosen as case study, and the methods described in Sec. 7.6 are adopted.

Article VI and Article VIII addressed objective 3.1 by investigating the theories and mechanisms of the RPT explosion for several fluid pairs through a thorough literature review (Sec. 7.1). Moreover, objective 3.2 is the focus of Article VI in which the method described in Sec. 7.4.4 are selected.

## 5.2. Research scope

The general goal of this PhD study is to gain knowledge in hydrogen safety. As previously mentioned, hydrogen safety is a very broad and multidisciplinary field. Therefore, only the consequences of the two atypical accident scenarios, BLEVE and RPT explosions, for $LH_2$ technologies are investigated in detail.

Despite the fact that previous $LH_2$ BLEVE and RPT events are sought and analysed, and the causes of the identified BLEVEs are investigated, the determination of probabilities associated to the phenomena is out of the scope of the thesis.

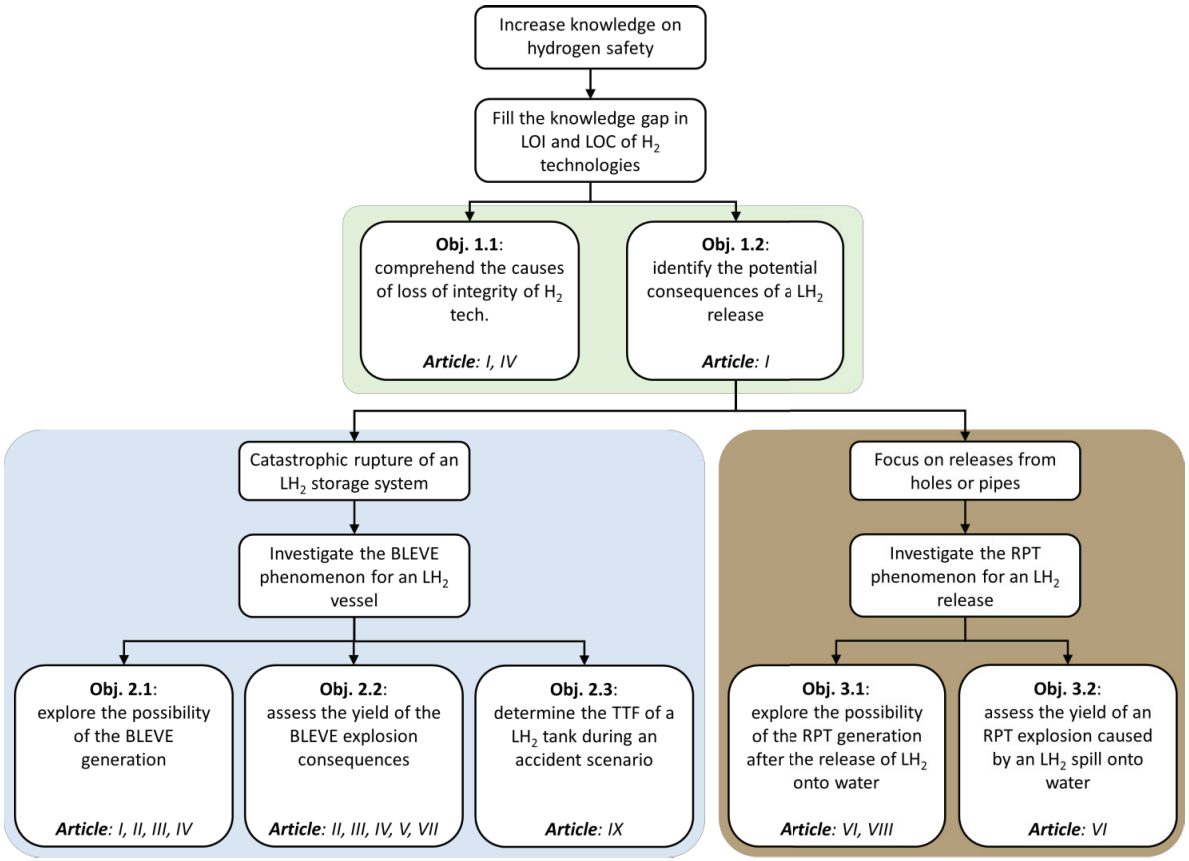


*Figure 1: Link between the objectives and the articles considered in this thesis (abbreviations LOI: loss of integrity, LOC: loss of containment, TTF: time to failure).*

# 6. Research methodology

Research methodology was defined by Buckley et al. (1976) as "the strategy or architectural design by which the researcher maps out an approach to problem-finding or problem-solving". Thus, the approach, i.e. the method, can be selected through the methodology.

The methodology adopted during the PhD is described in this section, while the methods are reported in Sec. 7. Firstly, the different research types according to the Frascati manual (OECD, 2015) are listed. Secondly the multidisciplinary research is explained. Finally, the research approach selected in the publications part of the PhD is reported together with the quality assurance process.

## 6.1. Research types

In the Frascati manual (OECD, 2015), the research and experimental development (R&D) is categorised in three main types of activity:

- Basic research: experimental or theoretical work undertaken primarily to acquire new knowledge of the underlying foundations of phenomena and observable facts, without any particular application or use in view.
- Applied research: original investigation undertaken to acquire new knowledge. However, it is directed primarily towards a specific, practical aim or objective.
- Experimental development: systematic work, drawing on knowledge gained from research and practical experience and producing additional knowledge, which is directed to producing new products or processes or to improving existing products or processes.

Moreover, an activity can be considered R&D, if all the following criteria are satisfied (OECD, 2015):

- Novelty: the work should aim at new findings.
- Creativity: the work should be based on original, not obvious, concepts and hypotheses.
- Uncertainty: the final outcome should be uncertain.
- Systematic: the work should be planned and budgeted.
- Transferability and/or reproducibility: the new knowledge should be transferred to allow other researchers to reproduce the results as part of their own R&D activities.

Initially, the PhD was supposed to carry out an experimental development research activity since the $SH_2IFT$ project experimental tests on $LH_2$ BLEVE and RPT were planned to take place during the first PhD year. Instead, the research conducted during the PhD study shifted to applied research due to the long delay in the experiments execution. In fact, the publications produced are original investigations aiming to broaden the knowledge in hydrogen safety. Moreover, the scientific articles respect the R&D criteria heretofore mentioned.

For instance, the experimental tests on $LH_2$ vessels (Pehr, 1996a, 1996b) are modelled by means of different approaches in Article II, Article III, Article IX. To the author's knowledge this has been done for the first time. New concepts and hypothesis which can satisfy the creativity criterion are formulated during the PhD and in many publications. A new method for the consequence analysis of liquefied gas tanks is provided in Article II. Most of the outcomes from the modelling activity are uncertain since a proper validation is still required. Furthermore, bind prediction studies of the $SH_2IFT$ project tests are conducted in Article II, Article IV and Article VII.

The research activities have been planned and budgeted within the $SH_2IFT$ project framework. A visiting period to the National Centre for Scientific Research (NCSR) "Demokritos" (Greece) was planned for the second year of the PhD and funded by the Research Council of Norway through additional funding associated to the $SH_2IFT$ project.

During the visiting period, a joint research activity between the Environmental Research Laboratory of the NCSR "Demokritos", and the candidate was undertaken.

## 6.2. Multidisciplinary research

Hydrogen safety is certainly a very broad topic. Paradoxically, if the focus is placed only on $LH_2$ safety, more factors must be considered for two main reasons: in an $LH_2$ system, gaseous hydrogen is always present (NASA, 2005), and $LH_2$ is a cryogenic fluid. Therefore, cryogenic technologies and processes must be taken into account and the $GH_2$ effects cannot be neglected. Moreover, an extensive knowledge on several disciplines ranging from materials for hydrogen equipment, regulations (e.g. safety codes and standards), physical and chemical phenomena (e.g. fires, explosions, releases and dispersions), and social awareness and acceptance might reduce potential risks of hydrogen deployment in new applications. For these reasons, often during this PhD study a multidisciplinary approach is sought.

## 6.3. Research approach

According to Creswell (2014), three types of research approach exist: quantitative, qualitative and mixed methods. Quantitative and qualitative approaches have not very well-defined boundaries. Both approaches exploit data and aim to increase knowledge. Usually, the main distinction between quantitative and qualitative research is that the first one utilises numbers and the second one words (Creswell, 2014). Moreover, a quantitative approach is selected to prove objective theories by verifying the relationship among variables which can be measured or calculated. On the other hand, the data gathered with a qualitative approach can be interpreted. With a mixed approach both quantitative and qualitative data are collected. It is assumed that with a combination of the quantitative and qualitative approaches, a more complete understanding of the research problem can be achieved compared with the first two research types.

During this PhD, mainly quantitative and mixed approaches are adopted. In particular, a quantitative research is adopted for the consequence analysis of the $LH_2$ BLEVE explosion conducted in Article II, Article III, Article V, Article VII, and in Article IX in

which the TTF of $LH_2$ vessels exposed to fires is determined. A mixture methods research is selected in article I where an exhaustive narrative review is coupled with a systematic one. A similar approach is used in Article IV and Article VI. Article VIII is the only one in which a qualitative method is selected to provide a review on theories and mechanisms of RPT for several types of fluids pairs.

### 6.4. Quality assurance

The scientific value of the publications is assured by different approaches. Plausibility is checked for each analysis by comparing the results with the ones from relevant studies on similar topics. Expert judgment is always adopted during the research process by consulting constantly the main supervisor. The expertise of the co-authors is exploited to ensure a high quality of each work. Monthly feedback on the research progress is received by the co-supervisor and the research group at collaborating on the RPT topic. The $SH_2IFT$ consortium provided feedback during the presentations of the advancement at the quarterly project meetings. Finally, all the presented articles underwent a peer review process when submitted to the international conferences and the journals, except Article III and Article IX which are still under revision. In Table 6, the research approaches and quality assurance for each article is reported.

*Table 6: Research methodology adopted in each publication.*

| Article no. | Research approach | Quality assurance |
|---|---|---|
| I | Mixed | – Expert judgment;<br>– Publication in a peer-reviewed journal. |
| II | Quantitative | – Expert judgment;<br>– Validation with experiments;<br>– Publication in a peer-reviewed journal. |
| III | Quantitative | – Expert judgment;<br>– Validation with experiments;<br>– Submission to a peer-reviewed journal. |

*Table 6: Research methodology adopted in each publication (continued).*

| Article no. | Research approach | Quality assurance |
|---|---|---|
| IV | Mixed | – Expert judgment;<br>– Publication in a peer-reviewed conference. |
| V | Quantitative | – Expert judgment;<br>– Publication in a peer-reviewed conference. |
| VI | Mixed | – Expert judgment;<br>– Publication in a peer-reviewed conference. |
| VII | Quantitative | – Expert judgment;<br>– Validation with experiments;<br>– Publication in a peer-reviewed conference. |
| VIII | Qualitative | – Expert judgment;<br>– Publication in a peer-reviewed conference. |
| IX | Quantitative | – Expert judgment;<br>– Validation with experiments;<br>– Submitted to a peer-reviewed conference. |

This page is intentionally left blank

# 7. Research methods

An introduction to the different methods, selected during the PhD study by applying the methodology described in Sec. 6, are reported in this section. Additional details on these methods can be found in the publications (Article I-Article IX).

## 7.1. Narrative and systematic review (Article I, III, IV, VI, VIII)

A narrative review (NR) is "aimed at identifying and summarizing what has been previously published, avoiding duplications, and seeking new study areas not yet addressed" (Ferrari, 2015). On the other hand, a systematic review (SR) is "a clearly formulated question that uses systematic and explicit methods to identify, select, and critically appraise relevant research, and to collect and analyse data from the studies that are included in the review" (The Cochrane Collaboration, 2005). The NR was mainly used in Article I and Article IV to address objective 1.1 and 1.2 (see Sec. 5) and in Article VI and Article VIII to focus on objective 3.1. Moreover, the results of the NR were used to define the queries of the SR in Article I. Hence, the SR was adopted only in Article I. It might be said that the NR is mainly a qualitative approach, while the SR is both a quantitative and qualitative analysis (Ferrari, 2015). The main differences between an NR and an SR are collected in Table 7.

A general framework is usually defined to perform the NR (Ferrari, 2015). This framework is composed by an introduction where the content together with objectives, scope and structure of the review are defined. Then the literature search in which the methodology selected for the NR may be reported by describing the searching strategy (databases and keywords), inclusion/exclusion criteria (languages, types of documents, time frame), is reported. Moreover, the researched references are cited and listed in the

literature search. Finally, discussion and conclusions follow as in conventional scientific publications. A similar framework can be recognised in the abovementioned articles.

All the methods used to carry out the SR must be presented to make the analysis reproducible. Two critical aspects of the analysis are the date in which the SR was completed, and the considered timespan (publication years). As for the NR, the selected databases and keywords should be mentioned. In addition, the exact queries chosen for the searching are listed. Several types of filters (e.g. language, type of document, category/field) can be applied in most common scientific databases (e.g. Web of Science, Scopus), and they should be mentioned among the details of the search. The outcomes of the search can be refined by means of dedicated tools or software. For instance, in Article I, the bibliometric data gathered by the SR analysis were "cleaned" with the aid of the OpenRefine tool, and the visualization of similarities (VOS) viewer software (van Eck and Waltman, 2007) was used to build co-authorship network maps of authors and countries, together with a cooccurrence map of key words. Even though the SR is a powerful technique, the probability to include false negative articles in the research always exists. An incorrect application of queries and filters may be the cause of misleading results. For further information see Article I.

*Table 7: Main differences between NR and SR (adapted from (Ferrari, 2015)).*

| Step | Narrative reviews | Systematic reviews |
|---|---|---|
| Main features | – Describe and appraise published articles.<br>– The methods employed to select the articles may be omitted. | – Well defined query.<br>– Clear definition of the criteria for the articles selection.<br>– Explicit methods of extraction and synthesis of the data.<br>– Comprehensive research to find all the relevant studies.<br>– Application of standards for the critical appraisal of the studies quality. |
| Uses/applications | – General debates, appraisal of previous studies and the current lack of knowledge.<br>– Rationales for future research.<br>– Speculate on new types of interventions available. | – Identify, assess and synthesize the literature gathered in response to a specific query.<br>– Collect what is known about a topic and identify the basis of that knowledge.<br>– Comprehensive report with explicit processes so that<br>– rational, assumptions and methods are open to<br>– examination by external organizations. |

*Table 7: Main differences between NR and SR (adapted from (Ferrari, 2015)) (continued).*

| Step | Narrative reviews | Systematic reviews |
|---|---|---|
| Limitations | – The assumptions and the planning are not often known.<br>– Selection and evaluation biases not known.<br>– Not reproducible. | – The scope is limited by the defined query, search terms, and the selection criteria.<br>– Usually, reader needs to reformulate the alternative questions that have not been answered by the main query. |

### 7.2. DyPASI technique (Article IV)

The Dynamic Procedure for Atypical Scenario Identification (DyPASI) technique was proposed by Paltrinieri (2010). DyPASI was used in Article IV to address the objective 1.1.

*Table 8: DyPASI procedure steps (adapted from (Paltrinieri et al., 2015)).*

| Step | Input | Output | Description |
|---|---|---|---|
| 0 | Input to conventional bow-tie technique | Generic bow-ties describing potential accident scenarios | DyPASI needs a preliminary application of the conventional bow-tie technique to identify relevant critical events |
| 1 | Information from accident databases and dedicated search systems | Risk notions on undetected potential hazards | A search for relevant information concerning hazards that may have not been considered in conventional bow-tie development is performed |
| 2 | Risk notions from step 1 | Early warnings triggering further analysis | A determination is made as to whether the data are significant enough to trigger further action and proceed with risk assessment |
| 3 | Bow-ties from step 0 and early warnings from step 2 | Bow-tie diagrams considering also atypical scenarios | Atypical scenarios are isolated from the early warnings; cause–consequence chains are built and integrated into the generic bow-ties |
| 4 | Integrated bow-ties from step 3 | Safety barriers for the atypical scenarios | Safety measures are defined for the atypical scenarios identified |

This is a hazard identification (HAZID) technique for the systematization of information from past accidents and inherent studies, usually coupled with a dynamic risk assessment (DRA). The idea is to dynamically update the HAZID, especially by taking into account atypical accidental scenarios which are not considered by traditional hazard identification processes (Paltrinieri et al., 2016). The main steps of the DyPASI technique are collected in Table 8. It can be noticed that different techniques and methodologies are employed in the DyPASI procedure. For instance, the conventional bow-tie diagram utilized as input of the first DyPASI step can be built with the methodology for the identification of major accident hazards (MIMAH) (Delvosalle et al., 2006). Moreover, the methodology for the identification of reference accident scenarios (MIRAS) (Delvosalle et al., 2006) can be employed in the step 4 of DyPASI for the definition of the safety barriers required to prevent or mitigate the atypical accident scenarios. The DyPASI technique was already employed by Paltrinieri et al. (2015) for the identification of atypical accident scenarios such as BLEVE and RPT, for innovative liquefied natural gas (LNG) regasification technologies. This technique is especially suited for emerging technologies which are challenging cases for a comprehensive and reliable hazard identification. For additional information, see Article IV.

### 7.3. Superheated liquids theory (Article II, III)

The superheat limit theory was exploited in Article II and Article III to comprehend under which operative conditions an $LH_2$ vessel can undergo a BLEVE (objective 2.1). In particular, what is the minimum tank pressure prior to the catastrophic rupture to achieve this event. In Figure 2, the saturation and liquid spinodal curves for a generic substance are reported. As an example of the application of the superheat limit theory is here provided. If the substance contained in the tank is at saturation conditions when the vessel fails (point A), and an isothermal depressurisation is considered (conservative assumption), the liquid will be superheated and in a metastable thermodynamic status. Instead, if the same substance has higher temperature and pressure (point B) and undergoes the same type of depressurisation, the liquid spinodal curve will be reached, thus the fluid will be in an unstable status and homogeneous nucleation will be initiated. Point B corresponds to the liquid spinodal temperature (or superheat limit temperature,

$T_{SL}$) at ambient pressure. According to the superheated liquids theory, a BLEVE can be generated if the substance is found at the conditions of point B or higher. The correspondent pressure ($P_B$) can be determined and is the minimum tank pressure required for a BLEVE to be generated. Similarly, the theory can be applied to a fluid (e.g. cryogen) released onto water. In this case, the substance is usually at saturation conditions virtually at atmospheric pressure (point C). If the heat flux received by the hotter fluid is such that a sudden increase in temperature leads the liquid toward its $T_{SL}$, the possibility for a violent boiling increases. The boiling curve of the substance, or at least its Leidenfrost temperature, are necessary to determine the regime (e.g. nucleate, transition or film boiling) according to the temperature different of the fluid pairs, thus the heat flux from the hotter to the colder fluid.

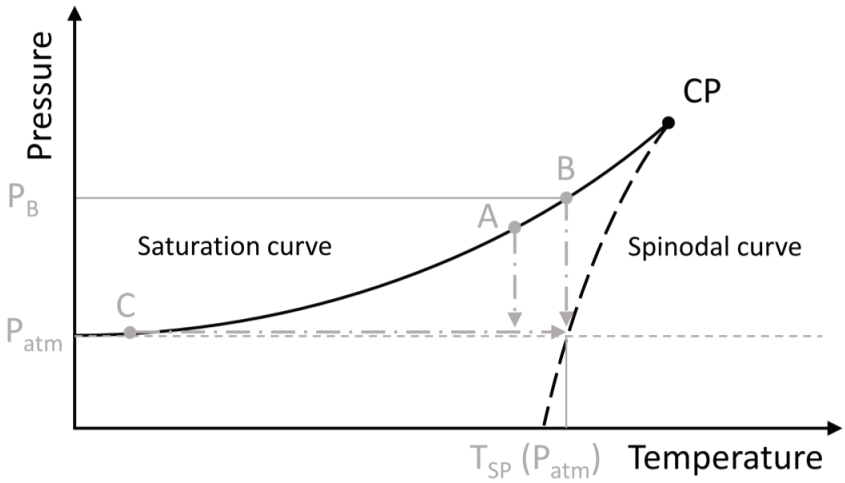


*Figure 2: saturation and liquid spinodal curve for a generic substance (abbreviations: CP: critical point, $T_{SP}$: spinodal temperature).*

The correlation proposed by Reid (1976) to estimate the $T_{SL}$ (Eq. (1)) is widely used for different substances and was selected in Article II:

$$T_{SL} = 0.895 \cdot T_C \tag{1}$$

where $T_C$ is the critical temperature of the substance in K, and 0.895 is the ratio between the liquid spinodal temperature at atmospheric pressure ($T_{SP(P_{atm})}$) and the critical temperature. The values of ratio estimated with different EoS are collected in Table 9. Salla et al. (2006) and Casal (2008) proposed two different methods to estimate the $T_{SL}$.

Both methods were selected in Article II and Article III. The first method estimates the $T_{SL}$ through an energy balance by considering an adiabatic vaporisation process during the depressurization (Salla et al., 2006). The second method exploit the saturation curve at the critical point (CP), and TSL can be estimated either graphically (building the tangent to the curve at the CP) or through the Clausius-Clapeyron equation (Casal, 2008). This latter is usually the most conservative approach. Further details can be found in Article II and Article III. The $T_{SL}$ is a critical indicator, and it was estimated together with the correspondent pressure at saturation by bearing in mind the limitations of the superheat limit theory, described in Sec. 3.2.

*Table 9: $T_{SP}(P_{atm})/T_C$ ratio values for the estimation of the $T_{SL}$ of hydrogen (adapted from (Ustolin et al., 2021)).*

| Proposed by | EoS | $T_{SP}(P_{atm})/T_C$ Normal $H_2$ |
|---|---|---|
| Reid, 1976 (Reid, 1976) | Redlich-Kwong | 0.8950 |
| Pinhasi et al., 2005 (Pinhasi et al., 2005) | Van der Waals | 0.8440 |
| | Soave | 0.9430 |
| | Peng-Robinson | 0.9480 |
| (Ustolin et al., 2021) | Helmholtz free energy | 0.8793 |

### 7.4. Analytical and empirical models

Different analytical and empirical models were selected to conduct the consequence analysis of $LH_2$ BLEVE explosions in Article II, Article V and Article VII, to address the objective 2.2. The models to assess each $LH_2$ BLEVE consequence (blast wave, missiles and fireball) are presented in the following. Moreover, the method chosen in Article VI to perform the RPT consequence analysis to focus on the objective 3.2 is described in Sec. 7.4.4.

### 7.4.1. Mechanical energy and pressure wave estimation (Article II, V)

As previously mentioned, Prugh (1991) proposed a correlation to calculate the liquid flashing fraction which enables to determine the total expansion volume ($V^*$) which is the sum of the gaseous phase and the liquid flashing volumes. The liquid flashing fraction correlation is given in Eq. (2):

$$f = 1 - \exp\left[-2.63\left[1 - \left(\frac{T_C - T_0}{T_C - T_b}\right)^{0.38}\right]\frac{c_{p,L0}}{\Delta h_{V0}}(T_C - T_b)\right] \quad (2)$$

where $T_0$, $T_C$ and $T_b$ are the atmospheric, critical and boiling temperatures respectively in K, $c_{p,L0}$ is specific heat of the liquid at boiling temperature in kJ kg$^{-1}$ K$^{-1}$, and $\Delta h_{V0}$ is the latent heat of vaporisation at boiling point in kJ kg$^{-1}$. The total volume is estimated with Eq. (3):

$$V^* = V_T + m_L\left(\frac{f}{\rho_V} - \frac{1}{\rho_L}\right) \quad (3)$$

where $V_T$ is the total volume of the tank in m$^3$, $m_L$ is the mass of the liquid in kg, $\rho_V$ and $\rho_L$ are the density of the vapour and liquid phase respectively in kg m$^{-3}$, and $f$ is the flashing fraction estimated with Eq. (2). The estimation of the total volume permits to adapt the model developed for explosive or pressurised vessels. Both ideal and real gas behaviour models were selected to calculate the mechanical energy generated by the explosion in Article II and Article V. Among the ideal gas behaviour models the following were chosen:

- isochoric process (Brode, 1959);
- adiabatic process (Prugh, 1991);
- thermodynamic availability (Crowl, 1992, 1991);
- isothermal process (Smith and Van Ness, 1996).

Instead, the selected real gas behaviour models for the mechanical energy estimation of the $LH_2$ BLEVE are:

- TNO model (van den Bosch and Weterings, 2005)
- Planas-Cuchi et al. (2004) model;

- superheating energy (SE) model – isentropic and irreversible processes (Casal and Salla, 2006);
- Genova et al. (2008) model;
- Birk et al. (2007) model.

The ideal and real gas behaviour model equations are provided in Table 10. The formulae for the estimation of the isentropic internal energies required by the TNO model (van den Bosch and Weterings, 2005) can be found in Article II, together with the intersection point between the variation of internal energy and the adiabatic irreversible expansion work ($x$) used in the Planas-Cuchi model. Only part of the mechanical energy generated by the explosion will be converted in pressure wave according to (Hemmatian et al., 2017). In fact, the released energy generates the following phenomena: pressure wave, missiles (kinetic energy and plastic deformation energy absorbed by the fragments), heating of the environment (negligible) (Planas-Cuchi et al., 2004). Therefore, empirical coefficients are employed to estimate the amount of energy which participate in the pressure wave formation. For instance, Casal et al. (2001) suggested that 40% and 80% of the released energy contributes to the generation of the pressure wave for ductile and fragile ruptures of the vessel, respectively. For this reason, the Planas-Cuchi model (Eq. (9)) is usually multiplied by 0.4 (40%). The values of the coefficients $k$ in the SE model (Eq. (10)) are 0.14 (isentropic process) and 0.05 (irreversible process), while the coefficient $\psi$ found in the Genova model (Eq. (11)) is equal to 0.07. On the contrary, the energy estimated by the TNO and Birk models (Eq. (8) and (12)) is doubled to account for the ground effect. Other coefficients consider the ground reflection and the geometrical effects (CCPS, 1999). The blast wave overpressure and impulse are then estimated from the mechanical energy with the aid of the trinitrotoluene (TNT) equivalent mass method or the Sachs scaling law (Sachs, 1944). These scaling laws approximate well the overpressure in the far field, whilst overpredict it in the near field. The correlations provided by Kinney and Graham (1985) are usually employed to estimate the overpressure and impulse in the far field. Additional details can be found in Article II.

*Table 10: Equations of the ideal and real gas behaviour models selected in Article II and Article V (adapted from (Ustolin et al., 2020)).*

| Reference | Equation | |
|---|---|---|
| (Brode, 1959); | $E_{Brode} = \frac{P - P_0}{\gamma - 1} V^*$ | (4) |
| (Prugh, 1991); | $E_{IE} = P \cdot V^* \cdot \ln \frac{P}{P_0}$ | (5) |
| (Crowl, 1992, 1991); | $E_{TA} = P \cdot V^* \left[ \ln\left(\frac{P}{P_0}\right) - \left(1 - \frac{P_0}{P}\right) \right]$ | (6) |
| (Smith and Van Ness, 1996) | $E_{Prugh} = \frac{P \cdot V^*}{\gamma - 1} \left(1 - \frac{P_0}{P}\right)^{\frac{\gamma - 1}{\gamma}}$ | (7) |
| (van den Bosch and Weterings, 2005) | $E_{TNO} = m_V \left(u_V - u_{V_{is}}\right) + m_L \left(u_L - u_{L_{is}}\right)$ | (8) |
| (Planas-Cuchi et al., 2004) | $E_{Planas} = -[(u_{L0} - u_{V0})\, m_T \cdot x - m_T \cdot u_{L0} + U_i]$ | (9) |
| (Casal and Salla, 2006) | $E_{SE} = k \cdot m_L \, (h_L - h_{L0})$ | (10) |
| (Genova et al., 2008) | $E_{Genova} = \psi \cdot m_L \cdot c_{p,L} \, (T_L - T_{L0})$ | (11) |
| (Birk et al., 2007) | $E_{Birk} = m_V \left(u_V - u_{V_{is}}\right)$ | (12) |

Notes: $m$, $u$, $h$, $T$, $U_i$ and $c_{p,L}$ refer to the masses in kg, internal energies in kJ kg$^{-1}$ (Planas model units are MJ kg$^{-1}$), the enthalpies in kJ kg$^{-1}$, the temperatures in K, the overall internal energy of the system before the explosion in MJ and the average specific heat at constant pressure of the liquid phase between the initial and final states of the expansion in kJ kg$^{-1}$ K$^{-1}$. The subscripts *V*, *V0*, *L*, *L0* indicates the vapor and liquid phases before and after (at atmospheric pressure) the explosion, respectively, while *T* and *is* refer to both liquid and vapour phases (total), and the isentropic process, respectively.

### 7.4.2. Missiles range determination (Article II)

(Birk, 1996) suggested a correlation to estimate the horizontal missiles range for propane BLEVE explosions, and it was implemented in Article II. The mass of the substance ($m_T$) and the vessel volume ($V_T$) are the only considered parameters in these correlations (Eq. (13) and (14)):

$$R = 90 \cdot m_T^{0.33} \quad \text{for } V_T < 5 \text{ m}^3 \tag{13}$$

$$R = 465 \cdot m_T^{0.1} \quad \text{for } V_T > 5 \text{ m}^3 \tag{14}$$

Usually, the most conservative range values are obtained with this method. Therefore, the approach suggested by CCPS (2010) was adopted as term of comparison. Firstly, the initial velocity of the fragments is calculated with the formula developed by Baum (1984). The velocity depends on the mechanical energy, obtained by the application of the most conservative methods (e.g. TNO model), the kinetic energy, fraction of energy responsible for the fragments ejection (0.04 for the BLEVE (van den Bosch and Weterings, 2005)), and the empty mass of the vessel. Therefore, the fluid dynamic forces (lift and drag) are neglected by this method. Secondly, the horizontal and vertical ranges depend on the initial angle of the trajectory: 5° ÷ 10° for vessels placed horizontally (CCPS, 2010), and 45° for vertically oriented tanks.

A third method which accounts for the fluid dynamic forces is implemented in Article II for the fragment analysis. In this case, the scaled velocity is calculated with the initial velocity (Baum equation), the air atmospheric density, gravitational acceleration constant, the fragment drag coefficient, cross-sectional area and mass. Thus, the number of fragments and their shapes and masses must be assumed adding uncertainties to the analysis outcomes. The scaled horizontal range is graphically determined from charts (Baker et al., 1983). Finally the horizontal range is calculated from the scaled one with the same parameters used to determine the scaled velocity except the gravitational acceleration.

### 7.4.3. Fireball models (Article II, VII)

The aftermath of the fireball ignited during an $LH_2$ BLEVE is estimated in Article II and Article VII to address the objective 2.2. As previously mentioned, several models were developed especially to determine the fireball diameter and duration of different substances. In Table 11, some of the empirical correlations used to determine the fireball diameter and duration of different substances are presented.

*Table 11: Empirical models for fireball diameter and duration for different substances (adapted from* (Abbasi and Abbasi, 2007a)*).*

| **Reference** | **Substance** | **Diameter, $D_{fb}$ (m)** | **Duration, $t_{fb}$ (s)** |
|---|---|---|---|
| (Fay and Lewis, 1977) | Propane | $6.28\ M^{0.333}$ | $2.53\ M^{0.167}$ |
| (Hasegawa and Sato, 1977) | Pentane | $5.28\ M^{0.277}$ | $1.10\ M^{0.097}$ |
| (Lihou and Maund, 1982) | Butane | $5.72\ M^{0.333}$ | $0.45\ M^{0.333}$ |
| (Lihou and Maund, 1982) | Rocket fuel | $6.20\ M^{0.320}$ | $0.49\ M^{0.320}$ |
| (Lihou and Maund, 1982) | Propylene | $3.51\ M^{0.333}$ | $0.32\ M^{0.333}$ |
| (Lihou and Maund, 1982) | Methane | $6.36\ M^{0.325}$ | $2.57\ M^{0.167}$ |
| (Lihou and Maund, 1982) | Propane | $3.46\ M^{0.333}$ | $0.31\ M^{0.333}$ |
| (Hardee and Lee, 1973) | LNG | $6.24\ M^{0.333}$ | $1.11\ M^{0.167}$ |

In Article II an Article VII, the fireball diameter, height and duration were determined by means of the empirical correlations proposed by Hord (1972) (Eq. (15)), Bagster and Pitblado (1989) (Eq. (16)) and Beyler (2016) (Eq. (17) and (18)):

$$D_{fb} \approx 7.93 \cdot m_T^{1/3} \tag{15}$$

$$H_{fb} = 2 \cdot R_{fb} \tag{16}$$

$$t_{fb} = 0.45 \cdot m_T^{1/3} \tag{17}$$

$$t_{fb} = 2.60 \cdot m_T^{1/6} \tag{18}$$

where $m_T$ is the $LH_2$ mass in kg and $R_{fb}$ is the fireball radius in m. Eq. (17) is called momentum-dominated fireball equation while Eq. (18), buoyancy-dominated. According to (CCPS, 2010), the first equation should be used if the mass is lower than 30,000 kg, as in Article II and Article VII where the BMW bursting scenario tests (Pehr, 1996b) were simulated. However, Zalosh and Weyandt (2005) found a better agreement between the outcome of the buoyancy-dominated correlation and the experiments in which the hydrogen mass was as small as 1.64 kg. Therefore, a comparison between these two methods was conducted to evaluate the shortest and longest fireball duration.

As previously noted, both diameter and duration are necessary for the estimation of the thermal radiation in which the geometric factor (e.g. view factor) and exposure time allow to determine the thermal dose at different distances. In Article II and Article VII, the fireball thermal radiation was assessed with the solid flame model (CCPS, 2010). It was assumed that the entire hydrogen content was ignited and burnt according to the considerations made by Gayle and Bransford (1965). Since no data on the surface emissive power (SEP) for $LH_2$ fireballs are publicly available, the SEP was estimated through the Stefan-Boltzmann's law (most conservative method). The transmissivity and view factor were also determined after the most conservative assumptions were made. For instance, the angle between the receptor surface normal and the distance between the fireball centre and the target was equal to zero (direct radiation). Once the fireball incident radiation ($q$) at difference distances from the fireball was calculated, the thermal dose ($Td$) was estimated with Eq. (19):

$$Td = q^{4/3} \cdot t_{fb} \tag{19}$$

Finally, the safety distance is determined as the distance where the thermal dose is equal or below 80 $(kW\ m^{-2})^{4/3}$ s which is the criterion measured by Rew (1997) to avoid any injuries to personnel. For more information on the fireball models, Article II and Article VII should be consulted.

### 7.4.4. RPT consequence analysis (Article VI)

An analytical model similar to the ones presented in Sec. 7.4.1 was used to estimate the blast wave overpressure of $LH_2$ RPT in Article VI to focus on objective 3.2. This model is described in detail in (Aursand and Hammer, 2018). In Article VI, it was exploited to estimate the energy released by two potential RPTs: one generated by a spill of $LH_2$ and the other one by the pouring of LNG onto water. The same volumes were compared. Further details can be found in Article VI.

### 7.5. Computation Fluid Dynamics analysis (Article III)

The CFD analysis of $LH_2$ BLEVE was performed in Article III to address the objective 2.2. As briefly discussed in Sec. 3.4.2, CFD codes were already used to investigate the BLEVE consequences of different substances, but not yet for $LH_2$ to the author's knowledge. ADREA-HF CFD code (Venetsanos et al., 2010) was selected to conduct this analysis. This is an in-house code developed by the Environmental Research Lab. of the NCSR "Demokritos". ADREA-HF is 3D time dependent finite volume code validated against several experiments involving flammable gas dispersion (Giannissi et al., 2020, 2014, 2013; Koutsourakis et al., 2012) and combustion (Tolias et al., 2020, 2017, 2014). The conservation equations of mass, momentum and energy for the mixture are solved together with the species total mass fraction conservation equation. Several turbulence models are implemented in the code, RANS and LES types. Multi-phase multi-component mixtures can be handled by the code by using the Eulerian methodology and assuming that the non-vapor (liquid and/or solid phase) is dispersed in the vapor mixture. The Homogeneous Equilibrium Model (HEM) is used by default, i.e. the phases have the same velocity and temperature. However, the Non-Homogeneous Equilibrium Model (NHEM), in which the phases (vapor and non-vapor) can develop different velocities, can be set (Giannissi and Venetsanos, 2018). The HEM method was utilized in the $LH_2$ BLEVE CFD analysis. The Raoult's law is used for the components phase distribution for ideal mixture, and the Rachford-Rice (R-C) methodology, effective for multi-component mixtures, is employed (Giannissi and Venetsanos, 2018). The governing equations and numerical details can be found in Article III.

The $LCO_2$ BLEVE experiments were reproduced by means of ADREA-HF and the outcomes were exploited to validate the code. Therefore, a parametric analysis was performed by simulating the $LH_2$ vessel tested during the BMW safety experiments (bursting tank scenario (Pehr, 1996b)). Several configurations were set in the analysis by varying the initial tank pressure and temperature, $LH_2$ and $GH_2$ mass content. The combustion was neglected to focus on the physics of the physical explosion and accurately analyse the dynamic of the pressure wave. However, the flammable hydrogen mass and cloud volume were estimated to investigate the hydrogen dispersion and provide

critical information on the fireball formation. The outcomes of the CFD analysis were compared with the BMW experimental results. All the details of the CFD parametric analysis are reported in Article III.

### 7.6. Thermal model (Article IX)

The analytical thermal model developed by Scarponi et al. (2016) to assess the thermal and mechanical response of LNG tanks exposed to a fire was tuned for $LH_2$ vessels in Article IX to address objective 2.3. This model is based on the thermal nodes approach, and the domain (vessel) is divided in eight nodes: the liquid and vapour hydrogen phases, the inner and outer shells walls, and the insulation in contact with the liquid and the vapour phases. The thermal and mass balances for the nodes can be found in (Scarponi et al., 2016) together with the models for evaporation and condensation and the equations for the determination of the discharging rate through the PRV.

In Article IX, the multiparameter Helmholtz-energy-explicit-type formulations was implemented in the model through the CoolProp package (Bell et al., 2014), to estimate the hydrogen thermodynamic properties. Moreover, the hydrogen boiling curve equations published in (Wang et al., 2016) were integrated in the model to model the heat transfer between the $LH_2$ and the inner shell wall. The $LH_2$ vessel investigated during the BMW fire tests was simulated engulfed in a propane fire. The thermal conductivity of the insulation and the sizing of the PRV was done by following the procedure described in the ISO 21013-3:2016 standard (ISO, 2016). The mechanical stress generated by the pressure build up in the inner vessel were estimated. The yield strength of the material was used to determine the admissible stress and set as a conservative criterion for the estimation of the time to failure of the tank estimation. Finally, the failure of the PRV was simulated to assess the TTF in the worst-case scenario. Further details on the model are reported in Article IX.

### 7.7. Model validation and comparison (Article II, III, VII, IX)

It is a good practise to validate the developed or adopted models by reproducing experimental tests or accident scenarios in the safety field. If a proper validation is not possible due to a high level of uncertainties, the results might not be reliable and additional experiments are required. Both analytical and numerical models must be validated. Borg et al. (2014) investigated different validation approaches for numerical simulations (CFD analysis). In Article II, Article III, Article VII and Article IX, the model outcomes were compared with the BMW safety tests (bursting tank scenario and fire) (Pehr, 1996b, 1996a) described in Sec. 3.3.1. Moreover, the ADREA-HF code employed for the CFD analysis of $LH_2$ BLEVE was validated with the $CO_2$ BLEVE experiments performed by van der Voort et al. (2012).

This page is intentionally left blank

## 8. Contributions

In this section, the summary of the contributions achieved during the PhD study are reported. These contributions are the results of the application of the methods reported in Sec. 7, and aim to answer to the objectives of the PhD (Sec. 5). The links between contributions and objectives are shown in Table 12 together with the correspondent articles and topics. This table can be used by the readers as index to navigate to the topic of interest. For a thorough description of the contributions, Part II of this thesis should be consulted.

*Table 12: Link between contributions, objectives, and scientific articles in the framework of the PhD.*

| Contribution | Sec. | Objective | Article(s) | Main topic |
|---|---|---|---|---|
| I | 8.1 | 1.1 | I, IV | Causes of loss of integrity of hydrogen technologies |
| II | 8.2 | 1.2 | I | Consequences of an $LH_2$ release |
| III | 8.3 | 2.1 | I-IV | Feasibility of a BLEVE for $LH_2$ storage systems |
| IV | 8.4 | 2.2 | II-V, Article VII | Consequences of an $LH_2$ BLEVE |
| V | 8.5 | 2.3 | IX | Time to failure of $LH_2$ tanks exposed to a fire |
| VI | 8.6 | 3.1 | VI, VIII | Theories and mechanisms of RPT |
| VII | 8.7 | 3.2 | VI | Consequence analysis of an $LH_2$ RPT |

## 8.1. Contribution I: Causes of LOI of hydrogen technology

This contribution addresses objective 1.1 and offers an overview on the phenomena and causal events which may lead to the LOI of hydrogen technology. This contribution is the result of Article I and Article IV.

The narrative review in Article I served to investigate the hydrogen life cycle, properties, and related safety aspects. The causal events (cause of the accident) are analysed together with the hazards, critical events and its consequences. Generally, all types of mechanical and physical failures can be considered as LOC causes. Some of the fault events can be collisions, mechanical failures of hydrogen equipment, hydrogen embrittlement and other phenomena responsible of material degradation. These types of failure are specified in Article I. It is found that most of the critical events (e.g. breach on the shell, leak from pipe, catastrophic rupture) are defined either as LOC or LOI (or loss of physical integrity, LPI) of the piece of equipment. The focus is then placed on the physical and chemical phenomena that can lead to an LOI such as hydrogen damages (HDs), and low temperature embrittlement and thermal deformation for $LH_2$ or cryogenic gaseous hydrogen. The mechanisms and theories that attempt to explain the HD formation are highlighted. The material behaviour during fatigue cycles is another issue that should be considered when analysing the LOI of hydrogen technologies and is introduced in Article I. Therefore, the material selection is a fundamental procedure that must be carefully carried out during the design of hydrogen equipment. Many critical indications on this practice are provided in Article I. The NR demonstrated that LOI topic related to the hydrogen technologies is a multidisciplinary subject.

The systematic review is conducted after the NR by exploiting the results of this latter. In fact, the focus of the SR is on the LOI and safety aspects of hydrogen technologies. As result, a limitation represented by the dearth of collaboration between the research groups from different areas is highlighted, especially between material scientists and safety experts. Finally, the causal events of the two $LH_2$ BLEVE identified through the DyPASI technique are described in Article IV. These events are represented by chains of events. In one case, an improper fire fighter technique provoked the failure of the PRV of the $LH_2$ vessel. A consequent pressure build up inside the tank led to a catastrophic rupture

of the container and the BLEVE explosion. In the second case, an O-ring failure initiated a jet fire from the solid rocket booster which impinged the $LH_2$ and LOX vessels until their failure. The catastrophic rupture of these tanks and consequent BLEVE explosion were the causes of the Space Shuttle Challenger disaster (Chirivella, 1997). The faults and escalation factor (e.g. improper firefighting technique) together with the direct consequences of the catastrophic rupture of the $LH_2$ vessel (BLEVE) allow to update the conventional bow-tie diagram built by means of the MIMAH technique. These are the main findings of Article IV regarding Contribution I, and additional information can be found in Part II.

### 8.2. Contribution II: $LH_2$ release consequences

Contribution II addresses objective 1.2 by investigating the causes of an $LH_2$ release after the LOC of a piece of equipment. As previously mentioned, the safety aspects of hydrogen technologies are analysed in Article I. Some of the highlighted consequences of an $LH_2$ release are: respiratory ailment and asphyxiation (especially in enclosed environment), frostbite and hypothermia after contact with $LH_2$, other physiological consequences due to exposure to blast wave overpressure or fireball (e.g. burns, lung damage), dispersion, pool formation, fires (e.g. pool, flash or jet fire), explosions (e.g. VCE, BLEVE). The focus is then placed on atypical accident scenarios (e.g. BLEVE and RPT) which are often not considered in a conventional risk analysis. More information can be found in Article I.

### 8.3. Contribution III: Feasibility of a BLEVE for $LH_2$ storage systems

The results of different articles (Article I-Article IV) are part of Contribution III which focusses on objective 2.1 regarding the possibility of the BLEVE formation for an $LH_2$ tank. Two different approaches are selected to determine this possibility: (i) through a literature review of this accident scenario and (ii) by applying the superheat limit theory. The first method, described in Sec. 7.1, is adopted in Article I and Article IV. The results of these scientific papers show that two previous BLEVEs occurred for $LH_2$ storage vessels. The first one in 1974 in a chemical industry facility where a 9,000 gal (34 $m^3$)

$LH_2$ tank failed almost three days after a fire ignited in the vicinity of the container (HydrogenTools, 2017). The cause was a failure of the PRV provoked by the intervention of the fire fighters brigade who sprayed the $LH_2$ vessel with water to cool it down. The water froze on the PRV impeding the venting of the evaporated $LH_2$ from the tank. The second accident occurred in 1986 over the Atlantic Ocean, off the coast of Cape Canaveral, Florida: the Space Shuttle Challenger disaster. The chain of events that led to the BLEVE of the $LH_2$ and LOX vessels has been described in Sec. 8.1. This type of approach usually allows to establish the probability for a type of scenario to occur. However, there are few publicly available information to determine the probability. Two accidents over a period of 47 years is an exceptional safety record, but one have to bear in mind that the applications in which $LH_2$ were employed until now are very limited compared to the $GH_2$ ones (< 1% globally (Ausfelder and Bazzanella, 2016)). Furthermore, $LH_2$ has been produced, handled, and utilised mostly in the chemical and aerospace industry, and often the accident reports are not made available.

As previously mentioned, the second approach exploits the superheat limit theory. This approach is adopted in Article II, Article III and Article IV. In this manner, the operative conditions under which the BLEVE might manifest can be determined with the different procedures described in Sec. 7.3. A large range of $T_{SL}$ of hydrogen is obtained with the least and the most conservative methods in Article III: 28.0 ÷ 32.6 K, which corresponds to a range of internal pressure of 5.7 ÷ 11.9 bar. This means that according to the most conservative method, a BLEVE might occur if the tank ruptures when its pressure is above 5.7 bar. A comparison with the $T_{SL}$ and correspondent pressure of $CO_2$ is carried out by using the same methods in Article III. The minimum pressure to achieve a BLEVE for a $CO_2$ vessel is 21.9 bar, four times large than the one for $LH_2$. This was expected since the $T_{SL}$ depends on the critical temperature of the substance, which is very low for hydrogen (33.145 K (NIST, 2019)) compared with other substances. However, this does not mean that a BLEVE is more likely for an $LH_2$ vessel than for the tanks of other substances, because the probability depends on several factors. Moreover, this theory has several limitations as explained in Sec. 3.2. Nevertheless, the $T_{SL}$ should be always estimated since can provide critical information. For instance, the PRV opening pressure can be set during the design phase in order to maintain the tank pressure below the

minimum pressure needed to achieve a BLEVE. Additional results are provided in Article II and Article III.

### 8.4. Contribution IV: Consequences of an $LH_2$ BLEVE

This contribution is in line with objective 2.2, which aims to quantify the consequences of an $LH_2$ BLEVE explosion. This consequence analysis is conducted with different approaches in Article II, Article III, Article IV, Article V, Article VII. In particular, analytical and empirical models are selected for the analyses in all these papers, except in Article III where a CFD analysis is performed. Moreover, only the pressure wave is investigated in Article III, Article IV and Article V, while the fireball is the only focus of Article VII. Only in Article II, all the three consequences of a BLEVE are analysed. The modelling of the $LH_2$ BLEVE consequences is one of the main activities of this PhD, and it is demonstrated by the large number of publications compared to the other contributions.

The idea of Article II, Article III, Article V, Article VII is to reproduce the BMW bursting tank scenario tests (Pehr, 1996b). It is demonstrated that the most conservative analytical models for the overpressure of the blast wave are the TNO model (van den Bosch and Weterings, 2005) and the Birk (Birk et al., 2007) model at sub- and supercritical conditions, respectively. The correlation proposed by Birk (1996) to estimate the fragment range is the most conservative one, but the obtained value is one order of magnitude larger than the experimental observations. The other correlations are strongly dependent on the initial trajectory angle of the fragments, or the number of fragments. A good approximation is achieved with the second method described in Sec. 7.4.2, proposed by CCPS (2010) with an initial suggested angle of 10°. Instead, the fireball dimensions as well as the duration are underpredicted by the empirical models proposed by (Hord, 1972) and (Beyler, 2016), respectively, reported in Sec. 7.4.3. A good agreement with the BMW tests is obtained by the CFD analysis considering that the combustion effect on the overpressure was neglected. Finally, a blind prediction study on the $SH_2$IFT BLEVE experiments is carried out in Article II after the methods were validated with the BMW tests. Additional information can be found in Part II of this thesis.

### 8.5. Contribution V: Time to failure of $LH_2$ tanks exposed to a fire

Contribution V is resulted from Article IX, where objective 2.3 is addressed. The heat transfer mechanisms, and thermal and mechanical stresses generated in the tank material when exposed to a fire are estimated. It is assumed that the mechanical stress depends mainly on the pressure build up inside the tank due to the evaporation of the $LH_2$. In this case, the BMW fire tests (Pehr, 1996a) are simulated. A very good agreement with the experiments is attained by considering a complete degradation of the insulation and lose of vacuum after only 115 s from the beginning of the test. The PRV opened after 347 s and the whole $LH_2$ content is vented after 854 s instead 900 s as measured during the test. On the other hand, a limitation of this thermal nodes approach is the calculation of temperatures due to the impossibility to estimate the temperature gradients developed in the tank and its lading. In fact, only one temperature is estimated for each thermal node. Moreover, the positions of the temperature measurement points in the vessel selected during the test are unknown. A second scenario in which a failure of the PRV occur was simulated. The estimated time to failure of the inner vessel was 632 s. This outcome could not be validated since the PRV was properly working and the tank did not rupture during the experiments. Additional information can be found in Article IX.

### 8.6. Contribution VI: Theories and mechanisms of RPT explosion

This contribution focusses on objective 3.1 which aims to explore the possibility of the RPT generation after the release of $LH_2$ onto water. The results of Article VI and Article VIII are part of this contribution. In Article VI, the knowledge gained in predicting the RPT event for LNG spills onto water is exploited. The focus is placed on delayed RPT which occurs several seconds after the LNG is poured onto water in a zone of the spreading pool different from the release one. It is demonstrated by estimating the hydrogen Leidenfrost point that this type of RPT is theoretically impossible for $LH_2$. In Article VIII, the common mechanisms between the RPT generated by the contact of different fluid pairs are sought to establish a universal theory. This is an arduous task due to the different composition and physical and chemical properties of the substances. Hence, it is decided to focus on the liquid nitrogen (LIN) RPT. It is found that the model

developed for LNG predicted that a delayed RPT is impossible for LIN as well. However, LIN RPTs manifested many times in the past, and this phenomenon can be easily reproduced at laboratory scale. The experiments conducted by Bang and Corradini (1991) on LIN RPT demonstrated that an RPT can triggered by hammering the tank containing the LIN and water initially in a stratified geometry (cryogenic pool). In this manner, the film boiling formed due to the low Leidenfrost temperature of LIN compared with the water temperature can be ruptured. It can be concluded that early and triggered RPT might occur when LIN is spilled onto water. It is speculated that a similar behaviour might be shown by a release of $LH_2$ onto water. However, the conditions under which an $LH_2$ RPT might manifest should be different than the ones of an LIN RPT due to the different properties such as density. Further information on the RPT mechanisms and theories are provided in Article VI and Article VIII, collected in Part II of this thesis.

### 8.7. Contribution VII: Consequence analysis of an $LH_2$ RPT

Objective 3.2 is addressed by contribution VII which resulted from Article VI. Beside the investigation of the RPT mechanisms, the aim of Article VI is to determine the yield of the consequences of an $LH_2$ RPT, and compare it with the intensity of an LNG RPT. The focus is placed on the mechanical energy generated by the two explosions and the peak overpressure of the shock wave. The same volumes of the two different substances are compared, and the estimated pressure peak for the $LH_2$ RPT was 7 bar, which is between 12% and 35% the yield of the explosion assessed for the LNG one (20-60 bar). The LNG pressure peak depends on the LNG composition. For some types of applications, it could be more indicative to compare the same energy content since the $LH_2$ density (70.9 kg $m^{-3}$ (NIST, 2019)) is one order of magnitude lower than the LNG one (an average value of 450 kg $m^{-3}$ can be considered (Aursand et al., 2020)). Therefore, additional investigation may be necessary. Further information on this contribution can be found in Article VI.

This page is intentionally left blank

# 9. Discussion

In this section, the contributions previously described are discussed. The discussion is divided according to the three main objectives of this thesis: investigation of the loss of integrity of hydrogen equipment (Sec. 9.1), BLEVE (Sec. 9.2) and RPT (Sec. 9.3) phenomena for $LH_2$ vessels and releases, respectively. Finally, a discussion of the overall PhD study follows in Sec. 9.4.

## 9.1. LOI of hydrogen equipment

The loss of integrity (LOI) phenomena are investigated mainly in Article I to comprehend their mechanisms and under which conditions they manifest. Firstly, the focus is placed on the hydrogen damages. It is found that a universal theory able to explain all the HDs has not been developed yet, and additional effort should be made to find a common thread between the different HDs. Secondly, low temperature embrittlement and thermal deformation must be always taken into account for $LH_2$. Thirdly, a significant reduction in fatigue lifetime of different metals suitable for hydrogen service was estimated by several authors. Therefore, supplementary studies must be conducted on the fatigue properties of hydrogen equipment materials. Finally, the material selection process is fundamental during the design phase of hydrogen equipment and can be influenced by the LOI phenomena investigation outcomes. Barely few materials, usually expensive alloys, are suitable for all hydrogen applications. For this reason, a careful analysis must be conducted for each utilization in order to minimize the costs and maximize the safety of the system.

The systematic review on the loss of integrity (LOI) of hydrogen equipment identified a heterogeneous variety of publications touching several research areas. Virtually all the works are focussed on hydrogen safety, marking its importance. Moreover, the SR

revealed an exponential growth in the number of papers published in the last two decades. This may be a consequence of the several hydrogen safety projects promoted worldwide during this period. A limitation emerged from the network maps, indicating that the collaborations between research groups from several fields are often missing. The hydrogen safety knowledge can be improved by the participation of experts from different areas in research projects related to this critical topic.

The aim of this investigation is to prevent a LOC, thus severe accidents by broadening the knowledge on these phenomena and optimise the material selection process. Two recent accidents occurred in June 2019 in a public hydrogen refuelling station in Norway (Nel Hydrogen, 2019) and in a hydrogen chemical plant in California (Genovese et al., 2020). They were both provoked by a LOC of the hydrogen storage system and resulted in explosion and fire. Beyond these direct consequences, the ceasing of many hydrogen refuelling stations service for few months as preventing measure was an additional aftermath in Norway. Thus, hydrogen fuelled cars were brought to a halt. These ruinous events witness the urgency for safety countermeasures to reassure the public opinion and future investors, and thus support the hydrogen deployment in several new fields and applications. Nevertheless, the root cause of the Norwegian accident was an assembly error of a specific plug in a high-pressure hydrogen tank, demonstrating that not only the LOI phenomena but many other aspects must be considered and investigated since hydrogen safety is a multidisciplinary topic.

Finally, the consequences of an $LH_2$ LOC are identified in Article I and Article IV. Particular attention is paid to the atypical accident scenarios such as BLEVE and RPT. The motivation is enhanced by the neglection of these phenomena by the conventional risk assessment techniques due to their low probabilities. This type of approach led to major accidents in the past (Sec. 3.1) and must be avoided. Furthermore, the extremely limited knowledge on $LH_2$ RPT is highlighted, hence further research on this event has to be pursued.

## 9.2. $LH_2$ BLEVE investigation

As previously explained in this thesis, different approaches and models are selected and employed to determine the possibility for a BLEVE to occur and its consequences. This subsection is then divided in three parts: discussion on the application of the superheat limit theory, analytical and empirical models, CFD analysis.

The minimum tank pressure at which a BLEVE might manifest after the catastrophic rupture of an $LH_2$ vessel is determined by applying the superheat limit theory. Different results are obtained because many EoS are selected for the estimation of the $T_{SL}$ and correspondent pressure. As expected, the minimum tank pressure according to the most conservative method (5.7 bar) is quite low compared to other substances. However, this is not directly related to the probability of the BLEVE occurrence due to mainly two factors: the BLEVE formation depends on the type of rupture of the tank, the probability depends on the time to failure. In the first case, the type of rupture of an $LH_2$ double walled vessel is supposed to be different from the single skin tank (e.g. propane tank). This is assumed because the energy required to rupture two shells might be higher than the one necessary to wreck one container, thus the mechanical energy generated by the explosion may be dissipated. Moreover, the $LH_2$ tanks are designed to work at lower pressures than other liquefied gas vessels. Therefore, if the $LH_2$ tank fails at a low pressure, a BLEVE explosion might be avoided. It must be said that currently these are speculations since additional safety experiments for $LH_2$ tanks are needed.

The analytical models for the estimation of the shock wave overpressure provided a wide range of outcomes. The limitations of these models are highlighted. For instance, few models are able to estimate the consequences when the tank lading is at supercritical conditions, and only few models provided conservative outcomes when the BMW tests were simulated. Moreover, some models consider only the gaseous or the liquid phase. This can lead to largely underestimate the overpressure when the considering phase is scarce in the tank. It seems that these models were developed for specific substances (e.g. propane) and configurations (e.g. filling degree of the tank equal to 50%), and usually validated barely with large-scale experiments. The same issues are valid for the fragments range correlations, even if these models tend to largely overpredict the experimental

results. Furthermore, many assumptions must be made when applying these methods because several parameters such as number of fragments, dimensions and initial trajectory angle are usually unknown. Finally, the fireball consequences (dimensions, height, duration, and thermal radiation) are estimated with empirical and theoretical models. These methods provided again a large underestimation of the maximum fireball diameter and duration. It is not possible to compare the radiation emitted by the fireball due to lack in experimental tests. In the past, the hydrogen fireball radiation was estimated by means of jet fire models. It is believed that a dedicated model must be developed since a luminous flames was observed after the explosion of both compressed gaseous (Zalosh and Weyandt, 2005) and liquid hydrogen tanks (Pehr, 1996b), while the hydrogen jet fires are known to have a scarce visibility (Schefer et al., 2009). It is extremely important to properly model the fireball since its consequences are often the most severe aftermath of the BLEVE explosion (Planas and Casal, 2016). Despite the fact that the safety distance is estimated by simulating the BMW tests and by predicting the future $SH_2IFT$ experiments, a further verification of these simulation outcomes is required.

The CFD analysis conducted with the ADREA-HF code focusses on the blast wave generation since the combustion was neglected. Again, the BMW bursting tank scenario tests are modelled. This type of analysis allows to estimate a number of parameters and observe in detail how the shock wave is generated and developed inside the domain at different instants. Moreover, the effects of the pressure, temperature, $LH_2$ amount, and liquid and gaseous phases are analysed thanks to the parametric analysis. It is observed that the duration of the explosion is shorter when only the cold gaseous hydrogen (at saturation conditions) is stored in the vessel compared to the $LH_2$ burst. This direct affects the impulse of the pressure wave. On the other hand, the maximum overpressure is not influenced by the phase type, thus the amount of hydrogen at the given pressure. Therefore, the dynamic of the shock wave is studied in detail, and critical indications are provided. The latter could be used to modify the existing analytical models. Even though this analysis could give many insights on the BLEVE accident scenario, several assumptions are still made due to the uncertainties in the BMW tests and the complexity of the phenomenon. Therefore, additional validation of the CFD code for the $LH_2$ BLEVE is necessary, and the combustion effect must be included.

## 9.3. $LH_2$ RPT investigation

This investigation is very arduous since no record of $LH_2$ RPT exists, and only one small-scale experiment on $LH_2$ release onto water, during which RPT did not occur, is available in literature. Furthermore, the delay in the $SH_2$IFT experiments could not provide any indication within the PhD framework. The theoretical approach was the only one left. The possibility of an RPT formation after the release of $LH_2$ onto water is investigated by exploiting the RPT knowledge for different substances and fluids pairs. Firstly, the model developed for LNG delayed RPT is applied to $LH_2$, and this type of RPT is excluded. This was lately confirmed by the analysis on LIN RPT. In fact, either early or triggered RPT can occur from the interaction of LIN and water, but the delayed one cannot. It is speculated that a similar behaviour can be manifested by the $LH_2$ water interaction. However, the conditions under which an RPT explosion can occur (e.g. temperatures, interface area between the fluids) should be different due to the differences between $LH_2$ and LIN properties (e.g. Leidenfrost temperature, density).

The analytical models that simulate the pool spreading of the cryogens onto water can be tuned for hydrogen. If the possibility for a delayed RPT for $LH_2$ is excluded, these models could aid the investigation of the evaporation and dispersion of $LH_2$ but not the RPT analysis. Complicated models such as CFD should be employed to simulate the mixing zone between water and $LH_2$ to estimate the interface area and temperatures in each point of the domain. These two parameters influence the heat flux between the fluids. This latter can be used as criterion to determine if the sudden heat transfer can heat the $LH_2$ up to the $T_{SL}$ and a violent boiling due to homogeneous nucleation may follow. Different models such as multiphase flow, heat transfer and phase change of $LH_2$, water and air must be applied for this kind of simulation, making it a complex and time demanding analysis. To the author's knowledge, this type of simulation for $LH_2$ release onto water was not conducted yet. Regarding the modelling of the potential RPT consequences, the comparison of the same volume of $LH_2$ and LNG showed that the maximum pressure peak is reached by this latter substance (20-60 bar), while expected overpressure for $LH_2$ is lower than 30% (7 bar) of the LNG one. Also in this case, additional verification must be carried out once the experiments will be conducted.

## 9.4. Implications of the PhD research

During this PhD study $LH_2$ BLEVE and RPT atypical accident scenarios were largely investigated. Some of the analyses were carried out for the first time for this substance. Even though the outcomes of this study require additional verification and validation with the experimental results, a good starting point was provided. In particular, the focus on consequence analysis of $LH_2$ BLEVE allowed validating some of the available models through mid-scale tests. Moreover, their limitations were highlighted, and critical information were provided for their modifications. Furthermore, the blind prediction study of the $SH_2$IFT experiments provided paramount indications for the experimental setting. Finally, it is believed that some knowledge on hydrogen safety was gained and important discussion on the atypical accident scenarios for emerging technologies was continued.

# 10. Conclusions

The main aim of this PhD study is to broaden the knowledge on hydrogen safety. The focus is placed on atypical accident scenarios for liquid hydrogen technologies. This topic is relatively broad and involves several disciplines. For this reason, a multidisciplinary approach was adopted in the PhD framework by focussing on risk assessment techniques, material science, thermodynamic theories, analytical and empirical as well as numerical modelling.

The loss of integrity and containment of hydrogen equipment was investigated, and two physical explosions were analysed: boiling liquid expanding vapour explosion (BLEVE) and rapid phase transition (RPT). The main contributions of this thesis are:

- investigation on the causes of LOI of hydrogen technology;
- identification of the $LH_2$ release consequences;
- understanding of the BLEVE feasibility for $LH_2$ storage systems;
- determination of the $LH_2$ BLEVE consequences;
- estimation of the time to failure of $LH_2$ tanks exposed to a fire;
- analysis of the theories and mechanisms of RPT explosions;
- determination of the $LH_2$ RPT consequences.

The systematic review used for the investigation on LOI of hydrogen technologies demonstrated that this is a multidisciplinary topic. A limitation represented by the dearth of collaboration between the research groups from different areas was highlighted. Thus, an extensive participation by different kind of experts would be beneficial to enlarge the knowledge on this topic. The identification of the $LH_2$ release consequences aid to direct the focus on the atypical accident scenarios (e.g. BLEVE, RPT), i.e. where the lack of knowledge is prevailing.

In the past, at least two BLEVE occurred for $LH_2$ vessels. The application of the superheat limit theory indicates that this type of event might manifest at a very low temperature and pressure for $LH_2$. However, the probabilities for a BLEVE to occur depend on several parameters such as the type of vessel and its insulation. Therefore, no further indications can be provided on this regard prior the $LH_2$ fire tests.

During the consequence analysis of $LH_2$ BLEVE, the drawbacks of the currently available analytical models and empirical corelations were highlighted together with several uncertainties such as the behaviour of the double walled tank and its content during the evolution of the BLEVE phenomenon. Paramount considerations on the dynamic of the blast wave were made by observing the outcomes of the $LH_2$ BLEVE CFD analysis. As a result, different modifications of the existing analytical models were suggested. Finally, a blind prediction study of the $SH_2$IFT $LH_2$ BLEVE experiments was carried out after the validation of the models with the BMW tests. Even though the outcomes of the blind prediction must be compared and verified with the tests results, critical information to aid the set up of the experiments were provided.

The thermal nodes approach allowed to simulate the behaviour of both the $LH_2$ vessel and its content when exposed to a fire. The BMW fire tests were simulated and a good agreement between the model and the experimental results was found. This validated model can be exploited for a blind prediction study of the $SH_2$IFT experiments. After these tests, further verification and validation can be conducted and propose it as a tool to aid the risk assessment of liquefied gas vessels.

The theories and mechanism of RPT explosion for different fluid pairs were broadly investigated. The probability and consequence of a potential RPT event caused by an $LH_2$ release onto water was evaluated based on established LNG and LIN research. It was assessed that the probability for a delayed RPT to happen for $LH_2$ is extremely low due to the very low Leidenfrost temperature of hydrogen. However, an early or triggered RPT during or after the spill of $LH_2$ onto or into water cannot be excluded. Further considerations cannot be provided without the support of experimental data. It can be concluded that in a hypothetical $LH_2$ RPT event, the estimated consequences of the vapor explosion are considerably smaller than the ones of an LNG RPT event.

Some of the research activities included in this study explore aspects of the physical explosions for the first time for $LH_2$ technologies. The dearth of knowledge is represented by the uncertainties in the formation of the $LH_2$ RPT event as well as the probability of failure of an $LH_2$ double walled vessel when exposed to a fire and thus the formation of the BLEVE explosion. The limitations of the currently available models to simulate $LH_2$ BLEVE and RPT were identified and highlighted. Knowledge gained for different substances were transferred to the liquid hydrogen system. However, the validity of the selected and applied methods must be validated further. Several aspects must be considered during the atypical accident scenarios analysis, thus the multidisciplinary approach was demonstrated to be effective.

The main goal of this PhD study was accomplished since new knowledge in hydrogen safety was provided and the outcomes of this thesis can be exploited as starting point for future studies. A list of the proposed future works is proposed in the next section.

This page is intentionally left blank

## 11. Future works

In this section, the future works proposed as results of the limitations and knowledge gap faced in this PhD study, are listed. The wide knowledge gap in $LH_2$ BLEVE and RPT phenomena could be fulfilled mainly by experimental work as planned during the $SH_2IFT$ project. The modelling activity can aid the prediction and prevention of future accidents and suggest modifications of the safety standards and codes as well as of risk assessment techniques and good practises. Certainly, the models must be thoroughly validated by the experimental results before employing them for a risk analysis.

The knowledge gap highlighted in LOI phenomena could be filled by enhancing the collaboration between experts of several fields. This is the aim of part of the new European project "Development of Tools Enabling the Deployment and Management of a Multi-Energy Renewable Energy Community with Hybrid Storage (H2 CoopStorage)" in which the material degradation provoked by the hydrogen-metal interactions will be investigated. A collaboration between material scientists and safety experts is ongoing to accomplish this objective. The material degradation modelling will provide paramount insights for modification of risk-based inspection techniques and good practices.

New empirical correlations to predict the aftermath of the hydrogen fireball must be found since underestimation cannot be tolerated during a consequence analysis, part of the risk assessment. Moreover, the fireball radiation must be measured, and an advanced thermal radiation model suited for hydrogen fireball must be developed. Therefore, the identification of the new models must be aided by the experimental data. The combustion process should be included in the CFD analysis of $LH_2$ BLEVE since it is believed that the overpressure generated by the combustion can be aggregated to the one from the blast wave. Finally, it should be investigated if it is necessary to implement the combustion in the analytical models used for the pressure wave estimation.

The CFD tools could be further applied to the study of the behaviour of the tank lading when exposed to a fire. In this manner, the pressure build up inside the tank which affects the mechanical resistance of the tank walls material can be accurately evaluated. Moreover, the temperature gradients developed in the tank can be estimated by allowing an additional thermal analysis of the vessel material. Therefore, the CFD outcomes can be used as input of a structural analysis of the tank to estimate its time to failure. This approach is supposed to be more precise than the thermal node model employed in this PhD study.

Additional effort should be made to model the $LH_2$ release onto water. As previously described, if the mixing zone of the two fluids is simulated to analyse the early RPT formation by means of a CFD code, this may result in a very complex simulation. However, a simulation strategy should be adopted to overcome the complexity and potential simulation of the CFD code. For instance, the domain could be split in several regions to simulate the interaction of one fluids pair per time (e.g. first water-$LH_2$, second $LH_2$-air).

Finally, appropriate and effective safety barriers should be suggested as result of the experimental tests and the modelling activity. These recommendations can be implemented in safety guidelines and standards.

## 12. References


Abbasi, T., Abbasi, S.A., 2008. The boiling liquid expanding vapour explosion (BLEVE) is fifty ... and lives on! J. Loss Prev. Process Ind. 21, 485–487. https://doi.org/10.1016/j.jlp.2008.02.002

Abbasi, T., Abbasi, S.A., 2007a. The boiling liquid expanding vapour explosion (BLEVE): Mechanism, consequence assessment, management. J. Hazard. Mater. 141, 489–519. https://doi.org/10.1016/j.jhazmat.2006.09.056

Abbasi, T., Abbasi, S.A., 2007b. Accidental risk of superheated liquids and a framework for predicting the superheat limit. J. Loss Prev. Process Ind. 20, 165–181. https://doi.org/10.1016/j.jlp.2005.11.002

Abdel-Jawad, M., 2020. Validation of BLEVE events using the hybrid code exploCFD. Process Saf. Prog. e12208, 1–9. https://doi.org/10.1002/prs.12208

Amaseder, F., Krainz, G., 2006. Liquid Hydrogen Storage Systems Developed and Manufactured for the First Time for Customer Cars. SAE Tech. Pap. 2006-01-0432. https://doi.org/https://doi.org/10.4271/2006-01-0432

Aursand, E., Hammer, M., 2018. Predicting triggering and consequence of delayed LNG RPT. J. Loss Prev. Process Ind. 55, 124–133. https://doi.org/10.1016/j.jlp.2018.06.001

Aursand, E., Odsæter, L.H., Skarsvåg, H.L., Reigstad, G.A., Ustolin, F., Paltrinieri, N., 2020. Risk and Consequences of Rapid Phase Transition for Liquid Hydrogen, in: 30th European Safety and Reliability Conference and 15th Probabilistic Safety Assessment and Management Conference (ESREL2020 PSAM15). https://doi.org/10.3850/978-981-14-8593-0

Ausfelder, F., Bazzanella, A., 2016. Hydrogen in the Chemical Industry, in: Stolten, D., Emonts, B. (Eds.), Hydrogen Science and Engineering: Materials, Processes, Systems and Technology. Wiley-VCH Verlag, pp. 19–39. https://doi.org/10.1002/9783527674268.ch02

Bader, B.E., Donaldson, A.B., Hardee, H.C., 1971. Liquid-Propellant Rocket Abort Fire Model. J. Spacecr. Rockets 8, 1216–1219.

Bagster, D.F., Pitblado, R.M., 1989. Thermal hazards in the process industry. Chem. Eng. Prog. 85, 69–75.

Baker, W.E., Cox, P.A., Kulesz, J.J., Strehlow, R.A., Westine, P.S., 1983. Explosion

Hazards and Evaluation. Elsevier Science, New York.

Balke, C., Heller, W., Konersmann, R., Ludwig, J., 1999. Study of the failure limits of a railway tank car filled with liquefied petroleum gas subjected to an open poolfire test - Final report of BAM project number 3215.

Bang, K.H., Corradini, M.L., 1991. Vapor explosions in a stratified geometry. Nucl. Sci. Eng. 108, 88–108. https://doi.org/10.13182/NSE91-A23809

Barbone, R., Frost, D.L., Makris, A., Nerenberg, J., 1995. Explosive boiling of a depressurized volatile liquid, in: S., M., L., V.W. (Eds.), IUTAM Symposium on Waves in Liquid/Gas and Liquid/Vapour Two-Phase Systems. Fluid Mechanics and Its Applications, Vol 31. Springer, Dordrecht, pp. 315–324. https://doi.org/https://doi.org/10.1007/978-94-011-0057-1_26

Barron, R.F., Nellis, G.F., 2016. Cryogenic Heat Transfer, 2nd ed. CRC Press, Boca Raton. https://doi.org/https://doi.org/10.1201/b20225

Barták, J., 1990. A study of the rapid depressurization of hot water and the dynamics of vapour bubble generation in superheated water. Int. J. Multiph. Flow 16, 789–798. https://doi.org/10.1016/0301-9322(90)90004-3

Barthelemy, H., Weber, M., Barbier, F., 2017. Hydrogen storage: Recent improvements and industrial perspectives. Int. J. Hydrogen Energy 42, 7254–7262. https://doi.org/10.1016/J.IJHYDENE.2016.03.178

Baum, M.R., 1988. Disruptive failure of pressure vessels: preliminary design guide lines for fragment velocity and the extent of the hazard zone. J. Press. Vessel Technol. 110, 168–176. https://doi.org/https://doi.org/10.1115/1.3265582

Baum, M.R., 1984. The Velocity of Missiles Generated by the Disintegration of Gas-Pressurized Vessels and Pipes. J. Press. Vessel Technol. 106, 362–368. https://doi.org/10.1115/1.3264365

BBC, 2019. Steel plant explosion: Two burned at Tata in Port Talbot [WWW Document]. URL https://www.bbc.com/news/uk-wales-48062141 (accessed 4.21.21).

Betteridge, S., Phillips, L., 2015. Large scale pressurised LNG BLEVE experiments, in: Hazard Symposium Series No 160. IChemE.

Beyler, C., 2016. Fire Hazard Calculations for Large, Open Hydrocarbon Fires, in: Hurley, M. (Ed.), SFPE Handbook of Fire Protection Engineering. Springer Science +Business Media, LLC, New York, pp. 2591–2663. https://doi.org/10.1007/978-1-4939-2565-0

Birk, A.M., 2002. On the Transition From Non-Bleve to Bleve Failure for a 1.8 m3 Propane Tank, in: ASME 2002 Pressure Vessels and Piping Conference. pp. 143–150. https://doi.org/https://doi.org/10.1115/PVP2002-1497

Birk, A.M., 1996. Hazards from propane BLEVEs: An update and proposal for emergency responders. J. Loss Prev. Process Ind. 9, 173–181. https://doi.org/https://doi.org/10.1016/0950-4230(95)00046-1

Birk, A.M., Cunningham, M.H., 1994. The boiling expanding vapour explosion. J. Loss Prev. Process Ind. 7, 474–480.

Birk, A.M., Davison, C., Cunningham, M., 2007. Blast overpressures from medium scale BLEVE tests. J. Loss Prev. Process Ind. 20, 194–206. https://doi.org/10.1016/J.JLP.2007.03.001

Birk, A.M., Heymes, F., Eyssette, R., Lauret, P., Aprin, L., Slangen, P., 2018. Near-field BLEVE overpressure effects: The shock start model. Process Saf. Environ. Prot. 116, 727–736. https://doi.org/10.1016/J.PSEP.2018.04.003

Birk, A.M., VanderSteen, J.D.J., 2006. On the Transition From Non-BLEVE to BLEVE Failure for a 1.8 M3 Propane Tank. J. Press. Vessel Technol. 128, 648. https://doi.org/10.1115/1.2349579

Borg, A., Paulsen Husted, B., Njå, O., 2014. The concept of validation of numerical models for consequence analysis. Reliab. Eng. Syst. Saf. 125, 36–45. https://doi.org/10.1016/j.ress.2013.09.009

Brode, H.L., 1959. Blast Wave from a Spherical Charge. Phys. Fluids 2, 217–229. https://doi.org/10.1063/1.1705911

Brown, T., Cederwall, R., Chan, S., Ermak, D., Koopman, R., Lamson, K., McClure, J., Morris, L., 1990. Falcon Series Data Report 1987 LNG Vapor Barrier Verification Field Trials.

Buckley, J.W., Buckley, M.H., Chiang, H., 1976. Research methodology & business decisions. National Association of Accountants.

Casal, J., 2008. Evaluation of the Effects and Consequences of Major Accidents in Industrial Plants. Elsevier, Amsterdam.

Casal, J., Arnaldos, J., Montiel, H., Planas-Cuchi, E., Vilchez, J., 2001. Modelling and understanding BLEVEs, in: Handbook of Hazardous Materials Spills Technology. McGraw-Hill, New York.

Casal, J., Hemmatian, B., Planas, E., 2016. On BLEVE definition, the significance of superheat limit temperature (Tsl) and LNG BLEVE's. J. Loss Prev. Process Ind. 40, 81. https://doi.org/10.1016/j.jlp.2015.12.001

Casal, J., Salla, J.M., 2006. Using liquid superheating energy for a quick estimation of overpressure in BLEVEs and similar explosions. J. Hazard. Mater. 137, 1321–1327. https://doi.org/10.1016/J.JHAZMAT.2006.05.001

CCPS, 2010. Guidelines for Vapor Cloud Explosion, Pressure Vessel Burst, BLEVE, and

Flash Fire Hazards, 2nd ed. Wiley Subscription Services, Inc., A. Wiley Company, New York. https://doi.org/10.1002/9780470640449

CCPS, 1999. Guidelines for Consequence Analysis of Chemical Releases. American Institute of Chemical Engineers, New York.

Chen, S., Sun, J., Wan, W., 2008. Boiling liquid expanding vapor explosion: Experimental research in the evolution of the two-phase flow and over-pressure. J. Hazard. Mater. 156, 530–537. https://doi.org/10.1016/j.jhazmat.2007.12.074

Chen, S.N., Sun, J.H., Chu, G.Q., 2007. Small scale experiments on boiling liquid expanding vapor explosions: Vessel over-pressure. J. Loss Prev. Process Ind. 20, 45–51. https://doi.org/10.1016/j.jlp.2006.09.002

Chirivella, J., 1997. Analysis of the "Phantom" Fires on the Space Shuttle External Tank Base and the Nature of the Space Shuttle "Phantom" Fires: LH2 Leaks, in: 34th Combustion Systems Hazards Subcommittee and Airbreathing Propulsion Subcommittee Joint Meetings JANNAF. Palm Beach, USA.

Clancey, V.J., 1974. The Evaporation and Dispersion of Flammable Liquid Spillages, in: Institution of Chemical Engineers Symposium Series No. 39a. pp. 80–98.

Creswell, J.W., 2014. Research Design: Qualitative, Quantitative, and Mixed Methods Approaches. SAGE.

Crowl, D.A., 1992. Calculating the energy of explosion using thermodynamic availability. J. Loss Prev. Process Ind. 5, 109–118. https://doi.org/10.1016/0950-4230(92)80007-U

Crowl, D.A., 1991. Using thermodynamic availability to determinethe energy of explosion. Plant/Operations Prog. 10, 136–142.

Deaves, D.M., Gilham, S., Mitchell, B.H., Woodburn, P., Shepherd, A.M., 2001. Modelling of catastrophic flashing releases. J. Hazard. Mater. 88, 1–32. https://doi.org/10.1016/S0304-3894(01)00284-9

Delvosalle, C., Fievez, C., Pipart, A., Debray, B., 2006. ARAMIS project: A comprehensive methodology for the identification of reference accident scenarios in process industries. J. Hazard. Mater. 130, 200–219. https://doi.org/10.1016/j.jhazmat.2005.07.005

DNV-GL, 2020. Energy Transition Outlook 2020, A global and regional forecast to 2050.

DOE, 2009. Energy requirements for hydrogen gas compression and liquefaction as related to vehicle storage needs.

Eckhoff, R.K., 2016. Water vapour explosions – A brief review. J. Loss Prev. Process Ind. 40, 188–198. https://doi.org/10.1016/J.JLP.2015.11.017

Ermak, D.L., Chapman, R., Goldwire, H.C.J., Gouveia, F.J., Rodean, H.C., 1988. Heavy gas dispersion test summary report. Lawrence Livermore National Laboratory Report No. UCRL-21210. Livermore, CA.

European Commission, 2020. Europe's moment: Repair and prepare for the next generation [WWW Document]. URL https://ec.europa.eu/commission/presscorner/detail/en/ip_20_940 (accessed 5.3.21).

Eyssette, R., Heymes, F., Birk, A.M., 2021. Ground loading from BLEVE through small scale experiments: Experiments and results. Process Saf. Environ. Prot. 148, 1098–1109. https://doi.org/10.1016/j.psep.2021.02.031

Eyssette, R., Heymes, F., Crawford, J., Birk, A.M., 2018. Near Field Effects of Small Scale Water BLEVE, in: Brebbia, C.A., Garzia, F., Lombardi, M. (Eds.), WIT Transactions on The Built Environment, Vol 174 - Safety and Security Engineering VII. pp. 465–473. https://doi.org/10.2495/SAFE170421

Fay, J.A., Lewis, D.H., 1977. Unsteady burning of unconfined fuel vapor clouds. Symp. Combust. 16, 1397–1405. https://doi.org/10.1016/S0082-0784(77)80424-4

Felbauer, G.F., Heigl, J.H., McQueen, W., Whipp, R.H., May, W.G., 1972. Spills of LNG on water - vaporization and downwind drift of combustible mixtures - Report No. EE61E - 72. Florham Park, New Jersey.

Ferrari, R., 2015. Writing narrative style literature reviews. Med. Writ. 24, 230–235. https://doi.org/10.1179/2047480615z.000000000329

FuelCellsWork, 2020. Norse Group Announces Launch of MF Hydra, World's First LH2 Driven Ferry Boat [WWW Document]. URL https://fuelcellsworks.com/news/norse-group-announces-launch-of-mf-hydra-worlds-first-lh2-driven-ferry-boat/ (accessed 3.16.21).

Gayle, J.B., 1964. Investigation of S-IV all systems vehicle explosion. NASA TN D-563.

Gayle, J.B., Bransford, J.W., 1965. Size and Duration of Fireballs from Propellant Explosions - NASA TM X-53314.

Genova, B., Silvestrini, M., Leon Trujillo, F.J., 2008. Evaluation of the blast-wave overpressure and fragments initial velocity for a BLEVE event via empirical correlations derived by a simplified model of released energy. J. Loss Prev. Process Ind. 21, 110–117. https://doi.org/10.1016/J.JLP.2007.11.004

Genovese, M., Blekhman, D., Dray, M., Fragiacomo, P., 2020. Hydrogen losses in fueling station operation. J. Clean. Prod. 248, 119266. https://doi.org/https://doi.org/10.1016/j.jclepro.2019.119266

Giannissi, S.G., Venetsanos, A.G., 2018. Study of key parameters in modeling liquid hydrogen release and dispersion in open environment. Int. J. Hydrogen Energy 43, 455–467. https://doi.org/10.1016/j.ijhydene.2017.10.128

Giannissi, S.G., Venetsanos, A.G., Hecht, E.S., 2020. Numerical predictions of cryogenic hydrogen vertical jets. Int. J. Hydrogen Energy 1–13. https://doi.org/10.1016/j.ijhydene.2020.08.021

Giannissi, S.G., Venetsanos, A.G., Markatos, N., Bartzis, J.G., 2014. CFD modeling of hydrogen dispersion under cryogenic release conditions. Int. J. Hydrogen Energy 39, 15851–15863. https://doi.org/10.1016/J.IJHYDENE.2014.07.042

Giannissi, S.G., Venetsanos, A.G., Markatos, N., Bartzis, J.G., 2013. Numerical simulation of LNG dispersion under two-phase release conditions. J. Loss Prev. Process Ind. 26, 245–254. https://doi.org/10.1016/j.jlp.2012.11.010

Giesbrecht, H., Hemmer, G., Hess, K., Leuckel, W., Stoeckel, A., 1981a. Analysis of Explosion Hazards on Spontaneous Release of Inflammable Gases into the Atmosphere - Part 2: Comparison of Explosion Model Derived from Experiments with Damage Effects of Explosion Accidents. Ger. Chem. Eng. 4, 315–325.

Giesbrecht, H., Hess, K., Leuckel, W., Maurer, B., 1981b. Analysis of Explosion Hazards on Spontaneous Release of Inflammable Gases into the Atmosphere - Part 1: Propagation and Deflagration of Vapour Clouds on the Basis of Bursting Tests on Model Vessels. Ger. Chem. Eng. 4, 305–314.

Goldwire, H., Rodean, H., Cederwall, R., Kansa, E., 1983. Coyote series data report, LLNL/NWC 1981 LNG spill tests dispersion, vapor burn and rapid phase transition , Vols. 1 and 2, UCID - 19953. Livermore, CA.

Hansen, O.R., Kjellander, M.T., 2016. CFD Modelling of Blast Waves from BLEVEs. Chem. Eng. Trans. 48, 199–204. https://doi.org/10.3303/CET1648034

Hardee, H.C., Lee, D.O., 1973. Thermal hazard from propane fireballs. Transp. Plan. Technol. 2, 121–128.

Hardee, H.C., Lee, D.O., Benedick, W.B., 1978. Thermal Hazard from LNG Fireballs. Combust. Sci. Technol. 17, 189–197. https://doi.org/10.1080/00102207808946829

Hasegawa, K., Sato, K., 1977. Study on the fireball following steam explosion of n-pentane, in: Second International Symposium on Loss Prevention and Safety Promotion in the Process Industries. pp. 297–304.

Hemmatian, B., Planas, E., Casal, J., 2017. Comparative analysis of BLEVE mechanical energy and overpressure modelling. Process Saf. Environ. Prot. 106, 138–149. https://doi.org/10.1016/j.psep.2017.01.007

Heymes, F., Eyssette, R., Lauret, P., Hoorelbeke, P., 2020. An experimental study of water BLEVE. Process Saf. Environ. Prot. 141, 49–60. https://doi.org/10.1016/j.psep.2020.04.029

High, R.W., 1968. The Saturn Fireball. Ann. N. Y. Acad. Sci. 152, 441–451. https://doi.org/https://doi.org/10.1111/j.1749-6632.1968.tb11992.x

Hord, J., 1972. Explosion criteria for liquid hydrogen test facilities - NBS Report.

HydrogenTools, 2017. Liquid Hydrogen Tank Boiling Liquid Expanding Vapor Explosion (BLEVE) due to Water-Plugged Vent Stack [WWW Document]. URL https://h2tools.org/lessons/liquid-hydrogen-tank-boiling-liquid-expanding-vapor-explosion-bleve-due-water-plugged-vent (accessed 6.3.20).

IEA, 2019. The Future of Hydrogen - Seizing today's opportunities.

ISO, 2016. Cryogenic vessels — Pressure-relief accessories for cryogenic service — Part 3: Sizing and capacity determination — ISO21013-3:2016.

Johnson, D.M., Pritchard, J.M., Wickens, M.J., 1991. Large Scale Experimental Study of Boiling Liquid Expanding Vapour Explosions (BLEVEs).

Jovanović, A.S., Baloš, D., 2013. INTeg-Risk project: Concept and first results. J. Risk Res. 16, 275–291. https://doi.org/10.1080/13669877.2012.729516

Jovanović, A.S., Löscher, M., 2014. iNTeg-Risk project: How much nearer are we to improved "Early Recognition, Monitorin and Integrated Management of Emerging, New Technology related Risks"?

Kamperveen, J.P., Spruijt, M.P.N., Reinders, J.E.A., 2016. Heat load resistance of cryogenic storage tanks – Results of LNG Safety Program.

Kaplan, S., Garrick, B.J., 1981. On the quantitative definition of risk. Risk Anal. 1, 11–27. https://doi.org/http://dx.doi.org/10.1111/j.1539-6924.1981.tb01350.x

Kinney, G., Graham, K., 1985. Explosive shocks in air. Springer, New York.

Kite, F.D., Webb, D.M., Bader, B.E., 1965. Launch Hazards Assessment Program, Report on Atlas/Centaur Abort - SC-RR-65-333.

Kneebone, A., Prew, L.R., 1974. Shipboard jettison tests on LNG on to the sea, in: 4th International Conference on LNG, Gastech ' 74. Algiers, pp. 13–14.

Koopman, R., Cederwall, R., Ermak, D., Goldwire, H., Hogan, W., McClure, J., McRae, T., Morgan, D., Rodean, H., Shinn, J., 1982. ANALYSIS OF BURRO SERIES 40-m3 LNG SPILL EXPERIMENTS. J. Hazard. Mater. 6, 43–83. https://doi.org/10.1016/0304-3894(82)80034-4

Koopman, R.P., Bowman, B.R., Ermak, D.L., 1980. Data and calculations on 5 m3 LNG spill tests. Liquefied Gaseous Fuels Safety and Environmental Assessment Program, Second Status Report, DOE/EV-0085, U.S. Department of Energy.

Koutsourakis, N., Venetsanos, A.G., Bartzis, J.G., 2012. LES modelling of hydrogen release and accumulation within a non-ventilated ambient pressure garage using the ADREA-HF CFD code. Int. J. Hydrogen Energy 37, 17426–17435.

Kovač, A., Paranos, M., Marciuš, D., 2021. Hydrogen in energy transition: A review. Int. J. Hydrogen Energy 46, 10016–10035. https://doi.org/10.1016/j.ijhydene.2020.11.256

Laboureur, D., Heymes, F., Aprin, L., Buchlin, J.M., Rambaud, P., 2012. BLEVE Overpressure: Small Scale Experiments and Multi-Scale Comparison with Literature Survey of Blast Wave Modeling, in: Global Congress on Process Safety 2012.

Laboureur, D., Heymes, F., Lapebie, E., Buchlin, J., Rambaud, P., 2014. BLEVE Overpressure: Multiscale Comparison of Blast Wave Modeling. Process Saf. Prog. 33, 274–284. https://doi.org/https://doi.org/10.1002/prs.11626

Li, G., Ji, T., 2016. Severe accidental water vapour explosions in a foundry in China in 2012. J. Loss Prev. Process Ind. 41, 55–59. https://doi.org/10.1016/j.jlp.2016.03.001

Li, J., Hao, H., 2021. Numerical simulation of medium to large scale BLEVE and the prediction of BLEVE's blast wave in obstructed environment. Process Saf. Environ. Prot. 145, 94–109. https://doi.org/10.1016/j.psep.2020.07.038

Li, J., Hao, H., 2020. Numerical study of medium to large scale BLEVE for blast wave prediction. J. Loss Prev. Process Ind. 65, 104107. https://doi.org/10.1016/j.jlp.2020.104107

Lihou, D.A., Maund, J.K., 1982. Thermal radiation hazard from fireballs, in: IChemE Symposium Series No. 71. pp. 191–225.

Lowesmith, B.J., Hankinson, G., 2013. Qualitative Risk Assessment of Hydrogen Liquefaction, Storage and Transportation - Deliverable 3.11, IDEALHY project.

McAllister, S., Chen, J.-Y., Fernandez-Pello, A.C., 2011. Fundamentals of Combustion Processes. Springer Science +Business Media, LLC, New York. https://doi.org/10.1007/978-1-4419-7943-8

McDevitt, C.A., Chan, C.K., Steward, F.R., Tennankore, K.N., 1990. Initiation step of boiling liquid expanding vapour explosions. J. Hazard. Mater. 25, 169–180. https://doi.org/10.1016/0304-3894(90)85076-F

Mires, R.W., 1985. Analysis of Liquid Hydrogen Explosion. Phys. Teach. 23, 533–535. https://doi.org/https://doi.org/10.1119/1.2341906

Moodie, K., Cowley, L.T., Denny, R.B., Small, L.M., Williams, I., 1988. Fire engulfment tests on a 5 tonne LPG tank. J. Hazard. Mater. 20, 55–71. https://doi.org/10.1016/0304-3894(88)87006-7

NASA, 2005. Safety standard for hydrogen and hydrogen systems, Guidelines for Hydrogen System Design, Materials Selection, Operations, Storage, and Transportation - NSS 1740.16.

Nasrifar, K., 2010. Comparative study of eleven equations of state in predicting the

thermodynamic properties of hydrogen. Int. J. Hydrogen Energy 35, 3802–3811. https://doi.org/10.1016/j.ijhydene.2010.01.032

Nazarpour, F., Dembele, S., Wen, J.X., 2017. Modelling Liquid Hydrogen Release and Spread on Water, in: 7th International Conference on Hydrogen Safety. Hamburg, Germany.

NCE Maritime Cleantech, 2019. Norwegian future value chains for liquid hydrogen.

Nel Hydrogen, 2019. Status and Q&A regarding the Kjørbo incident [WWW Document]. URL https://nelhydrogen.com/status-and-qa-regarding-the-kjorbo-incident/ (accessed 9.5.19).

NIST, 2019. NIST Chemistry WebBook [WWW Document]. URL webbook.nist.gov/ (accessed 3.19.19).

OECD, 2015. Frascati Manual 2015: Guidelines for Collecting and Reporting Data on Research and Experimental Development, The Measurement of Scientific, Technological and Innovation Activities. OECD Publishing, Paris. https://doi.org/https://doi.org/10.1787/9789264239012-en

Ono, R., Nifuku, M., Fujiwara, S., Horiguchi, S., Oda, T., 2007. Minimum ignition energy of hydrogen–air mixture: Effects of humidity and spark duration. J. Electrostat. 65, 87–93. https://doi.org/10.1016/J.ELSTAT.2006.07.004

Paltrinieri, N., 2010. Hazard identification review and assessment of unknown risks, Deliverable D1.4.4.3, EC project iNTeg-Risk, 7th FP, Grant: CP-IP 213345-2.

Paltrinieri, N., Dechy, N., Salzano, E., Wardman, M., Cozzani, V., 2013. Towards a new approach for the identification of atypical accident scenarios. J. Risk Res. 16, 337–354. https://doi.org/https://doi.org/10.1080/13669877.2012.729518

Paltrinieri, N., Dechy, N., Salzano, E., Wardman, M., Cozzani, V., 2012a. Lessons Learned from Toulouse and Buncefield Disasters: From Risk Analysis Failures to the Identification of Atypical Scenarios Through a Better Knowledge Management. Risk Anal. 32, 1404–1419. https://doi.org/10.1111/j.1539-6924.2011.01749.x

Paltrinieri, N., Landucci, G., Molag, M., Bonvicini, S., Spadoni, G., Cozzani, V., 2009. Risk reduction in road and rail LPG transportation by passive fire protection. J. Hazard. Mater. 167, 332–344. https://doi.org/10.1016/j.jhazmat.2008.12.122

Paltrinieri, N., Øien, K., Cozzani, V., 2012b. Assessment and comparison of two early warning indicator methods in the perspective of prevention of atypical accident scenarios. Reliab. Eng. Syst. Saf. 108, 21–31. https://doi.org/https://doi.org/10.1016/j.ress.2012.06.017

Paltrinieri, N., Tugnoli, A., Cozzani, V., 2015. Hazard identification for innovative LNG regasification technologies. Reliab. Eng. Syst. Saf. 137, 18–28. https://doi.org/10.1016/j.ress.2014.12.006

Paltrinieri, N., Villa, V., Khan, F., Cozzani, V., 2016. Towards dynamic risk analysis: A review of the risk assessment approach and its limitations in the chemical process industry. Saf. Sci. 89, 77–93. https://doi.org/10.1016/j.ssci.2016.06.002

Pehr, K., 1996a. Experimental examinations on the worst-case behaviour of LH2/LNG tanks for passenger cars, in: Proceedings of the 11th World Hydrogen Energy Conference, Stuttgart 23–28 June 1996. Stuttgart, pp. 2169–87.

Pehr, K., 1996b. Aspects of safety and acceptance of LH2 tank systems in passenger cars. Int. J. Hydrogen Energy 21, 387–395. https://doi.org/10.1016/0360-3199(95)00092-5

Pettitt, G., 1990. Characterisation of two-phase releases, Ph.D thesis. South Bank Polytechnic.

Pinhasi, G.A., Ullmann, A., Dayan, A., 2005. Modelling of Flashing Two-Phase Flow. Rev. Chem. Eng. 21, 133–264. https://doi.org/https://doi.org/10.1515/REVCE.2005.21.3-4.133

Planas-Cuchi, E., Salla, J.M., Casal, J., 2004. Calculating overpressure from BLEVE explosions. J. Loss Prev. Process Ind. 17, 431–436. https://doi.org/10.1016/J.JLP.2004.08.002

Planas, E., Casal, J., 2016. BLEVE-Fireball, in: Lackner, M., Winter, F., Agarwal, A.K. (Eds.), Handbook of Combustion. Wiley-VCH Verlag GmbH & Co. KGaA, Weinheim. https://doi.org/10.1002/9783527628148.hoc093

Pritchard, D.K., Rattigan, W.M., 2010. Hazards of liquid hydrogen RR769 Position paper.

Prugh, R.W., 1994. Quantitative evaluation of fireball hazards. Process Saf. Prog. 13, 83–91. https://doi.org/10.1002/prs.680130211

Prugh, R.W., 1991. Quantitative Evaluation of "BLEVE" hazards. J. Fire Prot. Eng. 3, 9–24.

Reid, R., 1976. Superheated Liquids. Am. Sci. 64, 146–156.

Reid, R.C., 1983. Rapid Phase Transitions from Liquid to Vapor. Adv. Chem. Eng. 12, 105–208. https://doi.org/10.1016/S0065-2377(08)60252-5

Rew, P.J., 1997. LD50 Equivalent for the Effect of Thermal Radiation on Humans - CRR 129/1997.

Roberts, T., Gosse, A., Hawksworth, S., 2000. Thermal Radiation from Fireballs on Failure of Liquefied Petroleum Gas Storage Vessels. Process Saf. Environ. Prot. 78, 184–192. https://doi.org/10.1205/095758200530628

Rüdiger, H., 1992. Design characteristics and performance of a liquid hydrogen tank

system for motor cars. Cryogenics (Guildf). 32, 327–329. https://doi.org/10.1016/0011-2275(92)90373-I

Sachs, R.G., 1944. The dependence of blast on ambient pressure and temperature, BRL Report no. 466, Aberdeen Proving Ground. Maryland.

Salla, J.M., Demichela, M., Casal, J., 2006. BLEVE: A new approach to the superheat limit temperature. J. Loss Prev. Process Ind. 19, 690–700. https://doi.org/10.1016/j.jlp.2006.04.004

Scarponi, G.E., Landucci, G., Birk, A.M., Cozzani, V., 2018. LPG vessels exposed to fire: Scale effects on pressure build-up. J. Loss Prev. Process Ind. 56, 342–358. https://doi.org/https://doi.org/10.1016/j.jlp.2018.09.015

Scarponi, G.E., Landucci, G., Ovidi, F., Cozzani, V., 2016. Lumped Model for the Assessment of the Thermal and Mechanical Response of LNG Tanks Exposed to Fire. Chem. Eng. Trans. 53, 307–312. https://doi.org/10.3303/CET1653052

Schefer, R.W., Kulatilaka, W.D., Patterson, B.D., Settersten, T.B., 2009. Visible emission of hydrogen flames. Combust. Flame 156, 1234–1241. https://doi.org/10.1016/J.COMBUSTFLAME.2009.01.011

Smith, J.M., Van Ness, H.C., 1996. Introduction to Chemical Engineering Thermodynamics, 5th ed. McGraw-Hill, Inc, NewYork.

Stawczyk, J., 2003. Experimental evaluation of LPG tank explosion hazards. J. Hazard. Mater. 96, 189–200. https://doi.org/10.1016/S0304-3894(02)00198-X

Taccani, R., Ustolin, F., Zuliani, N., Pinamonti, P., Pietra, A., 2018. Fuel cells and shipping emissions mitigation, in: NAV International Conference on Ship and Shipping Research. https://doi.org/10.3233/978-1-61499-870-9-885

The Cochrane Collaboration, 2005. Glossary of Terms in The Cochrane Collaboration - Version 4.2.5.

Tolias, I.C., Venetsanos, A.G., Kuznetsov, M., Koutsoukos, S., 2020. Evaluation of an improved CFD model against nine vented deflagration experiments. Int. J. Hydrogen Energy 46, 12407–12419. https://doi.org/10.1016/j.ijhydene.2020.09.231

Tolias, I.C., Venetsanos, A.G., Markatos, N., Kiranoudis, C.T., 2017. CFD evaluation against a large scale unconfined hydrogen deflagration. Int. J. Hydrogen Energy 42, 7731–7739. https://doi.org/10.1016/j.ijhydene.2016.07.052

Tolias, I.C., Venetsanos, A.G., Markatos, N., Kiranoudis, C.T., 2014. CFD modeling of hydrogen deflagration in a tunnel. Int. J. Hydrogen Energy 39, 20538–20546. https://doi.org/10.1016/j.ijhydene.2014.03.232

Tolias, I.C., Venetsanos, A.G., Vagiokas, N., 2016. CFD Modeling of Vapor Cloud Explosion, Cold BLEVE and Hot BLEVE in a Large Scale Tunnel, in: 12th

International Conference on Heat Transfer, Fluid Mechanics and Thermodynamics.

Tschirschwitz, R., Krentel, D., Kluge, M., Askar, E., Habib, K., Kohlhoff, H., Krüger, S., Neumann, P.P., Storm, S.-U., Rudolph, M., Schoppa, A., Szczepaniak, M., 2018. Experimental investigation of consequences of LPG vehicle tank failure under fire conditions. J. Loss Prev. Process Ind. 56, 278–288. https://doi.org/10.1016/J.JLP.2018.09.006

Ustolin, F., Paltrinieri, N., Landucci, G., 2020. An innovative and comprehensive approach for the consequence analysis of liquid hydrogen vessel explosions. J. Loss Prev. Process Ind. 68, 104323. https://doi.org/https://doi.org/10.1016/j.jlp.2020.104323

Ustolin, F., Tolias, I., Giannissi, S., Venetsanos, A., Paltrinieri, N., 2021. A CFD Analysis of Liquid Hydrogen Vessel Explosions Using the ADREA-HF Code (Under review - Submitted to the International Journal of Hydrogen Energy).

van Biert, L., Godjevac, M., Visser, K., Aravind, P.V., 2016. A review of fuel cell systems for maritime applications. J. Power Sources 327, 345–364. https://doi.org/10.1016/J.JPOWSOUR.2016.07.007

van den Bosch, C.J.H., Weterings, R.A.P.M., 2005. Methods for the Calculation of Physical Effects - Due to Releases of Hazardous Materials (liquids and gases), "Yellow Book." The Committee for the Prevention of Disasters by Hazardous Materials, Director-General for Social Affairs and Employment, The Hague.

van der Voort, M.M., van den Berg, A.C., Roekaerts, D.J.E.M., Xie, M., de Bruijn, P.C.J., 2012. Blast from explosive evaporation of carbon dioxide: experiment, modeling and physics. Shock Waves 22, 129–140. https://doi.org/10.1007/s00193-012-0356-0

van Eck, N.J., Waltman, L., 2007. VOS: A New Method for Visualizing Similarities Between Objects, in: R., D., H.J., L. (Eds.), Advances in Data Analysis. Studies in Classification, Data Analysis, and Knowledge Organization. Springer, Berlin, Heidelberg. https://doi.org/https://doi.org/10.1007/978-3-540-70981-7_34

Venetsanos, A.G., Papanikolaou, E., Bartzis, J.G., 2010. The ADREA-HF CFD code for consequence assessment of hydrogen applications. Int. J. Hydrogen Energy 35, 3908–3918. https://doi.org/10.1016/j.ijhydene.2010.01.002

Verfondern, K., Dienhart, B., 1997. Experimental and theoretical investigation of liquid hydrogen pool spreading and vaporization. Int. J. Hydrogen Energy 22, 649–660. https://doi.org/10.1016/S0360-3199(96)00204-2

Walls, W.L., 1978. What is a BLEVE? Fire J. 31, 46–47.

Wang, L., Li, Y., Zhang, F., Xie, F., Ma, Y., 2016. Correlations for calculating heat transfer of hydrogen pool boiling. Int. J. Hydrogen Energy 41, 17118–17131. https://doi.org/10.1016/j.ijhydene.2016.06.254

Wohletz, K., Zimanowski, B., Büttner, R., 2012. Magma-water interactions, in: Fagents, S.A., Gregg, T.K.P., Lopes, R.M.C. (Eds.), Modeling Volcanic Processes: The Physics and Mathematics of Volcanism. Cambridge University Press, pp. 230–257.

Woodward, J., Pitblado, R., 2010. LNG Risk Based Safety. John Wiley & Sons, New Jersey.

Woodward, J.L., Pitbaldo, R., 2010. LNG Risk Based Safety: Modeling and Consequence Analysis. John Wiley & Sons, Inc., Hoboken, New Jersey.

Yakush, S.E., 2016. Model for blast waves of Boiling Liquid Expanding Vapor Explosions. Int. J. Heat Mass Transf. 103, 173–185. https://doi.org/10.1016/j.ijheatmasstransfer.2016.07.048

Yu, C.M., Venart, J.E.S., 1996. The boiling liquid collapsed bubble explosion (BLCBE): A preliminary model, in: Journal of Hazardous Materials. Elsevier B.V., pp. 197–213. https://doi.org/10.1016/0304-3894(95)00071-2

Zalosh, R., Weyandt, N., 2005. Hydrogen Fuel Tank Fire Exposure Burst Test - SAE Technical Paper 2005-01-1886, in: SAE 2005 World Congress & Exhibition. https://doi.org/https://doi.org/10.4271/2005-01-1886

Zhao, Y., Liu, Z., Shi, X., Qian, X., Zhou, Y., Zhang, D., Li, Q., 2015. Numerical Simulation on BLEVE Mechanism of Supercritical Carbon Dioxide. Energy Procedia 75, 880–885. https://doi.org/10.1016/J.EGYPRO.2015.07.204

This page is intentionally left blank

# Part II

## Articles

This page is intentionally left blank

Ustolin F, Paltrinieri N, Berto F. Loss of integrity of hydrogen technologies: A critical review. Int J Hydrogen Energy 2020;45:23809–40. https://doi.org/https://doi.org/10.1016/j.ijhydene.2020.06.021.

This page is intentionally left blank

INTERNATIONAL JOURNAL OF HYDROGEN ENERGY 45 (2020) 23809–23840

Available online at www.sciencedirect.com

ScienceDirect

journal homepage: www.elsevier.com/locate/he

Review Article

# Loss of integrity of hydrogen technologies: A critical review

*Federico Ustolin*[*], *Nicola Paltrinieri*, *Filippo Berto*

*Department of Mechanical and Industrial Engineering, Norwegian University of Science and Technology NTNU, S.P. Andersens Veg 3, Trondheim, 7031, Norway*

## HIGHLIGHTS

- A systematic review on loss of integrity of hydrogen technologies was conducted.
- Loss of integrity phenomena are responsible for several hydrogen accident scenarios.
- Material selection may avoid the loss of integrity phenomena formation.
- Material science and hydrogen safety are often two separated research fields.
- Recent hydrogen accidents demonstrate the need for safety enhancement.

## ARTICLE INFO

*Article history:*
Received 16 January 2020
Received in revised form
17 May 2020
Accepted 3 June 2020
Available online 28 July 2020

*Keywords:*
Hydrogen
Loss of integrity
Safety

## ABSTRACT

Hydrogen is one of the main candidates in replacing fossil fuels in the forthcoming years. However, hydrogen technologies must deal with safety aspects due to the specific substance properties. This study aims to provide an overview on the loss of integrity (LOI) of hydrogen equipment, which may lead to serious consequences, such as fires and explosions. Substantial information regarding the hydrogen lifecycle, its properties, and safety related aspects has gathered. Furthermore, focus has placed on the phenomena responsible for the LOI (e.g. hydrogen embrittlement) and material selection for hydrogen services. Moreover, a systematic review on the hydrogen LOI topic has conducted to identify and connect the most relevant and active research group within the topic. In conclusion, a significant dearth of knowledge in material behaviour of hydrogen technologies has highlighted. It is thought that is possible to bridge this gap by strengthening the collaborations between scientists from different research fields.

*Abbreviations:* AIP, Air-Independent Propulsion; APU, Auxiliary Power Unit; bcc, body-centred cubic; BLEVE, Boiling Liquid Expanding Vapor Explosion; BOG, Boil-Off Gas; $CcH_2$, Cryo-Compressed Hydrogen; CCHP, Combined Cooling Heat and Power; CCS, Carbon Capture and Storage; CHHP, Combined Heat Hydrogen and Power; CHP, Combined Heat and Power; $CGH_2$, Compressed Gaseous Hydrogen; CTE, Coefficient of Thermal Expansion; DOT, Department of Transportation; DBTT, Ductile-Brittle Transition Temperature; DyPASI, Dynamic Procedure for Atypical Scenarios Identification; FC, Fuel cell; fcc, face-centred cubic; $GH_2$, Gaseous Hydrogen; HAZID, Hazard Identification; Hcp, hexagon close-packed; HD, Hydrogen Damage; HE, Hydrogen Embrittlement; HEE, Hydrogen Environment Embrittlement; HSC, Hydrogen Stress Cracking; IRAS, Integrated Refrigeration and Storage; $LH_2$, Liquid Hydrogen; LHV, Lower Heating Value; LIN, Liquid Nitrogen; LNG, Liquefied Natural Gas; LOC, Loss of Containment; LOHC, Liquid Organic Hydrogen Carrier; LOX, Liquid Oxygen; LPI, Loss of Physical Integrity; MLI, Multilayer insulation; MOF, Metal-Organic Framework; MWCNT, Multi-Walled Carbon Nanotubes; NEC, N-ethylcarbazole; NDT, Nil-Ductility Temperature; NDTT, Nil Ductility Transition Temperature; $NO_x$, Nitrogen Oxides; NREL, National Renewable Energy Laboratory; NTP, Normal Temperature and Pressure; OLEV, Office for Low Emission Vehicles; PEC, Photo-electrochemical; PCTFE, Poly-chloro-tri-fluoro-ethylene; PTFE, Poly-tetra-fluoro-ethylene; RPT, Rapid Phase Transition; $SLH_2$, Slush Hydrogen; SR, Systematic review; SSSH, Self Sufficient Solar House; tpd, tons per day; UAV, Unmanned Aerial Vehicle; VCE, Vapor Cloud Explosion; ZED, Zero Emission Digger.

* *Corresponding author.*
E-mail address: federico.ustolin@ntnu.no (F. Ustolin).

https://doi.org/10.1016/j.ijhydene.2020.06.021

Hydrogen damage
Hydrogen embrittlement



## Contents



## Introduction

Hydrogen can replace fossil fuels in order to reduce the pollutant emissions worldwide in the future [1]. In fact, only water, heat and traces of nitrogen oxides ($NO_X$) are produced from its combustion with air if a catalyst is used [2] or the flame temperature and oxygen concentration are controlled [3]. Furthermore, it is considered a renewable fuel if produced from water through electrolysis [4]. Although hydrogen is already widely used in the industry for several processes such as ammonia production for fertilizers [5], it is associated with crucial safety criticalities due to the specific substance properties [6]. For this reason, this study provides a critical review on the phenomenon of loss of integrity (LOI), which may lead to release and related serious consequences, such as fires and explosions.

Hydrogen has been employed in an increasing number of new technologies in the last two decades, and some of the most recent are listed below:

- First combined heat, hydrogen and power (CHHP) systems plant installed in California in 2016 [7].
- First hydrogen-fuelled stove for domestic application developed by Empa company in 2018 [2].
- Achievement of the longest duration flight of a multi-rotor unmanned aerial vehicle (UAV) by the hydrogen-fuelled drone developed by the EnergyOr company in 2015 [8].
- First hydrogen-fuelled train developed by Alstom in Germany in 2018 [9].

- First fuel cell and battery ferry should be operative in 2020 in Norway as result of the HYBRIDship project [10].

Hydrogen safety aspects may become more important in such new technologies as they may lead to emerging risks [11–13]. This is confirmed by the focus of some recent research projects, such as the project on the integrated design for demonstration of efficient liquefaction of hydrogen (IDEALHY) [14] also addressing the safety of hydrogen liquefaction, storage and transportation technologies. Currently, the Safe fuel Handling and use for efficient implementation ($SH_2IFT$) project [15] is studying safety implications of both $CGH_2$ and $LH_2$ technologies. Furthermore, a project named Prenormative research for safe use of liquid hydrogen (PRESLHY) [16] aims to lay the foundations for relevant safety regulations. This study aims to promote the prevention of hydrogen releases, and thus accidents, through a detailed review of LOI mechanisms and safety implications. The novelty of this work is to identify the overlap between material science and hydrogen safety which are usually two separated research areas. In particular, the common research aspects are pinpointed together with the most relevant experts in this field through a literature review hybrid approach (narrative and systematic) as described in the methodology.

The structure of this paper is presented in Fig. 1, where the methodology approach embraced for the present review (described in the methodology section) is also indicated. The shape of this schematic describes how the study narrows down from a broad topic as the hydrogen life cycle (described in Life cycle section) to hydrogen chemical and physical properties, LOI phenomena and relevant material selection. A systematic overview of scientific contributions on LOI of hydrogen equipment subsequently expands on the most relevant research groups and their collaborations. Finally, discussion and conclusion are provided.

## Methodology

Both the narrative (NR) and the systematic review (SR) approaches [17] are adopted for this study. Fig. 1 depicts how NR and SR are implemented in the structure of this work.

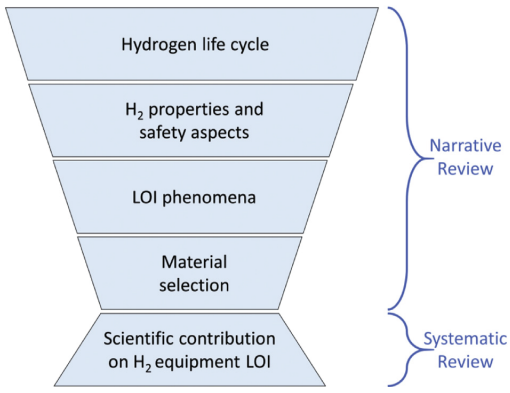


**Fig. 1 – Structure of the study. LOI: Loss of Integrity.**

An NR is "aimed at identifying and summarizing what has been previously published, avoiding duplications, and seeking new study areas not yet addressed" [17]. The general framework proposed by Ferrari in Ref. [17] was replicated for the NR. In particular, each section was composed by the following concepts: the hydrogen life cycle, its properties and safety aspects, the loss of integrity (LOI) phenomena and the material selection for hydrogen equipment. The information was gleaned from Scopus, Google Scholar and ScienceDirect databases by including reports, conference and journal papers as types of documents, while English was the only considered language. The discussions of each concept were collected in the namesake section at the end of this paper. Therefore, the NR results regarding LOI phenomena and material selection were used to sharpen the input (keywords) of the SR.

The systematic review (SR) is "a clearly formulated question that uses systematic and explicit methods to identify, select, and critically appraise relevant research, and to collect and analyse data from the studies that are included in the review" [18]. Several examples of SRs within the safety research area are present in literature, such as Li and Hale [19] and Merigó et al. [20]. In this case, the approach was selected to expand on the core topic of this study through a quantitative analysis. The novelty of this study consists in applying for the first time this methodology to the safety, loss of integrity phenomena and material selection of hydrogen technologies. This is conducted by highlighting the overlap and the discrepancies between these different topics and quantifying the experts who focus on these subjects and their publications.

The SR was completed on August 2, 2019. The data was retrieved from the Web of Science Core Collection database. On this platform, the key words selected for each query can be searched in several analysis fields such as topic (title, abstract, keywords), author, editor, publication name, DOI, publication year, organization-enhanced, conference, language, document type, ISSN, funding agency and grant number. In this review, all the analysis fields were selected, choosing the "ALL" option. In the queries, the quotations are used to search for an exact phrase, while the asterisk is used to find similar words (e.g. loss* = loss + losses). Hydrogen and safety are two key words that were always present in the queries of this study. When safety is not explicitly written, other words related to safety are already present in the query. Furthermore, the second and third queries were composed by loss of containment and hydrogen release that are consequences of the loss of integrity. Finally, the last three queries contained hydrogen embrittlement, low temperature embrittlement and thermal stress because these are three phenomena that can lead to a loss of integrity. In the attempt to make this SR repeatable and reproducible, all the chosen queries were collected in Table 1 (see Table 2).

Among the adopted filters, the sole considered language was English, whereas journal articles were the only type of document considered. Conference papers are not always or not accurately peer reviewed and for this reason, they were excluded from research. Several research areas related to health and agriculture were ignored. For the sake of completeness, the Web of Science categories (research subjects) embraced in this review were catalogued in Table 1 together with the other filters.

**Table 1 – Queries selected for the SR.**

| Query |
|---|
| "loss* of integrity" hydrogen |
| "loss* of containment" hydrogen |
| "hydrogen release*" safety |
| "release* of hydrogen" safety |
| "hydrogen embrittlement*" safety |
| "low* temperature* embrittlement" hydrogen |
| "thermal* stress*" hydrogen safety |

In addition, several source titles were eliminated as their articles are not related to this research topic. No limitations on the time span were applied. In conclusion, the co-authorship network maps of authors and countries, together with a co-occurrence map of key words were built with the aid of the visualization of similarities (VOS) viewer software [5], using the bibliometric data from the SR. Even though the SR is a powerful technique, the probability to include false negative articles in the research always exists. An incorrect application of queries and filters may be the cause of misleading results.

Finally, the NR and SR output related to safety, LOI phenomena and material selection was compared and deeply analysed. In particular, the statistical results from the SR regarding co-authorship, collaboration and research areas were necessary to confirm the trend highlighted by the NR.

## Hydrogen life cycle

Currently, hydrogen is mostly used in the chemical industry (63%) and refineries (31%) for several processes [5]. In most cases, hydrogen production and utilization take place within the same industrial facility. This choice is usually driven by a balanced combination of safety, logistic and economic aspects. For this reason, it is difficult to estimate the exact global production amount of hydrogen.

Fig. 2 depicts the hydrogen life cycle. This substance can be produced by means of different processes. After its production, hydrogen requires to be safely stored and transported to be employed in one of its several applications. The by-products of its utilization in a fuel cell (FC), which is a device used to generate electricity, are barely water and heat, while its combustion must be controlled to avoid nitrogen oxides ($NO_x$) formation [21].

The schematic illustrated in Fig. 2, represented the working principle of a self-sufficient system in which hydrogen is produced from water through an electrolyser, stored and supplied by means of a pipeline to a fuel cell in order to generate electricity when needed. In the past, many self-sufficient systems were developed, produced, tested and commercialized. For instance, the first self-sufficient solar house (SSSH) was built in Freiburg, Germany by the Fraunhofer Institute for Solar Energy Systems in the 1994 [22]. Nowadays, similar systems are commercially available such as the H2One system by Toshiba that is a hydrogen supply system $CO_2$-free from production to application [23].

### *Production*

Different techniques can be adopted to produce hydrogen. Heat, electric energy or sunlight are usually required as sources of energy by the majority of these methods. The most common and one of the cheapest techniques is the steam reforming in which hydrogen is produced from natural gas. Virtually 95% of the hydrogen in the world is produced from

**Table 2 – Filter selected for the SR.**

| Filter type | |
|---|---|
| Document type | Article |
| Language | English |
| Web of Science categories | Energy fuels, Chemistry Physical, Electrochemistry, Nuclear Science Technology, Engineering Chemical, Engineering Mechanical, Material Science Multidisciplinary, Metallurgy Metallurgical Engineering, Thermodynamics, Material Science Characterization Testing, Engineering Environmental, Environmental Sciences, Engineering Multidisciplinary, Mechanics, Green Sustainable Science Technology, Multidisciplinary Sciences, Physics Applied, Engineering Civil, Environmental Studies, Physics Nuclear, Transportation Science Technology |
| Source title excluded | Structure and Infrastructure Engineering, Strength of Materials, Steel Research, Physical Review Applied, Nuclear Technology, Metals, Mechanics Research Communications, Mechanics of Materials, Materials Science Medziagotyra, Materials Research Bulletin, Materials Performance, Materials Design, Kerntechnik, Journal of Mechanical Science and Technology, Journal of Engineering for Gas Turbines and Power Transactions of the ASME, International Journal of Pressure Vessels and Piping, International Journal of Plasticity, International Journal of Heat and Mass Transfer, Industrial Engineering Chemistry Research, Electrochemistry Communications, Corrosion, Chinese Science Bulletin, Chemical Engineering Technology, Catalysis Science Technology, Applied Physics Letters, Applied Materials Today, Scientific Reports, Journal of Failure Analysis and Prevention, Journal of Alloys and Compounds, International Journal of Mechanical and Materials Engineering, Computational Materials Science, Acta Metallurgical Sinica English Letters, Acta Materialia, Metallurgical and Materials Transactions a Physical Metallurgy and Materials Science, International Journal of Fatigue, Journal of Materials Science Technology, Journal of Power Sources, Journal of Nuclear Science and Technology, Corrosion Science |

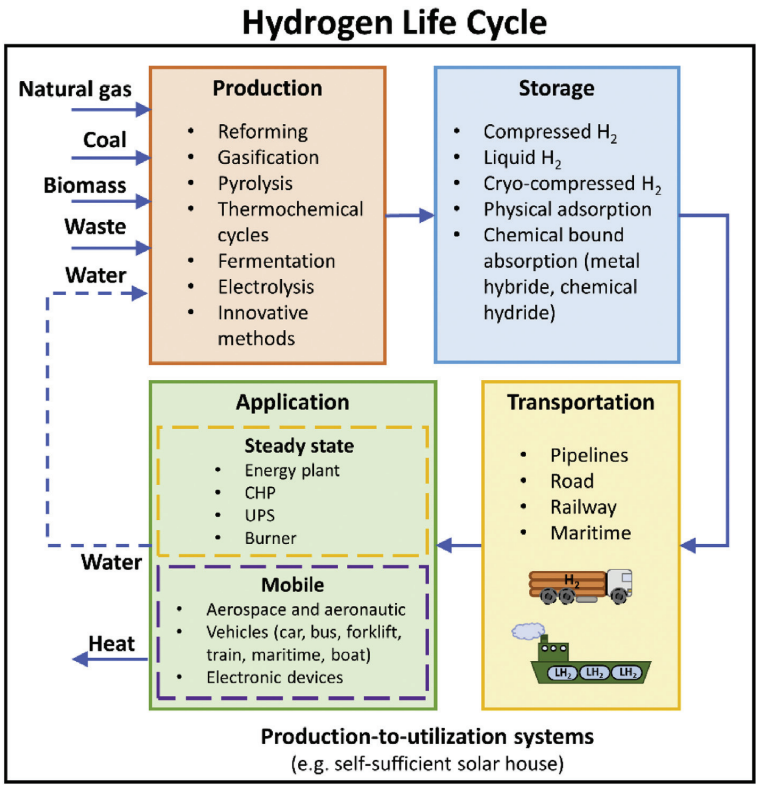


**Fig. 2 – Hydrogen life cycle. Potentially, the water produced after the hydrogen utilization can be the source of the hydrogen production.**

hydrocarbons [17]. In addition, hydrogen can be generated from coal, biomass, plastic mixtures, organic matter (refined sugars, corn stover, and wastewater), hydrides and water. If hydrogen is synthesized by coal, a gasification process is needed prior the reforming. Biomass is employed in gasification, pyrolysis and dark fermentation methods. Dark fermentation, differently from photo formation, does not required sunlight and oxygen, since an anaerobic digestion occurs during this process [24]. In Ref. [25], a review on different bio-hydrogen production techniques which exploit waste-based raw materials is conducted. In particular, the focus is placed on the bacteria activity improvement during the anaerobic fermentation to increase the hydrogen production rate.

Hydrogen is produced through hydrolysis from hydrides and other chemical compounds which contain hydrogen [26]. Hydrogen can be stored in the hydrides through a hydrogenation process [27], as described in the Storage subsection. Moreover, differently from steam reforming and gasification, hydrolysis is a $CO_2$-free process. Recently, different catalysts such as CoP nanoarray in situ grown on Ti mesh (CoP NA/Ti) [28], NiCoP nanosheet array on Ti mesh (NiCoP NA/Ti) [29] and Fe-doped CoP nanoarray on Ti foil (Fe–CoP/Ti) [30] were investigated to increase the hydrogen generation from ammonia borane and sodium borohydride ($NaBH_4$) respectively. Furthermore, the adoption of these non-noble-metal catalysts can reduce the hydrogen production costs.

Hydrogen is generated from water mainly by electrolysis. Other methods which use water are thermochemical cycles, photofermentation and sonochemical (ultrasound waves) processes. Currently, electrolysis is gaining more interest since an electrolyser can be coupled with the renewable energy systems (e.g. wind or solar) and exploit their energy surplus to generate hydrogen. Moreover, this method does not require an additional technique such as carbon capture and storage (CCS) in order to be emissions free. As for the hydrolysis process, several non-noble-metal catalysts were analysed to avoid the utilization of rare and precious metals such as platinum and therefore reduce the costs of this technique. In particular, $Zn_{0.08}Co_{0.92}P$ nanowall array on titanium mesh ($Zn_{0.08}Co_{0.92}P$/TM) [31], $NiMoS_4$ nanosheet array on Ti mesh ($NiMoS_4$/Ti) [32], CoP–$CeO_2$ hybrid nanosheet film on Ti mesh (CoP–$CeO_2$/Ti) [33], CoP nanosheet arrays on carbon cloth (CoP NA/CC) [34] and Mn-doped $Ni_2P$ nanosheet array on nickel

**Table 3 – Hydrogen production techniques.**

| Type | Technique | Hydrogen source | Energy source | CCS[a] required | Observations |
|---|---|---|---|---|---|
| Thermal | Steam reforming | Natural gas | Heat (steam at high temperature) | Yes | Cheapest method and used to produce virtually 95% of $H_2$ in the world [38]. |
| | Gasification and pyrolysis | Coal, biomass, plastic mixture [39] | Heat (steam at high temperature) | Yes | Pyrolysis is conducted in absence of oxygen [40]. |
| | Thermochemical cycles | Water and raw material | Nuclear, geothermal heat [41], solar power | No | Nuclear heat implies different environmental issues [37]. |
| | Hydrolysis | Hydrides or chemical compounds whit $H_2$ | Heat (low temperatures) | No | $H_2$ production rate and costs are influenced by the catalyst types [26]. |
| Biological | Photofermentation | Water, microorganism, organic matter | Sunlight, photosynthetic bacteria [42] | No | Higher hydrogen yield compared with dark fermentation [42] |
| | Dark fermentation | Biomass, organic matter | Bacteria, enzymes | No | Both light and oxygen are not required in this process. |
| Electrochemical | Electrolysis | Water | Electricity (solar [43,44], wind energy [45–47]) | No | Most suitable technique to exploit the surplus of the renewable energies. |
| | Photoelectrochemical (PEC) | Water, semiconductor materials | Sunlight | No | Developed by Fujishima and Honda in 1972 [48]. |
| Innovative | Sonochemical energy | Water | Electricity (ultrasound waves) | No | It has potentially a lower energy consumption than electrolysis [49]. |
| | Mobile electrolysis | Water | Electricity (solar, wind) | No | Energy Observer catamaran [50,51] is provided with one electrolyser. |

[a] CCS: carbon capture storage.

foam (Mn–$Ni_2P$/NF) [35] were found as the most suitable catalysts to replace platinum.

Finally, thermochemical cycles can produce hydrogen by splitting the water molecule with the aid of a raw material. There are more than 300 water-splitting cycles described in literature and they can be divided between direct and hybrid cycles [36]. Although direct cycles are simpler than hybrid cycles, higher operating temperatures are required. For instance, the cerium oxide two step is a typical direct cycle while two hybrid cycles are copper chloride [36] and Westinghouse [37]. In Table 3, the main hydrogen production methods are collected and compared.

A systematic and fully updated comparison between the main hydrogen production techniques is reported in Table 4. In particular, the hydrogen sources, energy consumptions and efficiencies of these methods were considered for the comparison. From the hydrogen source, the amount of fuel or the energy necessary to generate 1 kg of hydrogen can be estimated. For instance, 4.7 $Nm^3$ are required to produce 1 kg of hydrogen. The energy consumption is the energy contained in the fuel, i.e. its lower heating value (LHV) multiply by the fuel amount. Therefore, the energy consumption corresponds to the energy amount to produce 1 kg of hydrogen. The energy efficiency is estimated as the ratio between the hydrogen LHV (120.07 MJ/kg [52]) and the energy consumption. A similar approach was adopted in Ref. [53]. As result of the comparison, dark fermentation, steam reforming and electrolysis seem the most energy efficient techniques compared with the other methods.

### *Storage*

From a storage point of view, one of the main hydrogen drawbacks is the low density. Compared with other fuels, hydrogen requires a larger volume if stored at normal temperature and pressure (NTP) conditions (20 °C, 101.325 kPa [58]). In most of the hydrogen applications, the storage volume represents a limitation. For this reason, many hydrogen storage methods were studied and developed in the last decades.

The most common storage solution is compressed hydrogen up to 700 bar in metallic or composite tank. There are mainly four $CGH_2$ tank categorizes named type I, II, III and IV [59]. These tanks differ in the types of materials and the maximum allowable pressure. For instance, type IV tanks are composed by a polymer liner, wrapped in composite material (glass or carbon fibres embedded in epoxy resin) and can bear up to 100 MPa [59].

Compared with other storage solutions, liquid hydrogen ($LH_2$) offers a higher density up to 70.9 kg/$m^3$ at 20.4 K and atmospheric pressure [58]. Due to its extremely low boiling point (−253 °C), hydrogen can easily evaporate. For this reason, it is usually stored in double walled vessels, composed of two metal tanks separated by a vacuum jacket filled with insulated material (e.g. perlite powder) or a multi-layer insulation (MLI) [60]. The boil-off gas (BOG) formation is one of the main drawbacks of the $LH_2$ storage method. During the liquefaction process, hydrogen is converted from normal hydrogen (75% of ortho- and 25% of para-hydrogen at NTP conditions [61]) to 100% of the more stable para-hydrogen in order to reduce the BOG rate.

The maximum hydrogen density seems to be achievable with a cryo-compressed solution (80 kg/$m^3$ (300 bar, 38 K [59]). Another advantage of this technique is the reduction of the BOG since the vessel is designed to bear at least 350 bar and can be filled with either $LH_2$ or $CGH_2$ [59]. In this case, an insulate pressure vessel is needed [62], and the cost and weight of the tank result higher than the one for $LH_2$.

Hydrogen can be bonded with different material through adsorption and absorption. In the first case, porous materials such as metal organic frame (MOF) are employed. The limitations of this method are slow kinetic reaction and low operating temperature (77 K) or high pressure. Hydrogen can be absorbed by both metal and chemical hydrides and in this case the weight of the system and the energy necessary for both the hydrogenation and dehydrogenation processes are the main drawbacks of this solution.

In Table 5, the characteristics of the main hydrogen storage solutions are listed and compared. It should be remarked that the safety aspects must never be neglected when hydrogen is stored. In the past, several accidents occurred from hydrogen storage devices. For instance, one of the last accidents occurred in Kjørbo (Norway) on June 2019, where the high-pressure tank of a hydrogen filling station leaked the gas due to an assembly oversight [63]. The mixture of hydrogen and air was ignited leading to an explosion with consequent

**Table 4 – Systematic comparison of different hydrogen production techniques.**

| Technique | Hydrogen source | Fuel/energy amount for 1 $kg_{H2}$ | Energy consumption (MJ/$kg_{H2}$) | Efficiency (%) |
|---|---|---|---|---|
| Steam reforming [53] | Natural gas | 4.7 $Nm^3$ | 165 | 73.1 |
| Gasification [53] | Coal | 9.8 kg | 271 | 44.3 |
| | Biomass | 13.0 kg dry biomass | 242 | 48.3 |
| Thermochemical cycles (Nuclear) [53] | Water | $7.03 \times 10^{-5}$ kg uranium | 273 | 44.0 |
| Thermochemical cycles (Solar) [54] | Water | 160 kW h[a] | 577[a] | 20.8 |
| Hydrolysis [55] | Hydrides ($MgH_2$) | 74 kW h[a] | 265[a] | 45.3 |
| Photofermentation [56] | Waste | 33,353 kW h[a] | 120,070[a] | 0.1 |
| Dark fermentation [56] | Waste | 42 ÷ 56 kW h[a] | 150[a] | 80.0 |
| Electrolysis [57] | Water | 53 kW h | 192 | 73.0 |
| Photoelectrochemical (PEC) [56] | Water | 55,588 kW h[a] | 200,117[a] | 0.06 |

[a] Calculated from the efficiency ($LHV_{H2}$/Energy in). The hydrogen LHV is 120.07 MJ/kg [52].

**Table 5 – Hydrogen storage methods.**

| Storage method | | Hydrogen density/content | Gravimetric density ($kWh/kg_{sys}$) | Volumetric density ($kWh/L_{sys}$) | Storage temperature (°C) | Storage pressure (bar) | Energy provided during the storage process ($kWh/kg_{H2}$) | Vessel type | Substance used |
|---|---|---|---|---|---|---|---|---|---|
| Compressed gaseous hydrogen ($CGH_2$) | | 39.2 $kg/m^3$ at 700 bar [58] | 1.8 at 300 bar [65] | 0.8 at 700 bar [65] | 25 (298 K) | Up to 700 | 1.7 (from 20 to 350 bar) 6.4 (from 20 to 700 bar) [66] | Type I, II, III and IV) [59] | – |
| Liquid hydrogen ($LH_2$) | | 70.9 $kg/m^3$ at 1 bar [58] | 2.5 [67] | 1.1 [67] | −252.75 (20.4 K) at 1 bar [58] | Up to 7 | 10 ÷ 13 [66],[a] | Double walled tank [60] | – |
| Cryo-compressed ($CcH_2$) | | Up to 80 $kg/m^3$ at 300 bar, 38 K [59] | 2.3 at 500 bar [65] | 1.4 at 500 bar [65] | −235.15 (38 K) ÷ 25 (298 K) | Up to 500 | 2.0 [68] ÷ 8.0 [69] | Insulated pressurized vessel [69] | – |
| Physical adsorption | | Up to 5.60 wt% with $Mg_{95}Ni_5$–$TiO_2$/MWCNTs[b] [70] | 1.3 [65] | 0.7 [65] | ≈ −203 (70 K) [71] ÷ ≈ 100 (373 K) [70] | 1 [71] ÷ 100 [72] | 6.7 (at −176 °C and 40 bar) | Pressurized or insulated metal tank filled with porous or nanostructured material | MOF[c], zeolites [73], MWCNT[b], graphene [74] |
| Chemical bond (absorption) | Metal hydride | Up to 5.60 wt% with $NaAlH_4 \leftrightarrow Na_3AlH_6 \leftrightarrow NaH + Al + 3/2H_{2(g)}$ [75] | 0.4 [65] | 0.4 [65] | 25 (298 K) | Low pressure | 2.8 (for IM[d] at T < 80 °C, 50 bar) ÷ 11.0 (for $MgH_2$ at 300 °C, 30 bar) [76] | Pressurized metal tank filled with metal hydride | Alloys composed by Mg, Na, Al, Li, B, Ti, Zr and Fe [38] |
| | Chemical hydride | Up to 12.1 wt% with methanol [77] | 1.5 [65] | 1.3 [65] | 25 (298 K) | $P_{atm}$ | 6.3 (for ammonia at T > 425 °C) ÷ 11.2 (for MCH at 350 °C) [76] | Conventional steel tank [78] | Ammonia, methanol, formic acid, LOHC: DBT, NEC [77], MCH[e] [79] |

[a] according to Ref. [80], a potential energy consumption of 5.9 kW $h/kg_{H2}$ for an optimized liquefaction plan with a capacity between 25 and 100 tons per day ($tpd_{LH2}$) was estimated.
[b] MWCNT: multi-walled carbon nanotubes.
[c] MOF: metal-organic framework.
[d] IM: intermetallic hydride.
[e] LOHC: liquid organic hydrogen carrier; DBT: dibenziltoluene NEC: N-ethylcarbazole; MCH: methylcyclohexane.

**Table 6 – Hydrogen transportation methods (n. a.: not available).**

| Transportation method | Hydrogen storage method | Transport distance (km) | Pressure (bar) | Hydrogen content | Hydrogen amount | Tank volume ($m^3$) | BOG formation (vol % per day) | Example |
|---|---|---|---|---|---|---|---|---|
| Pipelines | $CGH_2$ | Up to 550 [81] | Up to 100 [81] | 99.9% [81] | n. a. | – | – | Between France and Belgium $H_2$ flows at 100 bar with high purity (99.9%) in a 550 km pipeline [81]. |
| | $LH_2/SLH_2$[a] | Up to 0.5 [60] | Up to 7[b] | 100% [60] | n. a. | – | n. a. | At Kennedy Space Center in Florida, long 500 m used for both $LH_2$ and LOX[c] [60]. |
| | Mixed with NG[d] | $> 10^3$ | Up to 100 [90] | 5 wt% [90] | n. a. | – | – | In Italy, Snam company is injecting 5% of $H_2$ in the traditional methane network [90]. |
| Road | $CGH_2$ | Short dist [91]. | 250 [92] | 100% | 600 kg per truck | <26 [93] | – | Titan module developed by Hexagon [94] carries 600 kg of $H_2$ at 250 bar. |
| | $LH_2$ | Mid-range dist [91]. | Up to 7[b] | 100% | 4 tons per truck [60] | <64 [95] | 0.5 [60] | Air Product [95] delivers $LH_2$ by means of semitrailer with a capacity of 17,000 gal (64 $m^3$). |
| | Metal or chemical hydride | n. a. | $P_{atm}$ | n. a. | – | – | – | Not an efficient solution for small amount of hydrogen over short distances [81]. No common practice. |
| Railway | $LH_2$ | $> 10^3$ | Up to 7[b] | 100% | 7 ton per rail car | 105 [60] | 0.2 [60] | In 2009, NREL[e] estimated that hydrogen railway delivery might be a more efficient method compared with $CGH_2$ and $LH_2$ trucks and pipelines for long distances and large $H_2$ amount [96]. |
| Maritime | $LH_2$ | Transoceanic delivery | Up to 7[b] | 100% | 60 ton per tank | 900 [60] | n. a. | $LH_2$ was transported in 900 $m^3$ containers onboard of barges to the NASA Space Center during the Apollo space program [60]. |

[a] $SLH_2$: slush hydrogen. It is a two-phase (solid and liquid) fluid [97].
[b] The maximum operating pressure is considered equal to 7 bar since at 7.4 bar the first pressure relief valve (PRV) opens [98].
[c] LOX: liquid oxygen.
[d] NG: natural gas (mainly composed by methane).
[e] NREL: National Renewable Energy Laboratory.

fire. Similarly, on June 1, 2019, a hydrogen tanker truck leaked the gas after the refuelling in a chemical plant in Santa Clara, California [64]. The hydrogen dispersion led to an explosion with consequent fire. Hydrogen safety is further discussed in the following sections.

### *Transportation*

Hydrogen can be transported by different means with continuous or batch approaches adopting different storage techniques previously described (see Table 6). The only manner to achieve a continuous hydrogen transport is through pipelines. Usually, these are installed within the facility where hydrogen is produced or until the plant in which the hydrogen is consumed [81]. The length of the pipelines is intentionally short in order to contain the capital and variable costs required by the maintenance. In 2007, Yang and Ogden [82] estimated that pipelines designed for $CGH_2$ are the most convenient delivery method for large amounts of hydrogen and short distances, compared with $CGH_2$ and $LH_2$ trucks.

When road transport is adopted, hydrogen can be stored onboard of trucks both as $CGH_2$ and $LH_2$. Hydrogen is commonly transported in pressurized vessels installed onboard of tube trailer when short distances must be covered. The road regulations of different countries limit the allowable $CGH_2$ tank pressure to 200–300 bar even though new generation type IV composite tanks are able to bear up to 700 bar [83]. Another constraint imposed by the road codes is the total mass of the trucks which must not exceed 40 tons [54]. From 2017 to 2018, the European Hydrogen Law (HyLaw) project aimed to change the road regulations together with other standards and safety codes which represent the legal barriers to the deployment of fuel cells and hydrogen applications [54]. $LH_2$ is delivered by means of road tanker, contained in the double walled tank. As mentioned before, the BOG formation is the main drawback of this storage method and impedes long distance shipments.

During railway transport, hydrogen is in liquid phase in order to increase the delivery amount. This transport method is not widely used due to a lack of $LH_2$ tank cars availability and railway time scheduling factor that can increase the BOG formation [53]. Finally, maritime transport is relatively suited for large quantities of hydrogen for long distances. The CO2-free Hydrogen Energy Supply-chain Technology Research Association Commences (HySTRA) organization, established by four Japanese companies, is aiming to demonstrate the marine transport feasibility of large amount of $LH_2$ [58]. Despite few projects studied and designed this kind of vessel, $LH_2$ carrier ships have not been built to date.

The common thread between these transport methods are the safety aspects which must be always considered. Different lessons were learned after several accidents and near misses occurred in the past, such as in 1991 at Porta Susa station in Turin, Italy where the whole content of a $LH_2$ railway wagon was harmlessly released [57].

#### *Related equipment*

When hydrogen is stored and delivered, substantial equipment is needed to move or contain it. Material selection is one of the main issues during hydrogen equipment design [84]. The selected material must be suitable for hydrogen environment, resistant to corrosion, hydrogen embrittlement and cryogenic temperatures if hydrogen is in liquid phase [85]. Therefore, the maintenance costs are reduced and the loss of integrity of hydrogen equipment can be avoided increasing the system safety by choosing the appropriate materials. Tanks and pipes are both complex equipment composed by valves, joints, welding, gaskets, compensators (for thermal contraction), safety devices, insulation, instrumentation and support structure. In the case of double walled $LH_2$ tanks, rods are needed to keep the inner tank suspended inside the outer vessel and manway or an inspection panel are needed when the tank has a large size [60]. During the design of these equipment, the mechanical stresses in the case of pressurized tanks and thermal dissipation and contraction for $LH_2$ and $CcH_2$ must be taken into account as well. Currently, reciprocating compressors are widely used to fill the hydrogen tanks. This equipment has low efficiency (45%) [86], is expensive and affected by operating and maintenance costs [87]. Ionic liquid piston compressor seems to be the most suitable device for hydrogen thanks to the lacking in solid moving parts, higher efficiency (70%) and reduced size and weight in comparison to a reciprocating compressor [88]. $LH_2$ pump is employed both to fill the $LH_2$ tank and to compress hydrogen from 3 bar at 24.6 K (liquid) up to 875 bar at 30–60 K (gaseous phase) [89]. The cryogenic pump has a low electricity consumption of 1.1 kW h/$kg_{H2}$ compared to the most performant hydrogen compressors in the same range of pressures (3 kW h/$kg_{H2}$). On the other hand, a larger energy demand is required by the liquefaction (10 kW h/$kg_{H2}$ [66]) compared with the compression process. The BOG formation during the pumping phase affects the pump efficiency but it can be reduced when large flowrates are required (more than 1000 $kg_{H2}$/day) [89].

### *Usage*

Fuel cells are the electrochemical devices that generate electric energy from the redox reduction of hydrogen and air (oxygen), hence without any combustion. This device was invented by Sir William Grove in 1839 [99]. During the 1960s, fuel cells were employed as power system for the Apollo lunar missions with a consequent enhancement of this technology. The advantages of these devices are a good weight-energy ratio, and water and heat as only by-products of the reaction. In the following, fuel cells are recognized as hydrogen technologies.

In Table 7, the hydrogen technologies are divided between two main categories: stationary and mobile systems. Most of the applications use hydrogen to produce electricity through a fuel cell device in order to supply an electric engine. In particular, this concept is adopted in vehicles because a higher efficiency can be obtained compared with traditional internal combustion engines (ICEs) [100]. The selection of this relatively new technology can increase the capital costs of the system since fuel cells are not produced on an industry large scale [101]. The high initial costs can sometime hamper the hydrogen distribution. Nevertheless, hydrogen can be employed as well as fuel in ICE to power cars or in gas turbine (GT) [102] either to produce electrical energy [103] or to thrust unmanned aerial vehicles (UAVs) [104]. In this manner, very

**Table 7 – Hydrogen usage.**

| | Type | Description | Examples |
|---|---|---|---|
| Stationary systems | Energy Plants | Electricity is produced through a fuel cell module [106,107] or a gas turbine (GT). | Hydrogen-fed GT in an Italian electric energy production managed by ENEL [103]. |
| | Combined Heat and Power (CHP) systems | Fuel cell (FC) are used to generated electricity and heat with a theoretical overall system efficiency of 95% [108]. | European project PACE on micro-CHP system [109]. |
| | Trigeneration Systems | Combined, cooling, heat and power (CCHP) [110], or combined heat, hydrogen and power (CHHP) systems. | In 2016, the world's first CHHP system was built in California [7]. |
| | Uninterruptible Power Systems (UPS) | Fuel cells are suitable as UPS devices with higher energy density of battery systems. | FCgen®-H2PM by Ballard [111] and HyPM™ XR fuel cell system by Hydrogenics [112]. |
| | Burners | The $H_2$ burners can be employed to cook, heat or cool through an absorption cycle. | $H_2$ burner/stove by the Swiss company Empa [2] for cooking, and $H_2$ burners for general purposes [113,114]. |
| | Chemical reactants | $H_2$ is employed in several chemical and metallurgical processes | Methanol and ammonia production [5]. |
| | Metal Hydride Solar Power | $H_2$, stored in metal hydride, is the motive fluid this type of pump. | In 1980, this pump was developed by Sandia National Laboratories [115]. |
| Mobile systems | Aerospace industry | Space missions use $H_2$ as propellant and as fuel to generate electricity onboard of space module through fuel cells. | Space applications of hydrogen and fuel cells by NASA [116]. |
| | Electronic devices | Portable and wearable electronic devices as well as auxiliary power unit (APU) can be powered by fuel cell. | Mobile phone and laptop [117] and APU, installed onboard of autonomous systems, battle ships and submarines [118] |
| | Internal combustion engine (ICE) | $H_2$ can fuel ICE for mobile applications. | In the 1990s, BMW prototyped the Hydrogen 7 model [119], powered by an ICE fuelled with $H_2$. |
| | Scooter and bike | Fuel cell powered scooters have been studied in different projects since 1998 [120]. | Suzuki is developing the Burgman scooter model [121]. HYSUN 3000 bike travelled from Berlin to Barcelona consuming 3.3 kg of $H_2$ [122]. |
| | Car and taxi | Several FC cars have been prototyped and developed in the last 50 years. | Toyota, Honda, Hyundai produce FC cars. Mercedes-Benz is developing the GLC F-CELL model [123]. In 2015, 60 Hyundai ix35 FC cars have been employed as taxi in the Hype project [124]. |
| | Bus and truck | FC technology is suitable for bus and truck, vehicles that require a long-distance range. | In [125], there is an overview of the current projects on FC buses. In 2018, the Norwegian company Asko ordered 4 FC trucks from Scania [126] and the deployment of 500 trucks in Shanghai, China has been planned [127]. |
| | Forklift | FC forklifts have no local emissions, long operational time, short refilling time [128] and are able to work in low temperature environment [129]. | In the USA between 2009 and 2017, the total number of FC deployment for applications in material handling equipment was 16,518 [130]. |
| | Train | FC trains are suitable for replacing diesel locomotives in railways without electricity supply. | In 2018, the first FC train, the Coradia iLint, entered in service in the Lower Saxony region (Germany) [9]. |
| | Boat, ship and submarine | FCs have been installed onboard of boats and ships as auxiliary power unit (APU). | In [131], a review of fuel cell system for maritime applications was conducted. Hydrogen has been employed in class 212 submarine as fuel of the air-independent propulsion (AIP) system [132]. |
| | Airplane and unmanned aerial vehicle (UAV) | FCs have been used since 2006 to power UAVs both fixed wing and multirotor. FCs can be used onboard airplane as APU in order to reduce emissions and fuel consumption [133]. | In 2015, the multi-rotor UAV H2QUAD 400 developed by EnergyOr reached the world record in time flight for its category [8]. Several projects on hydrogen fuelled aircrafts are been reported in Ref. [134]. |
| | Earth-moving machinery | $H_2$ has been used to fuel underground locomotives and mine loaders powered by fuel cell systems. | In 2000, the first fuel cell powered mince locomotive was developed and tested by the Fuelcell Propulsion Institute from Denver, Colorado [135]. Few projects regarding FC powered mine loader were carried out [112,113]. |

well-known technologies already available at large scale and competitive prices can be exploited. Another obstacle in the expansion of the hydrogen technology is the lack of infrastructures (e.g. refuelling stations) and the hydrogen availability to the public society compared with the conventional fuels such as hydrocarbons. The main barriers to build a spread and complete (from production to utilization) hydrogen network are cost, government policy, regulation and public opinion [105]. These barriers are mainly and directly influenced by safety, aspect that must be always guaranteed.

## Hydrogen Properties and Safety

### *Chemical and physical properties*

Hydrogen is the lightest element in nature, and it tends to rise in the atmosphere at normal conditions. It is not toxic, nor corrosive, and harmless for the environment. According to the International Agency Research on Cancer [85], hydrogen is not carcinogenic as well. At atmospheric conditions, it is a diatomic gas with a very low density (0.0838 kg/m$^3$ [136]). It is difficult to detect since it is colourless, odourless and tasteless. Moreover, its flame is considerably wicker compared with hydrocarbon flames [137], thus difficult to see with the naked eye. Although the hydrogen flame in air has a very high temperature (2321 K for 19.6%vol of $H_2$ in air [85]), it burns faster and produce significantly less thermal radiation than hydrocarbons such as LNG [138]. The atmospheric moisture has a significant effect on the thermal energy radiated by a hydrogen flame. In particular, the water contained in the air absorbs the thermal (infrared) radiation [138]. However, any kind of undesirable ignition sources should be always avoided during hydrogen applications due to its low ignition energy (0.017 mJ in air [139]). Furthermore, the flammability range is wider than other fuel (4.0% ÷ 75.0% in air [136]). Hydrogen has a high burning velocity which corresponds to a high explosive potential. This means that the containment or suppression of its flame and explosion are difficult to achieve. It must be notice that hydrogen is one of the few gases that increases its temperature when expanded at a temperature above its inverse Joule-Thomson temperature (193 K [85]). Some of the most important hydrogen physical and chemical characteristics are listed in Table 8.

**Table 8 – Thermophysical, chemical and combustion properties of hydrogen.**

| Property | Value |
|---|---|
| Normal Boiling point [136] | 20.268 K (−252.882 °C) |
| Melting point (0.101 MPa) [140] | 13.99 K (−259.16 °C) |
| Critical temperature [136] | 32.976 K (−240.174 °C) |
| Critical pressure [136] | 1.2928 MPa ab |
| Triple point temperature [136] | 13.803 K (−259.347 °C) |
| Triple point pressure [136] | 7.04 kPa ab |
| Density - gas (NTP) [136] | 0.0838 kg/m$^3$ |
| Density - liquid (NBP) [136] | 70.78 kg/m$^3$ |
| Lower Heating value (LHV) [52] | 120.07 MJ/kg |
| Higher Heating value (HHV) [52] | 141.80 MJ/kg |
| Heat of vaporization (NBP) [136] | 445.6 kJ/kg |
| Velocity of sound in air - adiabatic (NTP) [136] | 1294 m/s |
| Velocity of sound in air - adiabatic (NBP) [136] | |
| of vapour | 355 m/s |
| of liquid | 1093 m/s |
| Minimum ignition energy - in air [139] | 0.017 mJ |
| Flame temperature in air [136] | 2318 K (2044.85 °C) |
| Autoignition temperature [136] | 858 K (584.85 °C) |
| Limits of flammability in air (NTP) [136] | 4.0% ÷ 75.0% |
| Limits of detonability in air (NTP) [136] | 18.3% vol ÷ 59.0% vol |
| Joule-Thomson inversion temperature [136] | 193 K (−80.15) |
| Energy of explosion (theoretical explosive yield) [136] | 24 $g_{TNT}/g_{H2}$ |

NTP: Normal temperature and Pressure: 293 K and 101.3 kPa.
NBP: Normal Boiling point: 20.268 and 101.3 kPa.

### *Safety aspects*

In the following, the hydrogen safety aspects are presented according to the scheme depicted in Fig. 3. The schematic represents a simplified bow-tie diagram, in which hazards, faults, critical events and consequences are distinguished. A similar approach is provided by the software BowTieXP [141]. Each category is hereby briefly described. According to Refs. [142], hazard is "a source of danger", while risk is the "possibility of loss or injury". Therefore, the risk contains the likelihood of conversion of the hazard in a damage. The damage can be of different kind such as a loss or an injury. Thus, both critical event and consequences are considered as damages. In particular, a critical event is defined as the loss of containment (LOC) or loss of physical integrity (LPI) [143], while the consequences are the damages which occur due to the critical events. The fault event is the cause of the accident, thus the event that triggered other failures and errors which lead to the critical event (domino effect [144]) or directly this latter.

*Hazards*

In the case of hydrogen, the hazards consist of the hazardous physical and chemical properties of the substance in gaseous and liquid phase. The risk phrases R12 is attributed to hydrogen [145]. R12 corresponds to the hazard statement H220 "Flammable gas, Hazard Category 1" and H224 "Flammable

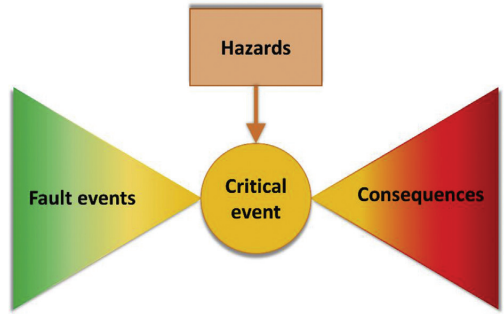


**Fig. 3 – Bow-tie approach adopted to describe the hydrogen safety aspects [141].**

liquid, Category 1" when it is in gaseous and liquid phase respectively. Category 1 means that the substance is extremely flammable. All the hazards analysed for $GH_2$ must be taken into account also with $LH_2$ since a gaseous phase is often present due to its continuous evaporation.

*Causal events*

All types of mechanical and physical failures can be considered as LOC causes. These failures include collision during transportation, mechanical failures of hydrogen equipment such as safety devices, storage vessels, vent, exhaust and vaporization systems. Hydrogen embrittlement is a well-known phenomenon responsible of material degradation and thus can be the cause of different types of equipment rupture. For this reason, the materials for hydrogen service must be selected in order to avoid any embrittlement phenomena. These issues were addressed in the Hydrogen Damage section. The embrittlement phenomena can lead to different critical events.

In case of $LH_2$, an inappropriate insulation of hydrogen equipment can provoke other failure mechanisms such as embrittlement or safety device failures due to its low boiling point. Moreover, at these extremely low temperatures, air can condensate over a hydrogen equipment such as a pipe, if it is not insulated properly. Therefore, explosive mixture can be created if the condensed air drips onto combustible materials such as tar or asphalt [85]. The low temperature of the liquefied air (−196 °C [146]) can brittle sensitive materials or flammable substances can be enriched with oxygen due to the higher density. Moreover, the humidity presents in the air can solidify over or inside safety devices such as pressure relief valves causing failures and thus severe consequences. A mixture of $LH_2$ and liquid or solid oxygen can be created if air flows into the tank during the filling [61] or $LH_2$ is spilled onto ground [147]. This mixture is sensible to variation in pressure and can be easily ignited due to its small ignition energy [148], and even an external generated shock wave can make it detonate [61]. Continuous evaporation of the $LH_2$ is an aspect that must be always considered. The BOG must be vented when the tank reaches a safety pressure value, otherwise, BOG production can be the cause of equipment rupture and a consequent physical or chemical explosion.

*Critical events*

According to the methodology for the identification of major accident hazards (MIMAH) [143], four types of critical events for hydrogen in gaseous phase at atmospheric conditions or stored in pressurized vessels can occur. In most of the applications, $GH_2$ is compressed in order to increase its density. The identified critical events are the following:

- start of fire (LPI);
- breach on the shell in vapor phase (three different sizes are defined);
- leak from gas pipe (three different sizes are defined);
- catastrophic rupture;

Three different sizes of breach or leak are defined which correspond different consequences severity. According to MIMAH, the critical events for a cryogenic hydrogen equipment in contact with a two-phase substance (liquid and vapor) are the same considered for the gaseous phase. Furthermore, the "breach on the shell in liquid phase" and "leak from liquid pipe" are two additional critical events. Conversely to $GH_2$, a $LH_2$ leak can be easily detected through the consequent formed cloud of condensed humidity. Although hydrogen has a higher density than air up to 23 K and atmospheric pressure, the cloud formed after its dispersion can float away blown by the wind. This can lead to severe consequences if the dispersed hydrogen encounters an ignition source.

*Consequences*

When hydrogen is dispersed, especially in an enclosed environment, it can cause respiratory ailment and asphyxiation. Other physiological consequences of physical or chemical phenomena are the overpressure of a blast wave or the radiation from a fireball. Physiological consequences such as frostbite and hypothermia can manifest when $LH_2$ is dispersed or splashed.

Consequences of loss of containment or catastrophic rupture can be fires and explosions when a mixture of hydrogen and air is present. The amount of energy necessary to reach the hydrogen ignition energy can be generated by mechanical sparks, electrostatic discharges, welding and cutting operations, catalyst particles and lightning strikes [85]. Deflagration, detonation and flash fire are the chemical explosions usually considered for hydrogen.

Boiling Liquid Expanding Vapor Explosion (BLEVE) is a physical explosion. It is a direct consequence of a catastrophic rupture of a tank containing a liquid (or liquid and vapor) at a temperature above its boiling point at atmospheric pressure [149]. Hence, BLEVE is usually considered for liquefied gases, both pressurized and cryogenic fluids. However, in Refs. [150], supercritical BLEVEs were tested and analysed. This is a type of BLEVE which can occur when a liquefied gas reaches the supercritical conditions due to considerable increase in pressure. BLEVE's consequences are the overpressure of the blast wave and the missiles. These latter are the debris of the tank blown away by the explosion. Another BLEVE consequence is the fireball that can be generated if an ignition source is present.

Rapid Phase Transition (RPT) is a physical explosion as well and should be considered when $LH_2$ is managed close to a water reservoir, sea, lakes or rivers. This is a well-known phenomenon for Liquefied Natural Gas (LNG) and liquid nitrogen (LIN). In the past, few accidents occurred when the LNG was spilled onto water [151]. The heat transfer between the water and the cryogenic fluid can leads to a violent expansion of the LNG due to the sudden phase change if certain conditions are met such as a well mixing between the two fluids [152]. RPT never occurred for $LH_2$ and it is not clear yet if it can happen. However, in Ref. [153–155], the authors assume that theoretically RPT can always occurs when a cryogenic fluid is spilled onto water.

During the $LH_2$ spilling caused by a leak, part of the hydrogen flash-vaporizes (more than 30% [154]) provoking also a gas dispersion as consequence. Two direct consequences of the gas dispersion are the vapor cloud explosion (VCE) and the flashfire. A pool formed during a series of

experimental tests carried out in Ref. [147] during which $LH_2$ was spilled on the ground. Although, the authors could not exactly estimate the composition of the pool, they assumed it was formed of $LH_2$ trapped by solidified and liquefied air (oxygen and nitrogen). In the case of pool ignition, a pool fire is the direct consequence.

*Atypical accident scenarios*

As previously mentioned, although hydrogen is a very well-known substance, emerging risks can arise when it is employed in new applications which correspond to emerging technologies [11]. From the emerging risks, different atypical accidents might occur. An accident scenario is atypical if it has not been identified by a conventional hazard identification (HAZID) technique [156]. In fact, some phenomena have not been analysed for hydrogen yet. For instance, in the case of $LH_2$, two physical explosions, BLEVE and RPT were not analysed and barley mentioned in few studies.

At least two BLEVE accidents for $LH_2$ occurred in the past. In 1974, an improper firefighting technique was the cause of an $LH_2$ 20,000 gal tank failure and the consequent BLEVE explosion [157]. The Challenger Space Shuttle disaster was initiated by an O-ring rubber seal failure installed in one solid rocket booster [158]. For this reason, the hot gases which could not be held anymore in this section, escaped and ignited. The generated flames burned against the external tank where the $LH_2$ and LOX vessels were installed. As consequence, the vessels breached and exploded [134]. The NASA theory established that this explosion was a BLEVE [159]. $LH_2$ BLEVE was considered during the IDEALHY project as result of the $LH_2$ risk assessment and consequence analysis [14] as well as in a recent study where the DyPASI technique able to identify atypical accident scenarios was applied to the $LH_2$ technologies [13]. On the other hand, there are no records of RPT for $LH_2$. During the $SH_2$IFT project [15], both $LH_2$ BLEVE and RPT will be analysed by conducting experimental tests and developing numerical simulation models in order to estimate the explosion consequences and comprehend their formation.

## Loss of integrity phenomena

In this section, the main physical and chemical phenomena that can lead to a loss of integrity of hydrogen equipment are described and analysed. These are some of the causal events, discussed in the Safety Aspects section and represented on the left-hand side of Fig. 3. Many critical events and thus accidents with severe consequences can be prevented by increasing the knowledge in loss of integrity phenomena, such as hydrogen damage (HD). Despite several studies were conducted in the past in order to prevent the formation of these phenomena, HD is still the cause of several failures and accidents. On the other hand, there are other processes such as low temperature embrittlement and thermal contraction which can occur for $LH_2$ and are not categorised as HD.

*Hydrogen damage (HD)*

HD is a categorization of different phenomena which can affect the characteristics and integrity of the hydrogen equipment materials. These phenomena can manifest even in applications in which hydrogen is not directly employed. As depicted in Fig. 4, the formation of the majority of these phenomena depends on three different factors. These are the environment (hydrogen amount, form and processes) and field type (mechanical, electrochemical, operating conditions) where the material is employed, and the selected material itself. Similarly to Fig. 4, Table 9 presents the three main factors which induce the HD formation (materials, hydrogen source and conditions) together with the main HD processes. In the following, these phenomena were briefly described.

According to Ref. [161], there are three main HD forms which are blisters caused by hydrogen diffusion into the metal, hydrogen-assisted cracking which includes different types of crack and metal hydrides formation. In Fig. 5, the

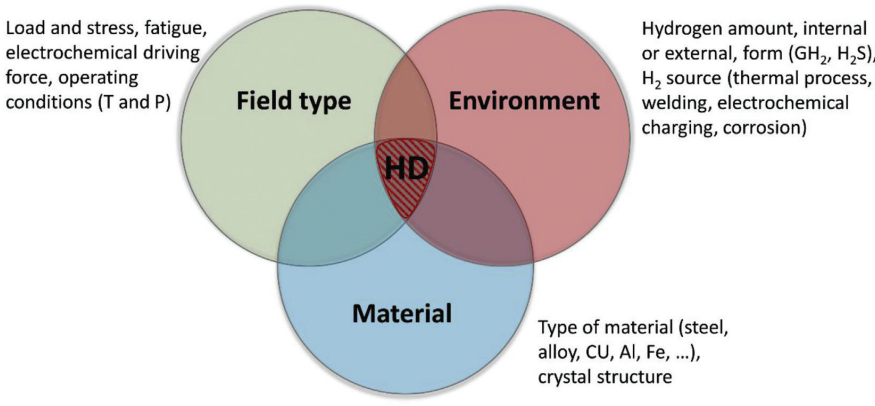


**Fig. 4 – Venn diagram of hydrogen damages (HDs) influencing factors (adapted from Ref. [160]).**

schematic of hydrogen attack, blistering and metal hydride formation phenomena is illustrated.

Hydrogen attack exhibits when carbon and low-alloy steels are exposed to hydrogen at high temperature and pressure for long time. As results, steel decarburization due to methane formation from hydrogen and carbon contained in the material, or generation of cracks and fissures making the alloy weaker [162]. Instead, blistering can occur for low-strength alloys if cleaned by pickling or exposed to corrosive environment, such as $H_2S$ [162]. A blister is a plastic deformation of the alloys provoked by the precipitation of atomic to molecular hydrogen, initially diffused inside internal defects of the material. This precipitation generates a localized high pressure. Finally, the hydrogen pickup from welding, heat treating, corrosion processes or melting, is the cause of precipitation of metal hydride phases with consequent degradation of mechanical properties and cracking of several metals such as magnesium, tantalum, niobium, vanadium, uranium, thorium, zirconium, titanium, and their alloys. Application of stress can increase the hydride formation [162].

Another large category, part of the HD, is named hydrogen embrittlement and includes hydrogen environment embrittlement (HEE), hydrogen stress cracking (HSC) and loss in tensile ductility. HEE can occur when the material is employed in a hydrogen atmosphere [61]. It affects more the materials with a low hydrogen solubility such as metals with body-centred cubic (bcc) and hexagon close-packed (hcp) lattice structure [61]. HEE is more severe at temperature of 20 °C, low strain-rate and high hydrogen purity and pressure [162]. The second hydrogen embrittlement type, HSC, is also called internal hydrogen embrittlement, it is a cracking mechanism for ductile steels that contain hydrogen able to freely move. This process happens when the material is under a sustained load between a certain threshold and its yield strength, resulting in brittle fracture. The threshold stress decreases when the strength of the material increases [163]. In the past, HSC occurred in components that were not employed in hydrogen environment but were treated with different techniques resulted as sources of hydrogen such as electroplating [61]. The last hydrogen embrittlement phenomena displays a reduced elongation and area in tensile test for steels, stainless steels, nickel-base, aluminium and titanium alloys subjected to hydrogen environment [163]. The loss in ductility is related to the hydrogen content of the material. This type of HE increases when the strain-rate decreases [162].

Shatter cracks, flakes, fisheyes are hydrogen damage similar to blistering and can occur in forgings, weldments and castings. These processes start during the melting operations due to hydrogen pickup and during the cooling phase due to hydrogen precipitation in material defects resulting in these features. Micro-perforation occurs at very high pressure and close to room temperature, mainly in steels. As consequence, small fissures are generated making the material permeable to gas and liquids [162]. On the other hand, the pressure has no influence for the degradation in flow properties phenomena. This degradation process appears when a hydrogen atmosphere is present for iron and steel at ambient temperature and for other alloys at high

**Table 9 – Hydrogen damage phenomena (adapted from Ref. [163]).**

| | Hydrogen embrittlement | | | Hydrogen attack | Blistering | Shatter cracks, flakes, fisheyes | Micro-perforation | Degradation in flow properties | Metal hydride formation |
|---|---|---|---|---|---|---|---|---|---|
| | Hydrogen environment embrittlement | Hydrogen stress cracking | Loss in tensile ductility | | | | | | |
| Materials | Steels, Ni-base alloys, metastable stainless steel, Ti alloys | Carbon and low alloy steels | Steels, Ni-base alloys, Be–Cu bronze, Al alloys | Carbon and low alloy steels | Steels, Cu, Al | Steels (forgings and castings) | Steels (compressor) | Fe, steels, Ni-base alloys | V, Nb, Ta, Ti,Zr, U |
| Source of hydrogen | $GH_2$ | Thermal processing, electrolysis, corrosion | $GH_2$, internal hydrogen from electrochemical charging | $GH_2$ | $H_2S$ corrosion, electrolytic charging,$GH_2$ | Water vapor reacting with molten steel | $GH_2$ | $GH_2$ or internal $H_2$ | Internal $H_2$ from melt; corrosion,electrolytic charging, welding |
| Conditions | $10^{-12} \div 10^2$ MPa, −100 ÷ 700 °C | 0.1 ÷ 10 ppm $H_2$ content, −100 ÷ 100 °C | 0.1 ÷ 10 ppm $H_2$ content,−100 ÷ 700 °C | Up to $10^2$ MPa at 200 ÷ 595 °C | $H_2$ activity 0.2 ÷ 1 × $10^2$ MPa at 200 ÷ 595 °C | Precipitation of dissolved ingot cooling | 2 ÷ 8 × $10^6$ MPa at 20 ÷ 100 °C< | 1 ÷ 10 ppm $H_2$ content, up to $10^2$ MPa | 0.1 ÷ $10^2$ MPa |

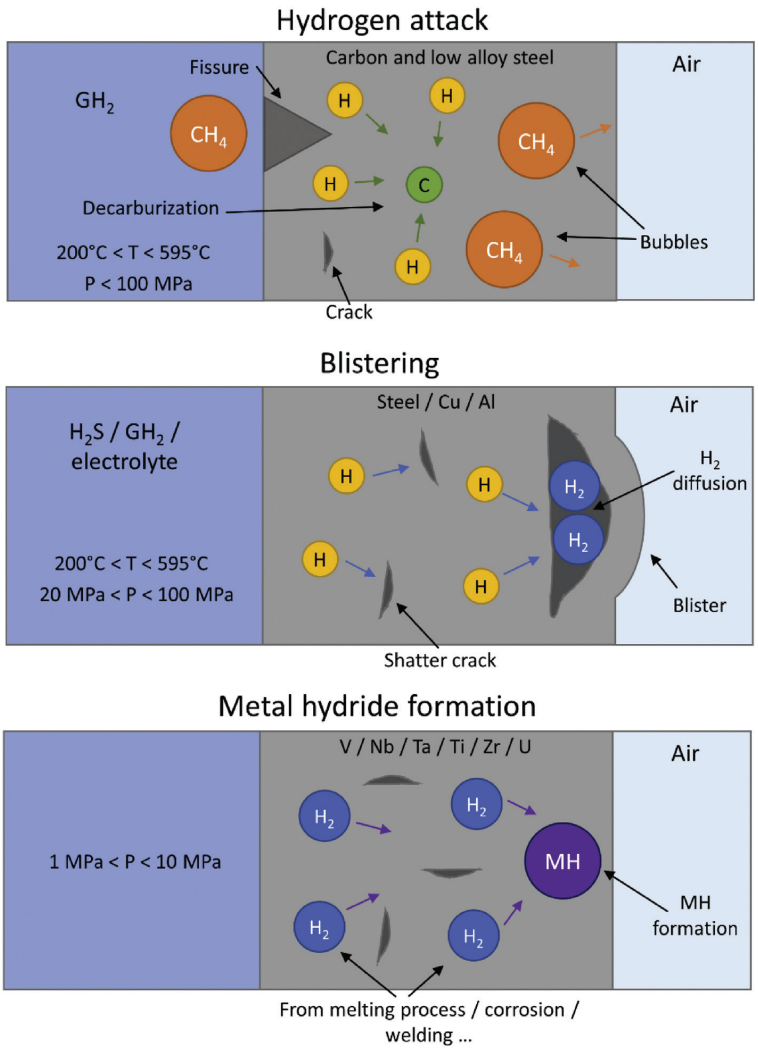


**Fig. 5 – Schematic of hydrogen attack, blistering and metal hydride formation phenomena.**

temperature. For some nickel-based alloys in hydrogen environment, the steady-state creep rate under constant load can increase [162].

### *Hydrogen damage mechanisms*

Even though the hydrogen damages are very well-known phenomena in the material science, many contrasting theories were developed to explain their complex formation mechanisms and a universal theory is yet missing. The HD formation can depends on several parameters which are the time of exposure to hydrogen, stress state, pressure, temperature, hydrogen concentration, physical and mechanical properties of the metal, microstructure, surface conditions, diffusion rates, purity of the hydrogen, nature of the crack front [61].

The pressure theory is one of the oldest one and thoroughly pinpoints the blistering and other loss in tensile ductility. On the other hands, this theory cannot explain other phenomena such as the hydrogen stress cracking [162]. Another important hydrogen damage is the metal hydride formation, which is very well described by the namesake mechanism. Instead, the hydrogen damage that occurs at high temperature can be characterize by the hydrogen attack mechanism. In Table 10, a brief description of the theories which aim to explain the hydrogen damages is provided.

**Table 10 – Hydrogen damage mechanism.**

| Mechanism | Proposed by | Explained HD | Starting process | Consequence |
|---|---|---|---|---|
| The pressure theory | Zapffe and Sims, 1941 [164] | Blistering and loss in tensile ductility | Hydrogen diffusion into the metal [162] | Voids growth or cracking due to high internal pressure [162] |
| The surface adsorption theory | Petch and Stables, 1952 [165] | Hydrogen embrittlement | Hydrogen adsorption on the Griffith crack surface [165] | Crack propagation increases due to reduction in work of fracture [165] |
| Decohesion | Pfeil, 1926 [166] | Hydrogen embrittlement | Hydrogen presence reduces the bond strength of the alloy atoms [167] | Rupture at lower levels of stress [167] |
| Enhanced plastic flow and instability | Beachem, 1972 [168] | Hydrogen-assisted cracking | Dislocation motion or generation due to hydrogen-steel interaction [168] | Different deformation processes ahead of the crack tip, decrease of microscopic plasticity [168] |
| Hydride formation | Gahr, Grossbeck and Birnbaum, 1977 [169] | Metal hydride formation | Hydride formation at the front of a crack [169] | Hydride precipitation which increases when stress is applied [169] |
| Hydrogen attack | Vitovec, 1982 [170] | Hydrogen attack and high temperature HD | Hydrogen diffusion into or at the surface of group Vb metals [162] | Surface or internal decarburization [162] |
| Hydrogen Trapping | Darken and Smith, 1949 [171] | Behaviour by alloys in different hydrogen bearing systems | Hydrogen diffusion in iron or steel [162] | Retardation in hydrogen diffusion rate or lag time due to traps filling by hydrogen [162] |

### *Low temperature embrittlement*

A brittle material, differently from a ductile one, does not show any permanent deformation before fracturing due to the absence of a yielding region. On the other hand, a ductile material can remain intact even though the applied load is higher than its yield stress by exhibiting plastic (permanent) deformation. Different ductile metals become brittle when the temperature is lowered. This phenomenon is called ductile-to-brittle behaviour and happens at the nil-ductility temperature (NDT), also named nil ductility transition temperature (NDTT) or ductile-brittle transition temperature (DBTT) which is different for each metal [61].

To measure the ductility of the materials, the Charpy test is used. If the reduction in area at the fracture location and the total elongation of the sample are considered, the tensile test can be applied as well. These tests can be conducted at different temperatures in order to analyse the ductile-to-brittle behaviour of the materials and estimate their NDT. For instance, the yield stress value of AISI 430 stainless steel increases faster than the tensile stress approaching the liquid nitrogen temperature (77 K at atmospheric conditions [58]). This means that this metal becomes brittle and not suitable for cryogenic applications [172]. Contrarily, 5086 aluminium has the opposite behaviour and increases its ductility at the same temperature. In general, metals used at cryogenic temperatures are metals with face-centred cubic (FCC) crystal structure such as aluminium, copper, nickel and some of their alloys and austenitic stainless steel [61].

Usually, the ductile-to-brittle behaviour is analysed by holding the metal in air. It would be interesting to investigate this behaviour for metals suitable for hydrogen service by placing them in contact with hydrogen. In 2008, Deimel and Sattler [173] demonstrated the influence of temperature and pressure on hydrogen embrittlement. Firstly, different stainless steels at −253 °C and ambient pressure were tested immersed in liquid hydrogen and in helium for comparison. Secondly, the steels were examined at 22 °C, 60 °C, 100 °C and 9 MPa in gaseous hydrogen and helium. As result, the reduction of area at fracture was more significant for the stainless steels tested in $LH_2$ and $GH_2$ than in helium at −253 °C, 22 °C and 60 °C. On the other hand, no critical variations in steels ductility were measured at 100 °C. Moreover, the authors compared the composition of the samples and concluded that nickel together with carbon and nitrogen should be considered when hydrogen embrittlement might manifest [173]. It seems that the hydrogen equipment employed at cryogenic temperature is susceptible to a sort of superposition of the low temperature embrittlement and hydrogen damage. Hence, during the design and maintenance phases, the influence of all these phenomena must be considered.

### *Thermal contraction*

Hydrogen equipment, especially for $LH_2$, is often subjected to thermal stresses. The coefficient of thermal expansion (CTE) is a characteristic of the material and depends on the operative temperature. This coefficient must be always considered during the design of components and systems. The majority

of the materials reduce their volume by decreasing the temperature. The CTE is not linear, usually the 90% of the total contraction take place between room temperature (298 K) and 77 K (nitrogen boiling point) [61]. In the following, the thermal stresses caused by dimensional change and thermal gradients were described.

*Stresses cause by dimensional change*

Usually, these stresses derive from thermal contraction due to the employment of the materials at cryogenic temperatures. For instance, the internal vessel of a double walled $LH_2$ tank must contract or expand freely during the filling and discharging phases respectively, otherwise tank failures might occur due to internal generated stresses. Furthermore, the suspension system and the interconnecting piping must be designed in order to accommodate the dimension variations of the inner shell after several contraction and expansion cycles [61]. One of the main issues for the $LH_2$ tanks is the shifting of the perlite powder in the vacuum jacket after the thermal contraction of the inner vessel. During the discharge of the $LH_2$, the inner tank expansion presses the powder which did not flow back to the original position. This phenomenon is known as perlite compaction and there are several solutions to overcome this problem. For example, a soft bat can be applied on the outer surface of the inner tank or a proper design of the support rod system [61]. The $LH_2$ vacuum-jacket pipe is another component that must be able to properly deform as well. The flexibility of the pipe can be increased through the installation of elbows, "U" bends and expansion bellows.

*Stresses caused by thermal gradients*

Different components, part of the hydrogen equipment, are subjected to thermal gradient during the filling and emptying operations or at steady state. The supporting rods of the inner tank in a $LH_2$ vessel are one example of the steady state gradient. In fact, one end of the beam is in contact with the outer vessel at ambient temperature while the other side is jointed to the inner shell reaching virtually a cryogenic temperature.

Three parameters which can influence the stresses generated by thermal gradients are the rate of cooling, thermal conductivity and thickness of the cooled material. A fatal combination of these parameters can provoke undesired stresses which might lead to the component failure. It was estimated that for a stainless steel flange, the thermal gradient generated by a $LH_2$ flow can provoke a compression and a tension of the outside and inside of the component respectively [61]. Thermal conductivity and thickness of the material can be selected during the design phase, while the cooling rate depends by the cryogenic flow rate setting during the operational phase. For lower-boiling cryogens such as hydrogen, a pre-cooling phase with liquid nitrogen or cold gaseous hydrogen is required. For instance, the bunkering duration for the $LH_2$ fuelled ferry S.F. Breeze estimated in Ref. [174] is hereby reported. The researchers had foreseen 40 min for the transferring line cooldown, 30 min for the $LH_2$ transfer and 30 min for purge and pipes warm-up before disconnecting.

Another issue during the cooldown of the long transfer lines is the two-phase hydrogen flow regime inside the pipe. The bottom of the tube, where the liquid phase is flowing, becomes cold faster than the top of the pipe and it tends to contract. A thermal gradient is generated again in the pipe section making it bow upward in the middle and generating unwanted stress both in the pipe and its supports [175]. To avoid bowing, the $LH_2$ flow should be higher than a lower limit in order to reduce the vapor phase. Another solution to avoid the two-phase flow is to cooldown the pipe by means of the BOG formed in the storage tank prior the $LH_2$ flow.

### *Material behaviour during fatigue cycles*

A fundamental aspect that must be taken into account during the design of a mechanical component is its fatigue life. In 2008, Murakami et al. [176] investigated the hydrogen embrittlement mechanism in fatigue of austenitic stainless steels. The authors concluded that the cause of HE is not the decohesion mechanism but the hydrogen diffusion and concentration to and at the crack tips respectively. Furthermore, hydrogen increases the fatigue crack growth rates and depends on cyclic load frequency [176]. In 2010, Nakamura et al. [177] investigated the degradation of fatigue properties of different metals in high pressure hydrogen environment. For comparison, the authors exposed the different materials to an argon environment as well. After the tests, the authors noted that the fatigue life of stainless steel 316 L was almost not affected by the hydrogen atmosphere compared with argon environment. On the other hand, the fatigue lives of the stainless steels A286 and 304 were shorter in hydrogen than in argon [177].

In [178], San Marchi et al. demonstrated the influence of hydrogen environment in reducing the fatigue life in the low-cycle regime of different grade austenitic stainless steel at different values of pressure and temperature, while hydrogen has no influence in high-cycle or very high-cycle regime. Differently, Iijima et al. [179] proved that the fatigue life in the high-cycle regime of austenitic stainless steels is increased at low temperature and is not affected by hydrogen. These studies demonstrate the need for further investigations on this topic.

## Material selection

As mentioned earlier, material selection is the base of the design phase of hydrogen equipment. The materials suitable for hydrogen applications must be resistant to hydrogen damage as well as to cryogenic conditions in case of $LH_2$ and $SLH_2$. In Table 11, the material compatible with hydrogen are collected by indicating if they are also suitable for cryogenic service.

In Table 12, the materials most indicated for the main components of hydrogen equipment were listed.

Further indications should be followed by hydrogen equipment designers and operators. For instance, the insulating materials such as powders or MLI must be composed of non-combustible materials for safety reasons (danger of

**Table 11 – Materials compatible with hydrogen (adapted from Ref. [85]).**

| Material | $GH_2$ | $CcGH_2/LH_2/SLH_2$ |
|---|---|---|
| Aluminium and its alloys | Yes | Yes |
| Austenitic stainless steels with >7% nickel (such as, 304, 304 L, 308, 316, 321, 347) | Yes | Yes |
| Copper and its alloys (brass, bronze, and copper-nickel) | Yes | Yes |
| Titanium and its alloys | Yes | Yes |
| Poly-chloro-tri-fluoro-ethylene (PCTFE or Kel-F®) | Yes | Yes |
| Poly-tetra-fluoro-ethylene (PTFE or Teflon®) | Yes | Yes |
| Carbon steels | Yes | No |
| Low-allow steels | Yes | No |
| Chloroprene rubber (Neoprene®) | Yes | No |
| Dacron® | Yes | No |
| Fluorocarbon rubber (Viton®) | Yes | No |
| Mylar® | Yes | No |
| Nitrile (Buna-N®) | Yes | No |
| Polyamides (Nylon®) | Yes | No |

explosion). Moreover, clad materials can be used in hydrogen technology, but they may be difficult to weld. Furthermore, welding is susceptible to hydrogen embrittlement in all hydrogen environments. Finally, during the cryogenic hydrogen equipment design, room temperature material properties must be considered since the materials strengths tends to increase as their temperature is lowered and they also operate at room (or higher) temperature during their life.

## Relevant expertise

In this section, the results of the systematic review on loss of integrity of hydrogen technologies are presented. This allows quantifying what has been done in the literature as well as demonstrating that this topic is multidisciplinary and includes chemistry, electrochemistry, nuclear science technology, material science, among the main fields. In particular, a precise overview of the loss of integrity of hydrogen equipment was achieved. After the application of the filters described in the methodology section, a total of 266 papers, written by 795 different authors, was found. As previously mentioned, no limitations on the publication year were adopted. Although the time span of the resulted papers goes from 1973 to 2019, as few as 7 papers were written before 2000. The publication years trend, illustrated in Fig. 6, indicates how the interest in this topic has strongly grown in the last 12 years.

Fig. 7 depicts the authors with the highest number of publications in this field. The first two authors are Venetsanos from the National Center for Scientific Research Demokritos and Molkov from the University of Ulster. They both have published 15 articles and studied the consequences of hydrogen accidents such as dispersion, fires and explosions, focusing on the numerical modelling.

**Table 12 – Materials suitable for the hydrogen equipment (adapted from Ref. [85]).**

| Component | $CGH_2$ | $CcGH_2/LH_2/SLH_2$ |
|---|---|---|
| Valves | Appropriate material[a] | Forged, machined, and cast valve bodies (304 or 316 stainless steel, or brass) with extended bonnet, and with other materials inside |
| Fittings | Appropriate material[a] | Stainless steel bayonet type for vacuum jackets |
| O-rings | Appropriate material[a] | Stainless steel, Kel-F®, or Teflon® |
| Gaskets | Appropriate material[a] | Soft Aluminium, lead, or annealed copper between serrated flanges; Kel-F®; Teflon®; glass-filled Teflon® |
| Flexible hoses | Stainless steel braided with Teflon-lining | Convoluted vacuum jacketed 316 or 321 stainless steel |
| Rupture disk assembly | 304, 304 L, 316, or 316 L stainless steel | 304, 304 L, 316, or 316 L stainless steel |
| Piping | 300 series stainless steel, carbon steel [180] | 304, 304 L, 316, or 316 L stainless steel |
| Outer tank of Dewar or tank ($CGH_2$) | 304, 304 L, 316, 316 L stainless steel, carbon fibre epoxy | 304, 304 L, 316, or 316 L stainless steel |
| Inner tank of Dewar | – | austenitic chrome-nickel steel with a high nickel content; aluminium alloys with very good weldability; copper and copper alloys, fcc metals |
| Insulation | – | Rockwool, perlite, mylar, aluminium and fiberglass |
| Lubricants | Dupont Krytox 240AC, Fluoramics OXY-8, Dow Corning DC-33, Dow Corning FS-3452, Bray Oil Braycote 601, General Electric Versilube, Houghton Cosmolube 5100, Braycote 640 AC, Dupont GPL 206, Halocarbon Series 6.3 oil, and Kel-F® oil | PTFE, PTFE carbon, PTFE bronze, fiberglass-PFTE graphite [60]. Graphite and molybdenum disulfide permit only very limited service life for bearings [181]. |

[a] Different commercial materials and product compatible with gaseous hydrogen at different conditions are available.

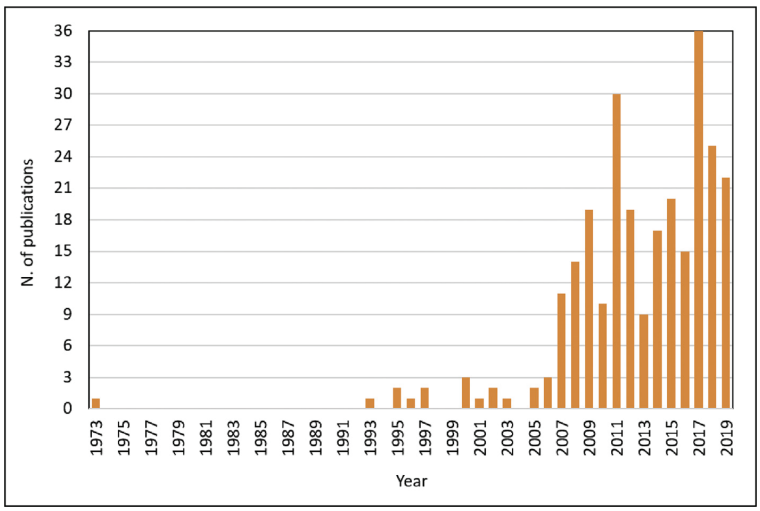


**Fig. 6 – Publication years of the selected papers.**

However, Molkov is not part of the top ten authors with the largest number of citations depicted in Fig. 8. The labels inside the bars of the chart indicate the number of publications per author in this field. Considering the authors with a minimum number of three papers, Venetsanos is the most cited one (263 times). Among the most cited authors, the researcher with the lowest number of publications is Xu with barely three articles but more than 150 citations.

The co-authorship network maps are shown in Fig. 9 and Fig. 10. Authors with fewer than three papers on this topic were excluded from these maps, and only the largest set of connections was reported. A total of 46 authors are indicated on these maps, showing their co-authorship links. In the first picture, each item (author) is weighted on the number of publications, whereas the number of citations is the weight type in the second figure. For this reason, the dimensions of the circles in the pictures clearly vary when the type of weight is modified. Moreover, the network map is formed by ten different clusters distinguished by diverse colours, which were created based on the author collaborations. In this case, one of the drawbacks of these maps is that the authors names with fewer publications (small circles) are omitted from the taken screenshot.

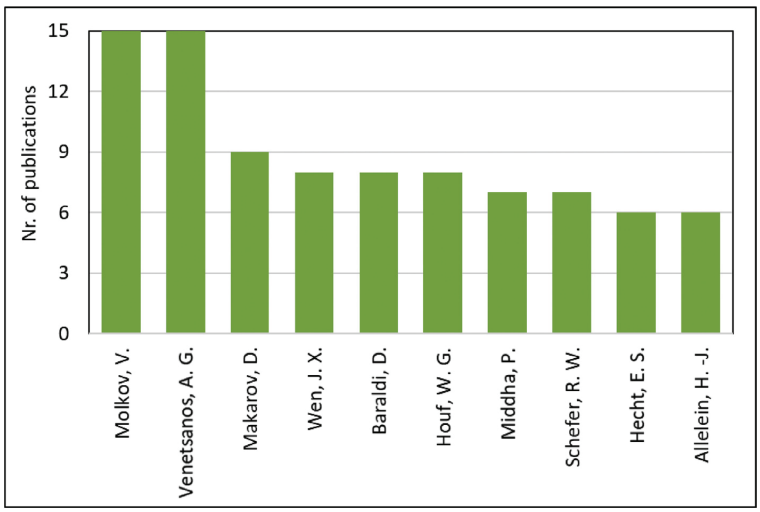


**Fig. 7 – Authors with the highest number of publications in the loss of integrity of hydrogen equipment field.**

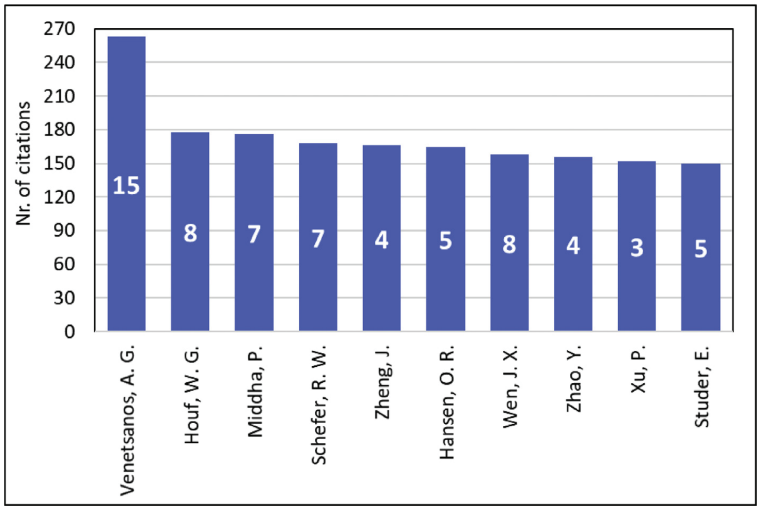


**Fig. 8 – Authors with the highest number of citations in the loss of integrity of hydrogen equipment field. The number of publications per author is written inside the bars.**

The co-authorship maps were also built for countries where the research institutions are sited and have published more than five articles. These maps are shown in Fig. 11 and Fig. 12. In both pictures, the weight was the number of publications, but in the latter image, this number was divided for the number of researchers working in the country. The number of researchers (academic and industrial) for the considered countries in the period 2005–2017 was retrieved from Ref. [182]. Then, an average over this time frame was calculated and reported in Table 13. As result from this sort of normalisation, Greece was the country with the highest number of publications per researcher, followed by Norway.

Finally, the co-occurrence network map was built for all types of keywords with a minimum of 7 occurrences in the considered papers. This map is depicted in Fig. 13 indicating

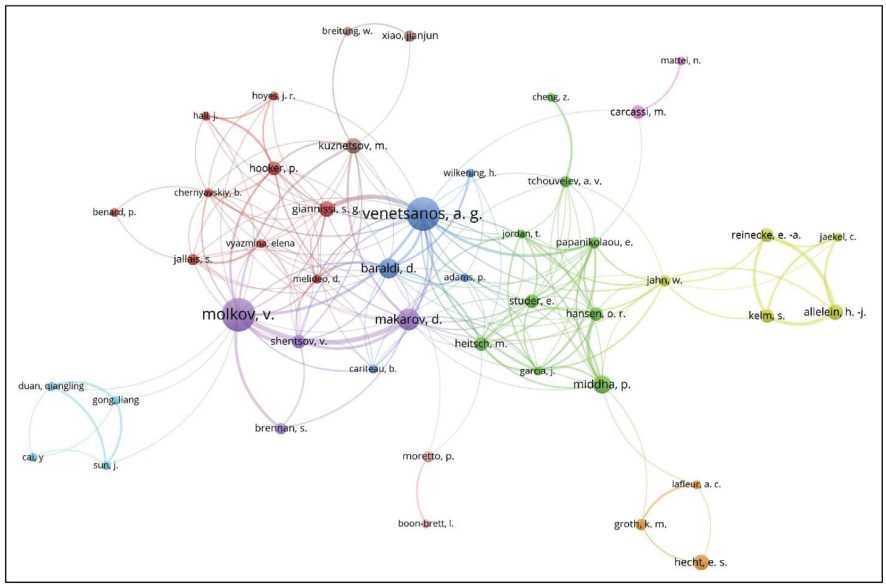


**Fig. 9 – Largest set of connection of the co-authorship network map weighted on the number of publications. Only authors with more than three publications were included.**

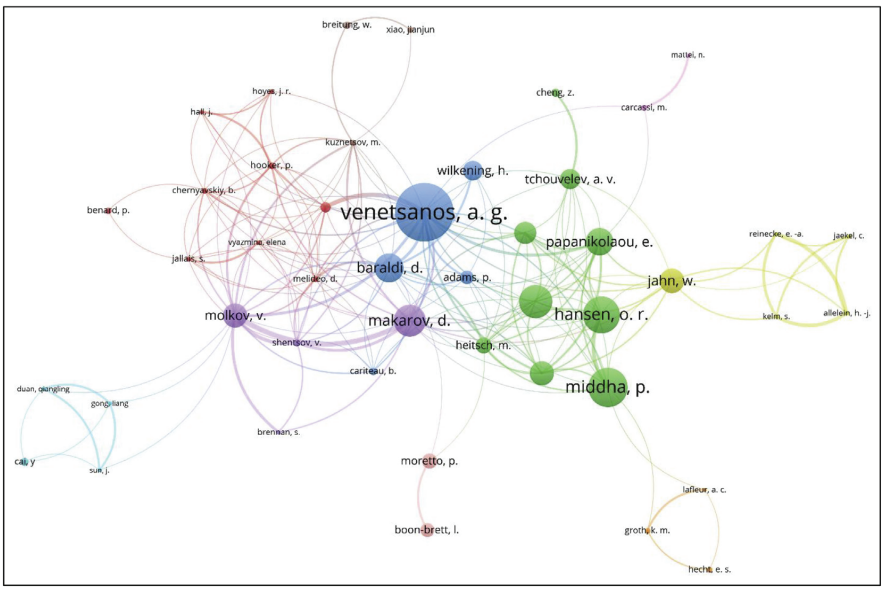


**Fig. 10 – Largest set of connection of the co-authorship network map weighted on the number of citations.**

that after "hydrogen", the keywords with the highest number of occurrences are "hydrogen safety", "dispersion" and "hydrogen embrittlement". Dispersion is a consequence of the loss of integrity, while hydrogen embrittlement is one of the phenomena that lead to it. Hence, both causes and consequences were examined in the analysed works, but they are often studied separately.

The research areas were considered an important parameter as well, enabling to enlarge the overview on this topic. Fig. 14 represents the research areas covered by the majority of the papers resulted from the SR. As evident from Fig. 14,

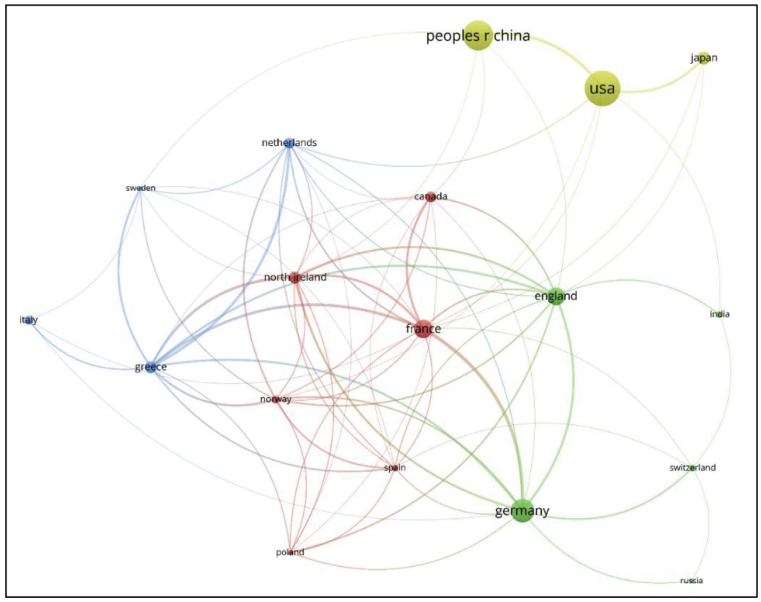


**Fig. 11 – Countries network maps weighted on the number of documents.**

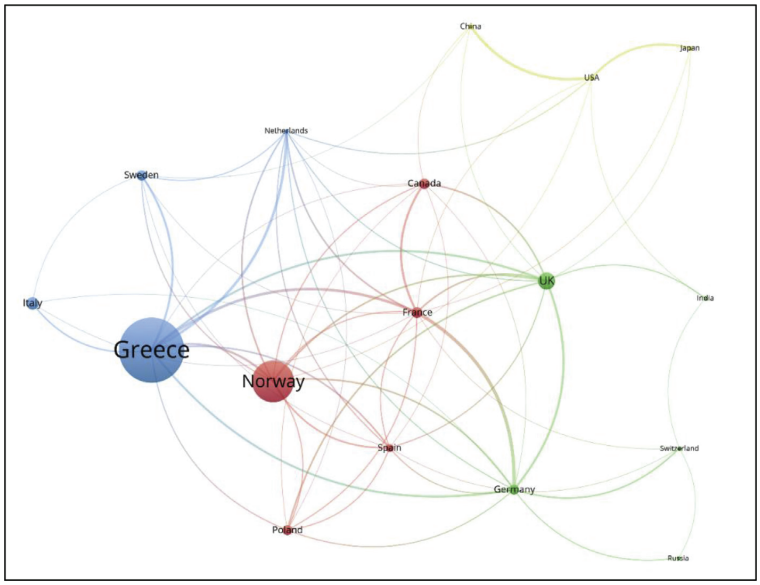


**Fig. 12 – Countries network map normalized on the number of researchers for each nation.**

there are different research fields in which the hydrogen loss of integrity related issues have been investigated. However, the safety field is missing from the chart because is not defined as a research area by the Web of Science platform and is thus enclosed in the other fields. As previously mentioned, the safety key word or a related word appears in all the selected queries. Therefore, the safety was assumed to be the research area common to all the papers. This means that each article can cover more than one research field. As prove of it, the sum of the papers reported in Fig. 14 is higher than the total number of studies found in the SR (266 papers).

All these examinations bring to the conclusion that the hydrogen loss of integrity is a multidisciplinary topic. The lack of collaboration between authors involved in different research fields is a problem that emerged from this multidisciplinary aspect. This is highlighted in Fig. 15 where the co-authorship network map is displayed with all the clusters demonstrating the absence of links between several research groups.

## Discussion

The hydrogen life cycle demonstrated the hydrogen flexibility. In particular, it can be produced from water, different hydrocarbons (especially methane), coal, biomass, hydrides, several types of waste and raw materials, by means of many techniques. These methods differ in costs, efficiency and $CO_2$ production. Usually, the cheapest techniques, such as steam reforming and gasification, require a carbon capture storage since $CO_2$ is generated during these processes. In the last two decades, the focus has been placed on generate hydrogen in a renewable and clean manner. Different techniques are able to achieve this goal. For instance, hydrogen can be produced through electrolysis by exploiting the renewable energy surplus, mainly from solar and wind technologies. New challenges such as the cost reduction, are faced during the development of new renewable and clean techniques. An effort has been made to identify non-noble metal catalysts in order to lessen the initial costs of many hydrogen production methods. The low density of hydrogen may represent a volume issue in some applications. For this reason, different storage solutions were studied in the past and some of these are still in a development phase. Hydrogen is stored under

**Table 13 – Number of researchers in the considered countries [182].**

| Country | Nr. of researchers | Nr. of publications by $10^5$ researchers |
|---|---|---|
| Canada | 156,924 | 9.6 |
| France | 260,811 | 1.0 |
| Germany | 361,726 | 9.1 |
| Greece | 28,971 | 58.7 |
| India | 366,445 | 2.5 |
| Italy | 117,616 | 11.1 |
| Japan | 667,762 | 2.7 |
| Netherlands | 74,223 | 20.2 |
| Norway | 29,072 | 37.8 |
| Popular Rep. of China | 1,511,812 | 2.8 |
| Poland | 78,073 | 9.0 |
| Russia | 440,282 | 1.4 |
| Spain | 123,460 | 7.3 |
| Sweden | 63,924 | 9.4 |
| Switzerland | 39,763 | 22.6 |
| UK | 273,160 | 15.4 |
| USA | 1,288,682 | 3.9 |

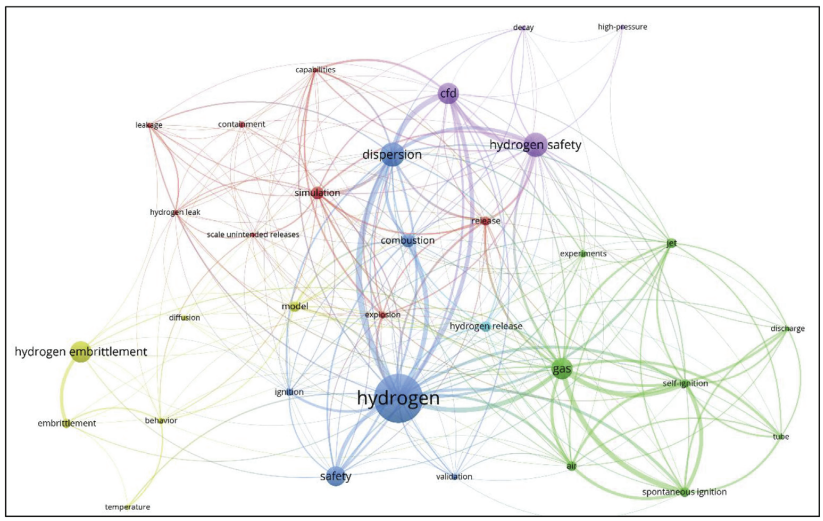


**Fig. 13 – Co-occurrence map for all types of keywords.**

different forms which are compressed gas, liquefied (cryogenic), cryo-compressed, and bounded to other substances through physical adsorption or chemical absorption. A new trend in hydrogen production and storage consists in generate hydrogen from water onboard of boats through electrolysers, compress and store it in appropriate pressurized vessels. Thus, the hydrogen storage volume can be reduced, and the surplus of electric energy produced onboard is exploited. An example of this innovative solution is the Energy Observer, the self-sustained catamaran previously mentioned [50]. Beyond the conventional hydrogen transportation methods (pipelines, road and rail) the maritime solution has been recently considered and the development of $LH_2$ tanker ships started few years ago. Hydrogen is suitable as clean fuel for a multitude of applications, and it seems clear that it could potentially replace the traditional hydrocarbons currently employed. Although the fuel cells are foreseen in the majority of the applications in order to increase the overall system efficiency, hydrogen can be used as fuel in available technologies such as ICE and GT reducing the capital costs of the systems.

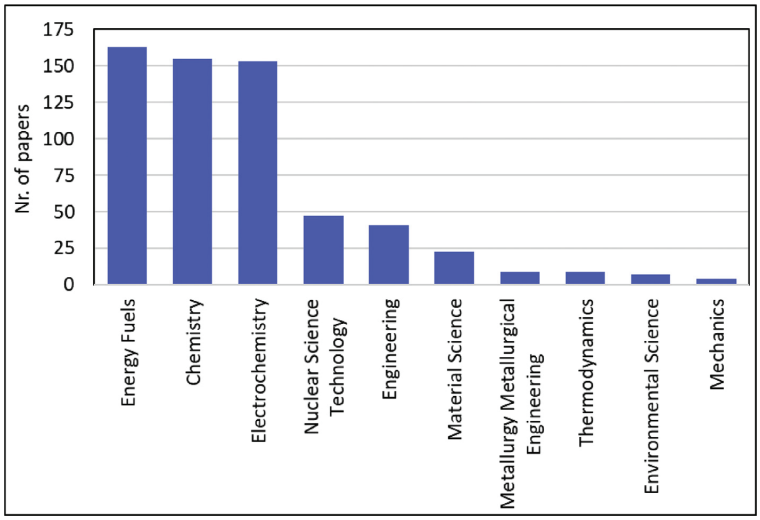


**Fig. 14 – Research areas covered by the papers found during the SR.**

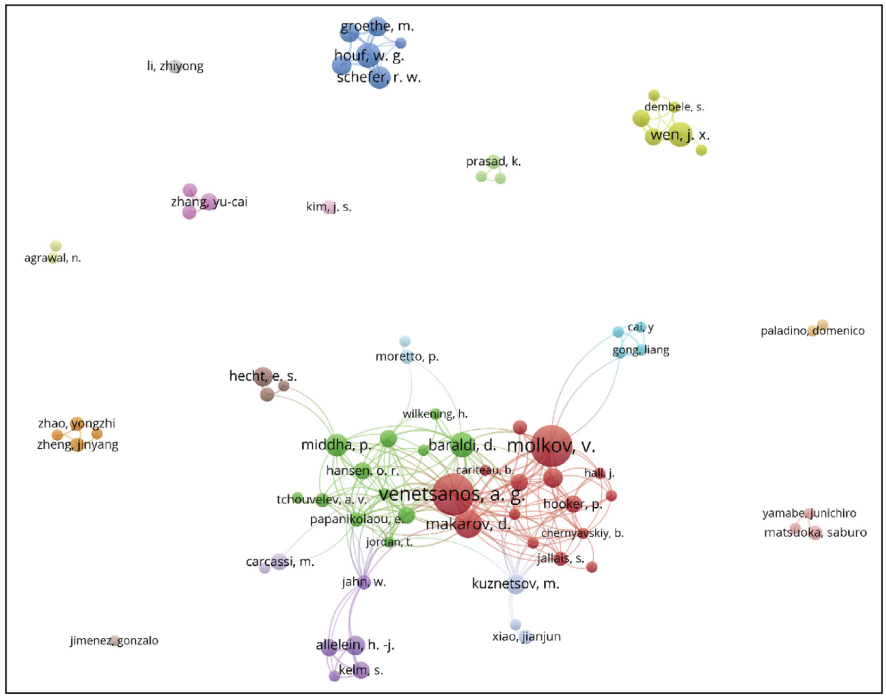


**Fig. 15 – Co-authorship network map weighted on the number of documents. Only authors with more than three publications were included.**

Hydrogen properties demonstrate its highly flammability and aptitude to escape from the storage equipment through undesired microscopic holes in the metal or in sealing and gasket. There are also several characteristics which make hydrogen safer than other conventional fuels such as the low thermal radiation of its flame and buoyancy in air. It must be highlighted again that it is not toxic nor corrosive and harmless for the environment. For this reason, all its properties must be considered for a thorough safety comparison between hydrogen and the fuels already employed in each application. Regarding the safety aspects, although it seems as safe as the traditional fuels, there is still a knowledge gap on few phenomena and consequences. In particular, the probability and formation of two physical explosions, BLEVE and RPT, are still not clear for $LH_2$. The consequences of these explosions and those of other phenomena have not been estimated yet for hydrogen. Currently, two important projects, $SH_2IFT$ and PRESLHY, are aiming to cover this knowledge gap. Furthermore, these projects demonstrate the growing interest in $LH_2$ as storage solution.

The loss of integrity (LOI) phenomena were described in this study in order to comprehend under which conditions they manifest, according to which mechanisms. It has been highlighted that an integrated theory able to explain all the LOI phenomena has not been proposed yet. Additional effort should be made to find a common thread between the mechanisms and understand which are the parameters that influence more the LOI occurrence. Moreover, other phenomena such as low temperature embrittlement and thermal contraction must be taken into account for $LH_2$. It is fundamental to investigate further on the fatigue properties of hydrogen equipment since a significant reduction in fatigue lifetime of different metals suitable for hydrogen service was estimated by different authors. Several accidents can be prevented by broadening the knowledge of these phenomena and considering them during both the design and maintenance phases. In the worst-case scenario, a loss of containment of hydrogen equipment might happen by neglecting these phenomena. For instance, two of the most recent hydrogen accidents occurred in June 2019 in a public hydrogen refuelling station in Norway [63] and in a chemical plant in California [64] were both provoked by a gas leakage with consequent explosion and fire. As additional aftermath, the service of many hydrogen refuelling stations was ceased as preventing measure for few months, and then several hydrogen fuelled cars were brought to a halt. These ruinous events witness the urgency for safety countermeasures to reassure the public opinion and future investors, and thus achieve a significant growth of the hydrogen technologies.

The material selection for hydrogen equipment is directly related with the LOI phenomena and fundamental during the design phase. There are just few materials suitable for all hydrogen applications. Usually these materials are expensive alloys. For this reason, a careful analysis must be conducted

for each utilization in order to minimize the costs and maximize the safety of the system. In Ref. [84] the authors demonstrated as the hydrogen compatibility with materials influences the hydrogen codes and standards. The authors confirmed that this compatibility is affected by the mechanical (structural integrity) and environmental variables (time, temperature, pressure), beyond the material conditions. All these aspects render the material selection a complex and critical analysis.

The systematic review (SR) on the loss of integrity (LOI) of hydrogen equipment resulted in a heterogeneous batch of papers. This heterogeneity is ought to the different research areas touched by the articles. Virtually all the works are focussed on hydrogen safety, marking its importance. Moreover, these articles accurately cover all the aspects described in the first sections of this study. For instance, the hydrogen service in new applications and the importance of appropriate safety measures were considered in Ref. [183]. Briottet et al. [184] expressed concern for the LOI phenomena, in particular for the hydrogen embrittlement and the existing knowledge gap on their formation mechanisms. This issue was highlighted also in the Hydrogen Damage Mechanisms section. Furthermore, the relevancy of the material selection during the apparatus design was clearly elucidated in Ref. [185]. This probably represents the main approach to prevent accidents provoked by the LOI phenomena. This matter is also related to the uncertainty about the material behaviour under fatigue cycles in hydrogen environment discussed in the Material Behaviour during Fatigue Cycles section, issue that must be considered together with the material behaviour during the design phase. The variety of these issues completely explain and highlight the multidisciplinary of the LOI topic.

Another compelling result of the SR is the publication years trend. In particular, the research revealed the exponential growth in the number of papers published in the last two decades. This may be an outcome of the several hydrogen safety projects promoted worldwide during this period. Most of the publications were written by scientists who work in European countries, as well as in North America (USA and Canada) and Asia (China, Japan and India). By normalising the amount of publications on the number of researchers, countries as Greece and Norway seem the most involved in this type of research. This can be explained by the fact that these two countries are currently involved in a number of European projects on hydrogen safety. Moreover, the Norwegian government policy is directed toward a sustainable and renewable energy mix by investing and supporting this research field.

The first achievement of this study is to appropriately confirm the information gathered in the first part of the paper through the SR. Therefore, the novelty of this work was respected, by successfully applying for the first time a well-known literature review technique to a complex topic: the hydrogen LOI. Lastly, a limitation emerged from the network maps, indicating that the collaborations between research groups from different fields are often missing. This lack is exacerbated by the multidisciplinary of this topic. It is believed that participation by experts from different areas in research projects related to this critical topic can significantly improve its knowledge. It can be concluded that various hydrogen related topics were addressed in this study, and the common thread between these issues is represented by related safety implications, which must never be neglected when hydrogen is employed. The safety aspects influence the costs, government policies, regulations and public opinion which can be obstacles against the hydrogen technologies distribution [105]. Therefore, the enhancement of hydrogen safety is suggested as result of this study since it can directly promote a broad implementation of this fuel.

## Conclusion and suggestions

In this study, a broad overview on the LOI of hydrogen equipment was presented. The innumerable hydrogen applications were described in the Life Cycle section, demonstrating the importance of this substance as future fuel. Currently, the hydrogen potential as clean renewable fuel cannot be compared with other substances or technologies. Its physical and chemical properties were discussed in the Properties and Safety section, clarifying why the safety aspects must never be neglected when hydrogen is employed in any kind of application. In Loss of Integrity Phenomena section, the focus was strongly placed on the LOI phenomena for hydrogen equipment, which are the main causes of accidents. The material selection, the fundamental aspect required to prevent the LOI phenomena formation, was examined in the Material Selection section. Finally, an SR on the LOI of hydrogen equipment was conducted in the Relevant Expertise section to confirm the aforementioned issues.

It can be concluded that safety is the common thread for all the topics considered in the paper, and it is one of the main aspects that can directly influence the future hydrogen technology distribution and development. LOI topic related to the hydrogen technologies was demonstrated to be a multidisciplinary topic. A limitation represented by the dearth of collaboration between the research groups from different areas was highlighted. For this reason, future research projects on the hydrogen LOI topic should include scientists and researchers from different fields. It is thought that an extensive participation by different kind of experts would be beneficial to enlarge the knowledge on this topic. Moreover, the government policies should support the development of sustainable and renewable technologies such as hydrogen during the emerging phase. Novel projects and investments able to increase the awareness on hydrogen safety may be initiated as consequence of the political decisions. Currently, the entire world is involved in an unprecedented crisis which involve the energy sector as well. It is believed that the hydrocarbons debacle could be one of the most suitable opportunities to promote the hydrogen technologies in a safe and responsible way.

## Declaration of competing interest

The authors declare that they have no known competing financial interests or personal relationships that could have appeared to influence the work reported in this paper.

## Acknowledgment

This study is part of the $SH_2IFT$(Safe Hydrogen Fuel Handling and Use for Efficient Implementation) project [grant number: 280964/E20] and the authors would like to acknowledge the financial support of the Research Council of Norway.

## REFERENCES

[1] International Energy Agency (IEA). Hydrogen Global Trends and Outlook for Hydrogen. 2017.
[2] Fumey B, Buetler T, Vogt UF. Ultra-low NOx emissions from catalytic hydrogen combustion. Appl Energy 2018;213:334–42. https://doi.org/10.1016/J.APENERGY.2018.01.042.
[3] Luo Q, Hu J-B, Sun B, Liu F, Wang X, Li C, et al. Experimental investigation of combustion characteristics and NOx emission of a turbocharged hydrogen internal combustion engine. Int J Hydrogen Energy 2019;44:5573–84. https://doi.org/10.1016/J.IJHYDENE.2018.08.184.
[4] Shiva Kumar S, Himabindu V. Hydrogen production by PEM water electrolysis – a review. Mater Sci Energy Technol 2019;2:442–54. https://doi.org/10.1016/J.MSET.2019.03.002.
[5] Ausfelder F, Bazzanella A. Hydrogen in the chemical industry. In: Stolten D, Emonts B, editors. Hydrog. Sci. Eng. Mater. Process. Syst. Technol. Wiley-VCH Verlag; 2016. p. 19–39. https://doi.org/10.1002/9783527674268.ch02.
[6] Najjar YSH. Hydrogen safety: the road toward green technology. Int J Hydrogen Energy 2013;38:10716–28. https://doi.org/10.1016/J.IJHYDENE.2013.05.126.
[7] Fuel Cell Technologies Office. Tri-Generation Success Story. 2016.
[8] EnergyOr. Energy or Demonstrates Multirotor UAV Flight OF 3 hours, 43 minutes. 2015. http://energyor.com/news/post:30. [Accessed 27 February 2019].
[9] Alstom fuel cell trains enter service in Germany. Fuel Cells Bull 2018;2018:1. https://doi.org/10.1016/S1464-2859(18)30310-9.
[10] ABB. ABB, SINTEF and Fiskerstrand test fuel cells for the world's first conversion of a hydrogen hybrid ferry. 2019. https://new.abb.com/news/detail/18654/abb-sintef-and-fiskerstrand-test-fuel-cells-for-the-worlds-first-conversion-of-a-hydrogen-hybrid-ferry. [Accessed 3 December 2019].
[11] Jovanović AS, Baloš D. INTeg-Risk project: concept and first results. J Risk Res 2013;16:275–91. https://doi.org/10.1080/13669877.2012.729516.
[12] Paltrinieri N, Tugnoli A, Buston J, Wardman M, Cozzani V. Dynamic procedure for atypical scenarios identification (DyPASI): a new systematic HAZID tool. J Loss Prev Process Ind 2013;26:683–95. https://doi.org/10.1016/J.JLP.2013.01.006.
[13] Ustolin F, Song G, Paltrinieri N. The influence of H2 safety research on relevant risk assessment. Chem Eng Trans 2019;74. https://doi.org/10.3303/CET1974233.
[14] Lowesmith BJ, Hankinson G. Qualitative risk assessment of hydrogen liquefaction. Storage and Transportation - Deliverable 2013;3(11).
[15] Sintef. SH2IFT - Safe Hydrogen Fuel Handling and Use for Efficient Implementation. https://www.sintef.no/projectweb/sh2ift/. [Accessed 2 September 2019].
[16] PRESLHY, Prenormative Research for Safe Use of Liquid Hydrogen, Research and Innovation Action Supported by the FCH JU 2.0 2019. https://preslhy.eu/(accessed June 22, 2019).
[17] Ferrari R. Writing narrative style literature reviews. Med Writ 2015;24:230–5. https://doi.org/10.1179/2047480615z.000000000329.
[18] The Cochrane Collaboration. Glossary of Terms in The Cochrane Collaboration -. 2005., Version 4.2.5.
[19] Li J, Hale A. Output distributions and topic maps of safety related journals. Saf Sci 2016;82:236–44. https://doi.org/10.1016/J.SSCI.2015.09.004.
[20] Merigó JM, Miranda J, Modak NM, Boustras G, de la Sotta C. Forty years of Safety Science: a bibliometric overview. Saf Sci 2019;115:66–88. https://doi.org/10.1016/J.SSCI.2019.01.029.
[21] Knop V, Benkenida A, Jay S, Colin O. Modelling of combustion and nitrogen oxide formation in hydrogen-fuelled internal combustion engines within a 3D CFD code. Int J Hydrogen Energy 2008;33:5083–97. https://doi.org/10.1016/J.IJHYDENE.2008.06.027.
[22] Stahl W, Voss K, Goetzberger A. The self-sufficient solar house IN freiburg. Sol Energy 1994;52:111–25.
[23] Toshiba opens tokyo integrated hydrogen application center. Fuel Cells Bull 2017;9. https://doi.org/10.1016/S1464-2859(17)30297-3.
[24] Łukajtis R, Hołowacz I, Kucharska K, Glinka M, Rybarczyk P, Przyjazny A, et al. Hydrogen production from biomass using dark fermentation. Renew Sustain Energy Rev 2018;91:665–94. https://doi.org/10.1016/J.RSER.2018.04.043.
[25] Wang H, Xu J, Sheng L, Liu X, Lu Y, Li W. A review on bio-hydrogen production technology. Int J Energy Res 2018;42:3442–53. https://doi.org/10.1002/er.4044.
[26] Khzouz M, Gkanas EI, Girella A, Statheros T, Milanese C. Sustainable hydrogen production via LiH hydrolysis for unmanned air vehicle (UAV) applications. Int J Hydrogen Energy 2020;45:5384–94. https://doi.org/10.1016/J.IJHYDENE.2019.05.189.
[27] Chen W, Ouyang LZ, Liu JW, Yao XD, Wang H, Liu ZW, et al. Hydrolysis and regeneration of sodium borohydride (NaBH4) – a combination of hydrogen production and storage. J Power Sources 2017;359:400–7. https://doi.org/10.1016/j.jpowsour.2017.05.075.
[28] Tang C, Qu F, Asiri AM, Luoa Y, Sun X. CoP nanoarray: a robust non-noble-metal hydrogen-generating catalyst toward effective hydrolysis of ammonia borane. Inorg Chem Front 2017;4:659–62. https://doi.org/10.1039/C6QI00518G.
[29] Li K, Ma M, Xie L, Yao Y, Kong R, Du G, et al. Monolithically integrated NiCoP nanosheet array on Ti mesh: an efficient and reusable catalyst in NaBH4 alkaline media toward on-demand hydrogen generation. Int J Hydrogen Energy 2017;42:19028–34. https://doi.org/10.1016/J.IJHYDENE.2017.06.092.
[30] Tang C, Zhang R, Lu W, He L, Jiang X, Asiri AM, et al. Fe-doped CoP nanoarray: a monolithic multifunctional catalyst for highly efficient hydrogen generation. Adv Mater 2017;29:1602441. https://doi.org/10.1002/adma.201602441.
[31] Liu T, Liu D, Qu F, Wang D, Zhang L, Ge R, et al. Enhanced electrocatalysis for energy-efficient hydrogen production over CoP catalyst with nonelectroactive Zn as a promoter. Adv Energy Mater 2017;7:1700020. https://doi.org/10.1002/aenm.201700020.
[32] Wang W, Yang L, Qu F, Liu Z, Du G, Asiri AM, et al. A self-supported NiMoS4 nanoarray as an efficient 3D cathode for the alkaline hydrogen evolution reaction. J Mater Chem 2017;5:16585. https://doi.org/10.1039/c7ta05521h.
[33] Zhang R, Ren X, Hao S, Ge R, Liu Z, Asiri AM, et al. Selective phosphidation: an effective strategy toward CoP/CeO2 interface engineering for superior alkaline hydrogen evolution electrocatalysis. J Mater Chem 2018;6:1985. https://doi.org/10.1039/c7ta10237b.

[34] Liu T, Xie L, Yang J, Kong R, Du G, Asiri AM, et al. Self-standing CoP nanosheets array: a three-dimensional bifunctional catalyst electrode for overall water splitting in both neutral and alkaline media. ChemElectroChem 2017;4:1840–5. https://doi.org/10.1002/celc.201700392.
[35] Zhang Y, Liu Y, Ma M, Ren X, Liu Z, Du G, et al. A Mn-doped Ni2P nanosheet array: an efficient and durable hydrogen evolution reaction electrocatalyst in alkaline media. Chem Commun 2017;53:11048. https://doi.org/10.1039/c7cc06278h.
[36] Office of Energy Efficiency & Renewable Energy. U.S. Department Of Energy. Hydrogen Production: Thermochemical Water Splitting. 2019. https://www.energy.gov/eere/fuelcells/hydrogen-production-thermochemical-water-splitting. [Accessed 25 October 2019].
[37] Sigfusson TI. Pathways to hydrogen as an energy carrier. Philos Trans R Soc A 2007;365:1025–42. https://doi.org/10.1098/rsta.2006.1960.
[38] Air Products and Chemicals. How do we produce hydrogen today?. 2015. http://www.airproducts.com/industries/Energy/Power/Power-Generation/faqs.aspx. [Accessed 2 March 2019].
[39] Alvarez J, Kumagai S, Wu C, Yoshioka T, Bilbao J, Olazar M, et al. Hydrogen production from biomass and plastic mixtures by pyrolysis-gasification. Int J Hydrogen Energy 2014;39:10883–91. https://doi.org/10.1016/J.IJHYDENE.2014.04.189.
[40] Office of Energy Efficiency & Renewable Energy. U.S. Department Of Energy. Hydrogen Production: Biomass Gasification. 2019. https://www.energy.gov/eere/fuelcells/hydrogen-production-biomass-gasification. [Accessed 25 October 2019].
[41] Hosseini SE, Wahid MA. Hydrogen production from renewable and sustainable energy resources: promising green energy carrier for clean development. Renew Sustain Energy Rev 2016;57:850–66. https://doi.org/10.1016/J.RSER.2015.12.112.
[42] Zhang Q, Zhang Z. Biological hydrogen production from renewable resources by photofermentation. Adv Bioenergy 2018;3:137–60. https://doi.org/10.1016/BS.AIBE.2018.03.001.
[43] Dini D. Hydrogen production through solar energy water electrolysis. Int J Hydrogen Energy 1983;8:897–903. https://doi.org/10.1016/0360-3199(83)90113-1.
[44] Siemens to supply first solar-driven hydrogen electrolysis for Dubai. Fuel Cells Bull 2018;2018:11–2. https://doi.org/10.1016/S1464-2859(18)30092-0.
[45] Japanese project under way to supply wind-produced hydrogen for fuel cell forklifts. Fuel Cells Bull 2017;2017:8. https://doi.org/10.1016/S1464-2859(17)30294-8.
[46] Asahi Kasei 'green' hydrogen demos under way in Germany, Japan. Fuel Cells Bull 2018;2018:7–8. https://doi.org/10.1016/S1464-2859(18)30205-0.
[47] Construction begins on Fukushima Hydrogen Energy Research Field. Fuel Cells Bull 2018;2018:9. https://doi.org/10.1016/S1464-2859(18)30332-8.
[48] Fujishima A, Honda K. Electrochemical photolysis of water at a semiconductor electrode. Nature 1972;238:37–8. https://doi.org/10.1038/238037a0.
[49] Islam MH, Burheim OS, Pollet BG. Sonochemical and sonoelectrochemical production of hydrogen. Ultrason Sonochem 2019;51:533–55. https://doi.org/10.1016/J.ULTSONCH.2018.08.024.
[50] Green-power Energy Observer boat plans round-the-world trip. Fuel Cells Bull 2016;2016:4. https://doi.org/10.1016/S1464-2859(16)30270-X.
[51] Race for Water electric catamaran sets off with Swiss Hydrogen tech. Fuel Cells Bull 2017;2017:5–6. https://doi.org/10.1016/S1464-2859(17)30144-X.
[52] Argonne National Laboratory. The Greenhouse Gases, Regulated Emissions, and Energy Use in Transportation Model (GREET) 1.8d1 2010.
[53] Melaina M, Penev M, Heimiller D. Resource Assessment for Hydrogen Production, Hydrogen Production Potential from Fossil and Renewable Energy Resources. 2013. NREL/TP-5400-55626.
[54] Charvin P, Stéphane A, Florent L, Gilles F. Analysis of solar chemical processes for hydrogen production from water splitting thermochemical cycles. Energy Convers Manag 2008;49:1547–56. https://doi.org/10.1016/j.enconman.2007.12.011.
[55] Zhong H, Wang H, Liu JW, Sun DL, Fang F, Zhang QA, et al. Enhanced hydrolysis properties and energy efficiency of MgH2-base hydrides. J Alloys Compd 2016;680:419–26. https://doi.org/10.1016/j.jallcom.2016.04.148.
[56] Nikolaidis P, Poullikkas A. A comparative overview of hydrogen production processes. Renew Sustain Energy Rev 2017;67:597–611. https://doi.org/10.1016/j.rser.2016.09.044.
[57] Diéguez PM, Ursúa A, Sanchis P, Sopena C, Guelbenzu E, Gandía LM. Thermal performance of a commercial alkaline water electrolyzer: experimental study and mathematical modeling. Int J Hydrogen Energy 2008;33:7338–54. https://doi.org/10.1016/j.ijhydene.2008.09.051.
[58] NIST. Nist. Chemistry WebBook 2019. webbook.nist.gov/. [Accessed 19 March 2019].
[59] Barthelemy H, Weber M, Barbier F. Hydrogen storage: recent improvements and industrial perspectives. Int J Hydrogen Energy 2017;42:7254–62. https://doi.org/10.1016/J.IJHYDENE.2016.03.178.
[60] Peschka W. Liquid Hydrogen - Fuel of the Future. 1st ed. Wien: Springer-Verlag; 1992. https://doi.org/10.1007/978-3-7091-9126-2.
[61] Edeskuty F, Stewart W. Safety in the Handling of Cryogenic Fluids. Springer Science +Business Media, LLC; 1996.
[62] Aceves SM, Espinosa-Loza F, Ledesma-Orozco E, Ross TO, Weisberg AH, Brunner TC, et al. High-density automotive hydrogen storage with cryogenic capable pressure vessels. Int J Hydrogen Energy 2010;35:1219–26. https://doi.org/10.1016/j.ijhydene.2009.11.069.
[63] Nel Hydrogen. Status and Q&A regarding the Kjørbo incident. 2019. https://nelhydrogen.com/status-and-qa-regarding-the-kjorbo-incident/. [Accessed 5 September 2019].
[64] Genovese M, Blekhman D, Dray M, Fragiacomo P. Hydrogen losses in fueling station operation. J Clean Prod 2020;248:119266. https://doi.org/10.1016/j.jclepro.2019.119266.
[65] U.S. DRIVE. Hydrogen Storage Tech Team Roadmap. 2017.
[66] DOE. Energy requirements for hydrogen gas compression and liquefaction as related to vehicle storage needs. 2009.
[67] Riis T, Sandrock G, Ulleberg Ø, Vie PJS. Hydrogen storage – gaps and priorities. HIA HCG Storage Pap; 2005.
[68] Ahluwalia RK, Hua TQ, Peng J-K. Fuel cycle efficiencies of different automotive on-board hydrogen storage options. Int J Hydrogen Energy 2007;32:3592–602. https://doi.org/10.1016/J.IJHYDENE.2007.03.021.
[69] U.S. Department of Energy. Technical Assessment: Cryo-Compressed Hydrogen Storage for Vehicular Applications. 2006.
[70] Tan Y, Zhu Y, Li L. Excellent catalytic effects of multi-walled carbon nanotube supported titania on hydrogen storage of a Mg-Ni alloy. Chem Commun 2015;51:2368–71. https://doi.org/10.1039/c4cc09350j.
[71] Schlegel MC, Többens D, Svetogorov R, Krüger M, Stock N, Reinsch H, et al. Conformation-controlled hydrogen storage in the CAU-1 metal-organic framework. Phys Chem Chem Phys 2016;18:29258–67. https://doi.org/10.1039/c6cp05310f.

[72] Kim J, Yeo S, Jeon J-D, Kwak S-Y. Enhancement of hydrogen storage capacity and hydrostability of metal–organic frameworks (MOFs) with surface-loaded platinum nanoparticles and carbon black. Microporous Mesoporous Mater 2015;202:8–15. https://doi.org/10.1016/J.MICROMESO.2014.09.025.
[73] Broom DP, Webb CJ, Fanourgakis GS, Froudakis GE, Trikalitis PN, Hirscher M. Concepts for improving hydrogen storage in nanoporous materials. Int J Hydrogen Energy 2019;44:7768–79. https://doi.org/10.1016/J.IJHYDENE.2019.01.224.
[74] Gangu KK, Maddila S, Mukkamala SB, Jonnalagadda SB. Characteristics of MOF, MWCNT and graphene containing materials for hydrogen storage: a review. J Energy Chem 2019;30:132–44. https://doi.org/10.1016/J.JECHEM.2018.04.012.
[75] Bellosta von Colbe J, Ares J-R, Barale J, Baricco M, Buckley C, Capurso G, et al. Application of hydrides in hydrogen storage and compression: achievements, outlook and perspectives. Int J Hydrogen Energy 2019;44:7780–808. https://doi.org/10.1016/J.IJHYDENE.2019.01.104.
[76] Andersson J, Grönkvist S. Large-scale storage of hydrogen. Int J Hydrogen Energy 2019;44:11901–19. https://doi.org/10.1016/J.IJHYDENE.2019.03.063.
[77] Niermann M, Beckendorff A, Kaltschmitt M, Bonhoff K. Liquid organic hydrogen carrier (LOHC) – assessment based on chemical and economic properties. Int J Hydrogen Energy 2019;44:6631–54. https://doi.org/10.1016/J.IJHYDENE.2019.01.199.
[78] Development Centre for, Systems Ship Technology and Transport. Perspectives for the Use of Hydrogen as Fuel in Inland Shipping, A Feasibility Study - Maritime Innovations in Green Technologies (MariGreen) project. 2018.
[79] Aziz M, Oda T, Kashiwagi T. Comparison of liquid hydrogen, methylcyclohexane and ammonia on energy efficiency and economy. Energy Procedia 2019;158:4086–91. https://doi.org/10.1016/J.EGYPRO.2019.01.827.
[80] Cardella U, Decker L, Sundberg J, Klein H. Process optimization for large-scale hydrogen liquefaction. Int J Hydrogen Energy 2017;42:12339–54. https://doi.org/10.1016/J.IJHYDENE.2017.03.167.
[81] Takahashi K. In: Hydrogen transportation Energy carriers convers. Syst. With emphas. Hydrog, vol. II. EOLSS Publications; 2009.
[82] Yang C, Ogden J. Determining the lowest-cost hydrogen delivery mode. Int J Hydrogen Energy 2007;32:268–86. https://doi.org/10.1016/J.IJHYDENE.2006.05.009.
[83] Antoniotti JP. Impact of high capacity CGH2-trailers, Deliverable 6.4. 2013. FCH-JU-2009-1 Grant Agreement Number 278796.
[84] San Marchi C, Hecht ES, Ekoto IW, Groth KM, LaFleur C, Somerday BP, et al. Overview of the DOE hydrogen safety, codes and standards program, part 3: advances in research and development to enhance the scientific basis for hydrogen regulations, codes and standards. Int J Hydrogen Energy 2017;42:7263–74. https://doi.org/10.1016/J.IJHYDENE.2016.07.014.
[85] NASA. Safety standard for hydrogen and hydrogen systems, guidelines for hydrogen system design, materials selection. Operations, Storage, and Transportation - NSS 1740;16:2005.
[86] Cornish AJ. Hydrogen Fueling Station Cost Reduction Study (March 2), Lakewood, Colorado: Engineering. Procurement & Construction, LLC; 2011.
[87] Cox K, Williamson K. Hydrogen: its technology and implications. In: Implication of hydrogen energy, vol. 5. CRC Press; 2018.
[88] Sdanghi G, Maranzana G, Celzard A, Fierro V. Review of the current technologies and performances of hydrogen compression for stationary and automotive applications. Renew Sustain Energy Rev 2019;102:150–70. https://doi.org/10.1016/J.RSER.2018.11.028.
[89] Petitpas G, Aceves SM. Liquid hydrogen pump performance and durability testing through repeated cryogenic vessel filling to 700 bar. Int J Hydrogen Energy 2018;43:18403–20. https://doi.org/10.1016/J.IJHYDENE.2018.08.097.
[90] Snam. Hydrogen IN the network. 2019. http://www.snam.it/en/Sustainability/news_and_tools/sustainability_news/Hydrogen_in_network.html. [Accessed 11 August 2019].
[91] U.S. Drive. Hydrogen Delivery Technical Team Roadmap. 2017.
[92] US Department of Energy. Hydrogen Tube Trailers. https://www.energy.gov/eere/fuelcells/hydrogen-tube-trailers. [Accessed 20 May 2019].
[93] Hydrogen Europe. Hydrogen transport & distribution. 2019. https://hydrogeneurope.eu/hydrogen-transport-distribution#Compressed. [Accessed 24 October 2019].
[94] Baldwin D, Lincoln Hexagon. Development of High Pressure Hydrogen Storage Tank for Storage and Gaseous Truck Delivery. Final Report; 2015.
[95] Air products and chemicals Inc. Liquid hydrogen. Safetygram 2014;9. https://doi.org/10.1016/j.ijhydene.2010.12.127.
[96] Sozinova O. H2A delivery components mode. In: DOE hydrogen program annual merit review proceedings; 2009.
[97] Ohira K. Slush hydrogen production, storage, and transportation. Compend Hydrog Energy 2016:53–90. https://doi.org/10.1016/B978-1-78242-362-1.00003-1.
[98] Rybin H, Krainz G, Bartlok G, Kratzer E. Safety demands for automotive hydrogen storage systems. Int. Conf. Hydrog. Saf. 2005:12.
[99] Appleby AJ. From Sir William Grove to today: fuel cells and the future. J Power Sources 1990;29:3–11. https://doi.org/10.1016/0378-7753(90)80002-U.
[100] U.S. Department of Energy. Fuel Cell Technology Office. FUEL CELL; 2015.
[101] Offer GJ, Howey D, Contestabile M, Clague R, Brandon NP. Comparative analysis of battery electric, hydrogen fuel cell and hybrid vehicles in a future sustainable road transport system. Energy Pol 2010;38:24–9. https://doi.org/10.1016/J.ENPOL.2009.08.040.
[102] Cappelletti A, Martelli F. Investigation of a pure hydrogen fueled gas turbine burner. Int J Hydrogen Energy 2017;42:10513–23. https://doi.org/10.1016/J.IJHYDENE.2017.02.104.
[103] Balestri M, Benelli G, Donatini F, Arlati F, Conti G. Enel's Fusina hydrogen-fed power generation plant. In: Int conf clean electr power, ICCEP '07 2007; 2007. p. 456–63. https://doi.org/10.1109/ICCEP.2007.384254.
[104] Ji Z, Qin J, Cheng K, Dang C, Zhang S, Dong P. Thermodynamic performance evaluation of a turbine-less jet engine integrated with solid oxide fuel cells for unmanned aerial vehicles. Appl Therm Eng 2019;160:114093. https://doi.org/10.1016/J.APPLTHERMALENG.2019.114093.
[105] Kim JW, Boo KJ, Cho JH, Moon I. 1 - key challenges in the development of an infrastructure for hydrogen production, delivery, storage and use. In: Basile A, editor. Iulianelli storage and distribution ABT-A in HP. Woodhead Publishing; 2014. p. 3–31. https://doi.org/10.1533/9780857097736.1.3.
[106] Ballard. FCveloCity®-HD. http://ballard.com/docs/default-source/motive-modules-documents/fcvelocity_hd_family_of_products_low_res.pdf. [Accessed 22 February 2019].
[107] Benjamin T, Gangi J, Curtin S. The Business Case for Fuel Cells: Delivering Sustainable Value. 2017.

[108] Herrmann A, Mädlow A, Krause H. Key performance indicators evaluation of a domestic hydrogen fuel cell CHP. Int J Hydrogen Energy 2018;44(35):19061–6.
[109] Fuel Cells and Hydrogen 2 Joint Undertaking (FCH JU). Pathway to a Competitive European Fuel Cell micro-Cogeneration Market 2019. http://www.pace-energy.eu/ (accessed February 22, 2019).
[110] Murugan S, Horák B. Tri and polygeneration systems - a review. Renew Sustain Energy Rev 2016;60:1032–51. https://doi.org/10.1016/J.RSER.2016.01.127.
[111] Ballard. Fuel Cell Backup Power Solutions - FCgen®-H2PM. 2019. http://ballard.com/docs/default-source/backup-power-documents/bup-flyer_final-version-low-res.pdf?sfvrsn=2. [Accessed 22 February 2019].
[112] Hydrogenics. Telecom & Data Centre Backup Power - HyPM$^{TM}$ XR fuel cell system. 2019. https://www.hydrogenics.com/hydrogen-products-solutions/fuel-cell-power-systems/stationary-stand-by-power/telecom-data-centre-backup-power/. [Accessed 22 February 2019].
[113] Giacomini. H$_2$ydroGEM, the hydrogen boiler by Giacomini 2019. https://www.giacomini.com/en/hydrogen-systems/h2ydrogem-hydrogen-boiler-giacomini (accessed February 28, 2019).
[114] Toyota. Toyota Develops World's First General-purpose Hydrogen Burner for Industrial Use n.d. https://global.toyota/en/newsroom/corporate/25260001.html (accessed February 28, 2019).
[115] Northrup C, Heckes AA. HYDROGEN-ACTUATED pump. Joumul Less-Common Met 1980;74:419–26.
[116] NASA. Explore Space Tech - Space Applications of Hydrogen and Fuel Cells. 2019. https://www.nasa.gov/content/space-applications-of-hydrogen-and-fuel-cells. [Accessed 2 September 2019].
[117] Technology indicators of portable power based on hydrogen-fed fuel cells. Portable Hydrog Energy Syst 2018;175–92. https://doi.org/10.1016/B978-0-12-813128-2.00010-3.
[118] Das N. Fuel cell technologies for defence applications. In: Raghavan K, Ghosh P, editors. Energy eng. Springer Singapore; 2017. p. 11. https://doi.org/10.1115/1.3267639.
[119] Wallner T, Lohse-Busch H, Gurski S, Duoba M, Thiel W, Martin D, et al. Fuel economy and emissions evaluation of BMW Hydrogen 7 Mono-Fuel demonstration vehicles. Int J Hydrogen Energy 2008;33:7607–18. https://doi.org/10.1016/J.IJHYDENE.2008.08.067.
[120] Hwang JJ. Review on development and demonstration of hydrogen fuel cell scooters. Renew Sustain Energy Rev 2012;16:3803–15. https://doi.org/10.1016/J.RSER.2012.03.036.
[121] London police trialing Suzuki scooters with Intelligent Energy units. Fuel Cells Bull 2017;2017:3–4. https://doi.org/10.1016/S1464-2859(17)30342-5.
[122] ExtraEnergy. HYSUN3000 2005. http://www.hysun.de/news_eng.php. [Accessed 27 February 2019].
[123] Daimler. Mercedes-Benz GLC F-CELL: Market launch of the world's first electric vehicle featuring fuel cell and plug-in hybrid technology. 2018. https://media.daimler.com/marsMediaSite/en/instance/ko/Mercedes-Benz-GLC-F-CELL-Market-launch-of-the-worlds-first-electric-vehicle-featuring-fuel-cell-and-plug-in-hybrid-technology.xhtml?oid=41813012. [Accessed 26 February 2019].
[124] Hyundai takes next STEP with largest fuel cell taxi fleet for Paris. Fuel Cells Bull 2016;2016:2. https://doi.org/10.1016/S1464-2859(16)30299-1.
[125] Fuel cells and hydrogen joint undertaking. Fuel Cell Electric Buses; 2019. https://www.fuelcellbuses.eu/. [Accessed 26 February 2019].
[126] ASKO orders Scania fuel cell trucks, starts hydrogen production. Fuel Cells Bull 2018;2018:3–4. https://doi.org/10.1016/S1464-2859(18)30005-1.
[127] Deployment of 500 Ballard-powered fuel cell trucks in Shanghai. Fuel Cells Bull 2018;2018:3–4. https://doi.org/10.1016/S1464-2859(18)30071-3.
[128] Lototskyy MV, Tolj I, Parsons A, Smith F, Sita C, Linkov V. Performance of electric forklift with low-temperature polymer exchange membrane fuel cell power module and metal hydride hydrogen storage extension tank. J Power Sources 2016;316:239–50. https://doi.org/10.1016/J.JPOWSOUR.2016.03.058.
[129] Gaines LL, Elgowainy A, Wang MQ. Full Fuel-Cycle Comparison of Forklift Propulsion Systems. 2008. https://doi.org/10.2172/946421.
[130] Davlin P, Greg M. Industry Deployed Fuel Cell Powered Lift Trucks. 2017.
[131] van Biert L, Godjevac M, Visser K, Aravind PV. A review of fuel cell systems for maritime applications. J Power Sources 2016;327:345–64. https://doi.org/10.1016/J.JPOWSOUR.2016.07.007.
[132] Sattler G. Fuel cells going on-board. J Power Sources 2000;86:61–7. https://doi.org/10.1016/S0378-7753(99)00414-0.
[133] Fernandes MD, de P, Andrade ST, Bistritzki VN, Fonseca RM, Zacarias LG, Gonçalves HNC, et al. SOFC-APU systems for aircraft: a review. Int J Hydrogen Energy 2018;43:16311–33. https://doi.org/10.1016/J.IJHYDENE.2018.07.004.
[134] Verfondern K. Safety Considerations on Liquid Hydrogen. Forschungszentrum Jülich GmbH; 2008.
[135] Miller AR. Tunneling and mining applications of fuel cell vehicles. Fuel Cells Bull 2000;5–9. https://doi.org/10.1016/S1464-2859(00)88922-1.
[136] McCarty R, Hord J, Roder H. Selected Properties of Hydrogen (Engineering Design Data). NBS Monogr. Boulder, Colorado: National Bureau of Standards; 1981.
[137] Schefer RW, Kulatilaka WD, Patterson BD, Settersten TB. Visible emission of hydrogen flames. Combust Flame 2009;156:1234–41. https://doi.org/10.1016/J.COMBUSTFLAME.2009.01.011.
[138] Klebanoff LE, Pratt JW, LaFleur CB. Comparison of the safety-related physical and combustion properties of liquid hydrogen and liquid natural gas in the context of the SF-BREEZE high-speed fuel-cell ferry. Int J Hydrogen Energy 2017;42:757–74. https://doi.org/10.1016/J.IJHYDENE.2016.11.024.
[139] Ono R, Nifuku M, Fujiwara S, Horiguchi S, Oda T. Minimum ignition energy of hydrogen–air mixture: effects of humidity and spark duration. J Electrostat 2007;65:87–93. https://doi.org/10.1016/J.ELSTAT.2006.07.004.
[140] Royal Society of Chemistry. Periodic Table n.d. http://www.rsc.org/periodic-table/element/1/hydrogen (accessed March 21, 2019).
[141] CGE Risk Management Solutions. BowTieXP. 2019. https://www.cgerisk.com/products/bowtiexp/. [Accessed 8 May 2019].
[142] Kaplan S, Garrick BJ. On the quantitative definition of risk. Risk Anal 1981;1:11–27. https://doi.org/10.1111/j.1539-6924.1981.tb01350.x.
[143] Delvosalle C, Fievez C, Pipart A, Debray B. ARAMIS project: a comprehensive methodology for the identification of reference accident scenarios in process industries. J Hazard Mater 2006;130:200–19. https://doi.org/10.1016/j.jhazmat.2005.07.005.
[144] Health and Safety Executive. Investigating accidents and incidents - hsg245. 2004.
[145] European Parliament, Council Union of the European Parliament. Regulation (EC) No 1272/2008 on classification,

labelling and packaging of substances and mixtures, amending and repealing. 2008.
[146] Lim Y, Al-atabi M, Williams RA. Liquid air as an energy storage: a review. J Eng Sci Technol 2016;11:496–515.
[147] Royle M, Willoughby D. Releases of unignited liquid hydrogen - RR986 - Health and Safety Laboratory. Harpur Hill (Buxton); 2014.
[148] Bunker R, Dees J, Eck M, Weaver R, Benz F. Large-Scale Hydrogen/Oxygen Explosion Project Special Interim Test Data Report. NASA; 1995. WSTF # 95-28791.
[149] Casal J, Hemmatian B, Planas E. On BLEVE definition, the significance of superheat limit temperature (Tsl) and LNG BLEVE's. J Loss Prev Process Ind 2016;40:81. https://doi.org/10.1016/j.jlp.2015.12.001.
[150] Laboureur D, Birk AM, Buchlin JM, Rambaud P, Aprin L, Heymes F, et al. A closer look at BLEVE overpressure. Process Saf Environ Prot 2015;95:159–71. https://doi.org/10.1016/J.PSEP.2015.03.004.
[151] Paltrinieri N, Tugnoli A, Cozzani V. Hazard identification for innovative LNG regasification technologies. Reliab Eng Syst Saf 2015;137:18–28. https://doi.org/10.1016/j.ress.2014.12.006.
[152] Woodward J, Pitblado R. LNG Risk Based Safety. New Jersey: John Wiley & Sons; 2010.
[153] Verfondern K, Dienhart B. Experimental and theoretical investigation of liquid hydrogen pool spreading and vaporization. Int J Hydrogen Energy 1997;22:649–60. https://doi.org/10.1016/S0360-3199(96)00204-2.
[154] Verfondern K, Dienhart B. Pool spreading and vaporization of liquid hydrogen. Int J Hydrogen Energy 2007;32:2106–17. https://doi.org/10.1016/j.ijhydene.2007.04.015.
[155] Watanabe T, Maehara H, Itoh S. Explosive evaporating phenomena of cryogenic fluids by direct contacting normal temperature fluids. Int J Multiphys 2012;6:107–14. https://doi.org/10.4028/www.scientific.net/msf.673.219.
[156] Paltrinieri N, Dechy N, Salzano E, Wardman M, Cozzani V. Lessons learned from toulouse and buncefield disasters: from risk analysis failures to the identification of atypical scenarios through a better knowledge management. Risk Anal 2012;32:1404–19. https://doi.org/10.1111/j.1539-6924.2011.01749.x.
[157] HydrogenTools. Liquid Hydrogen Tank Boiling Liquid Expanding Vapor Explosion (BLEVE) due to Water-Plugged Vent Stack. 2019. https://h2tools.org/lessons/liquid-hydrogen-tank-boiling-liquid-expanding-vapor-explosion-bleve-due-water-plugged-vent. [Accessed 25 September 2018].
[158] NASA. Report of the Presidential Commission on the Space Shuttle Challenger Accidentvol. 1997; 1986. http://science.ksc.nasa.gov/shuttle/missions/51-l/docs/rogers-commission/table-ofcontents.html. [Accessed 11 June 2019].
[159] Chirivella J. Analysis of the "phantom" fires on the Space Shuttle external tank base and the nature of the Space Shuttle "phantom" fires: LH2 leaks. 34th combust. In: Syst. Hazards subcomm. Airbreathing propuls. Subcomm. Palm Beach, USA: Jt. Meet. JANNAF; 1997.
[160] Barnoush A, Vehoff H. Recent developments in the study of hydrogen embrittlement: hydrogen effect on dislocation nucleation. Acta Mater 2010;58:5274–85. https://doi.org/10.1016/J.ACTAMAT.2010.05.057.
[161] Esaklul KA. Hydrogen damage. Trends Oil Gas Corros Res Technol 2017:315–40. https://doi.org/10.1016/B978-0-08-101105-8.00013-9.
[162] Burt V. Corrosion in the Petrochemical Industry. 2nd ed. Materials Park, Ohio: ASM International; 2015. https://doi.org/10.1179/bcj.1995.30.3.190.
[163] Hirth JP, Johnson HH. Hydrogen problems in energy related technology. Corrosion 1976;32:3–26. https://doi.org/10.5006/0010-9312-32.1.3.
[164] Zapffe CA, Sims CE. Hydrogen embrittlement, internal stress and defects in steel. Trans Am Inst Mining, Metall Pet Eng 1941;145:225–61.
[165] Petch NJ, Stables P. Delayed fracture of metals under static load. Nature 1952;169:842–3.
[166] Pfeil LB. The effect of occluded hydrogen on the tensile strength of iron. Proc. R. Soc. A Math. Phys. Eng. Sci. 1926;112:182–95. https://doi.org/10.1098/rspa.1926.0103.
[167] Robertson IM, Sofronis P, Nagao A, Martin ML, Wang S, Gross DW, et al. Hydrogen embrittlement understood. Metall Mater Trans B 2015;46:1085–103. https://doi.org/10.1007/s11663-015-0325-y.
[168] Beachem CD. A new model for hydrogen-assisted cracking (hydrogen "embrittlement"). Metall Mater Trans B 1972;3:441–55.
[169] Gahr S, Grossbeck ML, Birnbaum HK. Hydrogen embrittlement of Nb I—macroscopic behavior at low temperatures. Acta Metall 1977;25:125–34. https://doi.org/10.1016/0001-6160(77)90116-X.
[170] Vitovec FH. Modeling of hydrogen attack of steel in relation to material and environmental variables. In: Interrante CG, Pressouyre GM, editors. Curr. Solut. To hydrog. Probl. Steels. American Society for Metals; 1982.
[171] Darken LS, Smith RP. Behavior of hydrogen in steel during and after immersion in acid. Corrosion 1949;5:1–16. https://doi.org/10.5006/0010-9312-5.1.1.
[172] McClintock RM, Gibbons HP. Mechanical Properties of Structural Materials at Low Temperatures, A Compilation from the Literature. Washington, D.C.: National Bureau of Standards Monograph 13, U.S. Department of Commerce; 1960.
[173] Deimel P, Sattler E. Austenitic steels of different composition in liquid and gaseous hydrogen. Corros Sci 2008;50:1598–607. https://doi.org/10.1016/J.CORSCI.2008.02.024.
[174] Pratt JW, Klebanoff LE. Feasibility of the SF-BREEZE: a Zero-Emission. Hydrogen fuel cell, high-speed passenger ferry - sandia report. 2016. SAND2016-9719.
[175] Bronson JC, Edeskuty FJ, Fretwell JH, Hammel EF, Keller WE, Meier KL, et al. Problems in cool-down of cryogenic systems. In: Timmerhaus KD, editor. Adv. Cryog. Eng., vol. 7. New York: Plenum Press; 1960. p. 198–205.
[176] Murakami Y, Kanezaki T, Mine Y, Matsuoka S. Hydrogen embrittlement mechanism in fatigue of austenitic stainless steels. Metall Mater Trans 2008;39:1327–39. https://doi.org/10.1007/s11661-008-9506-5.
[177] Nakamura J, Miyahara M, Omura T, Semba H, Wakita M, Otome Y. Degradation of fatigue properties in high pressure gaseous hydrogen environment evaluated by cyclic pressurization tests. Procedia Eng 2010;2:1235–41. https://doi.org/10.1016/J.PROENG.2010.03.134.
[178] San Marchi C, Yamabe J, Schwarz M, Matsunaga H, Zickler S, Matsuoka S, et al. Global harmonization of fatigue life testing in gaseous hydrogen. In: Proc. ASME 2018 - Press. Vessel. Pip. Conf.; 2018. https://doi.org/10.1115/pvp2018-84898.
[179] Iijima T, Enoki H, Yamabe J, An B. Effect of high pressure gaseous hydrogen on fatigue properties of SUS304 and SUS316 austenitic stainless steel. In: Proc. ASME 2018 - Press. Vessel. Pip. Conf.; 2018. https://doi.org/10.1115/pvp2018-84267.
[180] NASA. Lewis Safety Manual, Chapter 6 "Hydrogen Propellant". NASA Technical Memorandum; 1992. vol. 104438.
[181] Wigley DA. The Properties of Nonmetals. Mech. Prop. Mater. Low Temp. Int. Cryog. Monogr. Ser.. Boston, MA: Springer; 1971. p. 177–252. https://doi.org/10.1007/978-1-4684-1887-3_4.

[182] OECD. Main science and technology indicators, vol. 2018. Paris: OECD Publishing; 2019. https://doi.org/10.1787/g2g9fae2-en. Issue 2.
[183] LaFleur AC, Muna AB, Groth KM. Application of quantitative risk assessment for performance-based permitting of hydrogen fueling stations. Int J Hydrogen Energy 2017;42:7529–35. https://doi.org/10.1016/J.IJHYDENE.2016.06.167.
[184] Briottet L, Moro I, Lemoine P. Quantifying the hydrogen embrittlement of pipeline steels for safety considerations. Int J Hydrogen Energy 2012;37:17616–23. https://doi.org/10.1016/J.IJHYDENE.2012.05.143.
[185] Saffers J-B, Molkov VV. Hydrogen safety engineering framework and elementary design safety tools. Int J Hydrogen Energy 2014;39:6268–85. https://doi.org/10.1016/J.IJHYDENE.2013.06.060.

Ustolin F, Paltrinieri N, Landucci G. An innovative and comprehensive approach for the consequence analysis of liquid hydrogen vessel explosions. J Loss Prev Process Ind 2020;68:104323. https://doi.org/https://doi.org/10.1016/j.jlp.2020.104323.

This page is intentionally left blank

Journal of Loss Prevention in the Process Industries 68 (2020) 104323

Contents lists available at ScienceDirect

Journal of Loss Prevention in the Process Industries

journal homepage: http://www.elsevier.com/locate/jlp

# An innovative and comprehensive approach for the consequence analysis of liquid hydrogen vessel explosions

Federico Ustolin [a,*], Nicola Paltrinieri [a], Gabriele Landucci [b]

[a] Department of Mechanical and Industrial Engineering, Norwegian University of Science and Technology NTNU, S.P. Andersens veg 3, Trondheim, 7031, Norway
[b] Department of Civil and Industrial Engineering, University of Pisa, Largo Lucio Lazzarino, Pisa, 56122, Italy

ARTICLE INFO

*Keywords:*
BLEVE
Hydrogen safety
Consequence analysis
Liquid hydrogen
Hydrogen explosion
Fireball

ABSTRACT

Hydrogen is one of the most suitable solutions to replace hydrocarbons in the future. Hydrogen consumption is expected to grow in the next years. Hydrogen liquefaction is one of the processes that allows for increase of hydrogen density and it is suggested when a large amount of substance must be stored or transported. Despite being a clean fuel, its chemical and physical properties often arise concerns about the safety of the hydrogen technologies. A potentially critical scenario for the liquid hydrogen ($LH_2$) tanks is the catastrophic rupture causing a consequent boiling liquid expanding vapour explosion (BLEVE), with consequent overpressure, fragments projection and eventually a fireball. In this work, all the BLEVE consequence typologies are evaluated through theoretical and analytical models. These models are validated with the experimental results provided by the BMW care manufacturer safety tests conducted during the 1990's. After the validation, the most suitable methods are selected to perform a blind prediction study of the forthcoming $LH_2$ BLEVE experiments of the Safe Hydrogen fuel handling and Use for Efficient Implementation ($SH_2IFT$) project. The models drawbacks together with the uncertainties and the knowledge gap in $LH_2$ physical explosions are highlighted. Finally, future works on the modelling activity of the $LH_2$ BLEVE are suggested.

## 1. Introduction

Hydrogen could be one of the options to shift the world energy production from fossil toward renewable and clean fuels. In order to be considered clean and renewable, hydrogen must be produced from non-fossil fuels such as biomass, organic material or waste, as well as from water (Ustolin et al., 2020). If hydrogen is generated from light hydrocarbons (e.g. natural gas), the carbon separation and sequestration technique must be employed to minimise the carbon dioxide emission in the atmosphere. The growth of renewable energies such as solar and wind may be supported by exploiting their surplus and producing hydrogen from water via electrolysis, as energy storage method (Maggio et al., 2019). The only by-products are water and heat when it is supplied to the fuel cells devices to produce electricity. Even when hydrogen is burnt, its combustion produces only water if the flame temperature is controlled or a catalyst is employed (Fumey et al., 2018).

After being stored, this fuel is suitable for transportation to the final users by different means thanks to its low weight (40.2 kg $m^{-3}$ at 700 bar and 15 °C (NIST, 2019)) and high energy content (120 MJ $kg^{-1}$ (McAllister et al., 2011)). The liquefaction process is one of the methods that can increase the hydrogen density (up to 70.9 kg $m^{-3}$ at ambient pressure and 20.3 K (NIST, 2019)), in order to transport a larger amount. Moreover, during liquefaction, hydrogen is converted from the normal composition (75% ortho-hydrogen, 25% para-hydrogen) to 100% para-hydrogen by means of a catalyst to increase its stability and hence reduce its evaporation (Zhuzhgov et al., 2018). To further reduce the boil-off gas (BOG) rate, the liquid hydrogen ($LH_2$) is then stored in highly insulated tanks (Barthelemy et al., 2017). These tanks are defined as double walled since they are composed by an inner vessel inside an outer one, separated by a vacuum jacket filled with insulating material. The two most common insulation types are perlite and the multilayer insulation (MLI), i.e. polymer sheets covered with a reflecting metal such as aluminium and separated by an insulating material (e.g. fiberglass) (Peschka, 1992). The residual gas pressure in the vacuum jacket has a high impact on the heat losses. For instance, the estimated thermal conductivity of a typical MLI with a layer density of 24 layers $cm^{-1}$ and boundary temperature of 300 and 90.5 K is almost 0.04 mW $m^{-1}$ $K^{-1}$ at $10^{-4}$ torr, while it increases up to 30 mW $m^{-1}$ $K^{-1}$ at $10^{2}$ torr (Barron and Nellis, 2016). The heat flux rate through the insulation of an $LH_2$ tank depends on many factors such as the type of insulation and its thickness, the residual gas pressure in the and the type of gas presents in

* Corresponding author.
*E-mail address:* federico.ustolin@ntnu.no (F. Ustolin).

https://doi.org/10.1016/j.jlp.2020.104323
Received 4 August 2020; Received in revised form 20 September 2020; Accepted 8 October 2020
Available online 10 October 2020

**List of symbols**

| | |
|---|---|
| $A_D$ | cross-sectional area of the fragment ($m^2$) |
| $A_{ke}$ | fraction of mechanical energy responsible for the ejection of the fragments (kinetic energy) |
| $A_L$: | external area of the fragment plane parallel to trajectory ($m^2$) |
| $c_{p,L}$: | average specific heat at constant pressure of the liquid phase between the initial and final states (kJ $kg^{-1}$ $K^{-1}$) |
| $C_D$ | drag coefficient of the fragment (−) |
| $C_L$: | lift coefficient of the fragment (−) |
| $c_{p,L0}$ | specific heat at constant pressure of the liquid at boiling point (kJ $kg^{-1}$ $K^{-1}$) |
| $d$ | distance from the tank (m) |
| $D_{fb}$ | diameter of the fireball (m) |
| $D_V$ | vessel diameter (m) |
| $E_{av}$ | available mechanical energy (J) |
| $E_{SEP}$ | surface emissive power (W $m^{-2}$) |
| $f$ | flashing fraction (−) |
| $F_{fb}$ | view factor of the fireball |
| $g$ | acceleration of gravity (m $s^{-2}$) |
| $H$ | vertical fragments range (m) |
| $h_L$: | specific enthalpy of the liquid phase immediately prior the explosion (kJ $kg^{-1}$) |
| $h_{L0}$ | specific enthalpy of the liquid phase at boiling point (kJ $kg^{-1}$) |
| $h_{V0}$ | specific enthalpy of the vapour phase at boiling point (kJ $kg^{-1}$) |
| $i_s$ | impulse of the pressure wave (Pa s) |
| $k$ | fraction of energy converted in overpressure (−) |
| $L$: | distance between the fireball centre and the target (m) |
| $M_C$ | empty mass of the vessel (kg) |
| $M_F$ | mass of fragment (kg) |
| $m_L$: | mass of the liquid phase (kg) |
| $m_V$ | mass of the vapour phase (kg) |
| $m_T$ | mass of the whole substance contained in the tank (kg) |
| $P$ | pressure before the explosion (Pa) |
| $P_a$ | pressure at the final state (usually equal to P0) (MPa) |
| $P_0$ | atmospheric pressure (Pa) |
| $P_C$ | critical pressure (Pa) |
| $p_s$ | side-on overpressure (Pa) |
| $p_w^0$ | partial pressure of saturated water vapour (Pa) |
| $R$ | horizontal fragment range (m) |
| $R_{fb}$ | radius of the fireball (m) |
| $RH$ | relative humidity of atmospheric air (%) |
| $\overline{R}$ | : Sachs scaled distance (−) |
| $\overline{R}_F$ | : scaled fragment range (−) |
| $q$ | incident radiation of the fireball (W $m^{-2}$) |
| $q_L$: | heat released by the liquid phase after the explosion (kJ $kg^{-1}$) |
| $q_V$ | latent heat of vaporisation (kJ $kg^{-1}$) |
| $s_L$: | specific entropy of the liquid phase before the explosion (kJ $kg^{-1}$ $K^{-1}$) |
| $s_{L0}$ | specific entropy of the liquid phase at boiling point (kJ $kg^{-1}$ $K^{-1}$) |
| $s_V$ | specific entropy of the vapour liquid phase before the explosion (kJ $kg^{-1}$ $K^{-1}$) |
| $s_{V0}$ | specific entropy of the vapour phase at boiling point (kJ $kg^{-1}$ $K^{-1}$) |
| $T$ | temperature of the substance inside the tank before the explosion (K) |
| $T_0$ | boiling point temperature (K) |
| $T_C$ | critical temperature (K) |
| $T_{fb}$ | fireball temperature (K) |
| $t_{fb}$ | duration of the fireball (s) |
| $T_{SL}$: | superheat limit temperature (K) |
| $U_i$ | overall internal energy of the system before the explosion (MJ) |
| $u_L$: | internal energy of the liquid phase before the explosion (kJ $kg^{-1}$) |
| $u_{L0}$ | internal energy of the liquid phase at boiling point (MJ $kg^{-1}$) |
| $u_{Lis}$ | internal energy of the liquid phase after the isentropic expansion (kJ $kg^{-1}$) |
| $u_V$ | internal energy of the vapour phase before the explosion (kJ $kg^{-1}$) |
| $u_{V0}$ | internal energy of the vapour phase at boiling point (MJ $kg^{-1}$) |
| $u_{Vis}$ | internal energy of the vapour phase after the isentropic expansion (kJ $kg^{-1}$) |
| $V^*$ | volume of the expanding fluid ($m^3$) |
| $v_i$ | initial velocity of the fragments (m $s^{-1}$) |
| $v_{L0}$ | specific volume of the liquid phase at boiling point ($m^3$ $kg^{-1}$) |
| $V_T$ | tank volume ($m^3$) |
| $v_{V0}$ | specific volume of the vapour phase at boiling point ($m^3$ $kg^{-1}$) |
| $x$ | vapour fraction after the irreversible expansion (−) |
| $x_{fb}$ | distance between the release point and the target (m) |
| $x_L$: | specific entropy fraction of the liquid phase (−) |
| $x_V$ | specific entropy fraction of the vapour phase (−) |
| $W_{TNT}$ | TNT equivalent mass ($kg_{TNT}$) |
| $Z$ | TNT scaled distance (m $kg^{-1/3}$) |
| $\alpha_i$ | initial angle of the fragments (°) |
| $\beta$ | fraction of mechanical energy which participates in the blast wave (−) |
| $\gamma$ | specific heat ratio (−) |
| $\Delta h_{V0}$ | latent heat of vaporisation at boiling point (kJ $kg^{-1}$) |
| $\varepsilon$ | emissivity of the body (−) |
| $\theta$ | angle between the receptor surface normal and L (°) |
| $\rho_a$ | density of atmospheric air (kg $m^{-3}$) |
| $\rho_L$: | density of the liquid phase (kg $m^{-3}$) |
| $\rho_V$ | density of the liquid phase (kg $m^{-3}$) |
| $\sigma$ | Stefan-Boltzmann constant ($5.67 \times 10^{-8}$ W $m^{-2}$ $K^{-4}$) |
| $\tau$ | atmospheric attenuation factor (transmissivity) (−) |
| $\psi$ | amount of energy which participate in the generation of the pressure wave (−) |

the vacuum jacket (e.g. air or nitrogen), the shape of the tank (cylindrical or spherical) as well as its size. For instance, Stochl and Knoll (1991) measured a total heat leak of 48.2 W from an $LH_2$ tank with a volume of 4.96 $m^3$, insulated with 34 layers of MLI, an external temperature of 350 K and an internal one of 20.3 K. This corresponds to an extremely low heat flux of 3.4 W $m^{-2}$ (Stochl and Knoll, 1991). Another option to maintain the hydrogen in liquid phase would be to refrigerate the tank insulation by exploiting the extremely cold BOG. This is achieved through vapour cooled shields installed inside the vacuum jacket and composed by coils of pipes where the BOG recirculates (Peschka, 1992). In addition, zero boil-off methods for large scale liquid hydrogen tanks were recently developed by NASA. These methods exploit an integrated refrigeration and storage system (Notardonato et al., 2017).

It must be mentioned that the hydrogen liquefaction is an energy

demanding process since up to 13.3 kWh per kg of hydrogen are requested, which corresponds to approximately 30% of the hydrogen lower heating value (LHV) (Bracha et al., 1994). However, the liquid phase seems to be the only fashion to transport large amount of hydrogen over long distances, or to be store onboard of large hydrogen fuelled vehicles such as ships (NCE Maritime Cleantech, 2019). Furthermore, Cardella et al. (2017) proposed a solution to optimise the liquefaction process and thus increase its efficiency and reduce the costs. Finally, Trevisani et al. (2007) suggested to produce electricity by recovering the thermal energy during the $LH_2$ vaporisation process through different systems such as a gas turbine or magnetohydrodynamic generator. In this manner, the overall efficiency of the liquefaction process can be improved.

Hydrogen is extremely flammable, odourless, and colourless, making it also difficult to detect (NASA, 2005). Thus, the safety aspects are crucial for hydrogen applications, which are progressively increasing in popularity, affecting the consumption of the hazardous substance (IEA, 2019) and its supply chain (Landucci et al., 2010). For instance, the first hydrogen fuelled train was deployed in Germany in 2018 (D'Ovidio et al., 2020), and the interest for this fuel is escalating in the maritime sector (van Biert et al., 2016) (NCE Maritime Cleantech, 2019). From emerging technologies, emerging risks might arise due to the lack of experience and knowledge (Jovanović and Baloš, 2013). For this reason, the atypical accident scenarios, which are the events not considered by the most common risk assessment techniques, must be investigated (Paltrinieri et al., 2012). When a vessel of liquefied gas is used, the boiling liquid expanding vapour explosion (BLEVE) is one of the atypical accident scenarios that might manifest. BLEVE is a physical explosion since it is not led by chemical reactions, yet by a rapid phase change and expansion (CCPS, 2010). One of the most recent BLEVE definitions states that this explosion may occur after the rupture of a tank containing a liquid at a temperature above its boiling point at atmospheric pressure, due to the expansion of both the vapour and liquid phases (Casal et al., 2016).

The first consequence of a BLEVE is the pressure wave generated by the explosion. The overpressure of the blast wave can cause different types of damages on structures, injuries or even death to humans, depending on its intensity (Baker et al., 1983). Part of the mechanical energy generated by the explosion contributes to the tear the vessel and throw away its debris. In the literature, this consequence is usually called missiles, projectiles, or fragments. In this study, this latter definition was adopted.

A fireball may be initiated from a BLEVE if the stored substance is flammable and an ignition source is present outside the vessel. According to the Centre for Chemical Process Safety (CCPS, 2010), the fireball is "a burning fuel-air cloud whose energy is emitted primarily in the form of radiant heat". In addition, this cloud tends to ascend and expand while burning due to the buoyancy of the hot gases. The fireball terminology was chosen because this cloud usually assumes a spherical shape or sometime a mushroom aspect since a stem might be created between the cloud and the fuel spilled on the ground (High, 1968). Under certain circumstances, an actual fireball does not take place. Instead, a fire starts on the ground after the loss of containment. This may represent a third type of BLEVE consequence. Bader et al. (1971) studied this event circumstances and determined the critical mass of the rocket propellants above which a fireball is formed and lift off.

Many causes could provoke the collapse of the vessel. The BLEVEs have been categorised in "fired" or "unfired" depending on the cause of the loss of containment (Paltrinieri et al., 2009). The fired or hot BLEVE is induced by a thermal source external to the tank, i.e. a jet or a pool fire. In this case, the heat transfer between the surrounding and the substance in the tank is enhanced, the vessel pressure rises due to the liquid evaporation and the decrease of density. Moreover, the external thermal source reduces the mechanical resistance of the tank wall material and the tank pressure increases the stress (Paltrinieri et al., 2009). On the other hand, an unfired or cold BLEVE can be caused by a violent impact (e.g. road accident), a pressure relief valves (PRVs) failure, or a defect on the insulation material.

Few $LH_2$ BLEVE accidents can be found in the literature, and in most of the cases the term BLEVE is not adopted by the authors of the accident reports. An example is provided by Gayle (1964), who describes the explosion of the S-IV All Systems Vehicle occurred on January 24, 1964, at the Douglas Aircraft Company, Sacramento. The author states that this was the second known accident involving large amount of liquid oxygen (LOX) and $LH_2$ at that time. In the report, the focus is placed on the fireball characterisation, the fragments range analysis, and the damages on the structures closed to the test facility. After this accident and during the 1960's, numerous test series, such as the PYRO project (Willoughby and Ullian, 1988) and Atlas/Centaur abort (Kite et al., 1965), were conducted to study the explosions of different types of liquid-propellants (e.g. RP-1/LOX, $LH_2$/LOX). Empirical correlations for the fireball development to estimate diameter and duration after the explosion of liquid-propellants were proposed by Gayle and Bransford (1965) and High (1968). A thermal radiation model for liquid-propellants was developed by Bader et al. (1971). Prugh (1994) assessed the thermal radiation for fireballs generated after BLEVEs as well, but $LH_2$ was not considered due to the high temperatures and low emissivity.

An $LH_2$ BLEVE accident occurred on January 1st, 1974 can be also found online (HydrogenTools, 2017), but its description focuses on the causes which provoked the phenomenon, neglecting its consequences. A similar $LH_2$ BLEVE event is analysed by Mires (1985). In this case, the fragments range is reported as consequence and a reverse analysis is conducted to comprehend the $LH_2$ amount involved and the tank pressure necessary to throw the tank end cap almost 76 m (180 ft) from the vessel. In both the accidents, a cold BLEVE occurred without ignition after the release. An example of hot $LH_2$ BLEVE took place during the Challenger space shuttle disaster in 1986 (NASA, 1997). In particular, hot gases ignited after their release from one solid rocket booster due to the failure of an O-ring rubber seal. The flames impinged the $LH_2$/LOX external tank provoking its rupture and a consequent BLEVE. This accident involved the LOX tank as well as all the tests conducted by NASA for the aerospace applications previously mentioned. Despite this event has occurred at least three times in the past, it might be still neglected during a risk assessment of $LH_2$ technologies (Ustolin et al., 2019).

The only experiments in which the $LH_2$ BLEVE phenomenon was simulated, were carried out by BMW car manufacturer on few automotive $LH_2$ tanks, in the period 1992–95 (Pehr, 1996). Although the three main BLEVE consequences (blast wave, fragments range and fireball) were considered and measured, some critical results were omitted (Ustolin and Paltrinieri, 2020). For instance, a thorough fragments analysis was disregarded. Furthermore, it was not possible to develop an experimental model to assess the absolute thermal radiation load in the fireball proximity, and the thermal radiation results were not published. These tests are described in detailed in Sec. 3.2.

During the integrated design for demonstration of efficient liquefaction of hydrogen (IDEALHY) project, an accurate qualitative risk assessment of hydrogen liquefaction, storage and transportation was carried out (Lowesmith et al., 2013). The consequences of the fireballs generated after different large scale $LH_2$ BLEVEs were estimated by means of empirical correlations and a model developed by the Loughborough University to assess the fireball radiation. As result of this project, the most severe event for both the transportation/storage and liquefaction/storage scenarios was the $LH_2$ BLEVE. Recently, the BLEVE phenomenon was considered for $LH_2$ by Hansen (2020), with a comparison between the consequences of an $LH_2$ and a liquefied natural gas (LNG) BLEVE. Currently, the safe hydrogen fuel handling and use for efficient implementation ($SH_2IFT$) project is investigating the safety aspects of a loss of containment of both liquid and compressed hydrogen tanks (Ustolin et al., 2019). In particular, the consequences of an $LH_2$ BLEVE explosion are analysed through either experimental tests or modelling activity. Furthermore, the project is focussing on the

consequences of the release of $LH_2$ onto water and compressed hydrogen from high pressurized vessels.

Given these premises, the aim of this work is to present a novel approach for the comprehensive assessment of the consequences of an $LH_2$ BLEVE. The approach is validated and employed to conduct blind predictions for the consequences of $LH_2$ accident scenarios. Moreover, this method is not limited to $LH_2$ but it could be applied to other substances as well.

To achieve the study objective, the BMW tests are considered for the first time and simulated by means of conventional risk assessment empirical and theoretical models. The idea was to investigate if these very well-known methods already validated for hydrocarbons BLEVE (e.g. propane and butane) are suitable for $LH_2$ BLEVE as well. These equations were never applied to $LH_2$ BLEVEs before, thus the outcomes of this analysis required to be validated with the experimental results. After the validation, the most suitable models for the $LH_2$ BLEVE consequence analysis are selected. The chosen models are applied to conduct a blind prediction study in order to estimate the consequences of a planned experimental tests set and generalize on potential BLEVE events for $LH_2$ under different conditions. For the first time, this approach allows assessing all the identified typologies of BLEVE consequences for both small- and mid-scale $LH_2$ accident scenarios. Therefore, the novelty of this study is mainly represented by the innovative methodology which allows to validate the available consequence analysis model and conduct a blind prediction study of the BLEVE phenomenon, and by considering and simulating for the first time the BMW safety tests.

In Sec. 2, the difference between a sub- and supercritical BLEVE is explained and the para-hydrogen properties are specified. The methodology adopted in this study and the results attained are reported in Sec. 3 and 4, respectively. In-depth discussion on the results and several observations on the employed models were provided in Sec. 5, and finally the conclusion together with the suggested future works are described in Sec. 6.

## 2. Subcritical and supercritical BLEVEs

According to Reid (1979), the liquid must be significantly superheated to consider the explosion after the tank rupture as severe as a BLEVE. When the superheated liquid or subcooled vapour approach the superheat limit temperature ($T_{SL}$), their states may shift either from metastable to equilibrium state under small perturbations or to unstable due to large perturbations (Casal, 2008). Under this thermodynamic state, a homogeneous nucleation may be attained as consequence of a rapid depressurisation. Therefore, a violent expansion which characterises the explosion is the aftermath of this nucleation type. It must be noticed that during such event, also the vapour phase contained in the tank contributes to the explosion yield. According to Birk et al. (2007), the pressure shock during a propane BLEVE is generated only by the vapour phase contribution since the liquid flashing is a slow process, thus not able to generate such an overpressure. However, this latter is responsible for fragments ejection and dynamic pressure loading of structures in the near field (Birk et al., 2007). On the other hand, the model developed by Casal and Salla (2006) to estimate the blast wave overpressure, takes into account barely the liquid phase contribution.

**Table 1**
Thermodynamic properties of parahydrogen.

| Property | Value | Units |
|---|---|---|
| Boiling temperature ($T_0$) | 20.277 | K |
| Critical temperature ($T_C$) | 32.938 | K |
| Critical pressure ($P_C$) | 12.838 | bar |
| Enthalpy of vapour @ BP[a] ($h_{V0}$) | 445.4 | kJ/kg |
| Enthalpy of liquid @ BP[a] ($h_{L0}$) | $-6.1 \times 10^{-13}$ | kJ/kg |

[a] BP: boiling point.

It might happen that during an accident, the substance contained in the vessel reaches the status of either compressible liquid or supercritical fluid due to the rise in pressure and temperature. Hence, the liquid and vapour phases are not present anymore. This can be caused by different events such as a fire external to the vessel or a defect in the tank insulation of the cryogenic tanks, leading to an undesired heat transfer between the substance and the surrounding. Therefore, if the catastrophic rupture of the vessel is attained when the status of the fluid is supercritical, the consequent explosion is called supercritical BLEVE (Laboureur, 2012; Laboureur et al., 2014, 2012a; 2012b; Zhang et al., 2016). Hydrogen has a low critical pressure (12.964 bar (NIST, 2019)) and an extremely low critical temperature (33.145 K (NIST, 2019)) compared with other substances and conventional fuels (hydrocarbons). For this reason, a supercritical BLEVE seems a likely scenario for a $LH_2$ tank. In this study, if the pressure and temperature inside the tank are lower than the critical point immediately prior the explosion the BLEVE is called subcritical, otherwise the explosion is referred as a supercritical BLEVE. The compressible liquid status is not covered in this paper because it is assumed that pressure and temperature of the substance inside the vessel follow the saturation curve before the critical point.

### 2.1. Para-hydrogen properties

As mentioned before, hydrogen is converted to para-hydrogen (p-$H_2$) during the liquefaction process in order to increase its stability and thus reduce the boil off (spontaneous evaporation) (Zhuzhgov et al., 2018). For this reason, only the properties of p-$H_2$ were considered in this study. Similarly to hydrogen, p-$H_2$ has a low critical pressure, (12.8377 bar (NIST, 2019)) and an extremely low critical temperature, (32.938 K (NIST, 2019)). In Table 1, the thermodynamic properties of p-$H_2$ are collected.

## 3. Methodology

### 3.1. Superheat limit temperature ($T_{SL}$) estimation for para-hydrogen

As described in Sec. 2, the superheat limit temperature aids to determine if the explosion may be considered as a BLEVE. The $T_{SL}$ is directly affected by the critical point of the substance. Thus, the $T_{SL}$ of p-$H_2$ (see Table 1) notably differs from most of the conventional fuels as well. In the scientific literature, many methods to estimate the superheat limit temperature are proposed (Casal, 2008). In this work, the p-$H_2$ $T_{SL}$ is calculated with three of the most representative models. These approaches were selected because they generally provide the highest, the lowest and the average values of the superheat limit temperature (Casal, 2008).

1. The first one is proposed by Reid (1976) and consists in a widely used correlation with the critical temperature (Eq. (1)):

$$T_{sl-T_C} = 0.895 \cdot T_C \tag{1}$$

This equation derives from bubble-column experiments conducted at different pressures for di-chlorodifluoromethane, n-pentane, n-hexane, n-heptane, and cyclohexane (Reid, 1976). It was demonstrated that for these substances, the $T_{SL}$ at atmospheric pressure was 0.89–0.90 times the critical temperature. In the following, this model is called Experimental Correlation (EC).

2. The second method, described by Casal (2008), estimates the $T_{SL}$ from the tangent to the saturation curve at the critical point ($T_{SL\text{-}t}$). Although this approach is not based on any thermodynamic law or equation, it is one of the most conservative methods (Casal, 2008). In this study, the tangent line was built graphically in order to avoid the significant error given by the Clausius-Clapeyron equation close to the critical point (CP) (Casal, 2008). The temperature intercepted by the tangent at ambient temperature ($P_0$) is the $T_{SL\text{-}t}$. In particular, this temperature was estimated with the straight line equation (Eq. (2)):

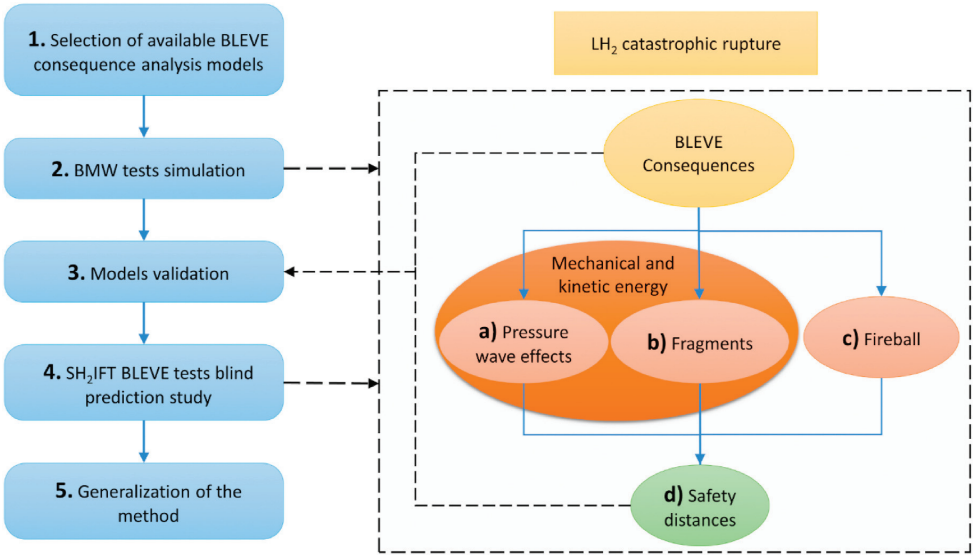


**Fig. 1.** Methodology steps and approach applied in the $LH_2$ consequence analysis.

**Table 2**
Equations of the ideal gas behaviour models selected in this study.

| Proposed by | Assumption | Equation | |
|---|---|---|---|
| Brode (1959) | Isochoric process | $E_{Brode} = \frac{P - P_0}{\gamma - 1} V^*$ | (5) |
| Smith and Van Ness (1996) | Isothermal process | $E_{IE} = P \cdot V^* \cdot \ln \frac{P}{P_0}$ | (6) |
| Crowl (1992, 1991) | Thermodynamic availability | $E_{TA} = P \cdot V^* \left[ \ln\left(\frac{P}{P_0}\right) - \left(1 - \frac{P_0}{P}\right) \right]$ | (7) |
| Prugh (1991) | Adiabatic process | $E_{Prugh} = \frac{P \cdot V^*}{\gamma - 1}\left(1 - \frac{P_0}{P}\right)^{\frac{\gamma - 1}{\gamma}}$ | (8) |

$$P = \tan\alpha \cdot T + b \quad (2)$$

where the gradient is the tangent of the angle $\alpha$, and the intercept $b$ was determine at CP, replacing the pressure and temperature with $P_C$ and $T_C$ respectively. This model is called Saturation Curve Tangent (SCT) in this study.

3. The third method, proposed by Salla et al. (2006), estimates the $T_{SL}$ through an energy balance. An adiabatic vaporisation process is considered after the depressurisation of the vessel in which part of the liquid cools down to the boiling point ($T_0$) at atmospheric pressure releasing a certain amount of heat ($q_L = h_L - h_{L0}$), partially or totally absorbed by a liquid fraction which vaporises. The $T_{SL\text{-}E}$ is the temperature at which the heat released by 50% of the liquid ($q_L$) is equal to the heat required by the other half of the liquid ($q_V = h_{V0} - h_L$) to vaporise. The $T_{SL\text{-}E}$ is then the temperature correspondent to $h_L$ on the saturated liquid line. This model was named Energy Balance (EB) in the following.

### 3.2. Approach for the comprehensive consequences assessment of an $LH_2$ BLEVE

The $LH_2$ BLEVE is studied and physically modelled in this work. In particular, the most significant consequence analysis models were selected (step 1 in Fig. 1) in order to create a suitable approach to assess the $LH_2$ BLEVE consequences. This approach is depicted by the black rectangle in Fig. 1 and it foresees to estimate the safety distance from the tank, from the results of the three main BLEVE consequences.

Then, the BMW safety tests were simulated (step 2) with the aforementioned approach. Therefore, a first validation of the chosen methods was possible (step 3). Hence, a blind prediction was accomplished by applying the same approach to the conditions of the $LH_2$ BLEVE tests which will be carried out during the $SH_2$IFT project. In this way, it was shown how the proposed methodology can be applied to future $LH_2$ BLEVE consequence analysis. In the following, the models and the steps adopted for the consequence analysis are described.

### 3.3. Model selection and consequence analysis approach

In this section, the models selected for the consequence analysis (step 1 in Fig. 1) are described, together with the approach proposed to estimate the safety distance from the tank (black dashed rectangle of

**Table 3**
Equations of the real gas behaviour models selected in this study.

| Proposed by | Equation | |
|---|---|---|
| van den Bosch and Weterings (2005) | $E_{TNO} = m_V (u_V - u_{V_a}) + m_L (u_L - u_{L_a})$ | (9) |
| Planas-Cuchi et al. (2004) | $E_{Planas} = -[(u_{L0} - u_{V0}) m_T \cdot x - m_T \cdot u_{L0} + U_i]$ | (10) |
| Casal and Salla (2006) | $E_{SE} = k \cdot m_L (h_L - h_{L0})$ | (11) |
| Genova et al. (2008) | $E_{Genova} = \psi \cdot m_L \cdot c_{p,L} (T_L - T_{L0})$ | (12) |
| Birk et al. (2007) | $E_{Birk} = m_V (u_V - u_{V_a})$ | (13) |

Fig. 1). The idea is to use the results of the three main BLEVE consequences to determine this distance. In the following, the mechanical energy models adopted to evaluate the pressure wave effects and the fragments range are reported together with the overpressure, impulse, fragments range and fireball models. It must be mentioned once again that these models have not been employed to $LH_2$ before, hence a verification with the experimental results is required.

### 3.3.1. Mechanical energy models

The approach proposed by (Hemmatian et al., 2017a) was adopted to estimate the mechanical energy generated by the explosion in order to determine the severity of the pressure wave (overpressure and impulse). This procedure foresees to compare different mechanical energy models. The ideal gas behaviour models proposed by the following authors were considered in this study:

1. Brode (1959);
2. Smith and Van Ness (1996);
3. Crowl (1992, 1991), thermodynamic availability (TA) model;
4. Prugh (1991).

These models, described below, depends only on the atmospheric and tank pressures, and the volume of the expanding fluid. The equations of the selected models are reported in Table 2, where $P$ and $P_0$ are the pressure inside the tank immediately prior the explosion and the atmospheric pressure respectively, in $P_a$, $\gamma$ is the heat specific ratio (1.4 for hydrogen) and $V^*$ is the sum of the vapour and flashing liquid fraction volumes in $m^3$ at subcritical conditions, and the total tank volume ($V_T$) at supercritical conditions. Prugh (1991) suggested the following method to estimate the total expansion volume (vapour and liquid fractions) during the explosion of a container of liquefied gas. The total volume is calculated with Eq. (3) at subcritical conditions:

$$V^* = V_T + m_L\left(\frac{f}{\rho_V} - \frac{1}{\rho_L}\right) \tag{3}$$

where $V_T$ is the total volume of the tank in $m^3$, $m_L$ is the mass of the liquid in kg, $\rho_V$ and $\rho_L$ are the density of the vapour and liquid phase respectively in kg $m^{-3}$, and $f$ is the flashing fraction estimated with Eq. (4):

$$f = 1 - \exp\left\{-2.63\left[1 - \left(\frac{T_C - T_0}{T_C - T_b}\right)^{0.38}\right]\frac{c_{p,L0}}{\Delta h_{V0}}(T_C - T_b)\right\} \tag{4}$$

where $T_0$, $T_C$ and $T_b$ are the atmospheric, critical and boiling temperatures respectively in K, $c_{p,L0}$ is specific heat of the liquid at boiling temperature in kJ $kg^{-1}$ $K^{-1}$, and $\Delta h_{V0}$ is the latent heat of vaporisation at boiling point in kJ $kg^{-1}$. It must be emphasized that when the substance in the vessel reaches supercritical conditions before the explosion, $V^*$ is equal to the total tank volume ($V_T$) in $m^3$.

Brode (1959) proposed Eq. (5) to estimate the total energy generated by the detonation of a spherical charge of TNT considering it as an isochoric process. Smith and Van Ness (1996) assumed an isothermal expansion (IE) process while developing their model (Eq. (6)). The thermodynamic availability (TA) model introduced by Crowl (1992, 1991) estimates the maximum mechanical energy extractable from a substance which reversibly reaches the equilibrium with the surrounding environment from the burst conditions. Eq. (7) can be used when the process is considered isothermal. Prugh (1991) proposed to apply Eq. (8), developed for high pressure containers to liquefied gas vessels by replacing the tank volume with the total volume of the expanding fluid (Eq. (4)) in order to determine the mechanical energy of a BLEVE explosion. The fluid is considered always as ideal and the process as adiabatic.

Furthermore, the following real gas behaviour models were utilised in this study and described below:

5) van den Bosch and Weterings (2005), TNO model;
6) Planas-Cuchi et al. (2004);
7) Casal and Salla (2006), superheating energy (SE) model – isentropic and irreversible processes;
8) Genova et al. (2008);
9) Birk et al. (2007).

The formulae of these models are collected in Table 3, where $m$, $u$, $h$, $T$, $U_i$ and $c_{p,L}$ refer to the masses in kg, internal energies in kJ $kg^{-1}$ (except for the Planas model where the units are MJ $kg^{-1}$), the enthalpies in kJ $kg^{-1}$, the temperatures in K, the overall internal energy of the system before the explosion in MJ and the average specific heat at constant pressure of the liquid phase between the initial and final states of the expansion in kJ $kg^{-1}$ $K^{-1}$. Moreover, the indexes $V$, $V_0$, $L$, $L_0$ indicates the vapour and liquid phases before and after (at atmospheric pressure) the explosion, respectively, while $T$ and is refer to both liquid and vapour phases (total) and the isentropic process, respectively.

The TNO model (van den Bosch and Weterings, 2005) in Eq. (9) considers the expansion of both the vapour and liquid phases, and assumes that this is an isentropic process. The thermodynamic properties are usually retrieved from a suitable database at saturation conditions. The specific internal energies after the isentropic expansion, $u_{Vis}$ and $u_{Lis}$ in kJ $kg^{-1}$, are estimated with Eqs. (14) and (15) reported in Table 4, where the ratios $x_V$ and $x_L$ are assessed with Eqs. (16) and (17), and $s$ indicates the entropies of the vapour and liquid phases before and after the explosion in kJ $kg^{-1}$ $K^{-1}$.

Planas-Cuchi et al. (2004) suggested a method which acknowledge that the explosion is an adiabatic irreversible process. The equation of this model is reported in Eq. (10), where $x$ is the intersection point between two equations: the variation in internal energy ($\Delta U$) and the adiabatic irreversible expansion work ($P_0 \cdot \Delta V$). Eq. (18) in Table 4 is employed to estimate the value of $x$, where $P_a$ is the pressure at the final state (usually equal to $P_0$) in MPa, $v_{V0}$ and $v_{L0}$ are the specific volumes of the vapour and liquid phases respectively in $m^3$ $kg^{-1}$. The authors of this model assume that only part of the mechanical energy contributes to the pressure wave, i.e. 80% if the tank ruptures in a fragile manner, or 40% the type of failure is ductile (Casal et al., 2001). It should be mentioned that these latter models (TNO and Planas) can be employed to barley estimate a subcritical BLEVE since both phases (vapour and liquid) are considered. The superheating energy (SE) model (Casal and Salla, 2006) directly assess the energy contribution to the pressure wave instead of

**Table 4**
Internal energies and entropy ratios employed in the TNO model, and the intersection point between the variation of internal energy and the adiabatic irreversible expansion work (x) used in the Planas model.

| Equation | |
|---|---|
| $u_{V_a} = (1 - x_L)\, u_{L0} + (x_L \cdot u_{V0})$ | (14) |
| $u_{L_a} = (1 - x_V)\, u_{L0} + (x_V \cdot u_{V0})$ | (15) |
| $x_V = \frac{s_V - s_{L0}}{s_{V0} - s_{L0}}$ | (16) |
| $x_L = \frac{s_V - s_{L0}}{s_L - s_{L0}}$ | (17) |
| $x = \frac{m_T \cdot P_a \cdot v_{L0} - V_T \cdot P_a + m_T \cdot u_{L0} - U_i}{[(u_{L0} - u_{V0}) - (v_{V0} - v_{L0})\, P_a]\, m_T}$ | (18) |

**Table 5**
Values of the coefficients of the real gas behaviour models.

| Model | $\beta$ | $K$ | $\psi$ |
|---|---|---|---|
| TNO (van den Bosch and Weterings, 2005) | 2.0 | – | – |
| Planas-Cuchi et al. (2004) | 0.4 | – | – |
| (Casal and Salla, 2006) – isentropic proc. | 1.0 | 0.14 | – |
| (Casal and Salla, 2006) – irreversible proc. | 1.0 | 0.05 | – |
| Genova et al. (2008) | 1.0 | – | 0.07 |
| Birk et al. (2007) | 2.0 | – | – |

**Table 6**
Multipliers for overpressure for cylindrical vessel at different $\overline{R}$ (van den Bosch and Weterings, 2005).

| $\overline{R}$ | |
|---|---|
| >1.6 and ≤ 3.5 | 1.6 |
| >3.5 | 1.4 |

the total mechanical energy. This energy is estimated considering the enthalpy variation of only the liquid phase and its mass (Eq. (11)). The overpressure energy of either an isentropic or an irreversible process are estimated by assuming different values of the coefficient $k$ in the model equation, i.e. 0.14 and 0.05 respectively. If this model is employed to simulate a supercritical BLEVE, the total mass of the fluid inside the tank must be considered, as well as the enthalpy of the fluid before (at supercritical conditions) and after the explosion. Similarly to the SE model, the method developed by Genova et al. (2008) takes into account only the liquid phase. The model assumes that the flashing liquid process is led by the excess heat stored in the vessel, determined with Eq. (12), where $\psi$ is the amount of energy which participate in the pressure wave generation. This coefficient was determined empirically for propane BLEVEs and it is equal to 0.07. Genova et al. (2008) suggested to neglect the variation of the specific heat at constant pressure of the liquid ($c_{p,L}$) due to the increase in temperature since these are usually very small (less than 1% for water between 25 and 100 °C). Instead, the change in $c_{p,L}$ is significant for hydrogen (from 9.7 to 70.2 kJ kg$^{-1}$ K$^{-1}$ at 20.3 and 32.0 K respectively). For this reason, an average $c_p$ value was estimated between the initial and final conditions (prior and after the explosion). The model proposed by Birk et al. (2007) is similar to the TNO model since a real gas behaviour and an isentropic expansion process are considered, but this is limited to the vapour phase. The model equation is presented in Eq. (13).

*3.3.1.1. Blast wave overpressure and impulse estimation.* The TNT equivalent mass method was employed both for the overpressure and impulse estimation since is the most conservative and only the far field was considered to determine the safety distance from the bursting vessel. Thus, the mechanical energies estimated with the models described above were converted in TNT masses by considering that 4680 kJ is equivalent to 1 kg of TNT (Salla et al., 2006). As previously mentioned, some models foresee that only part of the mechanical energy, hence TNT mass, contribute to the blast wave (Casal and Salla, 2006; Genova et al., 2008; Planas-Cuchi et al., 2004). On the other hand, the TNO and Birk models consider the reflection on the ground of the pressure wave, thus multiply the estimated energy (or the TNT mass) by a factor of 2. The Sachs scaled distance, estimated with Eq. (19), is usually applied to distinguish the near to the far field (Birk et al., 2007). In particular, the near field can be found when $\overline{R} < 2$.

$$\overline{R} = d\left(\frac{P_0}{\beta \cdot E}\right)^{1/3} \tag{19}$$

where $d$ is the distance from the tank in m, $P_0$ is the atmospheric pressure in Pa, $E$ is the mechanical energy estimated with one of the previously described models, and $\beta$ is the fraction of energy which participates in the blast wave. In this study, the $\beta$ factor was considered equal to 1 for the ideal gas behaviour models, while the values of the coefficients adopted for the real gas behaviour models are collected in Table 5.

The TNT scaled distance in m kg$^{-1/3}$, necessary to determine the overpressure and impulse from the TNT decay curve, is reported in Eq. (20):

$$Z = \frac{d}{(\beta \cdot W_{TNT})^{1/3}} \tag{20}$$

where $d$ is the distance from the centre of the explosion, $W$ is the TNT equivalent mass in kg, and $\beta$ is the fraction of energy which participates in the blast wave.

As mentioned above, only the far field ($\overline{R} > 2$) was considered in this study. Therefore, the equation proposed by Kinney and Graham (1985) can be employed to estimate the overpressure from the TNT scaled distance.

$$\frac{p_s}{P_0} = \frac{808\left[1 + \left(\frac{Z}{4.5}\right)^2\right]}{\sqrt{1 + \left(\frac{Z}{0.048}\right)^2}\sqrt{1 + \left(\frac{Z}{0.32}\right)^2}\sqrt{1 + \left(\frac{Z}{1.35}\right)^2}} \tag{21}$$

where $p_s$ is the overpressure in Pa, $P_0$ is the atmospheric pressure in Pa and $Z$ is the TNT scaled distance in m kg$^{-1/3}$. The impulse of the pressure wave was determined with a correlation proposed again by Kinney and Graham (1985), here reported in Eq. (22):

$$i_s = \frac{6.7\sqrt{1 + \left(\frac{Z}{0.23}\right)^4}}{Z^2\sqrt[3]{1 + \left(\frac{Z}{1.55}\right)^3}} W_{TNT}^{1/3} \tag{22}$$

where $Z$ is the TNT scaled distance in m k$^{-1/3}$ and $W_{TNT}$ is the equivalent mass of TNT in kg. the impulse is then determined in Pa s. Ullah et al. (2017) compared different methods to estimate the impulse of the blast wave and stated that the difference in the results of these correlations diminishes when $Z > 1$. It must be noticed that the TNO and Birk models take into account the influence of the tank geometry on the blast wave. The pressure wave has a different yield along the transversal and longitudinal axes when a cylindrical vessel fails, especially in the near field (Birk et al., 2007). In Table 6, the values of the multipliers to adjust the overpressure values according to the geometry effects are collected.

Finally, according to these two models, the overpressure should by multiply by 1.1 when $\overline{R} \geq 1$ and the tank is slightly elevated above the ground (van den Bosch and Weterings, 2005).

To determine the safety distance from a vessel, both overpressure and impulse must be taken into account. Molkov and Kashkarov (2015) adopted the data published for high explosives by Baker et al. (1983) to determine the harm effects on humans from high-pressure tank explosions. In this analysis, a similar approach was selected by considering only the overpressure and impulse threshold to avoid any kind of injuries on humans and damages on structures, correspondent to 1.35 kPa and 1 Pa s. This is a conservative threshold and was adopted to determine the safety distance from the tank due to the pressure wave effects. Moreover, an overpressure threshold to avoid injuries on humans caused directly by the pressure wave was set at 16.5 kPa by Molkov and Kashkarov (2015) and here employed when only the overpressure is considered.

*3.3.1.2. Fragments range.* The correlation suggested by (Birk, 1996) to estimate the horizontal range of the fragments of a propane tank during a BLEVE explosion was implemented in this work. This correlation, reported in Eqs. (23) and (24), depends only on the mass of the substance contained in the vessel ($m_T$) and its volume ($V_T$).

$$R = 90 \cdot m_T^{0.33} for VT < 5m^3 \tag{23}$$

$$R = 465 \cdot m_T^{0.1} for VT > 5m^3 \tag{24}$$

Since this method usually overestimates the fragments range, the methodology proposed by CCPS (2010) was adopted in this consequence analysis as well. The initial velocity of the fragments is estimated with the correlation presented by Baum (1984) in Eq. (25):

$$v_i = \sqrt{\frac{2 \cdot A_{ke} \cdot E_{av}}{M_C}} \quad (25)$$

where $E_{av}$ is the available mechanical energy usually estimated with the most conservative methods (IE or TNO models) in J, $A_{ke}$ is the portion of energy responsible for the fragments ejection (kinetic energy) equal to 0.04 for the BLEVE explosion (van den Bosch and Weterings, 2005), and $M_C$ is the empty mass of the vessel in kg. This second approach neglects the fluid dynamic forces (lift and drag) since the fragment characteristics (mass, dimensions, and shape) are usually difficult to gather or determine a priori. Eqs. (26) and (27) were utilised to calculate the horizontal ($R$) and vertical ($H$) ranges of the fragments respectively:

$$R = \frac{v_i^2 \cdot \sin(2 \cdot \alpha_i)}{g} \quad (26)$$

$$H = \frac{v_i^2 \cdot \sin(\alpha_i)^2}{2 \cdot g} \quad (27)$$

where $v_i$ is the initial velocity of the fragments previously estimated in m $s^{-1}$, $\alpha_i$ is the initial angle of the fragments ($5 \div 10°$ for cylindrical vessels horizontally placed (CCPS, 2010)), and $g$ is the acceleration of gravity (9.81 m $s^{-2}$). If the tank is placed vertically, an angle of 45° can be assumed as in (Gayle, 1964). Moreover, a third approach which instead considers the fluid dynamic force was adopted. The scaled velocity is estimated with Eq. (28):

$$\overline{v}_i = \frac{\rho_a \cdot C_D \cdot A_D \cdot v_i^2}{M_F \cdot g} \quad (28)$$

where $\rho_a$ is the atmospheric air density (1.229 kg $m^{-3}$ at 15 °C, 101.3 kPa (NASA, 2020)), $C_D$ is the drag coefficient of the fragment and $A_D$ is its cross-sectional area in $m^2$, $v_i$ is again the initial velocity estimated with Eq. (25) in m $s^{-1}$, $M_F$ is the fragment mass in kg, and $g$ the gravitational acceleration in m $s^{-2}$. Once the scaled velocity is estimated, the scaled range is determined with the aid of a graph published by Baker et al. (1983). The horizontal fragment range ($R$) is then calculated from Eq. (29):

$$\overline{R}_F = \frac{R \cdot \rho_a \cdot C_D \cdot A_D}{M_F} \quad (29)$$

where $\overline{R}_F$ is the scaled fragment range. The assumption that the tank ruptures in two pieces (end caps) was made. The end caps have hemispherical shape, hence $C_D \cdot A_D = 0.615 \cdot \pi / 4 \cdot D_V^2$, where $D_V$ is the vessel diameter in m and the tumbling of the fragment is considered, and the ratio $C_D \cdot A_D / C_L \cdot A_L = 0$ (van den Bosch and Weterings, 2005). This latter is used to select the curve on the chart provided in (Baker et al., 1983). The safety distance from the tank due to the fragments is then determined according to the most conservative fragments range result. In the following, the second and third methods are indicated as NFF (neglecting fluid dynamic forces) and CFF (considering fluid dynamic forces), respectively.

### 3.3.2. Fireball dimension, duration and radiation

Hydrogen is a highly flammable substance. After an $LH_2$ BLEVE, the formation of a fireball is a likely phenomenon, especially in the case of a hot BLEVE since the ignition source is already present externally to the tank. However, a fireball may be generated after a cold BLEVE as well due to the very low hydrogen ignition energy (0.017 mJ (Ono et al., 2007)). For instance, a spark has sufficient energy to ignite a hydrogen-air mixture, and this ignition source may be provoked during the rupture of the vessel. For this reason, the fireball dimensions (diameter and height), duration and radiation were estimated in this consequence analysis. The fireball diameter ($D_{fb}$) was calculated with Eq. (30) (Hord, 1972) which depends only on the total mass of the substance ($m_T$) in kg:

$$D_{fb} \approx 7.93 \cdot m_T^{1/3} \quad (30)$$

One of the most conservative equations to determine the height of the fireball centre ($H_{fb}$), provided by Bagster and Pitblado (1989), was adopted in this analysis:

$$H_{fb} = 2 \cdot R_{fb} \quad (31)$$

where $R_{fb}$ is the fireball radius in m. A comparison between both the momentum-dominated (Eq. (32)) and buoyancy-dominated fireball formula (Eq. (33)) was conducted in order to estimate the minimum and maximum fireball duration ($t_{fb}$) (Beyler, 2016).

$$t_{fb} = 0.45 \cdot m_T^{1/3} \quad (32)$$

$$t_{fb} = 2.60 \cdot m_T^{1/6} \quad (33)$$

In (CCPS, 2010), the employment of the momentum-dominated fireball equation is suggested if the mass of the substance is lighter than 30,000 kg. However, Zalosh and Weyandt (2005) better estimated the duration of the fireball experimentally initiated after the rupture of a compressed tank with a volume of 72.4 L and containing 1.64 kg of hydrogen at 35.7 MPa with the second equation rather than the first one. The radiation from the fireball was assessed through the solid flame model (CCPS, 2010) in which the fireball is approximated as a homogenous sphere. The fuel contribution to the fireball is usually a critical and challenging aspect to determine. According to (Gayle and Bransford, 1965), almost the whole $LH_2$ amount was completely consumed during the experiments of the Pyro project (Willoughby and Ullian, 1988). For this reason, it was assumed that 100% of the $LH_2$ mass contributes to the fireball. The incident radiation, $q$, which is the radiation received by a target in W $m^{-2}$, was calculated with Eq. (34):

$$q = F_{fb} \cdot E_{SEP} \cdot \tau \quad (34)$$

where $F_{fb}$ is the view factor, $E_{SEP}$ is the surface emissive power (*SEP*) in W $m^{-2}$, and $\tau$ is the atmospheric attenuation factor (transmissivity). The *SEP* is usually measured during the experiments, and Johnson et al. (1991) reported a *SEP* value up to 350 kW $m^{-2}$ for industrial size (>1000 kg) butane and propane BLEVE fireballs. This value is usually adopted for a conservative estimation. However, the fireball *SEP* is highly affected by the substance type and amount, and the tank pressure prior the release. In addition, the *SEP* is not constant on the fireball surface and during its duration. For these reasons, the *SEP* was theoretically assessed with the Stefan-Boltzmann's law (Eq. (35)).

$$E_{SEP} = \varepsilon \cdot \sigma \cdot T_{fb}^4 \quad (35)$$

where $\varepsilon$ is the emissivity of the body, $\sigma$ is the Stefan-Boltzmann constant ($5.67 \times 10^{-8}$ W $m^{-2}$ $K^{-4}$), and $T_{fb}$ is the fireball temperature in K. The fireball was considered as a black body ($\varepsilon = 1$) in order to obtain the most conservative estimation. The fireball temperature value was set equal to the stochiometric combustion temperature of hydrogen in air (2321 K (NASA, 2005)), since this value was assumed by Pehr (1996) as the peak temperature of the hydrogen fireballs. A similar procedure was adopted by High (1968) to estimate the thermal radiation from a Saturn V fireball where the highest temperature was 2400 K. When the distance between the release point and the target ($x_{fb}$) is longer than the fireball radius ($R_{fb}$), the view factor was estimated with Eq. (36):

$$F_{fb} = \left(\frac{R_{fb}}{L}\right)^2 \cos \vartheta \quad (36)$$

where $L$ is the distance between the fireball centre and the target in m, and $\theta$ is the angle between the receptor surface normal and $L$ in degree. It must be noticed that the higher value of $F_{fb}$ is attained when this angle is zero, i.e. the receptor is completely facing the fireball and receiving its radiation. In order to obtain a conservative result, $cos(\theta)$ was assumed to

**Table 7**
Summary of the BMW safety tests results (Pehr, 1996).

| BLEVE consequence | | Test | | | | | | | | |
|---|---|---|---|---|---|---|---|---|---|---|
| | | 2 | 3 | 4 | 5 | 6 | 7 | 8 | 9 | 10 |
| Tank pressure (bar) | | 4.0 | 11.0 | 2.1 | 15.0 | 3.7 | 2.0 | 4.0 | 11.0 | 11.3 |
| Overpressure (mbar) | | 110 | 470 | 33 | 150 | 60 | 167 | 77 | 133 | 150 |
| Fragments range (m) | | >15 | | | | | | | | |
| Fireball | Max. diameter (m) | 20 | | | | | | | | |
| | Max. height (m) | 20 | | | | | | | | |
| | Longest duration (s) | 4 | | | | | | | | |

**Table 8**
Characteristics of the $LH_2$ tanks selected for the consequence analysis.

| Case study | Type | Insulation | Orientation | $V_T$ ($m^3$) | $M_C$ (kg) |
|---|---|---|---|---|---|
| BMW test (Pehr, 1996) | Single walled | Foam | Horizontal | 0.12 | 60 |
| $SH_2$IFT project | Double walled | Vacuum jacket + perlite or MLI* | Horizontal and vertical | 1.00 | 730 (MLI), 1015 (perlite) |

Notes: *MLI: multi-layer insulation.

**Table 9**
Initial conditions of the consequence analysis.

| Simulation | $LH_2$ mass (kg) | Tank pressure before the explosion (bar) | Distance between the first pressure sensor and the tank (m) |
|---|---|---|---|
| BMW test ( Pehr, 1996) | 1.8 ÷ 5.4 | 2.0 ÷ 14.8 | 3.0 |
| $SH_2$IFT project | 35.4 | 14.0 ÷ 34.0 | 10.0 |

be equal to 1. Finally, the air transmissivity was determined with Eq. (37) (van den Bosch and Weterings, 2005):

$$\tau = 2.02 \cdot \left(RH \cdot p_w^0 \cdot \left(L - R_f\right)\right)^{-0.09} \quad (37)$$

where $RH$ is the relative humidity (50% in this analysis), $p_w^0$ is the partial pressure of saturated water vapour (1705 Pa at 15 °C (van den Bosch and Weterings, 2005)), $R_{fb}$ is the fireball radius in m, and $L$ is the distance from the fireball centre to the target in m. The injuries caused by the fireball radiation are affected by the thermal dose which depends on the incident radiation and the exposure time to the fireball. The thermal dose was then assessed with Eq. (38):

$$Thermal\ dose = q^{4/3} \cdot t_{fb} \quad (38)$$

where $q$ is the incident radiation in W $m^{-2}$, and $t_{fb}$ is the fireball duration in s. The thermal dose threshold to avoid any kind of injuries is 80 (kW $m^{-2}$)$^{4/3}$ s (Rew, 1997). The thermal dose was evaluated at difference distance from the fireball centre and this thermal dose was used as reference value to determine the safety distance due to the radiation emitted by the fireball. Finally, the safety distance from the failing vessel was determined by considering the longest distance among the ones previously determined due to the pressure wave, fragments range and fireball.

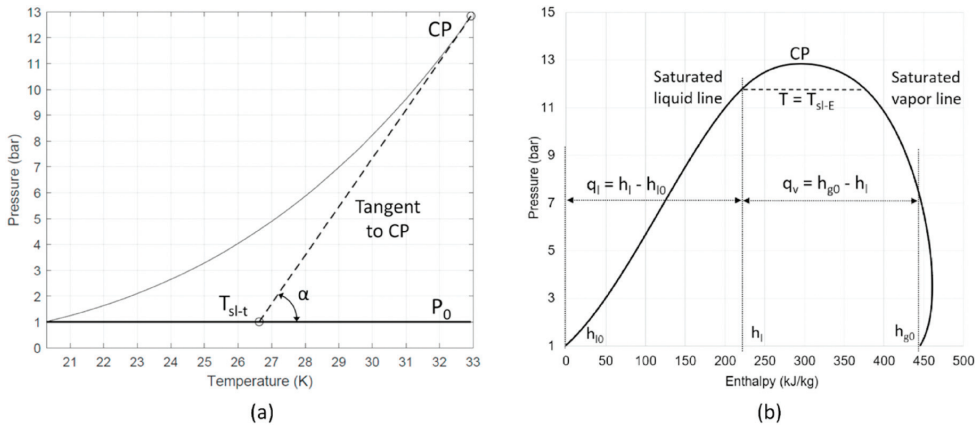


**Fig. 2.** (a) tangent to the parahydrogen saturation curve obtained from the application of the SCT model and (b) P-h diagram of parahydrogen obtained after the application of the EB model.

**Table 10**
Estimated superheat limit temperature ($T_{SL}$) for hydrogen.

| Models | $T_{SL}$ (K) | P (bar) |
|---|---|---|
| EC | 29.5 | 7.6 |
| SCT | 26.2 | 4.2 |
| EB | 32.4 | 11.9 |

### 3.4. BMW tests simulation and validation of the models

In the period 1992–1995, a safety research program on $LH_2$ tanks developed for automotive application was conducted by BMW car manufacturer in cooperation with the tank manufacturers Messer Grieshein GmbH, Linde AG and other relevant licensing and research

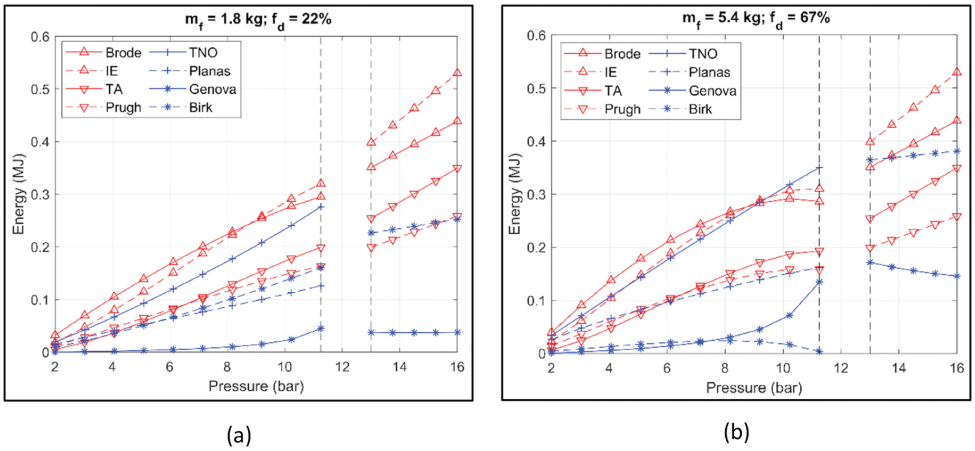


**Fig. 3.** Mechanical energy generated by BLEVE explosion at different tank pressures of a 0.12 $m^3$ tank containing (a) 1.8 kg and (b) 5.4 kg of $LH_2$, estimated by ideal (red) and real (blue) gas behaviour models. (For interpretation of the references to colour in this figure legend, the reader is referred to the Web version of this article.)

institutions (Pehr, 1996). Among different test types such as dynamic vibration, crash and skid, vacuum loss and fire tests (Rybin et al., 2005), the bursting tank scenario was investigated (Pehr, 1996). During this test series, ten single walled vessels with a volume of 0.120 $m^3$ insulated with a layer of foam and filled with different amounts of $LH_2$ (1.8 ÷ 5.4 kg) were wrecked at different internal pressures (2 ÷ 14.8 bar) by means of cutting charges. The description of this type of experiment corresponds to a cold BLEVE. The approach previously described was applied to simulate this case study (step 2 in Fig. 1). The results from the simulations were compared with the ones published in (Pehr, 1996) in order to validate the method for $LH_2$ BLEVE (step 3 in Fig. 1). The results of the BMW safety tests are collected in Table 7. During this phase, it was possible to determine which are the most suitable models for the $LH_2$ BLEVE consequence analysis.

### 3.5. Blind prediction and generalization of the method

A blind prediction is usually carried out when the experimental results are not available yet. The estimation of the consequences before the experiments may be useful to comprehend which type of instrumentation is required to record the pressure wave and fireball effects, and where it should be placed. Furthermore, a blind prediction of the BLEVE formation can determine the time to failure of the vessel, but this was not covered in this study. Finally, the predictive capabilities of the models employed in the blind prediction can be assessed by comparing its results with the experimental outcomes (Skjold et al., 2019). Different blind predictions were conducted for the consequences of hydrogen tests in the past (Skjold et al., 2019). In this work, a blind prediction of the $SH_2$IFT tests consequences was conducted (step 4 in Fig. 1) by employing the models selected after the validation.

During the $SH_2$IFT project, three double walled vessels filled at 50% with $LH_2$ will be engulfed in a propane fire. The tanks will be placed either horizontally or vertically and the insulations will be composed by both perlite powder and MLI inside the vacuum jackets in different tests. The pressure relief valves (PRVs) installed on the tanks will be closed to simulate a device failure. The experiment is foreseen to last until the

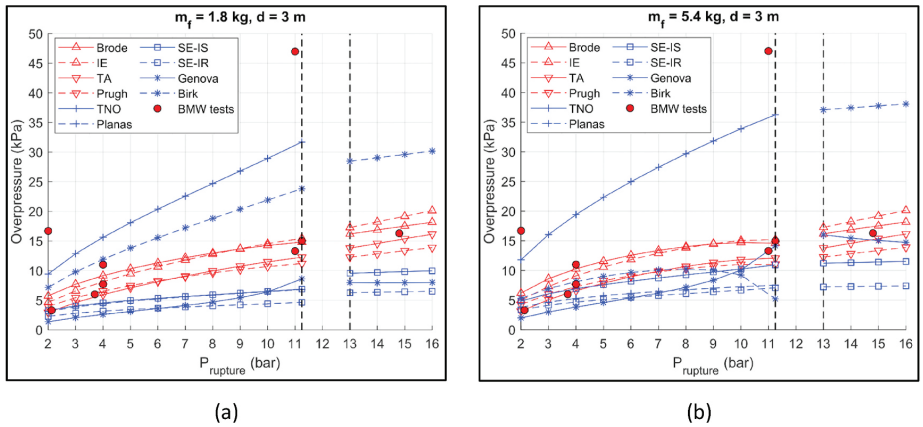


**Fig. 4.** Overpressure from the blast wave at 3 m from a sub- and supercritical BLEVE of a tank containing (a) 1.8 kg and (b) 5.4 of $LH_2$. Red circles indicates the overpressures measured during the BMW safety tests (Pehr, 1996). (For interpretation of the references to colour in this figure legend, the reader is referred to the Web version of this article.)

collapse of the vessels. In this manner, a hot BLEVE will be simulated if proper thermodynamic conditions will be reached inside the container. Since the bursting pressure is unknown, it was determined with the procedure proposed by Casal (2008). The failing pressure in the worst-case scenario should be four times the design pressure. According to (Rybin et al., 2005), the maximum allowable working pressure of an $LH_2$ tank is 8.2 bar. Hence, the highest failing pressure is foreseen to be 32.8 $bar_g$. Therefore, a failing pressure of 34 bar was the upper limit adopted in the analysis to simulate the most severe consequences.

Table 8 collects the characteristics of the $LH_2$ storage tanks of the BMW and $SH_2$IFT tests considered in this analysis, while the initial conditions of the simulations are reported in Table 9.

Laboureur et al. (2014) provided a distinction to differentiate small-, mid- and large-scale tests in terms of TNT equivalent mass, that is $m_{TNT} > 1$ kg for large-scales, $m_{TNT} \approx 1$ kg for mid-scales, and $m_{TNT} < 1$ kg for small-scales. Therefore, the BMW experiments were small-scale tests while the $SH_2$IFT ones will be mid-scale. In addition, a cold BLEVE was provoked during the BMW tests, while a fired BLEVE will be initiated during the $SH_2$IFT tests. In this way, the proposed approach can be generalized since applied to two different test scales and BLEVE types. However, the experimental outcomes are required to validate the models and the approach, and establish if their generalization and predictive capabilities are successful.

## 4. Results

A graphical representation of the SCT model is depicted in Fig. 2 (a) where the dashed line is the tangent to the saturation curve at the critical point (CP), while in Fig. 2 (b), the p-h diagram for parahydrogen obtained after the application of the EB model is displayed.

In Table 10, the values of $T_{SL}$ estimated for parahydrogen by the methods described in Sec. 3 are collected together with the correspondent pressures at saturation conditions. As shown, a BLEVE might occur after the catastrophic rupture of a $LH_2$ tank if the contained liquid has a temperature higher than 26.2 K, according to the most conservative method. The pressure correspondent to this temperature at saturation conditions is 4.2 bar.

Finally, Nishigaki and Saji (1983) identified experimentally the superheat temperature of oxygen, nitrogen, neon and hydrogen. The highest measured temperature for hydrogen at 1 atm was 28.1 K. This value is included in the range of temperatures theoretically estimated in this study. However, it is not clear if the hydrogen tested by Nishigaki and Saji (1983) had been converted in parahydrogen. There might be a small difference between the $T_{SL}$ of parahydrogen and normal hydrogen since their critical temperatures slightly differ (NIST, 2019). The first method applied in this work, proposed by Reid (1976), seems the most accurate when compared with the experimental results.

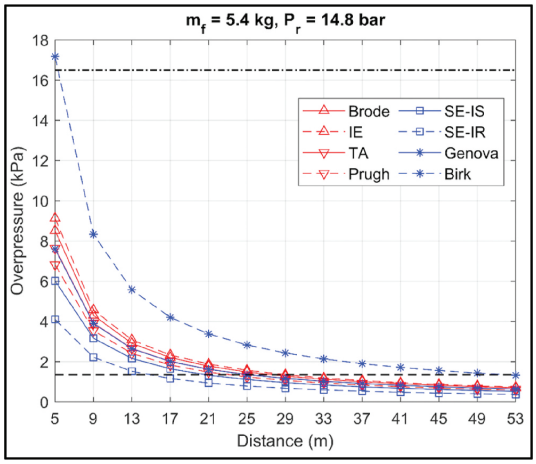


**Fig. 5.** Overpressure from the supercritical BLEVE blast wave at different distances from a tank failing at 14.8 bar and containing 5.4 kg of $LH_2$. Black dash-dotted and dashed lines indicate the overpressure thresholds at 16.5 and 1.35 kPa, respectively.

### 4.1. BMW safety test simulations

In the following, the consequence analysis results of the BMW safety tests are reported. Firstly, the mechanical energies estimated by the ideal and gas behaviour models for both sub- and supercritical BLEVEs are introduced. Secondly, the overpressures and impulses of the blast wave are presented. Finally, the fragments range and the fireball characteristics are described.

#### 4.1.1. Mechanical energy

The mechanical energy generated from the failure at different pressures of the tanks filled with different amounts of $LH_2$ (1.8 and 5.4 kg) are displayed in Fig. 3.

Both sub- and supercritical BLEVEs were simulated by means of the models previously described. The mechanical energy was not estimated close to the critical point because the selected models cannot provide reliable results. For instance, the Genova model is influenced by the specific heat of the substance which tends towards an infinite value at the critical pressure. Among the chosen models, this is the only one that foresees a reduction of mechanical energy when the failure pressure increases at supercritical conditions, because it follows the trend of the hydrogen specific heat. Increasing the hydrogen mass inside the tank, the ideal gas behaviour models tend to ebb in the vicinity of the critical pressure at subcritical conditions. It should be noticed that the Birk model estimates higher mechanical energy values when the $LH_2$ mass inside the tank is lower at subcritical conditions, because it barely depends on the vapour phase. As previously mentioned, the TNO and Planas models cannot be employed at supercritical conditions. The most conservative model is the isothermal expansion (Smith and Van Ness, 1996), as already demonstrated in previously studies (Hemmatian et al., 2017b).

#### 4.1.2. Overpressure and impulse from the blast wave

During the BMW safety tests (Pehr, 1996), the overpressure was measured at 3 m from the vessel, and the bursting pressures of the tanks were in the range from 2.0 to 14.8 bar. The subcritical and supercritical blast wave overpressures were then estimated by the ideal and real gas behaviour models at this distance from the tank in order to compare the experimental results (see Fig. 4). The failure pressure range was selected between 2.0 and 16.0 bar. It must be noticed that according to the results achieved in Sec. 3.1, the explosion which arise after the catastrophic rupture of the vessel can be considered as a BLEVE if the tank pressure before the explosion is higher than 4.2 bar. However, all the outcomes of the BMW tests were employed as comparison with the results of the selected models due to the scarcity in literature of small- and mid-scales $LH_2$ explosion experiments.

The most conservative estimation at subcritical conditions is provided by the TNO model with a maximum overpressure of 32 kPa at 11.25 bar. However, two BMW tests registered even a higher overpressure at 2 and 11 bar (16.7 and 47.0 kPa respectively). Pehr (1996) stated that during these two tests an over-proportional increase in overpressure was measured. The author supposed that the causes of these values can be attributed in one case to the overlap of the cutting charge and BLEVE effects (expanding of both vapour and liquid), and in the other case to an oxygen enrichment on the tank external wall due to an insulation damage. The highest overpressure (38.2 kPa) is attained by the Birk model at supercritical conditions when the tank fails at 16 bar and contains 5.4 kg of $LH_2$. For this reason, only the overpressures

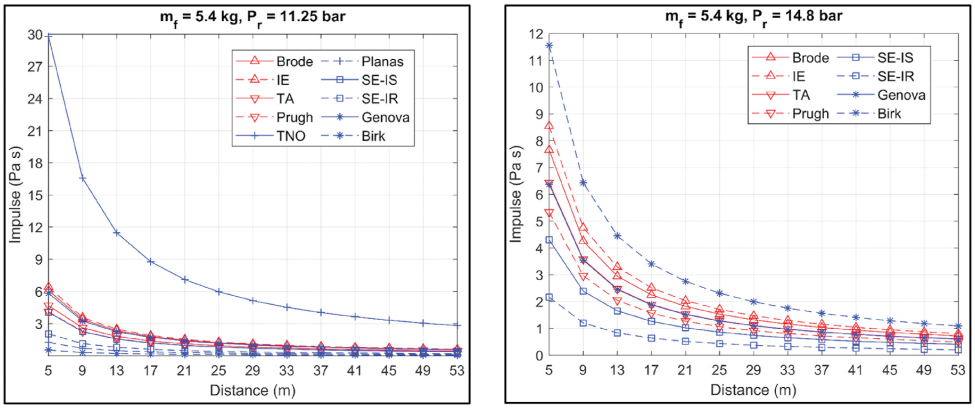


**Fig. 6.** Impulse from sub- and supercritical BLEVE blast waves at different distances from a tank containing 5.4 kg of $LH_2$ and failing at (a) 11.25 and (b) 14.8 bar, respectively.

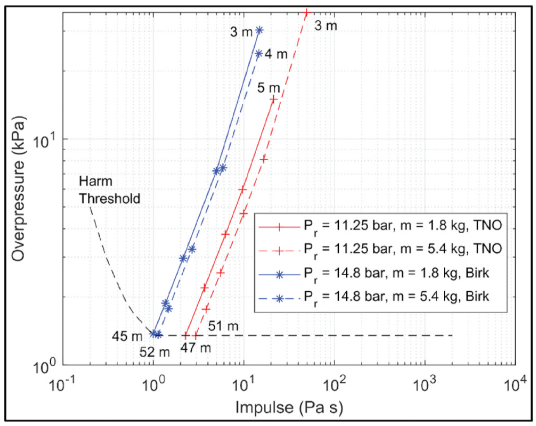


**Fig. 7.** Impulse and overpressure of both sub- and supercritical BLEVE blast waves at different distances from a tank failing at 11.25 and 14.8 bar respectively, containing 1.8 kg and 5.4 kg of $LH_2$, estimated with the most conservative models: TNO (red) and Birk (blue). The black dashed line indicates the harm threshold. (For interpretation of the references to colour in this figure legend, the reader is referred to the Web version of this article.)

**Table 11**
Fragments range for the sub- and supercritical BLEVEs occurred during the BMW safety tests estimated with the method proposed by (CCPS, 2010).

| BLEVE types | Conditions at the explosion | | | | *R* (and *H*) ranges (m) | | |
|---|---|---|---|---|---|---|---|
| | $m_{H2}$ (kg) | $P_{rup}$ (bar) | $E_k$ (kJ) | $v_i$ (m $s^{-1}$) | $\alpha_i$ = 5° | $\alpha_i$ = 10° | $\alpha_i$ = 45° |
| Subcritical BLEVE | 5.4 | 11.25 | 14 | 21.6 | 8 (2) | 16 (4) | 48 (17) |
| Supercritical BLEVE | 5.4 | 14.80 | 19 | 25.2 | 11 (3) | 22 (6) | 65 (23) |

estimated at different distances when the rupture pressure is 14.8 bar (highest rupture pressure of the BMW tests) and the $LH_2$ mass is 5.4 kg are depicted in Fig. 5.

The overpressure thresholds of 16.5 and 1.35 kPa described in the methodology are represented by the dash-dotted and dashed lines in Fig. 5, respectively. In this case, if only the overpressure is considered, the 1.35 kPa threshold is attained at 52 m according to the most conservative model (Birk).

Differently from the overpressure, the highest impulse is estimated by the TNO model at subcritical conditions. For this reason, the impulses calculated at different distances from the $LH_2$ tank for both sub- and supercritical BLEVEs are displayed in Fig. 6.

As previously mentioned, the TNO model gives the highest estimation at subcritical conditions (29.8 Pa s at 5 m from the vessel), while the Birk model is the most conservative at supercritical conditions (11.6 Pa s at 5 m). The combined effect of overpressure and impulse is displayed in Fig. 7 where the most conservative estimations for both sub- and supercritical BLEVEs are reported. The safety distance from the tank to avoid undesired injuries is determined when the lines cross the harm threshold curve. The longest safety distance is 52 m and was achieved for the supercritical BLEVE when the tank fails at 14.8 bar and contains 5.4 kg.

### 4.1.3. *Fragments range*

The number of fragments of a cylindrical vessel after a BLEVE should be between two and three pieces (van den Bosch and Weterings, 2005). During the BMW tests, the cylindrical vessels fragmented in several pieces. The cut explosive charges employed to trigger the explosion could be responsible for the high number of vessel debris. The distance reached by the fragments during these tests was longer than 15 m (Pehr, 1996). The first method to determine the fragments range proposed by Birk (1996) for vessels with a volume lower than 5 $m^3$, provides an extremely conservative value of 157 m. The fragments ranges were estimated for both sub- and supercritical BLEVEs with the NFF method which neglect the fluid dynamic forces. For the subcritical explosion, the most conservative result ($\alpha_i = 45°$) was 47.6 and 64.7 m for the failure pressures of 11.25 and 14.8 bar respectively. As suggested by CCPS (2010), the initial angle of the fragments trajectory for a cylindrical vessel horizontally placed should be between 5° and 10°. The results obtained for $\alpha_i = 10°$ agree with the BMW test results (>15 m). The horizontal (*R*) and vertical (*H*) fragments ranges are collected in Table 11 together with the conditions prior the explosion.

Finally, the fragments range was estimated considering the fluid dynamic forces (CFF model). As previously mentioned, it was assumed that the tank ruptured in two main fragments, the end caps which have a hemispherical shape. The vessel diameter and the fragments mass are

**Table 12**
Fragments range for the sub- and supercritical BLEVEs occurred during the BMW safety tests estimated by including the fluid dynamic forces.

| BLEVE types | Conditions at the explosion | | | Fragments characteristics | | | $R$ (m) |
|---|---|---|---|---|---|---|---|
| | $m_{H2}$ (kg) | $P_{rup}$ (bar) | $v_i$ (m s$^{-1}$) | $m_f$ (kg) | $C_D \cdot A_D$ | $\frac{C_L \cdot A_L}{C_D \cdot A_D}$ | |
| Subcritical BLEVE | 5.4 | 11.25 | 21.6 | 30 | 0.077 | 0 | 47 |
| Supercritical BLEVE | 5.4 | 14.80 | 25.2 | 30 | 0.077 | 0 | 63 |

**Table 13**
Consequences of the fireballs occurred during the BMW safety tests.

| Fireball parameters and safety distance | BMW test results | Consequence analysis | Relative error (%) |
|---|---|---|---|
| **Max. diameter (m)** | 20 | 13.9 | 43.9 |
| **Height (m)** | 20 | 13.9 | 43.9 |
| **Duration (s)** | 4.0 | 0.8 ÷ 3.4 | 17.6 ÷ 400 |
| **Surface Emissive Power (kW m$^{-2}$)** | – | 1880 | – |
| **Safety distance (therm. dose = 80 (kW m$^{-2}$)$^{4/3}$ s)** | – | 77.8 | – |

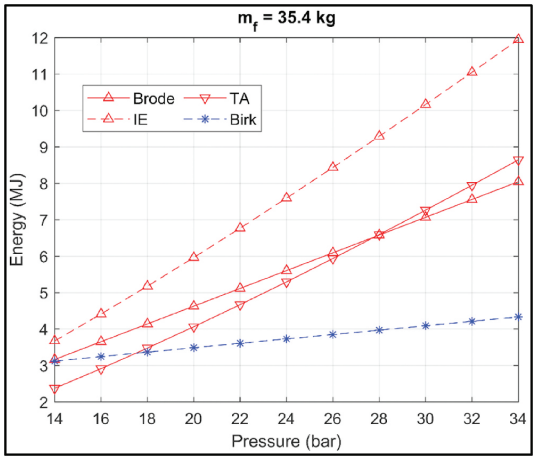


**Fig. 8.** Mechanical energy generated by supercritical BLEVE explosions at different tank pressures of a 1 m$^3$ tank containing 35.4 kg of $LH_2$, estimated by ideal (red) and real (blue) gas behaviour models. (For interpretation of the references to colour in this figure legend, the reader is referred to the Web version of this article.)

supposed to be 0.4 m and 30 kg respectively (the total tank mass is 60 kg). The results of the CFF method applied to the two BLEVE types are reported in Table 12, together with the fragments characteristics.

It must be noticed that similar ranges were obtained by the CFF and NFF models when an initial fragment angle of 45° was selected. These values are the most conservative results and can be assumed as upper limits, excluding the results achieved with the first method.

#### 4.1.4. Fireball dimensions and radiation

The fireball consequences, that is its dimensions, duration, radiation and distance to the thermal dose threshold, are listed in Table 13. The results obtained in this study seem underestimating the fireball consequences when compared with the BMW safety tests. In particular, the maximum fireball diameter and height of 20 m was measured in the experiments, while 13.9 m was the highest values achieved from the empirical model, which are 30.5% lower. These estimations provide almost 44% of relative error. The fireball duration calculated with the buoyancy-dominated fireball formula was closer to the measured duration compared with the value obtained with the momentum-dominated equation, while according to the literature it should be the opposite. The *SEP* estimated theoretically with the Stefan-Boltzmann's law was more than five time higher compared to the maximum value suggested for the propane fireballs (350 kW m$^{-2}$). However, the model developed by Bader et al. (1971) for rocket liquid-propellants estimated a peak heat flux from the fireball of 4543 kW m$^{-2}$ (400 Btu ft$^{-2}$ s$^{-1}$). A similar result was estimated by Kite et al. (1965) during the Atlas/-Centaur abort (425 Btu ft$^{-2}$ s$^{-1}$). In those analysis, large amounts of propellants were involved in the fireball, from 11,340 to 131,088 kg of both fuel and oxidizer, but the peak heat flux was not affected by the propellant mass. Considering the fireball duration and incident radiation, the thermal dose threshold of 80 (kW m$^{-2}$)$^{4/3}$ s was estimated at 77.8 m from the centre of the exploding tank.

#### 4.1.5. Safety distance

In this work, the safety distance is determined from the consequence analysis results. The highest value between the distance where the overpressure and impulse thresholds to avoid injuries are attained (52 m), the longest horizontal fragments range (65 m), the fireball diameter (13.9 m) and the distance to obtain the lowest thermal dose emitted from the fireball to the target (77.8 m), is considered as the safety distance. Therefore, it can be concluded that the safety distance from the vessel should be 77.8 m, due to the fireball radiation.

### 4.2. Models validation

The consequence analysis applied to the BMW safety tests, demonstrated that the most conservative models to estimate the overpressure from the blast wave in the sub- and supercritical conditions are the TNO and Birk ones, respectively. Furthermore, few models were able to provide higher overpressure values than the experimental results, if the highest BMW test outcomes attained at 2 and 11 bar (16.7 and 47.0 kPa, respectively) are excluded. These models are the Brode and IE, beyond the TNO and Birk ones. An observation must be made regarding the considerable underestimation obtained with the Birk model at subcritical conditions when the tank has a high filling degree and the liquid phase is preponderant. Moreover, the TA model foresees an overpressure increment when the rupture pressure increases at supercritical conditions (Fig. 4 (b)) slightly higher than the Brode model. In addition, the estimated overpressure by the TA model at supercritical condition is close to the experimental outcome. For these reasons, this model was considered valid as well. Finally, the selected energy models were the TNO, Birk, Brode, IE and TA. It must be remembered that the TNO model can be applied only at subcritical conditions. Laboureur et al. (2012b) simulated different small-scale supercritical propane BLEVE experiments by means of the models considered in this study. The comparison between the experimental and the estimated results demonstrated that the Birk and Prugh models provided the most conservative outcomes and were the only approaches that did not underestimated the measured overpressure.

Regarding the fragments range analysis, all three applied methods provided conservative results. However, the fragment range seems largely overestimated by the first method (157 m). For this reason, this model was not considered any further. On the other hand, the initial angle of the fragment must be chosen carefully when the NFF method is adopted, since the results obtained for angles lower than 10°

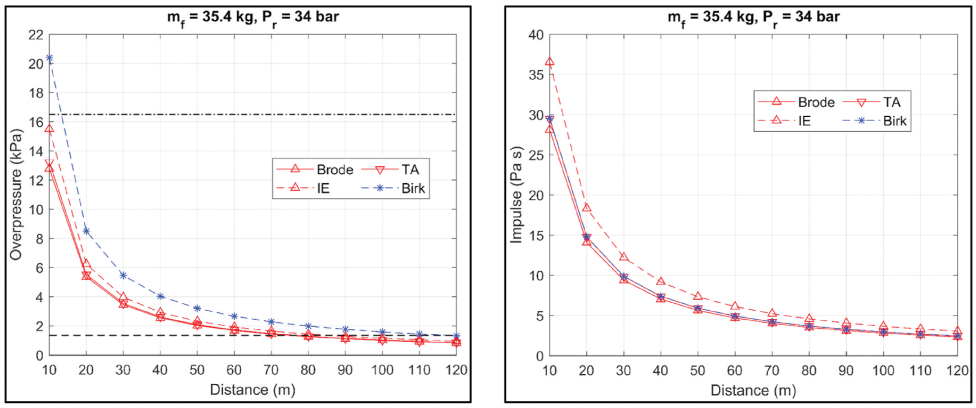


**Fig. 9.** (a) overpressure and (b) impulse at different distances from the blast wave of a supercritical BLEVE of a 1 $m^3$ tank containing 35.4 kg $LH_2$ and failing at 34.0 bar. The black dash-dotted and dashed lines represent the overpressure thresholds to avoid injuries.

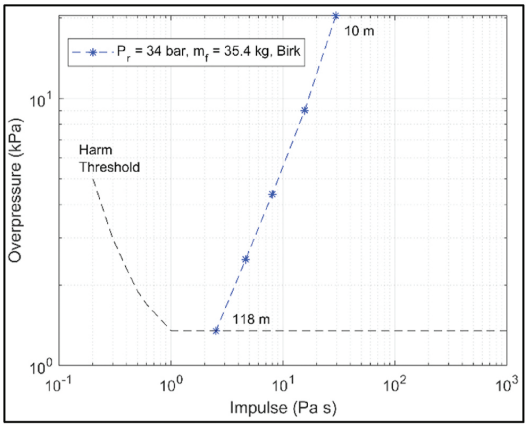


**Fig. 10.** Impulse and overpressure of the supercritical BLEVE blast wave at different distances from a tank failing at 34 bar and containing 35.4 kg of $LH_2$, estimated with the most conservative model (Birk). The black dashed line indicates the harm threshold.

**Table 14**
Fragments range for the supercritical BLEVE of the $LH_2$ tanks that will be tested during the $SH_2$IFT project, estimated by neglecting the fluid dynamic forces.

| Tank insulation and mass | Conditions at the explosion | | | | *R* (and *H*) ranges (m) | | |
|---|---|---|---|---|---|---|---|
| | $m_{H2}$ (kg) | $P_{rup}$ (bar) | $v_i$ (m $s^{-1}$) | $E_k$ (kJ) | $\alpha_i$ = 5° | $\alpha_i$ = 10° | $\alpha_i$ = 45° |
| MLI 730 kg | 35.4 | 34.0 | 36.2 | 478 | 23 (6) | 46 (12) | 133 (47) |
| Perlite 1015 kg | 35.4 | 34.0 | 30.7 | 478 | 17 (4) | 33 (8) | 96 (34) |

underestimated the experimental results. Finally, the CFF model provided outcomes similar to the most conservative results attained by the second method with an initial fragment angle equal to 45°. Therefore, only the NFF and CFF models were considered valid and employed in the blind prediction study.

**Table 15**
Fragments range for the supercritical BLEVEs of the $LH_2$ tanks that will be tested during the $SH_2$IFT project, estimated by including the fluid dynamic forces.

| Tank insulation and mass | Conditions at the explosion | | | Fragments characteristics | | | *R* (m) |
|---|---|---|---|---|---|---|---|
| | $m_{H2}$ (kg) | $P_{rup}$ (bar) | $v_i$ (m $s^{-1}$) | $m_f$ (kg) | $C_D \cdot A_D$ | $\frac{C_L \cdot A_L}{C_D \cdot A_D}$ | |
| MLI 730 kg | 35.4 | 34.0 | 36.2 | 365 | 0.88 | 0 | 135 |
| Perlite 1015 kg | 35.4 | 34.0 | 30.7 | 508 | 0.88 | 0 | 94 |

**Table 16**
Consequences of the fireballs expected during the $SH_2$IFT $LH_2$ BLEVE tests.

| Fireball parameters and safety distance | Blind prediction |
|---|---|
| Max. diameter (m) | 25.9 |
| Height (m) | 25.9 |
| Duration (s) | 1.5 ÷ 4.7 |
| Surface Emissive Power (kW $m^{-2}$) | 1880 |
| Safety distance (therm. dose = 80 (kW $m^{-2}$)$^{4/3}$ s) | 159.1 |

### 4.3. $SH_2$IFT project blind prediction study

The results of the blind prediction of the $SH_2$IFT project BLEVE tests are presented in this section with the same order of the previous section, starting from the mechanical energy generated by the explosion and related overpressure and impulse of the pressure wave and concluding with the fragments and fireball analysis.

#### 4.3.1. Mechanical energy

The mechanical energy was calculated when the 1 $m^3$ tank filled with 35.4 kg of $LH_2$ fails in a tank pressure range comprise between 14 and 34 bar. Thus, only the supercritical conditions were considered in this blind prediction study since the most severe consequences are sought. The mechanical energy results are displayed in Fig. 8.

The isothermal expansion model is the most conservative model in this case, as well as for the BMW safety tests analysis. Again, all the models linearly increase with the rise in internal tank pressure.

#### 4.3.2. Overpressure and impulse from the blast wave

Only the worst-case scenario was considered for the blind prediction

of the $SH_2$IFT $LH_2$ BLEVE tests. As previously mentioned, the maximum estimated failing pressure was 32.8 $bar_g$. Therefore, the overpressures and impulses were estimated at different distances from the vessel failing at 34 bar. In Fig. 9, both overpressures and impulses of the worst-case scenario are depicted.

The most severe overpressure estimations are achieved again by the Birk model, while the most conservative model to determine the impulse is the isothermal expansion. It must be noticed, that the ideal gas behaviour methods are not affected by the amount of fuel inside the tank at supercritical conditions, because the volume considered in the model equations corresponds to the total tank volume which is a fixed value. In Fig. 10, the plot of both overpressure and impulse against the harm threshold are depicted. In this case, the safety distance is attained at 118 m from the tank by the Birk model.

Ustolin et al. (2019) simulated with the aid of the Process hazard analysis software (PHAST) the overpressure from a BLEVE at different initial conditions for a tank with 1 $m^3$ volume and filled with different masses of $LH_2$. The authors obtained an overpressure of 2.07 kPa at 49.3 m when the tank pressure prior the explosion was 31.2 bar and 40 kg of $LH_2$ were contained in the vessel. Applying these conditions to the methodology selected in this study, this overpressure value is obtained at 47.5 and 75.1 m by the least (Brode) and the most (Birk) conservative models selected for this blind prediction study.

#### 4.3.3. Fragments range

As result from the validation process, only the second and third fragments range models were implemented for the $LH_2$ vessels which will be tested during the $SH_2$IFT project. As for the blast wave, the fragment range was calculated only for the supercritical BLEVE of the two $LH_2$ tank types (with MLI and perlite insulation) failing at 34 bar, with the second method. As expected, the most conservative results were achieved by the NFF model when the initial fragments angle was 45°. The horizontal ranges were 133 and 96 m for the tanks with MLI and perlite insulations, respectively. The results are reported in Table 14.

Similarly, to the fragment analysis conducted for the BMW vessels, two main fragments (the end caps) are expected after a supercritical BLEVE of the $LH_2$ cylindrical tanks. Again, the ranges estimated by the CFF method, are close to the most conservative estimations obtained with the previous model. The ranges calculated with the last method are collected in Table 15 together with the fragments characteristics.

As previously mentioned, one tank will be installed in a vertical position during these tests. The vessel orientation may have an influence on the initial fragment angle. Moreover, if the tank has a substantial height some fragments can reach longer distances by starting their trajectory many meters above the ground compared with a tank placed horizontally. For these reasons, the most conservative estimation ($\alpha_i = 45°$) seems more likely for the vessel installed vertically.

#### 4.3.4. Fireball dimensions and radiation

The maximum expected fireball diameter and height are 25.9 m, while the longest duration is 4.7 s. The safety distance from the $SH_2$IFT vessels should be 159.1 m in order to avoid a thermal dose higher than 80 $(kW\ m^{-2})^{4/3}$ s. Considering the comparison previously conducted in Sec. 4.1.4, these results might underestimate the real fireball consequences. The fireball dimensions and duration of the blind prediction study are reported in Table 16.

#### 4.3.5. Safety distance

In this case, the longest safety distance was 159.1 m due to the fireball radiation, compared with the distance to achieve the overpressure and impulse thresholds to avoid injuries (118 m), the fragments range (135 m), and the fireball diameter (25.4 m).

## 5. Discussion

The equations to calculate the mechanical energy of the explosion adopted in this study, provided a wide range of results, with a difference of one order of magnitude between the most and the least conservative models. In particular, the ideal gas behaviour models provided higher values compared with the real gas behaviour ones. The most conservative models were the isothermal expansion (Smith and Van Ness, 1996) and Brode (1959), as already ascertained by Hemmatian et al. (2017b), while the TNO approach (van den Bosch and Weterings, 2005) was the most conservative real gas behaviour model. Instead, the least conservative method was the one proposed by Genova et al. (2008). In general, if the vessel ruptures at subcritical conditions close to the critical pressure, all the models overpressure curves reach a plateau or have a decreasing trend, except the Genova and TNO methods. This trend can be noticed in Fig. 3 (b), especially for the ideal gas behaviour models. On the other hand, at supercritical conditions the employed models always have a rising trend except the Genova model which is affected by the specific heat at constant pressure ($c_p$) of the substance. Therefore, the Genova method seems not appropriate when applied to the BLEVE assessment for $LH_2$. As mentioned before, the models which take into account both the vapour and liquid phases (TNO and Planas (Planas-Cuchi et al., 2004)) cannot be applied at supercritical conditions. Instead, the models which depends on barely the vapour phase are more conservative when the tank has a low filling degree, and vice versa for the methods which are influenced only by liquid phase. This means that a significant error can be committed when the non-considered phase is dominant in the vessel (Hemmatian et al., 2017a). Moreover, the ideal behaviour models are not affected by the change in density (filling degree) at supercritical conditions because the entire volume of the tank and its pressure are the only two parameters considered by these methods.

The mechanical energy results are exploited in different manners to estimate the overpressure and impulse generated by the blast wave, and the fragments range. The ground reflection and tank geometry effects are included in the TNO and Birk methods to calculate the blast wave yield. For these reasons, the highest values of overpressure and impulse were obtained by these two approaches. On the contrary, according to the Planas, superheat energy (Casal and Salla, 2006) and Genova models, only a fraction of the mechanical energy contributes to the blast wave. This fraction depends on the tank fractur type (fragile, 80%, or ductile, 40%) for the Planas model, on the type of thermodynamic process (isentropic, 14%, or irreversible, 5%) for the SE model, and on empirical correlations (7% for propane) for the Genova method. In the case of double walled tank, used to contain cryogenic fluids such as $LH_2$, how will be affected this percentage? For instance, more energy should be spent to rupture the two tanks (inner and outer), or the outer vessel, designed to bear the vacuum pressure, does not influence the energy required for the fracture? These models (except the Genova one) were validated for butane and propane BLEVEs by Hemmatian et al. (2017b). However, they seem not accurate when applied to the $LH_2$ BLEVEs, even though the model outcomes were validated with the BMW safety tests results in which single walled $LH_2$ tanks were tested. As demonstration of this, the SE model provided the least conservative results for overpressures and impulses. Regarding the model validations with this set of results, only the outcomes of the TNO and Brode models had higher values than the experimental results at subcritical conditions, if the two tests with the over-proportional increase in overpressure are excluded. Since only one test was conducted at supercritical conditions, it is more crucial to conclude which are the most appropriate models at this thermodynamic status. However, the Birk (Birk et al., 2007), Brode, IE and TA (Crowl, 1992, 1991) models were the most conservative. In particular, the Birk method evaluated overpressure values which are more than 200% higher than the measured ones. Finally, it can be proposed to estimate the overpressure from the blast wave of an $LH_2$ BLEVE with the TNO model when the substance conditions are subcritical immediately prior the explosion, and with the Birk model for a supercritical BLEVE.

One observation regarding the TNT equivalent mass method

employed in this study must be made. In the case of BLEVE and high-pressure vessels, this method offers overly conservative estimations in the near field and conservative approximations in the far field due to the different energy release process of the high explosives (very fast) and the vessels explosion (slower than explosives) (Birk et al., 2007). The Sachs scaling law (Sachs, 1944), which derives always from experimental data on explosives, generally provides a less conservative estimation of the pressure wave effects. However, in this study, different underestimations were highlighted by the models previously discussed even adopting the most conservative method (TNT equivalent mass). It is true that in this analysis only the far field was considered due to the lack in experimental data, and more focus should be placed on the pressure wave effects in the near field in the future.

The results obtained for the blind prediction study of the mid-scale $SH_2$IFT tests cannot be compared since the only available tests in literature are the BMW ones, which are small scale experiments ($W_{TNT} < 1$ kg). It must be noticed that the distances at which the overpressure threshold to avoid any kind of injuries on humans was attained are 52 m in the worst-case scenario for the BMW tank containing 5.4 kg of $LH_2$ exploding at 14.8 bar, and 118 m for the $SH_2$IFT vessel containing 35.4 kg of $LH_2$ and failing at 34 bar. Thus, from one analysis to the other, the safety distance and the tank pressure increase almost 2.3 times, while the tank volume and $LH_2$ mass were almost 8.3 and 6.6 times larger. Further investigations and experiments are needed to comprehend which is the correlation between the vessel parameters to achieve a generalization of the approach. In this manner, the method can be applied to all the hydrogen accident scenarios in which BLEVE represents one of the consequences.

The estimation of the fragments range is critical for a BLEVE consequence analysis and is challenging due to several uncertainties. Firstly, the parameters which influence the range calculation such as the fragment shape, dimension, mass, and initial angle are unknown a priori. Secondly, the different methods provide quite contrasting results. For instance, the method proposed by Birk (1996) was the first one employed in this analysis and the most conservative. The results obtained with this approached were almost three times higher than the longest range foreseen by the other models, and thus was not employed in the blind prediction study. The NFF approach estimated quite different range by varying the fragment initial angle. In particular, the fragment range increased two times modifying the angle from 5° to 10°, and almost six times from 5° to 45° (most conservative case). In this case, the fluid dynamic forces were neglected, and this can lead to either an overestimation or an underestimation of the fragment range. This latter may be caused by the frisbee effect which manifests when disc-shape fragments are thrown with low initial angle (CCPS, 2010). In this case, high lift forces are generated under the debris, thus ensuing in an even longer range. However, the CFF approach selected in this study estimated similar range values to the most conservative estimation ($\alpha_i = 45°$) of the NFF model. The assumption of the last employed method (CFF) was that the tanks ruptures in two main pieces (the end caps) which have a hemispherical shape, therefore the frisbee effect was not considered.

Comparing the two case studies (BMW and $SH_2$IFT), it can be noticed that the fragment ranges do not vary linearly with the $LH_2$ mass contained in the tanks. In particular, the ranges increase from two to almost three times by using the first or the NFF and CFF methods, while the $LH_2$ mass increases five times and the maximum mechanical energy generated by the explosion is 24 times higher. The reason for this is that the equations of the models consider the mass of the empty vessels as well. In this regard, if this mass is lighter compared with a heavier vessel, as occurs for the MLI insulated tank, the range of the fragments may be longer when the same kinetic energy is produced by the explosion. Hence, the reduction of the vessel weight sought in many applications, such as the automotive one, would not aid the consequences mitigation of an eventual accident with subsequent explosion. Finally, the fragment range values obtained in this analysis seem extremely conservative when compared with the few $LH_2$ tank explosion accidents available in literature. The longest distance reached by the fragments after the S-IV all systems vehicle explosion was 457 m, and the $LH_2$ and LOX amounts were 7690 and 38,212 kg, respectively (Gayle, 1964). During the accident analysed by Mires (1985), the longest horizontal and vertical fragment ranges were 76 and 1.8 m for the 34 $m^3$ tank almost full with 2411 kg of $LH_2$. Another question arises regarding the influence of the vapour and liquid phases on the fragment range, since the container were filled mostly with hydrogen in liquid phase during the two considered accident scenarios ((Gayle, 1964) and (Mires, 1985)). Therefore, further investigations are needed also in this case, especially because the outcomes of this work indicated that the consequences provoked by the fragments are more severe than the ones caused by the pressure wave.

The consequences of the hydrogen fireball ignited after the explosion were estimated with the analytical models previously described and usually employed in risk analysis. These equations underestimated the fireball diameter and duration. It was not possible to validate the radiation emitted from the fireballs during the BMW safety tests because no data were reported in (Pehr, 1996). The radiation was calculated theoretically with the most conservative approach, i.e. the Stefan-Boltzmann's law. In fact, an extremely high value of *SEP* was obtained (1880 kW $m^{-2}$), more than five times higher than the theoretical *SEP* value of propane fireball. The reason for this value is the elevated temperature of the stochiometric combustion of hydrogen and air (2321 K (NASA, 2005)). Pehr (1996) assumed that the temperature of the burning gas inside the fireball reached this value during the BMW tests. From the incident radiation, the thermal dose threshold of 80 (kW $m^{-2})^{4/3}$ s was estimated at 77.8 and 159.1 m for the BMW and $SH_2$IFT tests, respectively. In (Shentsov et al., 2016), this thermal dose threshold was measured at 72.5 m for a compressed hydrogen tank containing 1.64 kg of hydrogen and failing at 35.7 MPa. This result seems to agree with the outcome of this study. However, further experimental results are needed to validate these analyses. Furthermore, different authors stated that the hydrogen fireballs generated in their experiments were quite luminous and the emitted radiation was largely different from the hydrogen jet fire. This was mentioned by Zalosh and Weyandt (2005), explaining that the propane fire which was burning beneath the vessel could have contribute to the fireball. Similar observation about the radiation were made by Pehr (1996), who reported the BMW tests results. As previously mentioned, cold BLEVEs were triggered during those tests, thus the authors explained that the radiation was provoked by the burning of solid particles in the air and insulating materials. Finally, High (1968) estimated through his empirical model, a radiation of 229.4 and 36.8 kW $m^{-2}$ (20.2 and 3.24 Btu $ft^{-2}$ $s^{-1}$), respectively at 610 and 1524 m (2000 and 5000 ft) from a fireball with a radius of 215 m and a duration of 33.9 s. The lowest value corresponds to a thermal dose of 4150 (kW $m^{-2})^{4/3}$ s, hence far from the 80 (kW $m^{-2})^{4/3}$ s threshold.

The assessment of the three main consequences was fundamental to comprehend which is the safety distance from the exploding tank. The blast wave effects do not strongly affect the safety distance. In fact, the overpressure and impulse threshold to avoid any kind of injuries was the shortest distance compared with the fragment range and the thermal dose threshold distance. This is confirmed by Planas and Casal (2016) who stated that fragments impact and thermal radiation from the fireball may have effects over a large area around the explosion, while the pressure wave usually do not reach distances far from the failing vessel. However, the blast wave can highly damage structures in the near field, therefore further experimental data are needed.

As previously mentioned, the tanks tested during the BMW experiments were single walled type, covered with a layer of foam as insulation. Therefore, the results obtained in these tests do not represent a realistic accident scenario, because double walled tanks are currently employed to store $LH_2$. The lack of experimental data lead to several uncertainties for the modelling activity of the BLEVE phenomenon. For instance, the fractions of mechanical energy responsible for the vessel

rupture, pressure wave generation, and fragments ejection, might be different from the traditional single walled propane tanks. Moreover, the propane tanks engulfed in fires usually fracture on the top immediately prior the BLEVE (Birk et al., 2007), because the specific heat of the vapour phase is lower than the liquid one, thus the heat absorbed by the tank wall is higher in the vapour region and the metal degrades faster. The parahydrogen specific heat at saturation conditions is slightly higher for the vapour rather than the liquid phase. This means that the vapour phase absorbs a larger amount if its mass is the same or heavier than the liquid one, i.e. when the tank filling degree is low. Therefore, additional studies are needed to understand the structural behaviour of the vessel as well.

Finally, the consequences of an $LH_2$ BLEVE estimated in this work should be thoroughly validated with further experimental results and then compared with the BLEVE consequences of other fuels. This comparison can be conducted in different manners due to the peculiar hydrogen properties. For instance, if the tank volume is adopted as reference, the parahydrogen mass would be much lower than the other fuels due to its density. On the other hand, if similar masses are compared, it would result in a considerable larger $LH_2$ tank volume. Probably the best fashion would be to compare the same tank energy content by taking into account the LHV of the different fuels. According to (Hansen, 2020), the consequences of an eventual $LH_2$ BLEVE should be less severe than an LNG tank explosion, but further data are required to confirm this assessment. From the results of the NASA projects about the rocket propellants explosions, Gayle (1964) concluded that the $LOX/LH_2$ consequences have a lower yield compare with the other propellants such as LOX/RP-1, but the probabilities for an accident to occur seem higher for the $LH_2$ due to its extreme flammability. Therefore, the probabilities should also be investigated in order to conduct an exhaustive risk analysis.

## 6. Conclusions

In this study, a thorough consequence analysis of $LH_2$ BLEVEs for both small- and mid-scale tests was conducted for the first time by evaluating all the consequence typologies (pressure wave, fragments, and fireball). The analytical and theoretical models usually employed in risk analysis were adopted, and an underestimation was observed when the outcomes were compared with the experimental results. The drawbacks of the models were highlighted together with different uncertainties such as the behaviour of the double walled tank and of $LH_2$ during the evolution of the BLEVE phenomenon. It can be concluded that a broad knowledge gap is still present regarding the $LH_2$ physical explosions.

The results of the different models were validated with the BMW safety tests outcomes, and the most appropriate methods were selected for the blind prediction study. The blind prediction case study addressed the planned $SH_2$IFT $LH_2$ BLEVE tests. The blind prediction results provided in this study must be validated by the experiments. This will further support the selection of the most appropriate consequence models and eventually serve as development of new approaches. Furthermore, effective safety barriers to prevent or mitigate the $LH_2$ BLEVE can be selected once the experimental results will be available. It is suggested to enhance the consequence analysis by employing innovative tools such as computational fluid dynamics (CFD) codes. Moreover, the finite elements method (FEM) can be adopted to conduct a suitable structural analysis of the double walled tank. Therefore, this analysis could be coupled with a CFD study to comprehend how the fluid inside the tank and the eventual external fire stress the tank material, by developing a Multiphysics simulation tool. Finally, a comparison between the consequences of the BLEVE for $LH_2$ and other conventional fuels (hydrocarbons) would be of high importance to aid the writing of safety codes and regulations. When the consequence analysis will be concluded, a probability analysis would be crucial in the case of hydrogen to provide a complete risk analysis overview.

## Author statement

**Federico Ustolin**: Conceptualization, Methodology, Software, Validation, Writing - Original Draft. **Nicola Paltrinieri**: Methodology, Writing - Review and Editing, Supervision, Funding acquisition. **Gabriele Landucci**: Writing - Review and Editing, Supervision.

## Declaration of competing interest

The authors declare that they have no known competing financial interests or personal relationships that could have appeared to influence the work reported in this paper.

## Acknowledgments

This work was undertaken as part of the research project Safe Hydrogen fuel handling and Use for Efficient Implementation ($SH_2$IFT), and the authors would like to acknowledge the financial support of the Research Council of Norway under the ENERGIX programme (Grant No. 280964).

## References

Bader, B.E., Donaldson, A.B., Hardee, H.C., 1971. Liquid-propellant rocket abort fire model. J. Spacecraft Rockets 8, 1216–1219.
Bagster, D.F., Pitblado, R.M., 1989. Thermal hazards in the process industry. Chem. Eng. Prog. 85, 69–75.
Baker, W.E., Cox, P.A., Kulesz, J.J., Strehlow, R.A., Westine, P.S., 1983. Explosion Hazards and Evaluation. Elsevier Science, New York.
Barron, R.F., Nellis, G.F., 2016. Cryogenic Heat Transfer, second ed. CRC Press, Boca Raton. http://dx.doi.org/10.1201/b20225.
Barthelemy, H., Weber, M., Barbier, F., 2017. Hydrogen storage: recent improvements and industrial perspectives. Int. J. Hydrogen Energy 42, 7254–7262. http://dx.doi.org/10.1016/J.IJHYDENE.2016.03.178.
Baum, M.R., 1984. The velocity of missiles generated by the disintegration of gas-pressurized vessels and pipes. J. Pressure Vessel Technol. 106, 362–368. http://dx.doi.org/10.1115/1.3264365.
Beyler, C., 2016. Fire hazard calculations for large, open hydrocarbon fires. In: Hurley, M. (Ed.), SFPE Handbook of Fire Protection Engineering. Springer Science + Business Media, LLC, New York, pp. 2591–2663. http://dx.doi.org/10.1007/978-1-4939-2565-0.
Birk, A.M., 1996. Hazards from propane BLEVEs: an update and proposal for emergency responders. J. Loss Prev. Process. Ind. 9, 173–181. http://dx.doi.org/10.1016/0950-4230(95)00046-1.
Birk, A.M., Davison, C., Cunningham, M., 2007. Blast overpressures from medium scale BLEVE tests. J. Loss Prev. Process. Ind. 20, 194–206. http://dx.doi.org/10.1016/J.JLP.2007.03.001.
Bracha, M., Lorenz, G., Patzelt, A., Wanner, M., 1994. Large-scale hydrogen liquefaction in Germany. Int. J. Hydrogen Energy 19, 53–59. http://dx.doi.org/10.1016/0360-3199(94)90177-5.
Brode, H.L., 1959. Blast wave from a spherical charge. Phys. Fluids 2, 217–229. http://dx.doi.org/10.1063/1.1705911.
Cardella, U., Decker, L., Sundberg, J., Klein, H., 2017. Process optimization for large-scale hydrogen liquefaction. Int. J. Hydrogen Energy 42, 12339–12354. http://dx.doi.org/10.1016/J.IJHYDENE.2017.03.167.
Casal, J., 2008. Evaluation of the Effects and Consequences of Major Accidents in Industrial Plants. Elsevier, Amsterdam.
Casal, J., Arnaldos, J., Montiel, H., Planas-Cuchi, E., Vilchez, J., 2001. Modelling and understanding BLEVEs. Handbook of Hazardous Materials Spills Technology. McGraw-Hill, New York.
Casal, J., Hemmatian, B., Planas, E., 2016. On BLEVE definition, the significance of superheat limit temperature (Tsl) and LNG BLEVE's. J. Loss Prev. Process. Ind. 40, 81. http://dx.doi.org/10.1016/j.jlp.2015.12.001.
Casal, J., Salla, J.M., 2006. Using liquid superheating energy for a quick estimation of overpressure in BLEVEs and similar explosions. J. Hazard Mater. 137, 1321–1327. http://dx.doi.org/10.1016/J.JHAZMAT.2006.05.001.
Ccps, 2010. Guidelines for Vapor Cloud Explosion, Pressure Vessel Burst, BLEVE, and Flash Fire Hazards, second ed. Wiley Subscription Services, Inc., A. Wiley Company, New York. http://dx.doi.org/10.1002/9780470640449.
Crowl, D.A., 1992. Calculating the energy of explosion using thermodynamic availability. J. Loss Prev. Process. Ind. 5, 109–118. http://dx.doi.org/10.1016/0950-4230(92)80007-U.
Crowl, D.A., 1991. Using thermodynamic availability to determine the energy of explosion. Plant/Operations Prog. 10, 136–142.
D'Ovidio, G., Ometto, A., Valentini, O., 2020. A novel predictive power flow control strategy for hydrogen city rail train. Int. J. Hydrogen Energy 45, 4922–4931. http://dx.doi.org/10.1016/j.ijhydene.2019.12.067.

Fumey, B., Buetler, T., Vogt, U.F., 2018. Ultra-low NOx emissions from catalytic hydrogen combustion. Appl. Energy 213, 334–342. http://dx.doi.org/10.1016/J.APENERGY.2018.01.042.
Gayle, J.B., 1964. Investigation of S-IV All Systems Vehicle Explosion, vol. 563. NASA TN D.
Gayle, J.B., Bransford, J.W., 1965. Size and Duration of Fireballs from Propellant Explosions - NASA TM X-53314.
Genova, B., Silvestrini, M., Leon Trujillo, F.J., 2008. Evaluation of the blast-wave overpressure and fragments initial velocity for a BLEVE event via empirical correlations derived by a simplified model of released energy. J. Loss Prev. Process. Ind. 21, 110–117. http://dx.doi.org/10.1016/J.JLP.2007.11.004.
Hansen, O.R., 2020. Liquid hydrogen releases show dense gas behavior. Int. J. Hydrogen Energy 45, 1343–1358. http://dx.doi.org/10.1016/j.ijhydene.2019.09.060.
Hemmatian, B., Casal, J., Planas, E., 2017a. A new procedure to estimate BLEVE overpressure. Process Saf. Environ. Protect. 111, 320–325. http://dx.doi.org/10.1016/J.PSEP.2017.07.016.
Hemmatian, B., Planas, E., Casal, J., 2017b. Comparative analysis of BLEVE mechanical energy and overpressure modelling. Process Saf. Environ. Protect. 106, 138–149. http://dx.doi.org/10.1016/j.psep.2017.01.007.
High, R.W., 1968. The Saturn fireball. Ann. N. Y. Acad. Sci. 152, 441–451. http://dx.doi.org/10.1111/j.1749-6632.1968.tb11992.x.
Hord, J., 1972. Explosion Criteria for Liquid Hydrogen Test Facilities. NBS Report.
HydrogenTools, 2017. Liquid hydrogen tank boiling liquid expanding vapor explosion (BLEVE) due to water-plugged vent stack [WWW Document]. URL. https://h2tools.org/lessons/liquid-hydrogen-tank-boiling-liquid-expanding-vapor-explosion-bleve-due-water-plugged-vent. (Accessed 6 March 2020).
IEA, 2019. The Future of Hydrogen - Seizing Today's Opportunities.
Johnson, D.M., Pritchard, J.M., Wickens, M.J., 1991. Large scale experimental study of boiling liquid expanding vapour explosions (BLEVEs). Contract report 15367, project M8411. Research and Technology division, British Gas.
Jovanović, A.S., Baloš, D., 2013. INTeg-Risk project: concept and first results. J. Risk Res. 16, 275–291. http://dx.doi.org/10.1080/13669877.2012.729516.
Kinney, G., Graham, K., 1985. Explosive Shocks in Air. Springer, New York.
Kite, F.D., Webb, D.M., Bader, B.E., 1965. Launch Hazards Assessment Program, Report on Atlas/Centaur Abort - SC-RR, pp. 65–333.
Laboureur, D., 2012. Experimental Characterization and Modeling of Hazards: BLEVE and Boilover (PhD Dissertation). Von Karman Institute for Fluid Dynamics (Universite Libre de Bruxelles).
Laboureur, D., Buchlin, J.M., Rambaud, P., 2012a. Small scale experiments on boiling liquid expanding vapor explosions: supercritical BLEVE. ASME 2012 Pressure Vessels and Piping Conference, pp. 51–60. http://dx.doi.org/10.1115/PVP2012-78283.
Laboureur, D., Heymes, F., Aprin, L., Buchlin, J.M., Rambaud, P., 2012b. BLEVE overpressure: small scale experiments and multi-scale comparison with literature survey of blast wave modeling. Global Congress on Process Safety.
Laboureur, D., Heymes, F., Lapebie, E., Buchlin, J., Rambauda, P., 2014. BLEVE overpressure: multiscale comparison of blast wave modeling. Process Saf. Prog. 33, 274–284. http://dx.doi.org/10.1002/prs.11626.
Landucci, G., Tugnoli, A., Cozzani, V., 2010. Safety assessment of envisaged systems for automotive hydrogen supply and utilization. Int. J. Hydrogen Energy 35, 1493–1505. http://dx.doi.org/10.1016/j.ijhydene.2009.11.097.
Lowesmith, B.J., Hankinson, G., Chynoweth, S., 2013. Safety issues of the liquefaction, storage and transportation of liquid hydrogen: studies in the IDEALHY project. In: International Conference on Hydrogen Safety. Brussels, Belgium.
Maggio, G., Nicita, A., Squadrito, G., 2019. How the hydrogen production from RES could change energy and fuel markets: a review of recent literature. Int. J. Hydrogen Energy 44, 11371–11384. http://dx.doi.org/10.1016/j.ijhydene.2019.03.121.
McAllister, S., Chen, J.-Y., Fernandez-Pello, A.C., 2011. Fundamentals of Combustion Processes. Springer Science +Business Media, LLC, New York. http://dx.doi.org/10.1007/978-1-4419-7943-8.
Mires, R.W., 1985. Analysis of liquid hydrogen explosion. Phys. Teach. 23, 533–535. http://dx.doi.org/10.1119/1.2341906.
Molkov, V., Kashkarov, S., 2015. Blast wave from a high-pressure gas tank rupture in a fire: stand-alone and under-vehicle hydrogen tanks. Int. J. Hydrogen Energy 40, 12581–12603. http://dx.doi.org/10.1016/J.IJHYDENE.2015.07.001.
NASA, 2020. Air properties definitions [WWW Document]. URL. https://www.grc.nasa.gov/www/k-12/BGP/airprop.html. (Accessed 27 May 2020).
NASA, 2005. Safety standard for hydrogen and hydrogen systems, guidelines for hydrogen system design, materials selection, operations, storage, and transportation. NSS 1740, 16.
NASA, 1997. Report of the presidential commission on the space shuttle challenger accident (1986) [WWW Document]. URL. http://science.ksc.nasa.gov/shuttle/missions/51-l/docs/rogers-commission/table-ofcontents.html. (Accessed 11 June 2019).
NCE Maritime Cleantech, 2019. Norwegian Future Value Chains for Liquid Hydrogen.
Nishigaki, K., Saji, Y., 1983. On the limit of superheat of cryogenic liquids. Cryogenics 23, 473–476. http://dx.doi.org/10.1016/0011-2275(83)90004-8.
NIST, 2019. NIST Chemistry WebBook [WWW Document]. URL. webbook.nist.gov/. (Accessed 19 March 2019).
Notardonato, W.U., Swanger, A.M., Fesmire, J.E., Jumper, K.M., Johnson, W.L., Tomsik, T.M., 2017. Zero Boil-Off Methods for Large Scale Liquid Hydrogen Tanks Using Integrated Refrigeration and Storage. NASA Technical Reports Server (NTRS). http://dx.doi.org/10.1088/1757-899X/278/1/012012.
Ono, R., Nifuku, M., Fujiwara, S., Horiguchi, S., Oda, T., 2007. Minimum ignition energy of hydrogen–air mixture: effects of humidity and spark duration. J. Electrost. 65, 87–93. http://dx.doi.org/10.1016/J.ELSTAT.2006.07.004.
Paltrinieri, N., Landucci, G., Molag, M., Bonvicini, S., Spadoni, G., Cozzani, V., 2009. Risk reduction in road and rail LPG transportation by passive fire protection. J. Hazard Mater. 167, 332–344. http://dx.doi.org/10.1016/j.jhazmat.2008.12.122.
Paltrinieri, N., Øien, K., Cozzani, V., 2012. Assessment and comparison of two early warning indicator methods in the perspective of prevention of atypical accident scenarios. Reliab. Eng. Syst. Saf. 108, 21–31. http://dx.doi.org/10.1016/j.ress.2012.06.017.
Pehr, K., 1996. Aspects of safety and acceptance of LH2 tank systems in passenger cars. Int. J. Hydrogen Energy 21, 387–395. http://dx.doi.org/10.1016/0360-3199(95)00092-5.
Peschka, W., 1992. Liquid Hydrogen - Fuel of the Future, first ed. Springer-Verlag, Wien. http://dx.doi.org/10.1007/978-3-7091-9126-2.
Planas-Cuchi, E., Salla, J.M., Casal, J., 2004. Calculating overpressure from BLEVE explosions. J. Loss Prev. Process. Ind. 17, 431–436. http://dx.doi.org/10.1016/J.JLP.2004.08.002.
Planas, E., Casal, J., 2016. BLEVE-Fireball. In: Lackner, M., Winter, F., Agarwal, A.K. (Eds.), Handbook of Combustion. Wiley-VCH Verlag GmbH & Co. KGaA, Weinheim. http://dx.doi.org/10.1002/9783527628148.hoc093.
Prugh, R.W., 1994. Quantitative evaluation of fireball hazards. Process Saf. Prog. 13, 83–91. http://dx.doi.org/10.1002/prs.680130211.
Prugh, R.W., 1991. Quantitative evaluation of "BLEVE" hazards. J. Fire Protect. Eng. 3, 9–24.
Reid, R., 1979. Possible mechanism for pressurized-liquid tank explosions or BLEVE's. Science 203 (80), 1263–1265. http://dx.doi.org/10.1126/science.203.4386.1263.
Reid, R., 1976. Superheated liquids. Am. Sci. 64, 146–156.
Rew, P.J., 1997. LD50 Equivalent for the Effect of Thermal Radiation on Humans - CRR 129/1997.
Rybin, H., Krainz, G., Bartlok, G., Kratzer, E., 2005. Safety demands for automotive hydrogen storage systems. International Conference on Hydrogen Safety.
Sachs, R.G., 1944. The Dependence of Blast on Ambient Pressure and Temperature, BRL Report No. 466. Aberdeen Proving Ground, Maryland.
Salla, J.M., Demichela, M., Casal, J., 2006. BLEVE: a new approach to the superheat limit temperature. J. Loss Prev. Process. Ind. 19, 690–700. http://dx.doi.org/10.1016/j.jlp.2006.04.004.
Shentsov, V., Cirrone, D.M.C., Makarov, D., Molkov, V., 2016. Simulation of fireball and blast wave from a hydrogen tank rupture in a fire. In: 7th International Symposium on Non-equilibrium Processes, Plasma, Combustion, and Atmospheric Phenomena, Sochi, Russia, pp. 139–146.
Skjold, T., Hisken, H., Bernard, L., Mauri, L., Atanga, G., Lakshmipathy, S., Lucas, M., Carcassi, M., Schiavetti, M., Chandra Madhav Rao, V., Sinha, A., Wen, J.X., Tolias, I. C., Giannissi, S.G., Venetsanos, A.G., Stewart, J.R., Hansen, O.R., Kumar, C., Krumenacker, L., Laviron, F., Jambut, R., Huser, A., 2019. Blind-prediction: estimating the consequences of vented hydrogen deflagrations for inhomogeneous mixtures in 20-foot ISO containers. J. Loss Prev. Process. Ind. 61, 220–236. http://dx.doi.org/10.1016/j.jlp.2019.06.013.
Smith, J.M., Van Ness, H.C., 1996. Introduction to Chemical Engineering Thermodynamics, fifth ed. McGraw-Hill, Inc, NewYork.
Stochl, R.J., Knoll, R.H., 1991. Thermal Performance of a Liquid Hydrogen Tank Multilayer Insulation System at Warm Boundary Temperatures of 630, 530 and 152 °R - NASA TM 104476.
Trevisani, L., Fabbri, M., Negrini, F., Ribani, P.L., 2007. Advanced energy recovery systems from liquid hydrogen. Energy Convers. Manag. 48, 146–154. http://dx.doi.org/10.1016/j.enconman.2006.05.002.
Ullah, A., Ahmad, F., Jang, H.-W., Kim, S.-W., Hong, J.-W., 2017. Review of analytical and empirical estimations for incident blast pressure. KSCE J. Civ. Eng. 21, 2211–2225. http://dx.doi.org/10.1007/s12205-016-1386-4.
Ustolin, F., Paltrinieri, N., 2020. Hydrogen fireball consequence analysis. Chem. Eng. Trans. 82, 211–216. http://dx.doi.org/10.3303/CET2082036.
Ustolin, F., Paltrinieri, N., Berto, F., 2020. Loss of integrity of hydrogen technologies: a critical review. Int. J. Hydrogen Energy 45, 23809–23840. http://dx.doi.org/10.1016/j.ijhydene.2020.06.021.
Ustolin, F., Song, G., Paltrinieri, N., 2019. The influence of H2 safety research on relevant risk assessment. Chem. Eng. Trans. 74 http://dx.doi.org/10.3303/CET1974233.
van Biert, L., Godjevac, M., Visser, K., Aravind, P.V., 2016. A review of fuel cell systems for maritime applications. J. Power Sources 327, 345–364. http://dx.doi.org/10.1016/J.JPOWSOUR.2016.07.007.
van den Bosch, C.J.H., Weterings, R.A.P.M., 2005. Methods for the Calculation of Physical Effects - Due to Releases of Hazardous Materials (Liquids and Gases), "Yellow Book." the Committee for the Prevention of Disasters by Hazardous Materials. Director-General for Social Affairs and Employment, The Hague.
Willoughby, A.B., Ullian, I.J., 1988. Analysis of Project PYRO Close-In Overpressure and Impulse Data - 8423-2RR.
Zalosh, R., Weyandt, N., 2005. Hydrogen fuel tank fire exposure burst test - SAE technical paper 2005-01-1886. SAE 2005 World Congress & Exhibition. http://dx.doi.org/10.4271/2005-01-1886.
Zhang, J., Laboureur, D., Liu, Y., Mannan, M.S., 2016. Lessons learned from a supercritical pressure BLEVE in nihon dempa kogyo crystal inc. J. Loss Prev. Process. Ind. 41, 315–322. http://dx.doi.org/10.1016/J.JLP.2016.02.012.
Zhuzhgov, A.V., Krivoruchko, O.P., Isupova, L.A., Mart'yanov, O.N., Parmon, V.N., 2018. Low-temperature conversion of ortho-hydrogen into liquid para-hydrogen: process and catalysts. Review. Catal. Ind. 10, 9–19. http://dx.doi.org/10.1134/S2070050418010117.

Ustolin F, Tolias I, Giannissi S, Venetsanos A, Paltrinieri N. A CFD Analysis of Liquefied Gas Vessel Explosions Using the ADREA-HF Code. (Submitted to the International Journal of Hydrogen Energy).

This article is awaiting publication and is not included in NTNU Open

This page is intentionally left blank

Ustolin F, Song G, Paltrinieri N. The influence of H2 safety research on relevant risk assessment. Chem Eng Trans 2019;74:1393–8. https://doi.org/10.3303/CET1974233.

This page is intentionally left blank

CHEMICAL ENGINEERING TRANSACTIONS
VOL. 74, 2019
A publication of AIDIC
The Italian Association of Chemical Engineering
Online at www.cetjournal.it
Guest Editors: Sauro Pierucci, Jiří Jaromír Klemeš, Laura Piazza

**ISBN** 978-88-95608-71-6; **ISSN** 2283-9216
DOI: 10.3303/CET1974233

# The Influence of $H_2$ Safety Research on Relevant Risk Assessment

Federico Ustolin*, Guozheng Song, Nicola Paltrinieri

Department of Mechanical and Industrial Engineering, Norwegian University of Science and Technology NTNU, S.P. Andersens veg 5, 7031 Trondheim, Norway
federico.ustolin@ntnu.no

Hydrogen is a valuable option of clean fuel to keep the global temperature rise below 2°C. However, one of the main barriers in its transport and use is to ensure safety levels that are comparable with traditional fuels. In particular, potential liquid hydrogen accidents may not be fully understood (yet) and excluded by relevant risk assessment. For instance, as hydrogen is cryogenically liquefied to increase its energy density during transport, Boiling Liquid Expanding Vapor Explosions (BLEVE) is a potential and critical event that is important addressing in the hazard identification phase. Two past BLEVE accidents involving liquid hydrogen support such thesis. For this reason, results from consequence analysis of hydrogen BLEVE will not only improve the understanding of the related physical phenomenon, but also influence future risk assessment studies. This study aims to show the extent of consequence analysis influence on overall quantitative risk assessment of hydrogen technologies and propose a systematic approach for integration of posterior results. The Dynamic Procedure for Atypical Scenario Identification (DyPASI) is used for this purpose. The work specifically focuses on consequence models that are originally developed for other substances and adapted for liquid hydrogen. Particular attention is given to the parameters affecting the magnitude of the accident, as currently investigated by a number of research projects on hydrogen safety worldwide. A representative example of consequence analysis for liquid hydrogen release is used in this study. Critical conditions identified by the numerical simulation models are identified and considered for subsequent update of the overall system risk assessment.

## 1. Introduction

Hydrogen is considered a clean fuel and could replace the fossil fuels in order to reduce the environmental pollution. Potentially, its combustion produces only water and heat if the flame temperature is controlled or a catalyst burner is adopted. Moreover, hydrogen has a specific energy value (120 MJ/kg (Verfondern, 2008)) higher than other commercial fuels such as gasoline or natural gas. Despite these and other advantages, hydrogen is considered a dangerous fuel mainly due to its flammability and low ignition energy (0.017 mJ in air (Ono et al., 2007)). Hence, when the transportation and utilization of hydrogen is taken into account, the safety aspects should not be neglected. Furthermore, hydrogen has a low density at atmospheric conditions (0.0838 kg/m$^3$ at 293 K, 101.3 kPa (McCarty et al., 1981)) compared with other fuels. Liquefaction increases the hydrogen density (70.9 kg/m$^3$ at 20.4 K, 101.3 kPa (NIST, 2019)) and that is why liquid hydrogen ($LH_2$) can be considered both for storage and transportation. For example, in the case of road transportation, a truck with a tube trailer of compressed gaseous hydrogen can be filled with 300-400 kg of hydrogen at 200-250 bar, while a truck with a vacuum insulated tank can hold up to 3.5 tons of $LH_2$ (Pritchard and Rattigan, 2010). On the other hand, when $LH_2$ is used, different potential accidents and hazards must to be considered. Some of these have not been fully understood or forecasted yet.

Boiling Liquid Expanding Vapour Explosion (BLEVE) and Rapid Phase Transition (RPT) are two physical explosions as consequence of a loss of containment and these are two atypical accidental scenarios. BLEVE is a very well-known phenomenon for different substances such as water, propane, Liquefied Petroleum Gas (LPG) and Liquefied Natural Gas (LNG). It can happen immediately after a catastrophic rupture of *"a vessel containing a liquid (or liquid plus vapour) at a temperature significantly above its boiling point at atmospheric*

Paper Received: 12 June 2018; Revised: 16 September 2018; Accepted: 12 February 2019

Please cite this article as: Ustolin F., Song G., Paltrinieri N., 2019, The Influence of H2 Safety Research on Relevant Risk Assessment, Chemical Engineering Transactions, 74, 1393-1398 DOI:10.3303/CET1974233

*pressure"* (Casal et al., 2016). While RPT can occur if Liquefied Natural Gas (LNG) is spilled onto water *"due to the sudden boiling or phase change from liquid to vapor, usually in a way that the LNG penetrates into and mixes well with water"* (Woodward and Pitblado, 2010). In the case of $LH_2$, it is not yet clear if and under which conditions these phenomena can happen, and which is the intensity of the consequences.
Several projects on hydrogen safety have been performed in the last decades. However, some of these studies did not consider BLEVE and RPT, such as the HyRAM tool (Groth and Hecht, 2017). Although, it does not mean these phenomena cannot happen for $LH_2$. In fact, the IDEALHY project has been focused on the $LH_2$ risk assessment, considering BLEVE among the potential consequences (Lowesmith et al., 2013). In a recent JRC report on hydrogen safety, it has been concluded that knowledge gaps still exist in hydrogen BLEVE/fire resistance among all the other considered areas (Azkarate et al., 2018). Moreover, $LH_2$ RPT has been theoretically predicted in a few studies such as in (Verfondern, 2008). This study identifies two past $LH_2$ BLEVE accidents. On the other hand, RPT never happened for $LH_2$.
The presented study is a preliminary introduction to the "Safe Hydrogen Fuel Handling and Use for Efficient Implementation" ($SH_2IFT$) project. This is a Norwegian project coordinated by the research institute SINTEF, in which the safety aspects of both liquid and gaseous hydrogen are studied. In the case of the $LH_2$, BLEVE and RPT will be analysed carrying out experimental tests and developing models both to forecast the formation and estimate the consequences.
The aim of this work is to integrate atypical accidental scenarios, such as $LH_2$ BLEVE, into the standard risk assessment of $LH_2$ technologies. The DyPASI technique was used to update the hazard identification phase, while relevant operational conditions of the $LH_2$ tank were considered as preliminary input to the consequence analysis phase. Furthermore, all the results obtained in this study will be confirmed during the $SH_2IFT$ project.

## 2. Methodology

In this study, DyPASI has been applied to $LH_2$ technologies following the methodology used in (Paltrinieri et al., 2015). In the following, DyPASI and its procedure are briefly described. Furthermore, the methodology adopted to carry out the $LH_2$ BLEVE consequence analysis has been reported.

### 2.1 Application of DyPASI technique to $LH_2$ technologies

In Figure 1, the phases described in the introduction have been schematized. Looking at this scheme, it is noticeable that to apply the DyPASI technique, other tools such as MIMAH (Methodology for the Identification of Major Accident Hazards) and MIRAS (Methodology for the Identification of Reference Accident Scenarios) are needed. As said before, the results obtained in this study will be confirmed during the $SH_2IFT$ project (dashed lines).

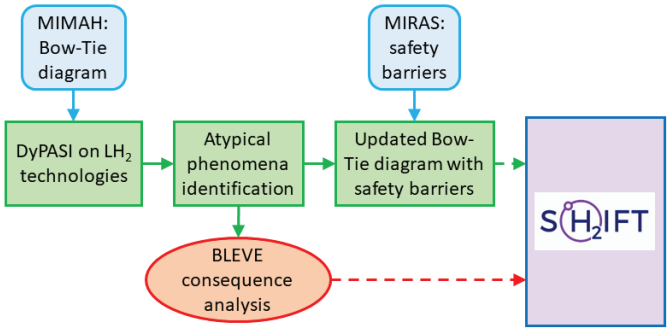


*Figure 1: Scheme of the phases followed in this study. Dashed line indicates the results will be confirmed during the $SH_2IFT$ project*

DyPASI is a hazard identification technique usually coupled with a Dynamic Risk Assessment (DRA) in order to update it taking into account atypical accidental scenarios which are not considered by traditional hazard identification processes (Paltrinieri et al., 2016). For example in (Russo et al., 2018), the explosion scenario has not been considered for the storage unit of the hydrogen refuelling station. MIMAH methodology has been used to develop the conventional bow-tie diagram utilized as input of the first DyPASI step (Delvosalle et al., 2006). DyPASI procedure is structured in different steps and these are described in Table 1. MIRAS methodology has been
used to define the safety barriers for the atypical scenarios in the step 4 of DyPASI (Delvosalle et al., 2006).

*Table 1: DyPASI procedure steps, adapted from (Paltrinieri et al. (2015)*

| Step | Input | Output | Description |
|---|---|---|---|
| 0 | Input to conventional bow-tie technique | Generic bow-ties describing potential accident scenarios | DyPASI needs a preliminary application of the conventional bow-tie technique to identify relevant critical events |
| 1 | Information from accident databases and dedicated search systems | Risk notions on undetected potential hazards | A search for relevant information concerning hazards that may have not been considered in conventional bow-tie development is performed |
| 2 | Risk notions from step 1 | Early warnings triggering further analysis | A determination is made as to whether the data are significant enough to trigger further action and proceed with risk assessment |
| 3 | Bow-ties from step 0 and early warnings from step 2 | Bow-tie diagrams considering also atypical scenarios | Atypical scenarios are isolated from the early warnings; cause–consequence chains are built and integrated into the generic bow-ties |
| 4 | Integrated bow-ties from step 3 | Safety barriers for the atypical scenarios | Safety measures are defined for the atypical scenarios identified |

### 2.2 $LH_2$ BLEVE consequence analysis

DyPASI technique can identify different kind of accidental scenarios consequences but other tools are needed to estimate these consequences. Hence, a study on $LH_2$ BLEVE consequences has been carried out.
The BLEVE consequences are the overpressure of the blast wave, the missiles (debrides formed after the vessel rupture) that fly away owing the explosion and the thermal radiation, if a fireball occur due to an ignition source outside the tank, such as fire (Casal, 2008). In this study, only the evaluation of the overpressure of the blast wave has been considered.
The superheat limit temperature theory (Reid, 1979) assumes that the liquid contained in the vessel must be superheated, otherwise the yield of the explosion cannot be compared with a BLEVE. To estimate the superheat temperature of a substance, several formulas have been developed by different authors. One of the most common equation used is the one proposed by Reid (Reid, 1976):

$$T_{shl} = 0.895 \cdot T_c = 29.66\ K \quad (1)$$

Eq(1) is a simple formula that depends only on the critical temperature. According to Eq(1), the superheat temperature of hydrogen is 29.66 K. There are other methods to estimate the superheat temperature, but these are more conservative. Casal et al. (Casal et al., 2016) explained that this theory is valid at small scale but not at large scale where there is always a non-homogeneous distribution of the heat in and around the vessel. Nevertheless, the superheat limit temperature is an important parameter because at this temperature the adiabatic energy transfer between the liquid and vapor interface is maximum (Salla et al., 2006). In this study, the inputs for the estimation of the consequence analysis have been chosen in order to reach a temperature higher than 29.7 K inside the tank. Furthermore, a correlation between the hydrogen mass contained in the tank, its pressure and the yield of the $LH_2$ BLEVE has been searched. The mass and pressure of hydrogen are operational parameters and, in the case of a storage facility, they can vary during the day.
A representative BLEVE consequence analysis has been carried out using the software PHAST 8.11 developed by DNV-GL. In this software, a BLEVE is simulated as a standalone model, hence the simulation is not time-dependent. The chosen tank has a volume of 1 $m^3$, a cylindrical shape with a diameter of 1.13 m and 1 m of length. The elevation of the tank is 1 m. The tank contains hydrogen in both phases, liquid and vapour. Three different pressures, 9, 11.9 and 31.2 bar gauge ($bar_g$) have been chosen to simulate the BLEVE. The first pressure, 9 $bar_g$, is approx. 1.21 times 7.4 $bar_g$, that is the pressure at which the first pressure relief valve (PRV) of the $LH_2$ vessel opens (Rybin et al., 2005). The same approach is suggested in (Uijt de Haag and Ale, 2005). Then, the yield of the BLEVE have been estimated when the vessel has a pressure of 11.9 $bar_g$, which is a value close to the hydrogen critical pressure (12.96 bar). The burst pressure of the $LH_2$ tank has been estimated to calculate the yield of the BLEVE in case of PRVs failure without fire engulfment of the tank (cold BLEVE). In this case, the value of the pressure inside the tank before its rupture is the highest compared with hot BLEVE. When the tank is exposed to fire, the tank material is subjected to thermal stress and the estimated bursting pressure has a lower value than the considered case. To evaluate the bursting pressure, the tank wall thickness has been calculated following the ASME Boiler and Pressure Vessel Code (BPVC) Sec. VIII (ASME, 2001). This code is used to design also cryogenic vessels. Eq(2) is used to calculate the tank wall thickness, *t*:

$$t = \frac{P \cdot R}{\sigma \cdot e - 6 \cdot P} = 2.76\ mm \quad (2)$$

where $P$ is the design pressure of the tank (7.4 $bar_g$ or 107 $psi_g$) and $R$ its radius (500 mm), $\sigma$ is the allowable stress equal to 20,000 psi for the AISI Stainless Steel 304 (Rana and Barthelemy, 2003) and $e$ is the weld joint efficiency factor considered 1. To estimate the burst pressure $P$, Eq(3) has been used (Casal, 2008):

$$P = P_0 + \frac{S_M \cdot t}{R + 0.6 \cdot t} = 3.22\ MPa = 32.2\ bar \quad (3)$$

where $P_0$ is the atmospheric pressure (0.1 MPa), $S_M$ is the mechanical strength of the material with a value of 565 MPa always for AISI Stainless Steel 304 (Casal, 2008). Eq(3) has been used for $LH_2$ tank because it is applied for cylindrical vessels with the pressure ($P - P_0$) lower than 0.385 times $S_M$ (Casal, 2008).
To simulate the BLEVE using PHAST, it is possible to set the pressure inside the tank, the temperature of the substance and the bubble point. The mass of the substance contained inside the tank is not an input, hence, to reach its desire value the other conditions such as pressure, temperature and liquid mole fraction should be changed. When the substance is in the supercritical state, only the temperature can be varied to set the mass at fixed pressure. When the pressure is 11.9 $bar_g$ inside the tank, the minimum and maximum values of the mass that can be reach are almost 26 and 40 kg respectively, due to the density of the vapour and the liquid at this pressure. For this reason, 26, 30 and 40 kg have been chosen as values of the hydrogen mass contained in the tank. In Table 2, the initial conditions of the different simulation have been collected.

*Table 2: Initial conditions of the different BLEVE consequence analysis scenarios*

| Pressure ($bar_g$) | Mass (kg) | Temperature (K) | Liquid mole fraction | Liquid mass fraction |
|---|---|---|---|---|
| 9 | 26 | 31.3 | 0.33 | 0.64 |
| | 30 | | 0.44 | 0.74 |
| | 40 | | 0.71 | 0.90 |
| 11.9 | 26 | 33.0 | 0.05 | 0.08 |
| | 30 | | 0.35 | 0.46 |
| | 40 | | 0.97 | 0.98 |
| 31.2 | 26 | 43.0 | 0 | 0 |
| | 30 | 40.7 | 0 | 0 |
| | 40 | 36.7 | 0 | 0 |

## 3. Results

### 3.1 Results of DyPASI application to $LH_2$ technologies

In the original bow-tie diagram obtained with the MIMAH tool, the catastrophic rupture of the cryogenic tank has been chosen as critical event. MIMAH suggests generic logic trees to build the bow-tie diagram. This methodology considers BLEVE as a domino effect, being the critical event of a secondary event tree.
Applying DyPASI, with the available information regarding the two past BLEVE accidents, this phenomenon becomes an event in the updated bow-tie diagram. Moreover, in the fault tree “improper firefighting technique” has been added as an escalation factor, following the procedure used in the software BowTieXP. This escalation factor triggers the PRV failure, leading to internal overpressure.
In the updated bow-tie diagram, three safety barriers have been added using the MIRAS methodology. These safety barriers are the “training” of the fire fighters and the “PRV” in order to prevent the PRV failures when the $LH_2$ tank is exposed to a fire and the increase in overcompression inside the tank respectively. The other safety barrier is the “blast walls”, usually utilized to mitigate the consequence of an explosion such as the overpressure of the blast wave. Only with the experimental tests that will carried out during the $SH_2$IFT project, the effectiveness of these safety barriers will be estimated.
In Figure 2, the updated bow-tie diagram is shown. The black branches form the bowtie diagram developed using the MIMAH methodology, while the blue branches have been integrated after the DyPASI application. The red boxes in the figure are the safety barriers.

### 3.2 $LH_2$ BLEVE consequence analysis results

The results of the BLEVE consequence analysis obtained with the PHAST software are the overpressure of the blast wave at different distances and the overpressure radii. The latter indicates at which distance the overpressure has a value of 0.02068 $bar_g$, which is the lowest value considered.

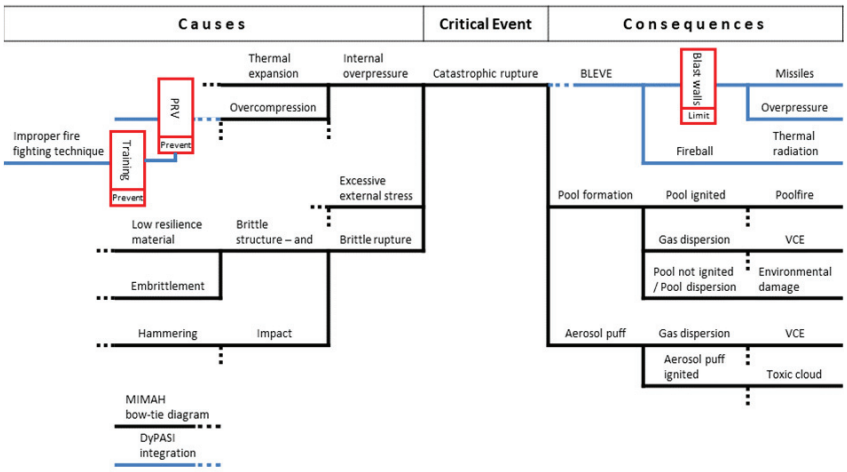


*Figure 2: Bow-tie diagram updated with the DyPASI integrations (light blue dotted line) adapted from (Paltrinieri et al., 2015). Safety barriers in red boxes to avoid the critical event or to limit the consequences*

In the presented study, the same overpressure values considered by PHAST that correspond to 3, 2 and 0.3 $psi_g$ (0.2068, 0.1379, 0.0207 $bar_g$ respectively) have been analysed. In the following, these values have been indicated as Overpressure 1, 2 and 3 respectively. In Table 3, the results of the BLEVE consequence analysis have been collected. In particular, the estimated distances at which the 3 values of overpressure occurred have been reported.

*Table 3: Results of the BLEVE consequence analysis at different conditions*

| Pressure in the tank ($bar_g$) | Mass (kg) | Distance downwind to Overpressure 1 (m) | Distance downwind to Overpressure 2 (m) | Distance downwind to Overpressure 3 (m) | Increasing of the distance to Overpressure 1 |
|---|---|---|---|---|---|
| 9 | 26 | 7.65 | 10.15 | 40.25 | |
| | 30 | 7.90 | 10.47 | 41.55 | +3.2 % |
| | 40 | 8.45 | 11.20 | 44.43 | +10.4 % |
| 11.9 | 26 | 8.38 | 11.02 | 43.31 | |
| | 30 | 8.74 | 11.49 | 45.14 | +4.2 % |
| | 40 | 9.43 | 12.39 | 48.71 | +12.4 % |
| 31.2 | 26 | 9.64 | 12.60 | 48.20 | |
| | 30 | 9.74 | 12.75 | 48.74 | +1.1 % |
| | 40 | 9.85 | 12.88 | 49.27 | +2.2 % |

As expected, when the hydrogen mass contained inside the vessel increases, the distance to overpressure increases as well. It is possible to note that the increase of mass influence more the distance when the tank pressure is 11.8 $bar_g$ (+12.4 %). Instead, when the hydrogen is in supercritical conditions, the mass has a weak influence on the results of the consequence analysis. The worst-case scenario is the third one, when the tank pressure is 31.2 $bar_g$, equal to the estimated bursting pressure of the tank.
For the considered cases, it seems that the tank pressure has a higher influence than the hydrogen mass on the consequence results. Comparing the same amount of hydrogen (26 kg) increasing the pressure from 9 to 31.2 $bar_g$, the distance to overpressure increase up to 19.8 %.
These results will be confirmed during the $SH_2IFT$ project when the experimental tests will be carried out to validate this model.

## 4. Conclusions

Usually, BLEVE is considered as a domino effect and not as a direct consequence of a critical event such as a catastrophic rupture. In this study, an atypical accidental scenario, such as $LH_2$ BLEVE, has been integrated into the standard risk assessment of $LH_2$ technologies. This allowed defining appropriate safety barriers to avoid, control, limit or prevent causes and consequences of the critical events are suggested. Moreover, a

preliminary consequence analysis has been carried out. The results of this analysis showed there is a correlation between the hydrogen mass contained in the vessel, its pressure and the distance to BLEVE overpressure. This will represent the very first basis to design robust safety barriers. A more accurate consequence analysis should be carried out, employing and adapting for $LH_2$ different models validated for other substances. The suggested safety barriers and the results of the BLEVE consequence analysis will be confirmed and validated by the experimental tests that will be carried out during the $SH_2$IFT project.

**Acknowledgments**

This study is part of the $SH_2$IFT (Safe Hydrogen Fuel Handling and Use for Efficient Implementation) project. Grant number: 280964/E20.

**References**

ASME, 2001. ASME Section VIII, Division 1, Pressure Vessel Code.

Azkarate, I., Barthélémy, H., Hooker, P., Jordan, T., Keller, J., Markert, F., Steen, M., Tchouvelev, A., 2018. Research Priority Workshop on Hydrogen Safety, JRC Conference and Workshop Report. Petten, Netherlands. https://doi.org/10.2760/77730

Casal, J., 2008. BLEVEs and vessel explosions, in: Casal, J. (Ed.), Evaluation of the Effects and Consequences of Major Accidents in Industrial Plants. pp. 147–193.

Casal, J., Hemmatian, B., Planas, E., 2016. On BLEVE definition, the significance of superheat limit temperature (Tsl) and LNG BLEVE's. J. Loss Prev. Process Ind. 40, 81. https://doi.org/10.1016/j.jlp.2015.12.001

Delvosalle, C., Fievez, C., Pipart, A., Debray, B., 2006. ARAMIS project: A comprehensive methodology for the identification of reference accident scenarios in process industries. J. Hazard. Mater. 130, 200–219. https://doi.org/10.1016/j.jhazmat.2005.07.005

Groth, K.M., Hecht, E.S., 2017. HyRAM: A methodology and toolkit for quantitative risk assessment of hydrogen systems. Int. J. Hydrogen Energy 42, 7485–7493. https://doi.org/10.1016/j.ijhydene.2016.07.002

Lowesmith, B.J., Hankinson, G., Chynoweth, S., 2013. Safety Issues of the Liquefaction, Storage and Transportation of Liquid Hydrogen: Studies in the IDEALHY Project, in: International Conference on Hydrogen Safety. Brussels, Belgium.

McCarty, R., Hord, J., Roder, H., 1981. Selected Properties of Hydrogen (Engineering Design Data), NBS Monogr. ed. National Bureau of Standards, Boulder, Colorado.

NIST, 2019. NIST Chemistry WebBook [WWW Document]. URL https://webbook.nist.gov/ (accessed 3.19.19).

Ono, R., Nifuku, M., Fujiwara, S., Horiguchi, S., Oda, T., 2007. Minimum ignition energy of hydrogen–air mixture: Effects of humidity and spark duration. J. Electrostat. 65, 87–93. https://doi.org/10.1016/J.ELSTAT.2006.07.004

Paltrinieri, N., Tugnoli, A., Cozzani, V., 2015. Hazard identification for innovative LNG regasification technologies. Reliab. Eng. Syst. Saf. 137, 18–28. https://doi.org/10.1016/j.ress.2014.12.006

Paltrinieri, N., Villa, V., Khan, F., Cozzani, V., 2016. Towards dynamic risk analysis: A review of the risk assessment approach and its limitations in the chemical process industry. Saf. Sci. 89, 77–93. https://doi.org/10.1016/j.ssci.2016.06.002

Pritchard, D.K., Rattigan, W.M., 2010. Hazards of liquid hydrogen RR769 Position paper.

Rana, M., Barthelemy, H., 2003. Development of ISO Standards for Cryogenic Vessels, in: ASME Pressure Vessels and Piping Conference 2003 (PVP2003). Cleveland Ohio, USA, pp. 1–10.

Reid, R., 1979. Possible Mechanism for Pressurized-Liquid Tank Explosions or BLEVE's. Science (80-. ). 203, 1263–1265. https://doi.org/10.1126/science.203.4386.1263

Reid, R., 1976. Superheated Liquids. Am. Sci. 64, 146–156.

Russo, P., De Marco, A., Mazzaro, M., Capobianco, L., 2018. Quantitative Risk Assessment on a Hydrogen Refuelling Station. Chem. Eng. Trans. 67, 739–744. https://doi.org/10.3303/CET1867124

Rybin, H., Krainz, G., Bartlok, G., Kratzer, E., 2005. Safety Demands For Automotive Hydrogen Storage Systems, in: International Conference on Hydrogen Safety. p. 12.

Salla, J.M., Demichela, M., Casal, J., 2006. BLEVE: A new approach to the superheat limit temperature. J. Loss Prev. Process Ind. 19, 690–700. https://doi.org/10.1016/j.jlp.2006.04.004

Uijt de Haag, P., Ale, B., 2005. "Purple Book", Guideline for quantitative risk assessment, CPR 18E.

Verfondern, K., 2008. Safety Considerations on Liquid Hydrogen. Forschungszentrum Jülich GmbH.

Woodward, J., Pitblado, R., 2010. LNG Risk Based Safety. John Wiley & Sons, New Jersey.

Ustolin F, Salzano E, Landucci G, Paltrinieri N. Modelling Liquid Hydrogen BLEVEs: A Comparative Assessment with Hydrocarbon Fuels. 30th Eur. Saf. Reliab. Conf. 15th Probabilistic Saf. Assess. Manag. Conf. (ESREL2020 PSAM15), 2020. https://doi.org/978-981-14-8593-0.

This page is intentionally left blank

# Modelling Liquid Hydrogen BLEVEs: a comparative assessment with hydrocarbon fuels

Federico Ustolin

*Department of Mechanical and Industrial Engineering, Norwegian University of Science and Technology NTNU, Norway. E-mail: federico.ustolin@ntnu.no*

Ernesto Salzano

*Department of Civil, Chemical, Environmental and Material Engineering, University of Bologna, Italy. E-mail: ernesto.salzano@unibo.it*

Gabriele Landucci

*Department of Civil and Industrial Engineering, University of Pisa, Italy. E-mail: gabriele.landucci@unipi.it*

Nicola Paltrinieri

*Department of Mechanical and Industrial Engineering, Norwegian University of Science and Technology NTNU, Norway. E-mail: nicola.paltrinieri@ntnu.no*

Hydrogen is one of the best candidates in replacing traditional hydrocarbon fuels to decrease environmental pollution and global warming. Its consumption is expected to grow in the forthcoming years. Hence its liquefaction becomes necessary to store and transport large amounts of this fuel. However, a liquid hydrogen ($LH_2$) boiling liquid expanding vapor explosion (BLEVE) is a potential accident scenario for these technologies, despite the fact it may be considered as atypical. A BLEVE is a physical explosion resulting from the catastrophic rupture of a tank of a liquid at a temperature above its boiling point at atmospheric pressure. Its consequences are the pressure wave, the missiles, which are the tank debris thrown away by the explosion, and a fireball if the substance is flammable and an ignition source is present. The aim of this paper is to estimate the consequences associated with BLEVEs from $LH_2$ storage and transport systems by means of integral models. Both ideal and real gas behavior models were considered to calculate the explosion overpressure. The physical models were employed to analyze the consequences of analogous fuel BLEVEs, in order to provide a comparative assessment of the results. BLEVE experimental results for $LH_2$ are not available in literature yet. For this reason, the developed models will be validated during the $SH_2IFT$ project in which $LH_2$ BLEVE experimental tests will be conducted.

*Keywords*: liquid hydrogen, comparative assessment, consequence analysis, BLEVE, explosion, integral models, numerical simulation models, risk assessment, atypical accident scenario.

## 1. Introduction

Hydrogen is considered a clean a renewable fuel able to replace the fossil fuels and reduce the environmental pollution. Its consumption is expected to increase in the next years (IEA Hydrogen, 2017). Hydrogen liquefaction seems to be one of the best options to transport large amount of this fuel by increasing its density up to 70.9 kg $m^{-3}$ (Landucci et al., 2008; NIST, 2019). This value is almost four times the density achieved in a conventional tube trailer which carries compressed hydrogen at 250 bar (Barthelemy et al., 2017). Currently, less than 1% of the hydrogen produced worldwide is liquefied (Ausfelder and Bazzanella, 2016). This could explain the knowledge gap still present in literature regarding the $LH_2$ behavior under certain conditions and its consequences.

The safety aspects must be always taken into account when hydrogen is considered in any application as it is highly flammable. Furthermore, it is colorless, odorless, buoyant in air and difficult to contain due to its very small molecule. Another safety issue is the extremely low boiling point (20.3 K at atmospheric pressure (NIST, 2019)). It becomes a cryogenic fluid when liquefied, with the tendency to evaporate even if contained in very well insulted vessels. In order to limit the boil-off gas formation, liquid hydrogen ($LH_2$) is converted from ortho- to parahydrogen and is usually stored in a double walled vessel (Edeskuty and Stewart, 1996). This type of tank is composed by an outer vessel in which the inner tank is installed. These tanks are then separated by a vacuum jacket in where an appropriate insulation is placed. This latter can be a powder of insulating material such as perlite or a multi-layer

*Proceedings of the 30th European Safety and Reliability Conference and the 15th Probabilistic Safety Assessment and Management Conference*
*Edited by* Piero Baraldi, Francesco Di Maio and Enrico Zio
*Published by* Research Publishing, Singapore.
ISBN: 978-981-14-8593-0; doi:10.3850/978-981-14-8593-0

insultation (MLI) formed by several metallized polymeric layers in order to prevent both convective and radiative heat losses (Peschka, 1992).

If hydrogen is employed for new applications, such as automotive or transport fuel (Landucci et al., 2010) it may be considered as an emerging technology with consequent emerging risks (Jovanović and Baloš, 2013). Atypical accident scenarios may be associated to emerging risks as the scenarios that may be well known by experts but disregarded by practitioners (Paltrinieri, 2013). Accidents scenarios are atypical if these have not been identified by a conventional hazard identification (HAZID) technique (Paltrinieri et al., 2012). For instance, a boiling liquid expanding vapor explosion (BLEVE) of $LH_2$ can be recognized as an atypical scenario. This phenomenon is a physical explosion which may occur after the catastrophic failure of a vessel containing a liquid (and vapor) at a temperature above its boiling point (Casal et al., 2016). Hence, this phenomenon may happen for any liquefied gas tank if the liquid phase is superheated. In the past, three $LH_2$ BLEVE accidents occurred (Ustolin et al., 2019). However, the yield of this phenomenon for an $LH_2$ tank is still unknown since very few experimental tests were conducted in this regard without achieving a BLEVE.

The aim of this study is to estimate which are the consequences of an $LH_2$ BLEVE in terms of mechanical energy generated by the explosion and the pressure wave overpressure at a certain distance from the tank. Then, an appropriate comparison with two conventional fuels such as propane and methane is conducted in order to comprehend if the $LH_2$ BLEVE consequences can be tolerated or additional safety barriers are required. After the description of the adopted methodology in Sec. 2, the results are reported and discussed in Sec. 3 and 4 respectively.

## 2. Methodology

In this study, the yield of an $LH_2$ BLEVE explosion was estimated. In particular, the mechanical energy generated by the explosion and the overpressure of the blast wave at different distances were calculated. Hydrogen has a low critical pressure (12.96 bar (NIST, 2019)) and temperature (33.1 K (NIST, 2019)). Therefore, there is the possibility for the $LH_2$ tank content to reach supercritical conditions during a BLEVE accident scenario. For this reason, both sub- and supercritical BLEVE were considered in this paper. In Fig. 1, the schematic of the methodology adopted in this study is illustrated.

A traditional (subcritical) BLEVE is usually characterized by the expansion of both the vapor and part of the liquid phases due to the depressurization after the catastrophic rupture of the tank. The amount of liquid that undergoes flash vaporization can be estimated by the vaporization fraction $f$ as indicated in Eq. (1) (Prugh, 1991):

$$f = 1 - e^{\left[-2.63\frac{c_{P,T_0}}{H_{V,T_0}}(T_C - T_0)\left(1-\left(\frac{T_C - T}{T_C - T_0}\right)^{0.38}\right)\right]} \quad (1)$$

where $T_0$ and $T_C$ are the boiling and critical temperature of the substance respectively at atmospheric pressure in K, $T$ is the temperature inside the tank prior the explosion in K, $c_{P,T0}$ is the specific heat of the liquid at $T_0$ in kJ kg$^{-1}$ K$^{-1}$ and $H_{V,T0}$ is the enthalpy of vaporization of the substance at $T_0$ in kJ kg$^{-1}$.

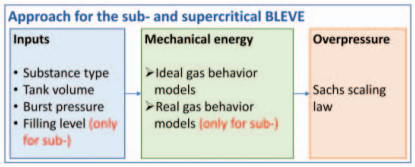


Fig. 1. Flowchart of the adopted methodology. Both ideal and real gas behavior models were adopted to calculate only the subcritical BLEVE mechanical energy.

Hence, the total volume $V^*$ of the substance involved in the explosion at subcritical conditions, is the sum of the vapor phase and the flashing liquid as shown in Eq. (2) (Casal, 2008):

$$V^* = V_V + V_L \cdot f \cdot \left(\frac{\rho_L}{\rho_V}\right) \quad (2)$$

where $V_V$ and $V_L$ are the volumes of the vapor and the liquid phases respectively inside the vessel immediately prior the explosion in m$^3$, $f$ is the vaporization fraction and $\rho_V$ and $\rho_L$ are the densities of the vapor and liquid phases respectively before the explosion in kg m$^{-3}$. Thus, $V^*$ is the volume considered in both the ideal and real gas behavior models when prior the explosion the subcritical conditions are met inside the tank. On the other hand, the whole volume of the vessel is considered for the supercritical BLEVEs.

### 2.1 *Mechanical energy estimation*

#### 2.1.1 *Subcritical BLEVE*

The methodology proposed by Hemmatian et al. (2017) was adopted and adapted for the subcritical BLEVEs. This methodology takes in consideration both ideal and real gas behavior models in order to estimate the mechanical energy

generated by the explosion. In this study, only the isothermal expansion (IE) was selected as ideal gas behavior model since it is usually the most conservative one (Hemmatian et al., 2017). The IE model proposed by Smith and Van Ness (1996) is reported in Eq. (3):

$$E = P \cdot V^* \cdot \ln\left(\frac{P}{P_0}\right) \quad (3)$$

where $P_0$ and $P$ are respectively the atmospheric and the bursting pressures of the vessel in Pa, and $V^*$ is the total expanding volume (vapor plus flashing liquid) in m$^3$.
The second and less conservative model is the real gas behavior and adiabatic expansion (RAIE), proposed by Planas-Cuchi et al. (2004). The mechanical energy is estimated by means of Eq. (4):

$$E = -[(u_{L0} - u_{V0}) \cdot m_T \cdot x - m_T \cdot u_{L0} + U] \quad (4)$$

where $u_{V0}$ and $u_{L0}$ are the internal energy of the vapor and liquid respectively, at the final state of the irreversible process in MJ kg$^{-1}$, $m_T$ is the overall mass of the substance in the vessel in kg, $U$ is the overall internal energy prior the explosion in MJ and $x$ is the intersection between the real expansion work line ($-P_0 \cdot \Delta V$) and the variation in internal energy of the vessel content (ΔU). The internal energy U is calculated with Eq. (5):

$$U = (m_V \cdot u_V) + (m_L \cdot u_L) \quad (5)$$

where $u_V$ and $u_L$ are the internal energies of the vapor and liquid phases respectively, prior the explosion in MJ kg$^{-1}$, and $m_L$ and $m_V$ are the masses of the liquid and vapor phases inside the tank before the explosion in kg. The above mentioned intersection $x$ is determined with Eq. (6).

$$x = \frac{m_T \cdot P_0 \cdot v_{L0} - V_T \cdot P_0 + m_T \cdot u_{L0} - U}{[(u_{L0} - u_{V0}) - (v_{V0} - v_{L0}) \cdot P_0] \cdot m_T} \quad (6)$$

where $v_{V0}$ and $v_{L0}$ are the specific volume of the vapor and liquid phases respectively at the final state of the irreversible process in m$^3$ kg$^{-1}$, and $V_T$ is the volume of the vessel in m$^3$.

2.1.2 *Supercritical BLEVE*

The bursting pressure of a pressure vessel is usually 3 to 4 times the maximum allowable working pressure (MAWP) (ASME, 2001). In the case of a $LH_2$ tank, the MAWP is 8.2 bar (Rybin et al., 2005). Hence, the maximum bursting pressure of an $LH_2$ tank should be 32.8 bar. According to Molkov and Kashkarov (2015), if hydrogen has a pressure below 10 MPa (100 bar), it can be considered as ideal gas. For this reason, only the ideal gas behavior models were embraced to estimate the mechanical energy generated by the supercritical BLEVE. In this case, Eq. (3) is employed again to calculate the mechanical energy, but the total expanding volume, $V^*$, is replaced by the total volume of the tank, $V$. In addition to the IE, the isentropic expansion (ISE) (Strehlow and Baker, 1975) model was considered as comparison, since the real gas behavior model is not applied. Among the ideal models, the ISE is usually the less conservative one. Its formula is reported in Eq. (7):

$$E = \frac{P \cdot V_T}{\gamma - 1}\left[1 - \left(\frac{P_0}{P}\right)^{\frac{\gamma-1}{\gamma}}\right] \quad (7)$$

where $P_0$ and $P$ are again the atmospheric and bursting pressures respectively in Pa, $V_T$ is the vessel volume in m$^3$, and $\gamma$ is the specific heat ratio of the considered substance.

### 2.2 *Blast wave overpressure calculation*

Part of the mechanical energy generated by the burst of the vessel contributes in the formation of the pressure wave. Hemmatian et al. (2017) demonstrated that for ductile tanks virtually 40% of this energy is converted in blast wave. This value was validated for conventional (single walled) propane tanks. $LH_2$ is commonly contained in double walled tanks due to its extremely low boiling point (20 K at atmospheric pressure (NIST, 2019)). Due to the lack of experimental tests, it is currently unknown if this percentage is valid for an $LH_2$ vessel. However, this contribution was assumed to be 40% as well for the $LH_2$ tank in this study.
The Sachs scaling law (Sachs, 1944) was adopted in order to estimate the overpressure of the pressure wave at a certain distance from the tank. The scaled distance was estimated with Eq. (8):

$$\bar{R} = R\left(\frac{P_a}{E \cdot \beta}\right)^{1/3} \quad (8)$$

where $R$ is the distance from the center of the explosion in m, $P_a$ is the atmospheric pressure (101325 Pa), $E$ is the mechanical energy in J, estimated with the models previously described and $\beta$ is the percentage of energy converted in pressure wave (40%). The overpressure is then found with the aid of appropriate diagrams reported in (Tang et al., 1996).
Moreover, only for the subcritical BLEVE, the liquid superheating energy (SE) model (Casal and Salla, 2006) was employed to directly calculate the contribution of the mechanical energy

dedicated to generate the pressure wave by means of Eq. (9):

$$E_w = k \cdot m_L \cdot SE \quad (9)$$

where $k$ is the amount of energy which participate in the BLEVE blast (0.04 for irreversible process), $m_L$ is the mass of liquid contained in the tank and $SE$ is the enthalpy difference estimated with Eq. (10):

$$SE = h_L - h_{L0} \quad (9)$$

where $h_{L0}$ and $h_L$ are the enthalpy of the liquid at boiling point and prior the explosion respectively in kJ kg$^{-1}$. This seems to be the most accurate model in the case of subcritical propane BLEVE (Hemmatian et al. 2017).

### 2.3 *Comparison with hydrocarbon fuels*

The idea of this study was to compare the results obtained for $LH_2$ with the BLEVEs from other fuels such as propane and methane. The densities of these fuels and their critical pressures are at least one order of magnitude larger (580.9 and 422.4 kg/m$^3$ for liquefied propane and methane respectively at atmospheric pressure (NIST, 2019)). In a safety comparison of different fuels, the same energy content is considered when an application is specified, as for the SF-BREEZE high-speed fuel cell ferry where $LH_2$ were compared with liquefied natural gas (LNG) (Klebanoff et al., 2017). Tanks of different fuels with the same fuel mass content were compared since an application was not specified in this study. This is a conservative assumption for $LH_2$ which has the highest energy content (120.1 MJ/kg (Argonne National Laboratory, 2010)) compared with the other fuels (46.3 and 48.6 MJ/kg for propane and methane respectively (Argonne National Laboratory, 2010)). The initial fuel mass present in the $LH_2$ tank at atmospheric pressure is 36.1 kg. For this reason, the volumes of the propane and methane tanks are 0.125 m$^3$ and 0.168 m$^3$ respectively. In the case of a subcritical BLEVE, the maximum failure pressure was the critical pressure of each substance, while the bursting pressure of each tank was the highest considered pressure for the supercritical BLEVE. The technique used to estimate the tank bursting pressure is explained Sec. 2.4.

### 2.4 *Initial conditions and boundaries*

All the thermodynamic conditions required by the models employed in this study were retrieved from the CoolProp database (Bell et al., 2014).
The inputs of the models were the type of substance (fuel) contained in the vessel, its volume and bursting pressure, and the liquid level only in the case of the subcritical BLEVE. The tank volume chosen was 1 m$^3$ since a vessel of this size will be tested during the Safe Hydrogen Fuel Handling and Use for Efficient Implementation ($SH_2IFT$) project. The bursting pressure was selected in the range from 2 bar to the critical pressure of the substance for the subcritical BLEVEs with a discretization of 1 bar. The maximum bursting pressure of the supercritical BLEVE was 4 times the MAWP of the vessels with the same discretization. As previously mentioned, the MAWP of an $LH_2$ tank is 8.4 bar, while 21.5 bar (US DOE - NHTSA, 2017) and 14.5 bar (Cummins Westport Inc., 2003) are the MAWPs of a liquefied petroleum gas (LPG) and LNG tank respectively. Since LPG and LNG are mainly composed by propane and methane respectively, these MAWP values were accepted. Therefore, the maximum bursting pressures were 32.8, 86 and 58 bar for the $LH_2$, liquefied propane ($LC_3H_8$) and methane ($LCH_4$) respectively. Finally, the liquid level prior the subcritical BLEVE was 50%.
Tschirschwitz et al. (2018) measured the blast wave overpressure at 7, 9 and 11 m for a series of LPG tanks with a volume of 0.064 m$^3$ engulfed in a fire. In this study, the overpressure was estimated at 9 m since the propane tank has a similar volume (0.125 m$^3$).

## 3. Results

In this section, the results are divided in sub- and supercritical BLEVE. The comparison with the other fuels is presented in both Sec. 3.1 and 3.2.

### 3.1 *Subcritical BLEVE*

The mechanical energies generated by the subcritical BLEVEs at different bursting pressures for parahydrogen ($LH_2$), propane and methane are depicted in Fig. 2.

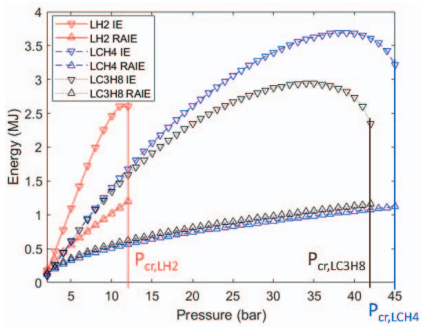


Fig. 2. Mechanical energy generated by a subcritical BLEVE at different bursting pressures for parahydrogen ($LH_2$) in red, liquefied propane ($LC_3H_8$)

in black and liquefied propane ($LCH_4$) in blue, estimated by means of the IE and RAIE models. The critical pressures ($P_{cr}$) of the substances are indicated on the chart with vertical lines.

In this chart, the highest value of the horizontal axis corresponds to the critical pressure of methane (46 bar (NIST, 2019)). The highest mechanical energy estimated with the most conservative model is 3.7 MJ for the liquefied methane tank, which bursting pressure is 38.8 bar. On the other hand, if the fuels are compared in the same bursting pressure range assumed for parahydrogen (from 2 to 12.9 bar), the highest mechanical energy value is 2.6 MJ reached by the $LH_2$ tank at 11 bar. The mechanical energy values estimated with the RAIE model are quite different. The highest value is 1.3 MJ, obtained for $LH_2$ at a pressure close to the critical one (12.7 bar). Similar values were calculated for the liquid propane and methane but at higher pressures. Comparing the same bursting pressure of 12.7 bar, $LH_2$ BLEVE generates two times the mechanical energy generated by the other fuels. In Tab. 1, the mechanical energy values estimated at different bursting pressures with both IE and RAIE models for the three types of fuels are collected.

Table 1. Comparison between the liquid hydrogen (LH2), propane ($LC_3H_8$) and methane ($LCH_4$) mechanical energy values generated by a subcritical BLEVE and estimated at different pressures with both IE and real RAIE models.

| | $LH_2$ | $LC_3H_8$ | $LCH_4$ |
|---|---|---|---|
| **IE model values** | | | |
| Max mech. en. (MJ) | 2.6 @ 11.0 bar | 2.9 @ 35.0 bar | 3.7 @ 39.0 bar |
| Mech. en. @ 11.0 bar (MJ) | 2.6 | 1.5 | 1.6 |
| **RAIE model values** | | | |
| Max mech. en. (MJ) | 1.3 @ 12.7 bar | 1.2 @ 42.0 bar | 1.1 @ 45.0 bar |
| Mech. en. @ 12.7 bar (MJ) | 1.3 | 0.6 | 0.6 |

As mentioned in Sec. 2.2, the blast wave overpressure depends by the mechanical energy, the percentage of this energy converted in pressure wave and the distance from the explosion. For this reason, the overpressure values collected in Tab. 2 and estimated at a distance of 9 m, follow the same trend found for the mechanical energy. The SE model outcome is reported as well in Tab. 2. This latter provided the less conservative values of overpressure but still close to the RAIE outcomes.

Table 2. Comparison between the liquid hydrogen (LH2), propane ($LC_3H_8$) and methane ($LCH_4$) overpressure of the blast wave generated by the subcritical BLEVEs, estimated at 9 m with the Sachs scaling law.

| | Max. overpressure (bar) | | |
|---|---|---|---|
| **Mech. en. model** | **$LH_2$** | **$LC_3H_8$** | **$LCH_4$** |
| **IE** | 0.06 @ 11.0 bar | 0.07 @ 35.0 bar | 0.08 @ 39.0 bar |
| **RAIE** | 0.05 @ 12.7 bar | 0.05 @ 42.0 bar | 0.05 @ 45.0 bar |
| **SE** | 0.03 @ 12.7 bar | 0.04 @ 34.0 bar | 0.04 @ 39.0 bar |

### 3.2 *Supercritical BLEVE*

The mechanical energy values obtained for parahydrogen with the IE and ISE models in the range of 13 to 33 bar are illustrated in Fig. 5, together with the results for liquefied propane (in the range of 42.5 and 86 bar) and liquefied methane (between 46 and 58 bar). The highest mechanical energy values are 8.6 and 4.7 MJ estimated for $LH_2$ with the IE and ISE models respectively, at a pressure of 32.8 bar.

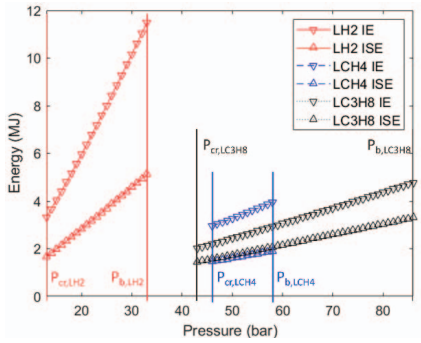


Fig. 5. Mechanical energy generated by a supercritical BLEVE of $LH_2$ (red lines), $LC_3H_8$ (black lines) and $LCH_4$ (blue lines) estimated with the IE and ISE models between the critical ($P_{cr}$) and bursting pressure ($P_b$) of the different substances.

The highest mechanical energy values reached by propane are 4.8 (IE) and 3.3 MJ (ISE) at 86 bar, while 3.9 (IE) and 1.9 MJ (ISE) are the values calculated for methane at 58 bar.
Both propane and methane are not in supercritical conditions in the range of pressures considered for $LH_2$. Only the values obtained by the IE model were compared even though the BLEVEs of propane and methane are subcritical. This

comparison is shown in Tab. 3, together with the maximum mechanical energy estimated for each fuel.

Similarly to Sec. 3.1, the maximum pressure wave overpressure values estimated for the supercritical BLEVEs are collected in Tab. 4. In this case, the SE model was not adopted since it takes into account exclusively the enthalpy of the liquid phase. The overpressure values follow again the mechanical energy trend.

Table 3. Comparison between the liquid hydrogen (LH2), propane ($LC_3H_8$) and methane ($LCH_4$) mechanical energy values generated by a sub- and supercritical BLEVE estimate at different pressures with the IE and ISE models.

| | $LH_2$ | $LC_3H_8$ | $LCH_4$ |
|---|---|---|---|
| **IE model values** | | | |
| Max mech. en. (MJ) | 8.6 @ 32.8 bar | 4.8 @ 86.0 bar | 3.9 @ 58.0 bar |
| Mech. en. @ 32.8 bar (MJ) | 8.6 (super) | 3.6 (sub) | 2.9 (sub) |
| **ISE model values** | | | |
| Max mech. en. (MJ) | 4.7 @ 32.8 bar | 3.3 @ 86.0 bar | 1.9 @ 58.0 bar |

Table 4. Comparison between the liquid hydrogen (LH2), propane ($LC_3H_8$) and methane ($LCH_4$) overpressure blast wave generated by the supercritical BLEVEs, estimated at 9 m with the Sachs scaling law.

| | Max. overpressure (bar) | | |
|---|---|---|---|
| **Mech. en. model** | $LH_2$ | $LC_3H_8$ | $LCH_4$ |
| **IE** | 0.18 @ 32.8 bar | 0.12 @ 86.0 bar | 0.11 @ 58.0 bar |
| **ISE** | 0.12 @ 32.8 bar | 0.10 @ 86.0 bar | 0.09 @ 58.0 bar |

The values obtained for propane and hydrogen are similar, while the pressure wave generated by the methane tank failure seems to be the weakest.

## 4. Discussion

The results of this study show that the consequences of a subcritical BLEVE (mechanical energy and overpressure) are similar when the bursting pressures are closed to the critical pressures of the considered fuels. Nevertheless, the consequences of a supercritical $LH_2$ BLEVE are virtually twice higher than the propane and methane explosions even though their expected failure pressures (86 and 58 bar respectively) are higher than the hydrogen one (32.8 bar). The models employed in this study seem to provide reliable results for the propane tank. During the tests conducted in Tschirschwitz et al. (2018), similar values of overpressure (0.05 ÷ 0.12 bar) were measured at 9 m, for an LPG tank of 0.0638 $m^3$ which failed between 74 and 79 bar. Both ideal (IE and ISE) and real (RAIE) gas behavior models were adopted in this study. The ideal models are usually the most conservative as demonstrated by the presented outcomes. A first limitation of the IE model is that only the pressure and the volume of the tank are taken into account, without considering the type of substance. Moreover, the results of this model are not reliable when the tank fails at a pressure close to the critical one. The independency of the fuel mass content inside the tank at supercritical conditions is another limitation of all the ideal gas behavior models. Additional models such as the thermodynamic availability (TA) or the real gas behavior and isentropic expansion (RISE) should be adopted in the future studies in order to estimate more accurate consequences.

The comparison between the chosen fuels was one of the main difficulties of this study due to their diverse physical and chemical properties. On one hand, hydrogen has a lower density and needs larger containments than propane and methane. On the other hand, it has much lower critical temperature and pressure, thus the probability to reach a supercritical status is higher than the conventional fuels. The $LH_2$ properties influence the characteristics of the vessel, which requires high performance insulation to prevent heat losses. Therefore, the $LH_2$ double walled vessel is composed by an internal tank installed inside the external one and separated by the aforementioned insulation, and additional energy may be required to disrupt both shells. For this reason, the mechanical energy contribution dedicated to generate the pressure wave ($\beta$) might be lower than the conventional tank. The same speculation may be valid for the LNG (or liquefied methane) which has a temperature of 112 K (NIST, 2019), and the other cryogenic fluids. Moreover, the $LH_2$ tank is design with a MAWP lower than the conventional pressure vessels due to its properties. The MAWP affects the foreseen bursting pressure of the tank, which depends on the material and structure of the container and other external parameters, such as the presence of fire. The yield of the explosion is mainly influenced by the bursting pressure and the volume. Further investigations such as a tank structural analysis or experimental tests are needed to determine the effective failure pressure of this type of vessels. Furthermore, experimental tests are needed to validate the results of these models for the $LH_2$ BLEVE. This type of tests will be conducted during the Norwegian $SH_2$IFT project. If the results of this study will be validated, appropriate and effective safety barriers

must be suggested in order to prevent or mitigate the $LH_2$ BLEVE phenomenon. In a future assessment for hydrogen and other conventional fuels, the same tank energy content instead of the fuel mass could provide a more meaningful and realistic comparison if a specific application will be considered.

## 5. Conclusion

In this study the consequences of both sub- and supercritical $LH_2$ BLEVE were estimated by means of ideal and real gas behavior models. In particular, the mechanical energy generated by the explosion and the blast wave overpressure at a fixed distance from the tank were calculated. Similar estimations were conducted for liquefied propane and methane tanks in order to conduct a meaningful hazard assessment.
Different challenges were tackled especially during the fuel safety comparison due to the different properties of the considered fuels. The lack of knowledge still present in literature for the $LH_2$ BLEVE phenomenon was highlighted justifying the necessity for future studies and experimental tests. Future test results will be used to validate for the $LH_2$ BLEVE the model adopted in this study.

## Acknowledgement

This work was undertaken as part of the research project Safe Hydrogen fuel handling and Use for Efficient Implementation ($SH_2IFT$), and the authors would like to acknowledge the financial support of the Research Council of Norway under the ENERGIX programme (Grant No. 280964).

## References

American Society of Mechanical Engineering (2001). ASME Section VIII, Division 1, Pressure Vessel Code.

Argonne National Laboratory (2010), The Greenhouse Gases, Regulated Emissions, and Energy Use in Transportation Model (GREET) 1.8d1.

Ausfelder, F., and A. Bazzanella (2016). Hydrogen in the Chemical Industry. In D. Stolten and B. Emonts *Hydrogen Science and Engineering: Materials, Processes, Systems and Technology*, pp. 19–39. Wiley-VCH Verlag.

Barthelemy, H., M. Weber, and F. Barbier (2017). Hydrogen Storage: Recent Improvements and Industrial Perspectives. *International Journal of Hydrogen Energy 42*, 7254–62.

Bell, I., J. Wronski, S. Quoilin, and V. Lemort (2014). Pure and Pseudo-Pure Fluid Thermophysical Property Evaluation and the Open-Source Thermophysical Property Library CoolProp. *Industrial & Engineering Chemistry Research 53*, 2498–2508.

Casal, J., and J. Salla (2006). Using Liquid Superheating Energy for a Quick Estimation of Overpressure in BLEVEs and Similar Explosions. *Journal of Hazardous Materials 137*, 1321–27.

Casal, J. (2008). Evaluation of the Effects and Consequences of Major Accidents in Industrial Plants. Elsevier.

Casal, J., B. Hemmatian, and E. Planas (2016). On BLEVE Definition, the Significance of Superheat Limit Temperature (Tsl) and LNG BLEVE's. *Journal of Loss Prevention in the Process Industries 40*, 81.

Cummins Westport Inc. (2003). Advanced LNG Onboard Storage System (ALOSS) - Financial Technical Report for DOE Financial Assistance Award DE-FC36-02CH11138.

Edeskuty, F. and W. Stewart (1996). *Safety in the Handling of Cryogenic Fluids*. Springer Science +Business Media, LLC.

Hemmatian, B., E. Planas, and J. Casal (2017). Comparative Analysis of BLEVE Mechanical Energy and Overpressure Modelling. *Process Safety and Environmental Protection 106*, 138–49.

International Energy Agency (IEA) Hydrogen (2017). Global Trends and Outlook for Hydrogen.

Jovanović, A. and D. Baloš (2013). INTeg-Risk Project: Concept and First Results. *Journal of Risk Research 16*, 275–91.

Klebanoff, L., J. Pratt, and C. LaFleur (2017), Comparison of the safety-related physical and combustion properties of liquid hydrogen and liquid natural gas in the context of the SF-BREEZE high-speed fuel-cell ferry, *Int. J. Hydrogen Energy 42*, 757–774.

Landucci, G., A. Tugnoli, V. Cozzani (2010). Safety assessment of envisaged systems for automotive hydrogen supply and utilization, *International Journal of Hydrogen Energy* 35, 1493–1505.

Landucci, G., A. Tugnoli, V. Cozzani (2008). Inherent safety key performance indicators for hydrogen storage systems, *Journal of Hazardous Materials* 159, 554–566.

Molkov, V., and S. Kashkarov (2015). Blast Wave from a High-Pressure Gas Tank Rupture in a Fire: Stand-Alone and under-Vehicle Hydrogen Tanks. *International Journal of Hydrogen Energy 40*, 12581–12603.

National Institute of Standards and Technology (2019). NIST Chemistry WebBook, SRD 69.

Paltrinieri, N., N. Dechy, E. Salzano, M. Wardman, and V. Cozzani (2012). Lessons Learned from Toulouse and Buncefield Disasters: From Risk Analysis Failures to the Identification of Atypical Scenarios Through a Better Knowledge Management. *Risk Analysis, 32*, 1404–1419.

Paltrinieri, N., A. Tugnoli, J. Buston, M. Wardman, and V. Cozzani (2013). Dynamic Procedure for Atypical Scenarios Identification (DyPASI): A New Systematic HAZID Tool. *Journal of Loss Prevention in the Process Industries 26*, 683–95.

Peschka, W. (1992). *Liquid Hydrogen - Fuel of the Future*. Springer-Verlag.

Planas-Cuchi, E., J. Salla, and J. Casal (2004). Calculating Overpressure from BLEVE Explosions. *Journal of Loss Prevention in the Process Industries 17*, 431–36.

Prugh, R. (1991). Quantitative Evaluation of 'BLEVE' Hazards. *Journal of Fire Protection Engineering 3*, 9–24.

Rybin, H., G. Krainz, G. Bartlok, and E Kratzer (2005). Safety Demands for Automotive Hysrogen Storage Systems. In *International Conference on Hydrogen Safety 12*.

Sachs, R. (1944). The Dependence of Blast on Ambient Pressure and Temperature. BRL Report No. 466, Aberdeen Proving Ground, Maryland.

Smith, J. and H. Van Ness (1996). Introduction to Chemical Engineering Thermodynamics (Edition 5th). McGraw-Hill.

Strehlow, R., and W. Baker (1975). The Characterization and Evaluation of Accidental Explosions - NASA CR 134779.

Tang, M., C. Cao, and Q. Baker (1996). Blast Effects from Vapor Cloud Explosions. In *International Symposium on Loss Prevention, Bergen, Norway*.

Tschirschwitz, R., D. Krentel, M. Kluge, E. Askar, K. Habib, H. Kohlhoff, S. Krüger, et al. (2018). Experimental Investigation of Consequences of LPG Vehicle Tank Failure under Fire Conditions. *Journal of Loss Prevention in the Process Industries 56*, 278–88.

U.S. Department of Transportation - National Highway Traffic Safety Administration (2017). Evaluation of Methodology for LPG Fuel System Integrity Tank Test - DOT HS 812 377.

Ustolin, F., G. Song, and N. Paltrinieri (2019). The Influence of H2 Safety Research on Relevant Risk Assessment. *Chemical Engineering Transactions 74*.

Aursand E, Odsæter LH, Skarsvåg HL, Reigstad GA, Ustolin F, Paltrinieri N. Risk and Consequences of Rapid Phase Transition for Liquid Hydrogen. 30th Eur. Saf. Reliab. Conf. 15th Probabilistic Saf. Assess. Manag. Conf. (ESREL2020 PSAM15), 2020. https://doi.org/10.3850/978-981-14-8593-0.

This page is intentionally left blank

# Risk and Consequences of Rapid Phase Transition for Liquid Hydrogen

E. Aursand, L. H. Odsæter, H. Skarsvåg, G. Reigstad

*SINTEF Energy Research, Postboks 4761 Torgarden, 7465 Trondheim, Norway.*
*E-mail: lars.odsater@sintef.no*

F. Ustolin, N. Paltrinieri

*Department of Mechanical and Industrial Engineering, Norwegian University of Science and Technology NTNU, 7491 Trondheim, Norway.*

Safe handling of liquid hydrogen ($LH_2$) has gained extra attention over the last years due to an increase in usage to mitigate climate changes. Rapid phase transition (RPT) is a potential safety concern when cryogens, like $LH_2$ and liquefied natural gas (LNG), are accidentally spilled onto water. A theoretical assessment of the risk and consequences of $LH_2$ RPT has been conducted. The assessment is based on the RPT theory established from LNG research, as well as published reports on actual $LH_2$ spills. We give a review of the established theory on LNG RPT, examine the probability of an $LH_2$ RPT event, and give estimates on the theoretical consequence in terms of the peak pressure and the explosive energy yield. There are two main findings of this study. Firstly, the known theoretical pathways to LNG RPT are impossible or very unlikely when applied to $LH_2$ spills. Secondly, the theoretical consequences of an explosive $LH_2$ RPT event are low compared to LNG RPT. The expected peak pressure is about 25% of an LNG RPT, while the expected explosive energy yield is only about 10% of an LNG RPT, given the same volume of participating cryogen. Combined with the knowledge that LNG RPT events are only moderately dangerous, the hypothetical $LH_2$ RPT event is possibly characterized by a low destructive potential.

*Keywords*: Liquid hydrogen, Safe fuel handling, Cryogens, Rapid phase transition, Spill accidents, Risk and consequence analysis

## 1. Introduction

Hydrogen technology is pointed out as one of the solutions to reduce emissions in the transport and energy sectors. The high volumetric energy density of liquid hydrogen ($LH_2$) compared to gaseous hydrogen is an advantage for transport and storage of large quantities. $LH_2$ is considered a cryogen due to its extremely low boiling point (20 K). With an increase in usage, transportation and storage, the need for more knowledge of safe handling is important.

Liquefied natural gas (LNG) is another cryogenic fuel that has been widely used over the last decades. If LNG is accidentally spilled onto water it has been observed in some cases, seemingly at random, to undergo a localized explosive vaporization (Reid, 1983; Cleaver et al., 1998; Luketa-Hanlin, 2006; Melhem et al., 2006; Koopman and Ermak, 2007). This is known as a rapid phase transition (RPT) and has the potential to have devastating consequences (Luketa-Hanlin, 2006; Havens and Spicer, 2007; Pitblado and Woodward, 2011; Forte and Ruf, 2017). Predicting triggering and consequence of LNG RPT was subject to a recent study by Aursand and Hammer (2018). The literature on LH2 RPT is very limited, and to the best of our knowledge, no RPT-like event as a consequence of an $LH_2$ spill has been reported. This does not mean that $LH_2$ RPT is impossible.

In this study, we examine the probability and consequences of the hypothetical $LH_2$ RPT event. The assessment is based on the RPT theory established from LNG research, as well as published reports on actual $LH_2$ spills. Our focus is RPT events caused by the cryogen being spilled onto water, since this is a likely scenario for transportation and storage in a marine environment. We recognize that other scenarios may also cause RPT events, e.g., when water is released onto a cryogenic pool. An introduction to RPT and a review of the established theory on LNG RPT is given in Sec. 2. This theory is then applied to $LH_2$ in Sec. 3. In particular, we apply the approach by Aursand and Hammer (2018) to estimate the consequences of an RPT event in terms of the peak pressure of the vapor-explosion and the explosive energy yield. Finally, we summarize the main conclusions of this study in Sec. 4.

## 2. LNG Rapid Phase Transition (RPT)

Natural gas is a common fossil fuel whose main component is methane (about 90%), with the remainder consisting of progressively smaller amounts of the heavier alkanes. For long-range

*Proceedings of the 30th European Safety and Reliability Conference and the 15th Probabilistic Safety Assessment and Management Conference*
*Edited by* Piero Baraldi, Francesco Di Maio and Enrico Zio
*Published by* Research Publishing, Singapore.
ISBN: 978-981-14-8593-0; doi:10.3850/978-981-14-8593-0

transportation, natural gas is sometimes cooled down below its boiling point ($-162\,^{\circ}\mathrm{C}$ at atmospheric pressure) to form liquefied natural gas (LNG) (Kumar et al., 2011).

### 2.1. *The phenomenon of RPT*

When LNG is spilled onto water it will in the majority of cases eventually boil off without further incident. However, in some cases it is observed to suddenly, and seemingly at random, undergo a localized explosive vaporization. This is an RPT event, and is considered one of the main safety concerns of the LNG industry (Reid, 1983; Pitblado and Woodward, 2011). Still, the attention given to RPT risk in LNG safety reviews is highly variably, ranging from significant discussion (Pitblado and Woodward, 2011; Cleaver et al., 2007; Luketa-Hanlin, 2006; Shaw et al., 2005) to little more than a brief mention (Alderman, 2005; Hightower et al., 2005; Havens and Spicer, 2007; Raj and Bowdoin, 2010; Forte and Ruf, 2017).

RPT is not an explosion in the common meaning of the word, since it does not involve combustion or other chemical reactions. RPT events are what is sometimes called a vapor explosion or a physical explosion. It is still destructive in nature, and poses a danger to both people and equipment. Its peak pressures and released mechanical energy can be large enough to displace and damage heavy equipment (Luketa-Hanlin, 2006; Pitblado and Woodward, 2011; Forte and Ruf, 2017) and could theoretically cause secondary structural damage and cascading containment failures (Havens and Spicer, 2007). Whether or not an RPT event will occur in any given spill has been notoriously difficult to predict. From extensive tests performed by LLNL in the 1980s (Luketa-Hanlin, 2006; Koopman and Ermak, 2007; Melhem et al., 2006) it was found that RPT occurred in about one third of spills. It was also observed that a single spill may lead to more than ten distinct RPT events. The yields of single RPT events seem quite random, and may apparently have TNT equivalents of anything from a few grams to $6\,\mathrm{kg}$ (about $25\,\mathrm{MJ}$) (Koopman and Ermak, 2007; Melhem et al., 2006; Cleaver et al., 1998; ABS Consulting, 2004; Hightower et al., 2004).

The general macroscopic chain-of-events of a marine LNG spill is as follows:

(i) *Containment breach*: Due to some unintended event, the containment of LNG in a tank or transfer line is broken. If the breach is above sea level, the LNG may fall towards the water surface in the form of a jet.
(ii) *Jet impact*: The LNG jet impacts the water surface, which will break it up into separate droplets.
(iii) *Droplet/water mixing*: If the momentum of the the jet is large enough, the droplets will initially penetrate the surface and become submerged in water. This forms a chaotic *mixing region*.
(iv) *Pool formation and spreading*: Since the density of LNG is about half of that of water, the droplets will be buoyant and will eventually rise to the surface. This forms an LNG pool that spreads on top of the water surface.
(v) *Boil-off*: The boiling point of LNG is at about $-162\,^{\circ}\mathrm{C}$ (at atmospheric pressure), while the water holds a temperature relatively close to $0\,^{\circ}\mathrm{C}$, so the spreading pool will start boil while spreading. Since methane is by far the most volatile component, the resulting vapor is almost purely methane. This causes a gradual compositional change, which increases the relative amounts of the heavier alkanes such as ethane, propane and butane.

See Fig. 1 for an illustration of the scenario. As indicated, there is an established distinction between two kinds of RPT events depending on when and where it occurs in a spill event (Luketa-Hanlin, 2006; Koopman and Ermak, 2007). An *early RPT* is defined as any RPT that occurs in the mixing region at any time during the spill event, while a *delayed RPT* is defined as any RPT that is not an early RPT, which means that it must occur somewhere in the spreading pool, not in the mixing region. Reports indicate that delayed RPT only occurs a considerable time (on the scale of minutes) after the start of the LNG spill event.

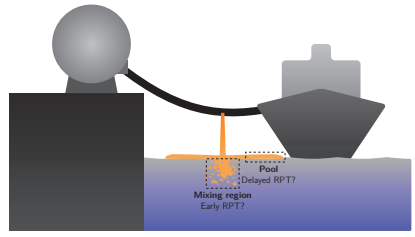


Fig. 1. An illustration of a spill-scenario, where a breach in a fueling line causes the release of cryogen in the form of a falling jet. Also shown are the origins of the two kinds of RPT event: *early RPT* from the mixing region, and *delayed RPT* from the spreading pool.

### 2.2. *The theory of RPT*

After the possibility of LNG RPT was discovered in the 1960s, a handful of research groups went to work on understanding the mechanisms behind the phenomenon. By the first half of the 1970s, they had arrived at a general consensus for a theory of RPT (Katz and Sliepcevich, 1971;

Katz, 1972; Nakanishi and Reid, 1971; Enger, 1972; Enger and Hartman, 1972a,b; Enger et al., 1973). This is a theory about what occurs on the small scales at the local time and position where a single RPT event is observed, and is relevant for both early and delayed RPT. The theory may be summarized by the following chain-of-events:

(i) *Film-boiling stage*: The temperature difference between the sea water and the LNG is so large that boiling occurs far into the *film boiling* regime, see Fig. 2. This means that the LNG pool or droplet is insulated from the water by a vapor film consisting mainly of methane. Because of this the heat flux stays relatively low and the evaporation stays in a quasi-equilibrium regime. All of the energy transferred into the LNG is spent on evaporation, and the LNG temperature stays close to the bubble-point, which is initially about $-162\,^{\circ}\mathrm{C}$.

(ii) *Film-boiling collapse (liquid-liquid contact)*: For some reason there is a sudden and localized *film-boiling collapse*. The suggested mechanisms for film-boiling collapse will depend on whether one is considering early or delayed RPT. In either case, this means that there is considerable direct contact between the water and the LNG, which increases the heat flux by orders of magnitude.

(iii) *Rapid superheating to the superheat limit*: Because a liquid-liquid interface has relatively few nucleation sites, the evaporation rate is initially unable to keep up with the dramatic increase in heat flux. Instead, much of the heat is spent on *superheating* the LNG, which means that the liquid is heated significantly beyond its boiling temperature. The superheated liquid is in a meta-stable state, and may transition to its corresponding equilibrium state if disturbed. If not disturbed sufficiently, there is a maximum temperature at which the liquid must transition regardless of external disturbances. This is called the *superheat limit*.

(iv) *Homogeneous nucleation*: Once the liquid approaches its superheat limit, vaporization spontaneously occurs throughout its volume by *homogeneous nucleation*. This is the start of a rapid transition from a liquid state to a two-phase state.

(v) *Explosive expansion*: If in mechanical equilibrium with its surroundings, the new state would take up over 100 times the volume of the original superheated liquid state. The fluid is initially forced to fit in the original volume, so the pressure increases dramatically before it has time to expand. Since this transition happens fast, it is observed as a loud and destructive vapor explosion. The event involves high-pressure waves and considerable energy release through expansion work.

### 2.3. *Predicting triggering of RPT*

The main challenge when predicting the occurrence of RPT is predicting step two, the sudden film-boiling collapse and subsequent liquid–liquid contact. We refer to this as the *triggering event*. The approach depends on whether one considers early RPT (droplet boiling) or delayed RPT (pool boiling).

#### 2.3.1. *Delayed RPT*

For delayed RPT, the relevant mode of boiling is *pool boiling*. This is usually quantified in terms of the *boiling curve* (Dhir, 1998). A general illustration of a boiling curve is shown in Fig. 2.

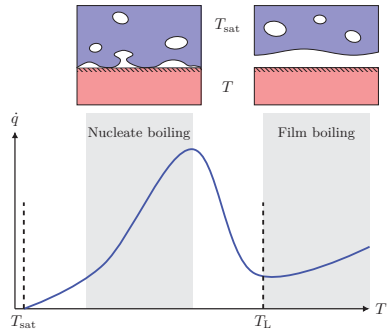


Fig. 2. Illustration of a typical boiling curve for saturated pool boiling, showing boiling heat flux ($\dot{q}$) as a function of surface temperature ($T$). In our case, the cryogen is the boiling fluid (blue shape), while water takes the role as the hot surface (red shape). Once $T > T_{\mathrm{sat}}$ the surface is considered superheated, and the difference $T - T_{\mathrm{sat}}$ is called the *surface superheat*. At moderate surface superheat we are in the conventional *nucleate boiling regime*. Once the surface superheat becomes very large there is a transition into a *film-boiling regime*, which comes with a dramatic drop in heat flux due to the formation of a continuous vapor film. The lower end of the film boiling regime is the Leidenfrost temperature ($T_{\mathrm{L}}$), and crossing this from right to left is called *film-boiling* collapse.

In the present case, LNG takes the role of the boiling fluid and water takes the role of the hot surface. According to the theory described above RPT is triggered on film-boiling collapse, which for pool boiling is defined by the position on the

boiling curve:

$$\begin{aligned} T_{\mathrm{L}} < T_{\mathrm{w}} &: \text{Film boiling (no RPT)} \\ T_{\mathrm{L}} > T_{\mathrm{w}} &: \text{Liquid-liquid contact (risk of RPT),} \end{aligned} \quad (1)$$

where $T_{\mathrm{w}}$ is the temperature of the water. The Leidenfrost temperature of a fluid such as LNG is difficult to predict (or even measure) with good accuracy, but it has generally been found that it is close to, but slightly below, the fluid's critical temperature (Spiegler et al., 1963),

$$T_{\mathrm{L}} \approx \frac{27}{32} T_{\mathrm{crit}}. \quad (2)$$

The critical point of a typical LNG mixture is in the region of $T_{\mathrm{crit}} \approx 203\,\mathrm{K}$ ($-70\,^{\circ}\mathrm{C}$), yielding $T_{\mathrm{L}} \approx 171\,\mathrm{K}$ ($-102\,^{\circ}\mathrm{C}$). By comparison, since the water is normally not observed to freeze in large-scale LNG spills, the surface holds a temperature close to zero, $T_{\mathrm{w}} \approx 0\,^{\circ}\mathrm{C}$. Hence, we are safely in the "Film boiling (no RPT)" part of Eq. (1).

The above calculations are only true for LNG with its initial (stored) composition. As boil-off proceeds, the composition changes in such a way that the critical temperature of the mixture increases. According to Eq. (2), this means that the Leidenfrost temperature will also increase. Eventually it reaches the water temperature, which according to Eq. (1) gives a risk of RPT. See Fig. 3 for an illustration of this *LNG RPT boil-off* effect.

Thus, the challenge of predicting the triggering of delayed LNG RPT is reduced to the prediction of when and where the condition $T_{\mathrm{L}} > T_{\mathrm{w}}$ may be satisfied. In our previous work, Aursand and Hammer (2018), this was analyzed extensively in terms of the methane fraction necessary to satisfy the the triggering criterion. In short, the results can be summarized as follows. The LNG must boil down to approximately 30-50 mol% methane before meeting the condition for delayed RPT triggering ($T_{\mathrm{L}} \approx T_{\mathrm{w}}$). This depends on the relative amounts of the heavier alkanes. By the time the triggering condition is met, only 10-20% of the original amount of LNG is remaining.

#### 2.3.2. *Early RPT*

As indicated in Fig. 1, so-called early RPT occurs in the chaotic mixing region beneath the point of LNG jet impact. This region contains film-boiling LNG droplets submerged in water, which initially move downwards due to inertia but eventually move back to the surface due to buoyancy. According to the general theory of RPT presented in Sec. 2.2, the triggering event is initiated by sudden significant liquid-liquid contact. Predicting this for early RPT is much more difficult than in the case of delayed RPT, since the degree of liquid-liquid contact is no longer governed by a simple boiling curve. In this case it would require a detailed multi-phase simulation of the mixing region over sufficiently long time-scales. This has to our knowledge not been achieved, and we consider early RPT an unsolved problem in the LNG industry.

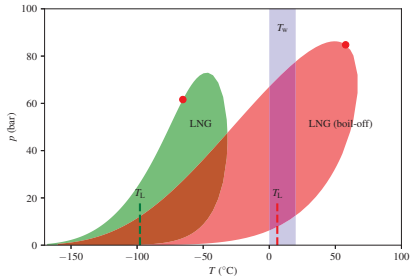


Fig. 3. An illustration of how the two-phase region (filled shapes) and the critical point (red dot) shifts to higher temperatures as methane is removed from the mixture due to boil-off. In this particular example the LNG boils down from 90 mol% methane to 40 mol% methane. This causes the Leidenfrost temperature ($T_{\mathrm{L}}$), according to Eq. (2), to shift up into the typical seawater temperatures (blue bar), which satisfies the condition for delayed RPT triggering.

### 2.4. *RPT consequence quantification*

Our work in Aursand and Hammer (2018) also included a method of partially quantifying the consequence of RPT. According to the theoretical chain-of-events listed in Sec. 2.2, after film-boiling collapse (Leidenfrost transition) there is rapid superheating, homogeneous nucleation and explosive expansion. Here we enable consequence quantification by simplifying the final two steps in the chain-of-events (steps 4-5) by the following idealized two-step process:

(i) *Equilibration*: Calculate the energy and density of the the mixture exactly when it reaches the superheat limit after film-boiling collapse. The temperature of this state is the superheat limit ($T_{\mathrm{SHL}}$) corresponding to the composition at the time when the triggering criterion was reached. Then, find the corresponding quasi-equilibrium state, with the same energy, density and composition. This yields a new high-pressure intermediate state $(T^*, p^*)$.

(ii) *Isentropic expansion*: The intermediate state $(T^*, p^*)$ is called a quasi-equilibrium state because while it is in local equilibrium, it is not in mechanical equilibrium with the surroundings ($p^* \gg 1\,\mathrm{atm}$). This leads to a rapid expansion, which is approximated as an isentropic process. The end-state of this expansion may then be found as the state at

atmospheric pressure that has the same entropy as the high-pressure intermediate state.

There are two significant numbers to take away from such a calculation. Firstly, the *peak pressure* ($p^*$) is found as the pressure of the intermediate state before expansion. The value may be interpreted as an estimate for the peak pressure seen in the vapor-explosion event very close to the source. Secondly, the *explosive energy yield* ($E$) is found as the mechanical work done by the expansion process. Since the process is assumed to be isentropic (reversible and adiabatic), it follows from classical thermodynamics that the work done by the process is simply the difference in total enthalpy between the initial and final states of the expansion. Note that this merely yields an energy per amount triggered (i.e. per mole or kilogram), not a total amount.

Even with these simplifying assumptions, performing this calculation involves a set of quite complex thermodynamic algorithms. Firstly, an algorithm to calculate the superheat limit ($T_{\mathrm{SHL}}$). Here we use the method described in Aursand and Hammer (2018). Secondly, an algorithm to calculate the two-phase equilibrium state, given either values for energy and density or values for entropy and pressure. Here we use the implementations in SINTEF's in-house software (Wilhelmsen et al., 2017), which are based on algorithms described by Michelsen and Mollerup (2007).

The result of such a calculation is shown in Fig. 4. This result will depend on the initial LNG composition, which will vary some. In Aursand and Hammer (2018) the range of outcomes given a plausible range of LNG compositions was explored, and the conclusions were the following. The predicted explosive yield from LNG RPT ($E$) is in the range of 50–80 $\mathrm{kJ/kg}$, which is equivalent to about 12–20 $\mathrm{gTNT}$ per $\mathrm{kg}$ LNG. In terms of spilled liquid volume, this is about 5–10 $\mathrm{gTNT}$ per litre. The predicted peak pressure from LNG RPT ($p^*$) is in the range of 20 $\mathrm{bar}$ to 60 $\mathrm{bar}$.

Note that the predicted yield is only found in terms of energy per liquid amount that participates in the event. Since there is currently no way of predicting how much liquid will participate in a single event, the explosive yield of single RPT events cannot be predicted. However, the calculations give useful upper bounds on the explosive potential of an LNG pool. They also give numbers that may be compared with other substances, such as $LH_2$.

## 3. Assessment of $LH_2$ RPT

To our knowledge, no RPT-like incident has ever been reported in relation to $LH_2$ spills. Pritchard and Rattigan (2010) reported in 2010 that "...no record of a RPT resulting from a $LH_2$ spill has been found", and subsequent reports addressing hydrogen safety does not mention RPT (Batt, 2014; Royle and Willoughby, 2014; Ekoto et al., 2014; Kotchourko et al., 2014; Rivkin et al., 2015; Ruiz, Vega, del Mar Arxer, Jimenez, and Rausa, Ruiz et al.; Keller et al., 2016). Furthermore, experimental activity on $LH_2$ spills on water is limited to the BAM trials in 1994 (Verfondern and Dienhart, 1997, 2007), were no RPT-like events was observed. In this section we will assess the probability and consequences of a hypothetical $LH_2$ RPT event based on the theory for LNG RPT presented in Sec. 2.

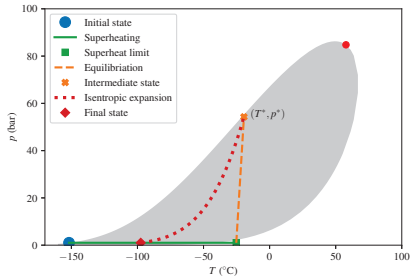


Fig. 4. The result of an RPT consequence calculation, as described in Sec. 2.4, for an LNG mixture that is triggered after boiling down to 40 mol% methane. In this particular example the theoretical explosive yield ($E$) is 20 $\mathrm{gTNT}$ per kg LNG, or about 10 $\mathrm{gTNT}$ per liter of spilled LNG. The predicted peak pressure ($p^*$) is about 55 $\mathrm{bar}$.

### 3.1. *Triggering of $LH_2$ RPT*

#### 3.1.1. *Delayed RPT*

If we assume that the basic principles and theories for LNG RPT also apply for the hypothetical $LH_2$ RPT, the triggering criterion Eq. (1) for delayed RPT should still hold. In other words, triggering may only occur if the Leidenfrost temperature ($T_{\mathrm{L}}$) is at or above the water temperature. According to the approximate model in Eq. (2), the Leidenfrost temperature of hydrogen is about 28 $\mathrm{K}$. This is somewhat consistent with the value of 24 $\mathrm{K}$ reported by Wang et al. (2016). In either case, the triggering criterion is far from being satisfied:

$$T_{\mathrm{L}} \ll T_{\mathrm{w}} \implies \text{No triggering.} \tag{3}$$

Furthermore, a pure fluid like $H_2$ has no compositional shift as boil-off proceeds. This is in contrast to LNG, where the initial stable situation like Eq. (3) is eventually lost due to methane depletion. In terms of Fig. 2, $LH_2$ will be far into the film-boiling regime throughout the boil-off process, which will prevent RPT. The conclusion is the following: As long as the surface (water) temperature stays anywhere near 0 °C, delayed $LH_2$ RPT is impossible given that the applied theory is valid.

#### 3.1.2. *Early RPT*

We should also consider the possibility of early RPT, as described for the case of LNG in Sec. 2.3.2. As illustrated in Fig. 1, early RPT occurs in the mixing-region below the location where the cryogen jet penetrates the water surface. As mentioned in Sec. 2.3.2, there is no satisfactory method for quantifying the probability of early RPT. From experience of LNG spills, it seems to be an event of quite high probability, occurring in about one third of spills. In contrast, no early RPT has ever been observed in $LH_2$ spills, and we may speculate why this is the case:

- *Small mixing region*: This relates to the mixing region illustrated in Fig. 1, where all early RPT events occur by definition. LNG on water has a density-ratio of about $1/2$, which allows for an appreciable mixing region. In contrast, $LH_2$ on water has a density-ratio of less than $1/10$. Unless the jet has a very high velocity, it is unlikely to have enough inertia to penetrate the water and create an significant mixing region. Additionally, if a droplet is submerged, it will be brought to the surface by buoyancy very quickly.
- *Stable film-boiling droplets*: As mentioned the Leidenfrost temperature is very low compared to the water temperature. While this value is usually measured for pool boiling, the stability of film boiling around submerged droplets is likely quite related to this. This suggests that even if an $LH_2$ droplet is submerged in water, it will likely stay separated from the water by a vapor film, and thus not satisfy the fundamental criterion for RPT triggering (film-boiling collapse).

#### 3.1.3. *Hypothetical pathways to $LH_2$ RPT*

Note that the above argument is based on the assumption of no ice-formation, i.e. a situation where the $LH_2$ is spilled on top of liquid water that holds an approximately constant temperature of $0\,^{\circ}\mathrm{C}$. Moreover, we neglect other triggering criteria such as water waves, that could increase the mixing region and hence possibly facilitate an RPT. For large-scale (unconfined) LNG-on-water spills very little or no ice-formation is usually reported (Luketa-Hanlin, 2006; Cleaver et al., 2007), despite the very low LNG temperature ($-162\,^{\circ}\mathrm{C}$). It appears that the film-boiling heat transfer is not sufficiently strong to overcome the convective heat transfer in the water, and thus is unable to create the sub-cooling necessary to nucleate and grow solid ice. However, $LH_2$ is considerable colder ($-253\,^{\circ}\mathrm{C}$), which presumably could be enough to cause noticeable ice-formation. The formation of continuous and thick (several $\mathrm{mm}$) layers of ice when $LH_2$ is spilled on water has been reported in experiments (Verfondern and Dienhart, 1997, 2007). This may be important for (at least) the following reasons:

- *Sub-cooled ice*: The presence of an ice sheet allows for a new potential mechanism for the triggering of delayed RPT. If there is no freezing, the surface temperature would essentially be locked to a constant $T_{\mathrm{w}} \approx 0\,^{\circ}\mathrm{C}$, leading to the conclusion that the only way to satisfy Eq. (1) is to increase the Leidenfrost temperature, which is not possible for $LH_2$. However, the formation of ice allows for the further cooling of $T_{\mathrm{w}}$. If the ice surface cools all the way down to $T_{\mathrm{L}}$, the triggering criterion can be satisfied despite $T_{\mathrm{L}}$ being constant. The maximum heat flux achieved after film-boiling collapse (*critical heat flux*) is quite high ($1 \times 10^5\,\mathrm{W/m^2}$ (Wang et al., 2016)), despite the temperature difference being less than $10\,\mathrm{K}$ at that point. This is almost as high as the critical heat flux of methane (Sciance et al., 1967).
- *Jet-on-ice impact*: The presence of an ice sheet makes the incoming jet impact a solid surface instead of a liquid surface. One could imagine this leading to a new kind of early RPT.

Both of the above hypothetical pathways lead to liquid-solid contact after film-boiling collapse. This may make RPT unlikely, as the fundamental theory outlined in Sec. 2.2 often stress the importance of a liquid-liquid interface between the cryogen and the hot substrate. A liquid-liquid interface has no nucleation sites, which allows the sudden heat-flux increase to be spent on superheating instead of rapid heterogeneous nucleation. Sudden liquid-solid contact after film-boiling collapse may merely lead to normal (but rapid) nucleate boiling instead of an explosive RPT event.

It is also worth mentioning that the temperature of $LH_2$ ($20\,\mathrm{K}$) is below the freezing points of both oxygen ($54\,\mathrm{K}$) and nitrogen ($63\,\mathrm{K}$). This means that there is a potential to both condense and freeze oxygen gas and nitrogen gas from the air and mix it into the $LH_2$ pool. Such mixing may have unpredictable consequences, and should be studied further.

### 3.2. *Consequences of $LH_2$ RPT*

Regardless of the actual probability of triggering, we may apply the procedure described in Sec. 2.4 to quantify the consequence of $LH_2$ RPT assuming that it does occur. The results of such a calculation are shown in Fig. 5, which is the equivalent of what Fig. 4 showed for LNG. Note that in this case, as opposed to the case of LNG, a single calculation is representative for all scenarios because there is no composition variable in a pure fluid. The results are summarized and compared with LNG in Tab. 1.

Table 1. The predicted consequences of $LH_2$ RPT compared to LNG RPT. The energy yields per volume were calculated using densities of $450\,kg/m^3$ for LNG and $71\,kg/m^3$ for $LH_2$.

| | LNG | $LH_2$ | $LH_2$ compared to LNG |
|---|---|---|---|
| Peak pressure ($p^*$) | 20–60 bar | 7 bar | 12% – 35% |
| Yield (energy per mass) | 50–80 kJ/kg | 38 kJ/kg | 48% – 76% |
| Yield (energy per volume) | 22000–36 000 kJ/m$^3$ | 2700 kJ/m$^3$ | 7.5% – 12% |

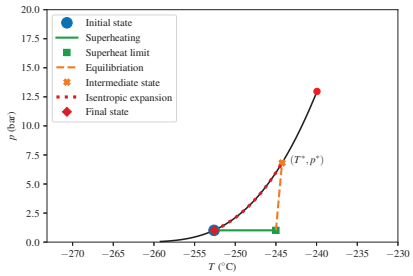


Fig. 5. The result of an RPT consequence calculation, as described in Sec. 2.4, applied to pure hydrogen. Theoretical explosive yield ($E$) is 9.2 gTNT per kg LNG, or about 0.65 gTNT per liter of spilled LNG. The predicted peak pressure ($p^*$) is about 6.8 bar.

## 4. Conclusions

The probability and consequence of a hypothetical RPT event caused by a $LH_2$ spill (release) onto water has been evaluated based on established LNG research. We may draw the following conclusions from this assessment.

The probability of an explosive $LH_2$ RPT event similar to the well known phenomenon of LNG RPT seems to be low. The theoretical pathways to RPT known from LNG research seem unlikely due to the very low Leidenfrost temperature of hydrogen, the lack of a shift in the Leidenfrost temperature due to boil-off, and the presumably very small mixing region at the point of jet impact in the absence of waves. The formation of an ice sheet could theoretically allow the triggering of RPT, but this would require the ice to have time to cool down to extremely low temperatures. This theoretical risk assessment is supported by the fact that no RPT incidents have ever been reported from real $LH_2$ spills.

In a hypothetical $LH_2$ RPT event, the estimated consequence of the vapor explosion is considerably smaller than an LNG RPT event. The predicted peak pressure is only about 25% of that from LNG RPT. The predicted explosive energy yield is about 60% by mass (or about 10% by volume) compared to LNG RPT.

Based on these arguments, we judge the hypothetical $LH_2$ RPT to be an issue of only minor concern. It should be noted that there have been relatively few $LH_2$ spills on water, experimental or accidental, when compared to LNG spills. Thus, the fact that no $LH_2$ RPT has been reported is not conclusive evidence for it being impossible and additional experiments is recommended. Experimental activity on $LH_2$ spill on water designed to investigate triggering and consequences of $LH_2$ RPT is planned to be conducted as part of the project "Safe $H_2$ fuel handling and Use for Efficient Implementation ($SH_2IFT$)".

## Acknowledgements

This work was undertaken as part of the research project "Safe $H_2$ fuel handling and Use for Efficient Implementation ($SH_2IFT$)", and the authors would like to acknowledge the financial support of the Research Council of Norway under the ENERGIX programme (Grant No. 280964).

## References

ABS Consulting (2004). Consequence assessment methods for incidents involving releases from liquefied natural gas carriers. Technical Report GEMS 1288209, Federal Energy Regulatory Commission.

Alderman, J. A. (2005). Introduction to LNG safety. *Process Saf. Prog. 24*(3), 144–151.

Aursand, E. and M. Hammer (2018). Predicting triggering and consequence of delayed LNG RPT. *J. Loss Prev. Process Ind. 55*, 124–133.

Batt, R. (2014). Modelling of liquid hydrogen spills. Technical Report RR985, Health and Safety Laboratory.

Cleaver, P., C. Humphreys, M. Gabillard, D. Nédelka, R. Heiersted, and J. Dahlsveen (1998). Rapid phase transition of LNG. In *12th International Conference on Liquefied Natural Gas*, Perth, Australia.

Cleaver, P., M. Johnson, and B. Ho (2007). A summary of some experimental data on LNG safety. *J. Hazard. Mater. 140*(3), 429–438.

Dhir, V. K. (1998). Boiling heat transfer. *Annu. Rev. Fluid Mech. 30*(1), 365–401.

Ekoto, I. W., E. Hecht, C. San Marchi, K. M. Groth, A. C. Lafleur, N. Natesan, M. Ciotti, and A. Harris (2014). Liquid hydrogen release and behavior modeling: State-of-the-art knowledge gaps and research needs for refueling infrastructure safety. Technical Report SAND2014-18776, Sandia National Laboratories.

Enger, T. (1972). Explosive boiling of liquefied gases on water. In *Proceeding of the conference on LNG import and terminal safety*, Boston.

Enger, T. and D. Hartman (1972a). Mechanics of the LNG-water interaction. In *AGA Distribution Conference*, Atlanta.

Enger, T. and D. E. Hartman (1972b). Explosive boiling of liquefied gases on water. In *Proceeding of the conference on LNG import and terminal safety*, Boston.

Enger, T., D. E. Hartman, and E. V. Seymour (1973). Explosive boiling of liquefied hydrocarbon/water systems. In K. D. Timmerhaus (Ed.), *Advances in Cryogenic Engineering*, pp. 32–41. Boston: Springer US.

Forte, K. and D. Ruf (2017). Safety challenges of LNG offshore industry and introduction to risk management. In *36th International Conference on Ocean, Offshore and Arctic Engineering*. American Society of Mechanical Engineers.

Havens, J. and T. Spicer (2007). United states regulations for siting LNG terminals: Problems and potential. *J. Hazard. Mater. 140*(3), 439 – 443.

Hightower, M., L. Gritzo, and A. Luketa-Hanlin (2005). Safety implications of a large lng tanker spill over water. *Process Saf. Prog. 24*(3), 168–174.

Hightower, M., L. Gritzo, A. Luketa-Hanlin, J. Covan, S. Tieszen, G. Wellman, M. Irwin, M. Kaneshige, B. Melof, C. Morrow, and D. Ragland (2004). Guidance on risk analysis and safety implications of a large liquified natural gas (LNG) spill over water. Technical Report SAND2004-6258, Sandia National Laboratories, Albuquerque, New Mexico.

Katz, D. L. (1972). Superheat-limit explosions. *Chem. Eng. Prog. 68*(5), 68.

Katz, D. L. and C. M. Sliepcevich (1971). LNG/Water explosions: Cause & effect. *Hydrocarbon Process. 50*(11).

Keller, J., L. Hill, K. Kiuru, K. M. Groth, E. Hecht, and W. James (2016). Hysafe research priorities workshop report. Technical Report SAND2016-2644, Sandia National Laboratories.

Koopman, R. and D. Ermak (2007). Lessons learned from LNG safety research. *J. Hazard. Mater. 140*, 412 – 428.

Kotchourko, A., D. Baraldi, P. Bénard, N. Eisenreich, T. Jordan, J. Keller, A. Kessler, J. LaChance, V. Molkov, M. Steen, A. Tchouvelev, and J. Wen (2014). State of the art and research priorities in hydrogen safety. Science and policy report, Joint Research Centre of the European Commission.

Kumar, S., H.-T. Kwon, K.-H. Choi, W. Lim, J. H. Cho, K. Tak, and I. Moon (2011). LNG: An eco-friendly cryogenic fuel for sustainable development. *Appl. Energy 88*(12), 4264–4273.

Luketa-Hanlin, A. (2006). A review of large-scale LNG spills: Experiments and modeling. *J. Hazard. Mater. 132*, 119 – 140.

Melhem, G., S. Saraf, and H. Ozog (2006). LNG properties and hazards, understanding LNG rapid phase transitions (RPT). *An ioMosaic Corporation Whitepaper*.

Michelsen, M. L. and J. M. Mollerup (2007). *Thermodynamic models: Fundamentals and computational aspects* (second ed.). Holte, Denmark: Tie-Line Publications.

Nakanishi, E. and R. Reid (1971). Liquid natural gas - water reactions. *Chem. Eng. Prog. 67*(12), 36 – 41.

Pitblado, R. M. and J. L. Woodward (2011). Highlights of LNG risk technology. *J. Loss Prev. Process Ind. 24*(6), 827 – 836.

Pritchard, D. K. and W. M. Rattigan (2010). Hazards of liquid hydrogen: Position paper. Technical Report RR769, Health and Safety Laboratory.

Raj, P. K. and L. A. Bowdoin (2010). Underwater LNG release: Does a pool form on the water surface? What are the characteristics of the vapor released? *J. Loss Prev. Process Ind. 23*(6), 753 – 761.

Reid, R. C. (1983). Rapid phase transitions from liquid to vapor. *Adv. Chem. Eng. 12*, 105–208.

Rivkin, C., R. Burgess, and W. Buttner (2015). Hydrogen technologies safety guide. Technical Report NREL/TP-5400-60948, National Renewable Energy Laboratory.

Royle, M. and D. Willoughby (2014). Releases of unignited liquid hydrogen. Technical Report RR986, Health and Safety Laboratory.

Ruiz, P., L. F. Vega, M. del Mar Arxer, C. Jimenez, and A. Rausa. *Hydrogen: applications and safety considerations* (1st ed.). MATGAS 2000 AIE.

Sciance, C. T., C. P. Colver, and C. M. Sliepcevich (1967). Pool boiling of methane between atmospheric pressure and the critical pressure. In K. D. Timmerhaus (Ed.), *Advances in Cryogenic Engineering*, Boston, MA, pp. 395–408. Springer US.

Shaw, S., J. Baik, and R. Pitblado (2005). Consequences of underwater releases of LNG. *Process Saf. Prog. 24*(3), 175–180.

Spiegler, P., J. Hopenfeld, M. Silberberg, C. F. Bumpus, and A. Norman (1963). Onset of stable film boiling and the foam limit. *Int. J. Heat Mass Transfer 6*(11), 987–989.

Verfondern, K. and B. Dienhart (1997). Experimental and theoretical investigation of liquid hydrogen pool spreading and vaporization. *Int. J. Hydrogen Energy 22*(7), 649–660.

Verfondern, K. and B. Dienhart (2007). Pool spreading and vaporization of liquid hydrogen. *Int. J. Hydrogen Energy 32*(13), 2106–2117.

Wang, L., Y. Li, F. Zhang, F. Xie, and Y. Ma (2016). Correlations for calculating heat transfer of hydrogen pool boiling. *Int. J. Hydrogen Energy 41*(38), 17118–17131.

Wilhelmsen, Ø., A. Aasen, G. Skaugen, P. Aursand, A. Austegard, E. Aursand, M. Gjennestad, H. Lund, G. Linga, and M. Hammer (2017). Thermodynamic Modeling with Equations of State: Present Challenges with Established Methods. *Ind. Eng. Chem. Res. 56*(13), 3503–3515.

Ustolin F, Paltrinieri N. Hydrogen Fireball Consequence Analysis. Chem Eng Trans 2020;82:211–6. https://doi.org/10.3303/CET2082036.

This page is intentionally left blank

CHEMICAL ENGINEERING TRANSACTIONS
VOL. 82, 2020
A publication of AIDIC
The Italian Association of Chemical Engineering
Online at www.cetjournal.it
Guest Editors: Bruno Fabiano, Valerio Cozzani, Genserik Reniers

**ISBN** 978-88-95608-80-8; **ISSN** 2283-9216
DOI: 10.3303/CET2082036

# Hydrogen Fireball Consequence Analysis

Federico Ustolin*, Nicola Paltrinieri

Department of Mechanical and Industrial Engineering, Norwegian University of Science and Technology NTNU,
S.P. Andersens veg 3, 7031 Trondheim, Norway
federico.ustolin@ntnu.no

A fireball may occur after the catastrophic rupture of a tank containing a flammable substance such as a fuel, if an ignition source is present. The fireball is identified by the combustion of the flammable cloud created after the fuel release and composed by the mixture of the latter and air. In particular, the fuel concentration is higher at the center of the fireball compared with the external layers where the ignition takes place. After its formation, the fireball tends to rise vertically due to the buoyancy of the hot gases involved in the combustion. Moreover, the fireball emits its energy mainly through radiant heat. Hence, the fireball formation may be one of the consequences of both a liquid and a compressed gaseous hydrogen tank explosion. For instance, the fireball is a consequence of a boiling liquid expansion vapor explosion (BLEVE). A BLEVE may occur after the catastrophic rupture of a tank containing a liquid at a temperature higher than its boiling point at atmospheric pressure. The explosion is characterized by the rapid expansion of the liquid and vapor phases due to the depressurization of the vessel.
The aim of this study is to model a liquid hydrogen ($LH_2$) fireball generated subsequently the BLEVE phenomenon. Different empirical correlations were selected to estimate the fireball dimensions and duration. Moreover, the fireball radiation was estimated by means of a theoretical model. As case study, the fireball generated from the explosion of the $LH_2$ tank with a volume of 1 $m^3$, which will be tested during the safe hydrogen fuel handling and use for efficient implementation ($SH_2IFT$) project, was simulated. The results achieved from the fireball numerical models can be employed to estimate the safety distance from an $LH_2$ tank and propose appropriate safety barriers. Furthermore, these outputs can aid the writing of critical safety guidelines for hydrogen technologies. Finally, the outcome of this study will be validated with the experimental results during the $SH_2IFT$ project.

## 1. Introduction

Hydrogen is a highly flammable substance with a very low density at atmospheric conditions (0.0883 kg $m^{-3}$ (NIST, 2019)). For this reason, it is usually stored at high pressures (up to 70 MPa (Kikukawa et al., 2008)). The liquefaction process can increase the hydrogen density (up to 70.9 kg $m^{-3}$) by cooling the gaseous hydrogen down to its boiling point (20.3 K at atmospheric pressure) (NIST, 2019). Currently, less than 1% of the hydrogen worldwide produced is liquefied (Ausfelder & Bazzanella, 2016). However, the liquid hydrogen ($LH_2$) production might grow in the forthcoming years as response to the foreseen consumption increase (IEA, 2017). Therefore, $LH_2$ may be employed in new applications, thus considered as emerging technology from which emerging risks might arise (Jovanović & Baloš, 2013). Boiling Liquid Expanding Vapor Explosion (BLEVE) is a physical explosion, consequence of the catastrophic failure of a vessel which contains a liquefied gas at temperature above its boiling point at atmospheric pressure (Casal et al., 2016). The consequences of a BLEVE are the overpressure of the blast wave, the tank debris thrown away by the explosion and a fireball if the substance contained in the vessel is flammable. This latter can cause damages to the structures in the vicinity of the tank and injuries to the personnel due to the high radiation produced, and it must not be neglected during a risk assessment of a flammable liquefied gas storage vessel (Hemmatian et al., 2017).
In the past, few experiments on $LH_2$ fireball were conducted. In the 1960s, NASA conducted a series of tests to determine the blast hazards of liquid propellants (including $LH_2$) as consequence of two disastrous incidents: the Atlas-Centaur rocket failure during the booster phase of its first launch in 1962, and the Saturn-

Paper Received: 26 January 2020; Revised: 9 April 2020; Accepted: 1 July 2020
Please cite this article as: Ustolin F., Paltrinieri N., 2020, Hydrogen Fireball Consequence Analysis, Chemical Engineering Transactions, 82, 211-216 DOI:10.3303/CET2082036

IV explosion at the beginning of its firing test in 1964 (Gayle, 1964). In these tests, $LH_2$ fireballs were generated after the explosion of several vessels which contained different amounts of propellant, i.e. fuel ($LH_2$) and oxidizer (liquid oxygen, LOX) with a 1:5 ratio, in the range of 200 ÷ 100,000 lb (~91 ÷ 45,359 kg) (Gayle & Bransford, 1965). $LH_2$ fireballs were obtained also during the research programme conducted by BMW, car manufacture, in the period 1992-1996 (Pehr, 1996). BLEVE explosions were triggered by means of cutting charges installed on the $LH_2$ tanks designed for the hydrogen powered cars. The $LH_2$ tank mass content varied from 1.8 to 5.4 kg during the experiments. In 2005, a hydrogen fireball were achieved from a pressurized vessel during the fire exposure test conducted by Zalosh & Weyandt (2005). In that case, the composite tank with a volume of 72.4 L was filled with 1.64 kg of hydrogen at 34.3 MPa, engulfed in a propane fire. A thorough qualitative risk analysis was conducted in the European project Integrated design for demonstration of efficient liquefaction of hydrogen (IDEALHY) (Lowesmith & Hankinson, 2013). BLEVE explosion was considered as consequence of the loss of containment of a storage vessel provoked by an external fire. The fireballs generated after the explosion of tanks with different hydrogen mass contents (3 ÷ 700 t) were simulated by means of theoretical and empirical models. As result of this analysis, the most severe consequence for both the transportation and liquefaction applications was a BLEVE of a road tanker and of a storage tank respectively. Currently, the consequences of handling and use of large amount of hydrogen are investigated in the Safe Hydrogen fuel handling and Use for Efficient Implementation ($SH_2$IFT) project (Sintef, 2019). BLEVE is one of the two physical explosions analyzed in this project. Both experimental tests and modelling activity will be carried out within the project. The aim of this study is to conduct a preliminary consequence analysis of the hydrogen fireball generated after the BLEVE of an $LH_2$ tank as part of the $SH_2$IFT project. Theoretical models and empirical correlations are employed in this investigation. The idea is to estimate the consequences of the BMW bursting tests previously described, in order to validate the models for $LH_2$. Furthermore, a sort of blind simulation is performed by providing the fireball parameters expected after the explosion of the $LH_2$ vessels during the $SH_2$IFT experimental tests. The methodology adopted in this study is described in Sec. 2, while the results and the discussion are reported in Sec. 3 and 4 respectively.

## 2. Methodology

One of the most critical and arduous challenges of a fireball consequence analysis is the determination of the fuel amount which participates in the fireball formation. In this study, it was assumed that the whole tank content is burnt in the fireball in order to assess the worst-case scenario. The fireball diameter, duration and height, depicted in Figure 1, were estimated together with the radiative heat flux emitted toward a target to determine the safety distance from the vessel. In the following, the selected methodology is described in detail.

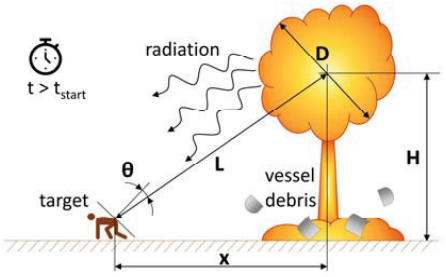


*Figure 1: fireball parameters considered during a consequence analysis: diameter D, duration t, height of the fireball center H, horizontal distance from the release to the target x, distance from the fireball center to the target L, and angle between the target surface normal and the fireball axis θ.*

### 2.1 Diameter

Different correlations to estimate the $LH_2$/LOX fireball diameter were proposed as result of the blast hazards tests of liquid propellant conducted by NASA (Gayle & Bransford, 1965), (High, 1968). In this study, Eq(1) proposed by Hord (1972) was used to estimate the fireball diameter:

$$D \approx 7.93 \cdot {W_f}^{1/3} \tag{1}$$

where $D$ is the maximum fireball diameter in m and $W_f$ is the fuel mass in kg.

### 2.2 Duration

The fireball dynamic, thus its duration, depends on the release momentum which derives from the flash evaporation of liquefied gases during a BLEVE. Therefore, Beyler (2016) categorized the fireballs in momentum- and buoyancy-dominated. The correlations proposed by Gayle & Bransford (1965) and High (1968) for liquid propellant fireballs, are similar to the momentum-dominated fireball formula (Eq(2)) proposed by CCPS (2010):

$$t = 0.45 \cdot m^{1/3} \tag{2}$$

where *m* is the fuel mass in kg. The duration correlation for buoyancy-dominated fireball is reported in Eq(3):

$$t = 2.6 \cdot m^{1/6} \tag{3}$$

where *m* is again the fuel mass in kg. CCPS (2010) suggested to use Eq(2) for fuel masses lighter than 30,000 kg, and Eq(3) otherwise. In this analysis a comparison between both equations was conducted.

### 2.3 Height of the fireball center

The fireball raise height depends on the fireball type (momentum- or buoyancy-dominated) as demonstrated by Fay & Lewis (1977). In this analysis, the equation proposed by van den Bosch & Weterings (2005) (Eq(4)) was selected to calculate the maximum height of the center of the fireball.

$$H = D_{max} \tag{4}$$

where $D_{max}$ is the maximum fireball diameter in m, estimated with Eq(1).

### 2.4 Radiative heat flux and thermal dose

The solid flame model, employed in this study, is widely used to estimate the incident radiation per unit area and unit time from a fireball (CCPS, 2010). The model approximates the fire geometry with a basic geometrical shape (e.g. sphere). Furthermore, the whole thermal radiation is assumed as diffused from the shape surface. Therefore, the incident radiation from the fireball is estimated with Eq(5):

$$q = \tau \cdot F \cdot E \tag{5}$$

where $\tau$ is the atmospheric attenuation (transmissivity), *F* is the view factor, and *E* is the surface emissive power (SEP) in W m$^{-2}$. This latter is the radiative heat flux which is emitted from the fireball surface per unit time and is usually measured during experimental tests by means of pyrometers. It can be theoretically estimated with the Stefan-Boltzmann's law (Eq(6)) as performed in this study.

$$E = \varepsilon \cdot \sigma \cdot T^4 \tag{6}$$

where $\varepsilon$ is the emissivity, $\sigma$ is the Stefan-Boltzmann constant equal to 5.67 × 10$^{-8}$ W m$^{-2}$ K$^{-4}$, and *T* is the flame temperature in K. In this analysis, the maximum theoretical SEP value was determined by assuming that the flame is a black body ($\varepsilon = 1$) and its temperature is close to the stochiometric combustion temperature (2318 K for hydrogen in air (Pehr, 1996)). The view factor in Eq(5) correlates the radiation received by the receptor and the SEP emitted by the fireball surface. Assuming a spherical fireball, the view factor is calculated with Eq(7) when the distance from the release point to the target, *x*, is longer than the fireball radius (*D/2*), (Beyler, 2016):

$$F = \left(\frac{R}{L}\right)^2 \cos\theta \tag{7}$$

where *R* is the fireball radius in m, *L* is the distance from the fireball center to the target in m and $\theta$ is the angle between the target surface normal and the fireball axis in degree (Figure 1). In this study, the value of this angle was zero to provide the most conservative estimation. The incident radiation is attenuated by the atmospheric transmissivity ($\tau_a$) which is function of the atmospheric air temperature, path length (between the fireball and the target) and chemical species present in air (primarily water vapor, i.e. humidity). Eq(8), proposed by van den Bosch & Weterings (2005), was selected in this analysis.

$$\tau_a = 2.02 \cdot (p_w \cdot (L - R))^{-0.09} = 2.02 \cdot (RH \cdot p_w^0 \cdot (L - R))^{-0.09} \tag{8}$$

where $p_w$ is the partial pressure of vapor water in air in Pa, *L* is again the distance between the fireball center and the target in m, *R* is the fireball radius in m, *RH* is the relative humidity (70% in this analysis), and $p_w^0$ is the partial pressure of saturated vapor water (1705 Pa at 15°C (van den Bosch & Weterings, 2005)). Burn injuries depends on the duration of exposure to the radiative het flux, i.e. the thermal dose which is estimated with Eq(9):

$$Thermal\ dose = q^{4/3} \cdot t \quad (9)$$

where $q$ is the incident radiation in kW m$^{-2}$ and $t$ is the duration of exposure (fireball duration) in s. The relationship between burn level and thermal dose from infrared radiation are published in (Rew, 1997). The maximum tolerable thermal dose which does not provoke any injury is 80 kW$^{4/3}$ m$^{-2/3}$ s. The safety distance from the tank for personnel during the explosion is the distance value between the release point and the target ($x$) for which this thermal dose threshold is attained. In this study, the safety distance is only based on the thermal contribution neglecting the overpressure from the blast wave. Finally, the described theoretical models and empirical correlations were validated with the outcomes of the BMW tests and an estimation of the fireball generated during the forthcoming $SH_2$IFT $LH_2$ BLEVE tests was provided.

## 3. Results

A total of 10 single walled $LH_2$ tanks, insulated with a layer of foam, were destroyed by means of cutting charges during the BMW bursting tests. The $LH_2$ mass content in the vessels varied from 1.8 to 5.4 kg. Despite these tanks were equipped with temperature, pressure and $LH_2$ level sensors, the fireball results are not correlated with these parameters. Pehr (1996) reported a maximum fireball diameter of 20 m, height of the fireball center between 16 and 20 m, and 4 s as longest duration between the fireball ignition and extinction. Moreover, a radiation spectroscopy was carried out during the tests highlighting ultraviolet (from OH-radicals and $H_2O$ molecules), infrared and visible radiations (from solid particles). However, the radiative flux emitted from the fireball at a certain distance was not provided in (Pehr, 1996). Similar results were obtained by applying the methodology previously described in Sec. 2. The highest hydrogen mass (5.4 kg) was adopted to calculate the most conservative case. A maximum diameter and height of the fireball center of 13.9 m were estimated for a total duration of 0.8 s (with momentum-dominated fireball equation) and 3.4 s (with buoyancy-dominated fireball equation). The safety distance from the tank to the target (personnel) was 77.8 m. The maximum error values between the estimations and the test results were 30.5% in the case of the maximum diameter and height of the fireball center and 80% for the fireball duration.
During the $SH_2$IFT project, three double walled $LH_2$ tanks with a volume of 1 m$^3$ filled at 50% will be engulfed in a propane fire until the tank failure will cause a BLEVE. Considering the $LH_2$ density (70.9 kg m$^{-3}$) initially stored at 1 bar at a temperature close to the boiling point (20.3 K), the hydrogen mass content in the tank will be 35.5 kg (NIST, 2019). This mass was used in the blind simulation of the fireball, consequence of an $LH_2$ BLEVE. According to this evaluation, the fireball will last from 1.5 to 4.7 s expanding to a maximum diameter and height of 25.9 m. The thermal dose of 80 kW$^{4/3}$ m$^{-2/3}$ s for a target exposed to the fireball is expected at 159.1 m, thus this is the safety distance from the $LH_2$ tank. In Table 1, the results of this analysis are reported for comparison.

*Table 1: Comparison between the experimental data from the BMW bursting tests (Pehr, 1996) and the empirical model outcomes for the BMW and $SH_2$IFT $LH_2$ BLEVE tests.*

| Fireball parameters and safety distance | BMW tests | BMW tests estimation | Error (%) | $SH_2$IFT BLEVE tests blind simulation |
|---|---|---|---|---|
| $LH_2$ mass (kg) | 1.8 ÷ 5.4 | 5.4 | --- | 35.5 |
| Max. diameter (m) | 20.0 | 13.9 | 30.5 | 25.9 |
| Duration (s) | 4.0 | 0.8 ÷ 3.4 | 80.0 ÷ 15.0 | 1.5 ÷ 4.7 |
| Height (m) | 16.0 ÷ 20.0 | 13.9 | 13.1 ÷ 30.5 | 25.9 |
| Safety distance (thermal dose = 80 kW$^{4/3}$ m$^{-2/3}$ s) (m) | --- | 77.8 | --- | 159.1 |

## 4. Discussion

According to (Gayle & Bransford, 1965), the fireballs generated by propellant explosions after rocket failures have a diameter similar to those for high explosives, while the duration for the propellants is appreciably longer. Furthermore, the authors observed that the diameter depends on the cube root of the propellant weight and it varies inversely with the cube root of the atmospheric pressure. Pehr (1996) noticed that the diameter was influenced by the tank pressure as well. However, both the atmospheric pressure and the tank pressure prior the explosion are not included in any correlation. In (Gayle & Bransford, 1965), a standard error of 30% was estimated for the data scatter with the fitting curve. This was also noted in this study, where the maximum diameter of the BMW tests was underestimated of about 30% by using the (Hord, 1972) equation. Moreover, Zalosh & Weyandt (2005) estimated with the same correlation a fireball diameter value 19% higher than the

experimental results for the hydrogen pressurized tank. According to these observations, the diameter estimated in the blind simulation of the $SH_2$IFT tests might vary by ± 30% in the range of 18.1 ÷ 33.7 m. Even though these results may be within the error interval estimated by Gayle & Bransford (1965), an underestimation is not acceptable when a risk assessment is performed, and the most severe consequences are sought. During the NASA test series, it was difficult to estimate the exact fireball duration probably due to the variation in photography techniques (Gayle & Bransford, 1965). For this reason, the data scatter provided a standard error of 84%. The authors proposed to estimate the fireball duration with the same correlation for all types of liquid propellant tested This equation is similar to the momentum-dominated fireball formula described in Sec. 2. In this study, the duration calculation gave a similar error (80%) using this approach, while adopting the buoyancy-dominated fireball equation, the error was reduced to 15%. This latter equation gave a more accurate evaluation of the fireball duration also in (Zalosh & Weyandt, 2005). According to CCPS (2010), the momentum-dominated fireball equation should provide a more precise time estimation for small amount of fuel (< 30,000 kg). The results of this analysis are not in agreement with this theory, and again an underestimation was provided by these correlations.

The lift-off velocity of the fireball is nearly independent of the propellant weight (High, 1968) and it was not assessed in this study since the available test results are not sufficiently detailed. The maximum height of the fireball center was estimated with the equation proposed by van den Bosch & Weterings (2005) since it provides the most conservative estimation. Bader et al. (1971) developed a model to estimate the minimum propellant weight for the fireball to liftoff. If the propellant mass is lower than this critical value, the fireball will not form, and the propellant will burn on the ground as residual fires. This model was validated with the results of the Pyro test series (Willoughby et al., 1968) where explosion of a propellant weight (1:5 fuel-oxidizer ratio) lower than 200 lb (90.7 kg, equivalent to 15.1 kg of $LH_2$) did not lift-off. During the BMW tests the fireballs rose up to a height between 16 and 20 m when the hydrogen mass content in the $LH_2$ vessel prior the explosion was between 1.8 and 5.4 kg. The model developed by Bader et al. (1971) should be tuned according to these results. A fireball generated by the explosion of an $LH_2$ vessel emits ultraviolet, infrared and visible radiations (Pehr, 1996). The hydrogen fireball seems to have a high luminosity (Zalosh & Weyandt, 2005), while the hydrogen flame is well-known to have a low visibility compared with the other hydrocarbons (Schefer et al., 2009). One reason for this can be the participation of the tank material in the combustion (polyethylene products and carbon fiber fragments) or other fuels burnt externally to the vessel (propane) (Zalosh & Weyandt, 2005). Furthermore, very high temperatures were locally measured in the hydrogen fireball both during the BMW and NASA tests. The highest temperature was close to the stoichiometric combustion temperature of hydrogen in air (2318 K) (Pehr, 1996). This affects the surface emissive power estimated with the Stefan Boltzmann's law, and hence the incident radiation and thermal dose. The SEP can be estimated with the method prosed by (van den Bosch & Weterings, 2005) in which the fuel mass and the heat of combustion of the flammable substance are considered. In this case, this method presents a less conservative estimation compared with the Stefan-Boltzmann's law. According to CCPS (2010), the SEP is influenced by the fuel mass and the pressure of the vessel prior the release. This latter parameter is usually not considered in the theoretical models. Pehr, (1996) stated that was not possible to develop a thermal radiation model close to the hydrogen fireball since the particles distribution, gas concentration and fireball temperature were unknown due to the rapid fireball expansion. Moreover, Prugh (1994) developed a model for hydrocarbons fireball thermal radiation without including hydrogen in the discussion because its flame temperature is very high and its emissivity is very low. The thermal dose criterion was employed to assess the safety distance from the $LH_2$ vessel during an explosion. The results achieved are very conservative since the lower threshold of the range (80 ÷ 130 $kW^{4/3}$ $m^{-2/3}$ s) suggested by Rew (1997) was adopted in this analysis.

These observations should lead to future studies on the hydrogen fireball consequences either by improving and tuning the existing theoretical models or by exploiting the CFD tools for a more accurate and thorough assessment of all the fireball parameters. Multiphysics analysis could provide a wide overview on how the parameters influence the fireball consequences. For instance, a structural analysis may determine if the vessel type (single or double walled) affect the explosion consequences such as the blast wave overpressure and the fireball characteristics. The experimental data available in the literature are not sufficient to validate the developed models. A broader amount of data is required to comprehend the complex physical phenomena involved in the combustion of hydrogen as consequence of a BLEVE, and the $SH_2$IFT project will partially fill this knowledge dearth.

## 5. Conclusions

A consequence analysis on hydrogen fireball generated after an $LH_2$ BLEVE explosion was conducted. In particular, the fireball dimensions, duration and radiation were estimated by means of empirical and theoretical

models. The evaluation of the radiation at different distances allowed the determination of the safety distance from an $LH_2$ tank. The safety distance is a fundamental parameter for the selection of appropriate safety barriers and in the writing of safety guidelines. In this analysis, the BMW bursting tests were simulated obtaining an underestimation of the fireball diameter and duration. Furthermore, a sort of blind simulation of the $SH_2$IFT $LH_2$ BLEVE tests was carried out. The results of the $SH_2$IFT project will be used to validate the results of this analysis and fulfill part of the knowledge gap in hydrogen fireball.

**Acknowledgments**

This work was undertaken as part of the research project Safe Hydrogen fuel handling and Use for Efficient Implementation ($SH_2$IFT), and the authors would like to acknowledge the financial support of the Research Council of Norway under the ENERGIX programme (Grant No. 280964).

**References**

Ausfelder, F., & Bazzanella, A., 2016, Hydrogen in the Chemical Industry, In D. Stolten & B. Emonts (Eds.), Hydrogen Science and Engineering: Materials, Processes, Systems and Technology (pp. 19–39). Wiley-VCH Verlag.

Bader, B. E., Donaldson, A. B., & Hardee, H. C., 1971, Liquid-Propellant Rocket Abort Fire Model, Journal of Spacecraft and Rockets, 8, 1216–1219.

Beyler, C., 2016, Fire Hazard Calculations for Large, Open Hydrocarbon Fires, In M. Hurley (Ed.), SFPE Handbook of Fire Protection Engineering (5th ed., pp. 2591–2663). New York: Springer Science +Business Media, LLC.

van den Bosch, C. J. H., & Weterings, R. A. P. M., 2005, Methods for the Calculation of Physical Effects - Due to Releases of Hazardous Materials (liquids and gases), “Yellow Book.” The Hague: The Committee for the Prevention of Disasters by Hazardous Materials, Director-General for Social Affairs and Employment.

Casal, J., Hemmatian, B., & Planas, E., 2016, On BLEVE definition, the significance of superheat limit temperature (Tsl) and LNG BLEVE’s, Journal of Loss Prevention in the Process Industries, 40, 81.

CCPS., 2010, Guidelines for Vapor Cloud Explosion, Pressure Vessel Burst, BLEVE, and Flash Fire Hazards, 2nd ed. Wiley Subscription Services, Inc., A. Wiley Company, New York.

Fay, J. A., & Lewis, D. H., 1977, Unsteady burning of unconfined fuel vapor clouds, Symposium (International) on Combustion, 16, 1397–1405. Elsevier.

Gayle, J. B., 1964, Investigation of S-IV all systems vehicle explosion. NASA TN D-563.

Gayle, J. B., & Bransford, J. W., 1965, Size and Duration of Fireballs from Propellant Explosions - NASA TM X-53314.

Hemmatian, B., Casal, J., & Planas, E., 2017, Essential Points in the Emergency Management in Transport Accidents which Can Lead to a BLEVE-Fireball, Chemical Engineering Transactions, 57, 439–444.

High, R. W., 1968, The Saturn Fireball, Annals of the New York Academy of Sciences, 152, 441–451.

Hord, J., 1972, Explosion criteria for liquid hydrogen test facilities - NBS Report.

International Energy Agency (IEA) Hydrogen., 2017, Global Trends and Outlook for Hydrogen.

Jovanović, A. S., & Baloš, D., 2013, INTeg-Risk project: Concept and first results, Journal of Risk Research, 16, 275–291.

Kikukawa, S., Yamaga, F., & Mitsuhashi, H., 2008, Risk assessment of Hydrogen fueling stations for 70 MPa FCVs, International Journal of Hydrogen Energy, 33, 7129–7136. Pergamon.

Lowesmith, B. J., & Hankinson, G., 2013, Qualitative Risk Assessment of Hydrogen Liquefaction, Storage and Transportation - Deliverable 3.11, IDEALHY project.

NIST., 2019, NIST Chemistry WebBook. <webbook.nist.gov/> accessed 03/19/2019

Pehr, K., 1996, Aspects of safety and acceptance of LH2 tank systems in passenger cars, International Journal of Hydrogen Energy, 21, 387–395. Pergamon.

Prugh, R. W., 1994, Quantitative evaluation of fireball hazards, Process Safety Progress, 13, 83–91.

Rew, P. J., 1997, LD50 Equivalent for the Effect of Thermal Radiation on Humans - CRR 129/1997.

Schefer, R. W., Kulatilaka, W. D., Patterson, B. D., & Settersten, T. B., 2009, Visible emission of hydrogen flames, Combustion and Flame, 156, 1234–1241. Elsevier.

Sintef., 2019, SH2IFT - Safe Hydrogen Fuel Handling and Use for Efficient Implementation. <https://www.sintef.no/projectweb/sh2ift/> accessed 09/02/2019

Willoughby, A. B., Wilton, C., & Mansfield, J., 1968, Liquid Propellan Explosive Hazards, Volumes I-III, AFRPL-TR-68-92, Final Report. Edwards, CA.

Zalosh, R., & Weyandt, N., 2005, Hydrogen Fuel Tank Fire Exposure Burst Test - SAE Technical Paper 2005-01-1886, SAE 2005 World Congress & Exhibition.

Ustolin F, Odsæter LH, Reigstad G, Skarsvåg HL, Paltrinieri N. Theories and Mechanism of Rapid Phase Transition. Chem Eng Trans 2020;82:253–8. https://doi.org/10.3303/CET2082043.

This page is intentionally left blank

CHEMICAL ENGINEERING TRANSACTIONS
VOL. 82, 2020
A publication of AIDIC
The Italian Association of Chemical Engineering
Online at www.cetjournal.it
Guest Editors: Bruno Fabiano, Valerio Cozzani, Genserik Reniers

**ISBN** 978-88-95608-80-8; **ISSN** 2283-9216
DOI: 10.3303/CET2082043

# Theories and Mechanism of Rapid Phase Transition

Federico Ustolin[a,*], Lars H. Odsæter[b], Gunhild Reigstad[b], Hans L. Skarsvåg[b], Nicola Paltrinieri[a]

[a]Department of Mechanical and Industrial Engineering, Norwegian University of Science and Technology NTNU, S.P. Andersens veg 3, 7031 Trondheim, Norway
[b]SINTEF Energy Research, Postboks 4761 Torgarden, 7465 Trondheim, Norway
federico.ustolin@ntnu.no

Light hydrocarbons and hydrogen can replace high-alkane fuels with the benefit of reduced $CO_2$ emissions. Their liquefaction to a cryogenic state is one of the most suitable solutions for storage and transport. An unexpected release of these fuels might lead to a rapid phase transition (RPT). RPT is a physical explosion well-known for liquefied natural gas (LNG), and may occur when this substance is spilled onto water. The heat provided by the water to the cryogenic fuel might lead to a sudden evaporation of the liquid, resulting in an explosion. The generated blast wave has the potential to damage equipment and personnel. The RPT phenomenon can also occur in different types of industrial applications when molten metals accidentally come in contact with water. In these cases, the water is the cold fluid which expands violently.
In this study, the RPT phenomenon is investigated for cryogenic fluids (liquefied hydrocarbons, nitrogen and hydrogen) as well as for smelts (molten inorganic salts) and molten metals (aluminum). The contribution has a twofold purpose as it addresses relevant past accidents and lay the foundation for future modelling activities to simulate the cryogenic-pool formation on water, triggering of an RPT event and the RPT explosion consequences. Furthermore, the RPT theories and mechanisms comprehension is critical to qualitatively evaluate the probability for a liquid hydrogen ($LH_2$) RPT. In particular, a comparison between liquid nitrogen ($LN_2$) and $LH_2$ is conducted to understand under which conditions an $LH_2$ RPT might occur. The results of this study are to be validated through the Safe Hydrogen Fuel Handling and Use for Efficient Implementation ($SH_2IFT$) project, in which a series of $LH_2$ spill tests onto water will be conducted.

## 1. Introduction

Hydrogen is considered a clean and renewable fuel that can replace hydrocarbon fuels, thus reducing the environmental pollution. The liquefaction of hydrogen increases its density so that it can be transported in larger amounts. The gaseous hydrogen is cooled down below its boiling point (-253°C (NIST, 2019)) obtaining a cryogen fluid. This is an energy intensive process, but can be advantageous for large-scale transport and applications where a high energy density is required (DOE, 2009). Although hydrogen is employed in several industrial processes, its application in new technologies might unveil unexpected risks. For this reason, hydrogen can be considered an emerging technology and emerging risks could arise from different accident scenarios (Jovanović & Baloš, 2013). For instance, it is still unclear how liquid hydrogen ($LH_2$) behaves when accidentally spilled onto water. In the case of liquefied natural gas (LNG), stored at -161°C (NIST, 2019), this type of accident scenario may lead to a physical explosion known as rapid phase transition (RPT), which is the sudden evaporation of a cryogenic fluid after contact with a heat source (Woodward & Pitbaldo, 2010). RPT can be found in the literature under different names which are water explosion, vapor explosion, steam explosion, explosive boiling, thermal explosion, thermal interaction, thermal detonation and molten fuel coolant interaction (MFCI). Verfondern & Dienhart (1997) spilled $LH_2$ onto a pool of water without observing any RPT, and there are no records in the literature for such a phenomenon. However, the stochastic nature of the RPT phenomenon calls for additional experiments and a thorough analysis of the underlying mechanisms before a conclusion is drawn. RPT might occur for different fluid pairs (one cold and one hot liquid) in various industrial applications such as in the paper (water – smelts) or metallurgic industries (water – molten metals) and nuclear plants (water – molten fuel). In these cases, water is the colder liquid which explosively vaporizes.

Paper Received: 20 January 2020; Revised: 7 April 2020; Accepted: 24 July 2020
Please cite this article as: Ustolin F., Odsaeter L., Reigstad G., Skarsvag H., Paltrinieri N., 2020, Theories and Mechanism of Rapid Phase Transition, Chemical Engineering Transactions, 82, 253-258 DOI:10.3303/CET2082043

Similar phenomenon has also been observed with mineral oils or other hydrocarbons instead of water (Burgess et al., 1970). The aim of this study is to comprehend from a theoretical point of view if an RPT can occur when $LH_2$ is spilled onto water. Hence, theories developed for the fluid pairs listed above were collected to provide a qualitative overview on the RPT mechanisms for different substances. After the methodology description, the different system configurations for which an RPT has occurred are analyzed. Finally, the common aspects of the different theories are summarized in the discussion and used to discuss the $LH_2$-water system.

## 2. Methodology

Different RPT events with different underlying mechanisms depending on the fluids involved and the setup, were reviewed and qualitatively compared. In particular, the considered systems can be divided in two categories. In the first one, water is the subcooled liquid which transfers heat to the colder fluid, while in the second category water acts as the coolant. The following substances were considered for the first and second category, respectively:

1. Liquefied Natural Gas (LNG), liquefied hydrocarbons (e.g. propane, ethane), liquid nitrogen ($LN_2$) and liquid refrigerants (e.g. R22 -$CHClF_2$-).
2. Smelt (molten inorganic salts) and molten metals (e.g. aluminum, tin).

Moreover, an RPT can happen in three geometrical arrangements: spilling of the hot liquid into the cold one, injection of the cold liquid into the hot one or, stratified layers of the hot and cold liquids (Bang & Corradini, 1991). All three geometries were considered in this study, and an overview of the theories and mechanisms developed for each system is provided. The purpose is to pinpoint the common aspects of the theories even though the conditions to achieve an RPT vary for each configuration due to the different properties of the involved substances. The approach of Archakositt et al. (2004), where the fuel-coolant interaction of a nuclear plant was simulated by a water-liquid nitrogen interaction, is an example of how the common aspects can be used. In this paper, the knowledge gained on molten metals RPT is exploited to understand this explosion for cryogenic fluids. The common steps leading to an RPT event are the liquid-liquid interaction (with eventual mixing), film boiling formation and consequent collapse, and nucleation (heterogenous or homogenous). Finally, these steps are evaluated in case of an $LH_2$-water interaction.

## 3. RPT theories and underlying mechanisms for different liquid-liquid systems

In this section, the theoretical models for describing the RPT event for the different liquid-liquid systems previously mentioned are presented. In this study, “early” indicates the RPT that occurs immediately after the release of one liquid onto or inside the other, while a "delayed" explosion manifests several seconds after the spill, usually when the liquid-liquid system has a stratified geometry. Furthermore, an RPT event can be spontaneous due to film-boiling collapse or externally triggered (e.g., by an artificial pressure pulse or waves).

### 3.1 LNG – water

The first well documented LNG RPT accident occurred in 1968 during the Bureau of Mines test series (Burgess et al., 1970). Several small- and large-scale tests followed to investigate this phenomenon. Porteous & Reid (1976) conducted small-scale experiments where they spilled LNG onto water to understand under which conditions an early spontaneous RPT may be achieved. They observed that (i) a liquid-liquid interface must be present to obtain an RPT (e.g. RPT will not occur when LNG is spilled on ice), (ii) the hot liquid temperature must exceed a lower limit, i.e. the homogeneous nucleation temperature (called also superheat-limit temperature, $T_{sl}$) of the cold fluid, (iii) the time scale of the event is very short (< 5 ms), (iv) the probability of an RPT event depends on the LNG (or hydrocarbon) composition, (v) a high momentum of the cryogenic fluid on top of the hot one can trigger the explosion, (vi) the RPT are rare if ice is formed, and (vii) the RPT probability decreases if the hot liquid temperature is much higher than the $T_{sl}$ of the cold liquid. Moreover, the authors noted that spontaneous film boiling collapse occurs only if the LNG has a low methane content (< 19%mol) and no other perturbation are present. From these observations, the superheat theory was developed by Reid (1976). According to this theory, the following steps lead to a small-scale early spontaneous LNG RPT:

- Film boiling due to the high temperature difference between the two fluids: The LNG and water are separated by a thin vapor film which prevent large heat transfer. This happens when the water has a temperature higher than the LNG Leidenfrost temperature ($T_L$).
- Film-boiling collapse due to a triggering process leading to transition boiling. The vapor film is less stable if the water temperature is close to $T_L$.

- Rapid increase of heat transfer due to the direct liquid-liquid contact with consequent metastable temperature rise of the LNG toward its $T_{sl}$ temperature. In this phase, the liquid has a temperature higher than its boiling point at atmospheric pressure, hence it is thermodynamically metastable.
- Violent expansion of the cold liquid caused by a perturbation when the liquid is vaporizing by heterogeneous nucleation. If the $T_{sl}$ is reached, the homogeneous nucleation leads to an extremely rapid vaporization even without any perturbation.

The LNG RPT chain of events is depicted in Figure 1.

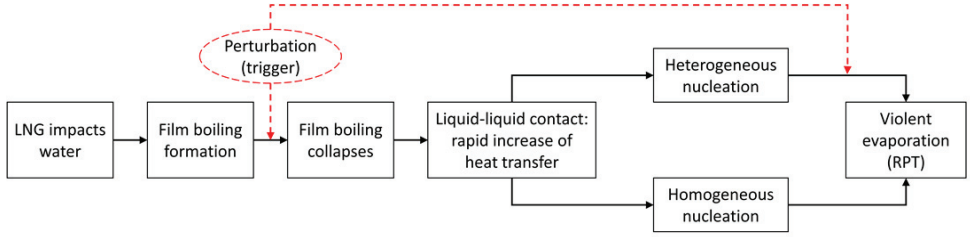


*Figure 1: chain of the events for an LNG RPT.*

During some of the large-scale tests (Goldwire et al., 1983), early and delayed spontaneous RPTs occurred close to the spill origin, or on the evaporating pool formed on top of water after the LNG release respectively. The triggering conditions to generate an early RPT can be attributed to the LNG impact with water or the high degree of mixing of the two fluids. For delayed RPT, evaporation of methane causes a shift in the Leidenfrost temperature, eventually leading to film-boiling collapse. For this reason, even LNG with an initially high methane content could undergo either an early or a delayed spontaneous RPT. Furthermore, Reid (1983) proposed that the following criteria must be satisfied to reach an early spontaneous RPT from large spills of LNG with a high methane content: (i) significant LNG and water mixing , (ii) the water-LNG interface temperature must be higher than the $T_{sl}$ of LNG, and (iii) a triggering event that produces a significant pressure pulse to collapse the vapor film. For this early-RPT event, LNG-water-temperature ratios are not in the range defined by the superheat theory. Therefore, this theory should be slightly modified to explain this RPT type.

### 3.2 Liquefied hydrocarbons and refrigerants – water

Porteous & Reid (1976) poured onto water both pure and mixtures of hydrocarbons during the tests described in Sec. 3.1. Spontaneous RPTs were achieved under certain conditions for ethane, propane, isobutane, propylene and isobutylene during these tests. Recently, the combustion-induced RPT phenomenon which may occur after the ignition of methane, $CO_2$ and air mixtures was investigated by Salzano et al. (2013).
In the 1970s, numerous tests of liquid refrigerants spill on water were conducted. In most of these experiments, R-22 ($CHClF_2$) was investigated and spontaneous RPTs for this substance were obtained when injected into water with temperature higher than 350 K (Anderson & Armstrong, 1977). The results attained in these analysis for both liquefied hydrocarbons and refrigerants are in agreement with the superheat theory since the RPTs occurred only when the estimated interface temperature was closed to the $T_{sl}$ of the cold fluid (Reid, 1983).

### 3.3 Liquid nitrogen – water

Bang & Corradini (1991) analyzed the formation and consequences of the $LN_2$ RPTs starting from a stratified geometry ($LN_2$ over water). These authors demonstrated that a delayed spontaneous RPT cannot occur for this configuration, because the interfacial temperature between water at 0°C and saturated $LN_2$ is -30°C (~243 K) while the $LN_2$ $T_L$ is around -150°C (~123 K). Therefore, the water surface solidifies before film boiling becomes unstable. As follow-up of these investigations, different $LN_2$ RPTs were achieved by forcing the film-boiling collapse with external pressure pulse by means of an electromagnet or a detonator. The necessary pressure can also be achieved by injecting the $LN_2$ onto water with a high velocity (Anderson & Armstrong, 1972). In later studies, RPTs occurred when $LN_2$ was injected directly into water. For instance, Archakositt et al. (2004) measured the overpressure generated by the $LN_2$ vaporization and the heat transfer from the cryogenic liquid to water by varying the $LN_2$ jet velocities and pressures. The $LN_2$ RPTs achieved by Bang & Corradini (1991) and Archakositt et al. (2004) have the same chain of events shown in Figure 1. Moreover, Zhang et al. (2017) observed a similar boiling process for LNG and $LN_2$ when injected into water, confirming

that this chain of events is suitable for different cryogenic substances. However, the superheat theory cannot be directly applied since the water temperature is much higher than the $LN_2$ $T_{sl}$, as previously mentioned.

### 3.4 Water – smelt

Soda and kraft smelts are mixtures of molten inorganic salts employed in the paper industry. The soda smelt is mainly composed by sodium carbonate ($Na_2CO_3$) (Shiang et al., 1989) while the kraft smelt contains in addition a large amount of sodium sulfide ($Na_2S$) (Nelson & Kennedy, 1956). If water enters the boiler in which the smelt is contained due to operational errors or equipment failures, an RPT might be generated by the rapid evaporation of water (Reid, 1983). Sallack (1955) discovered that NaCl and NaOH were responsible for the explosion of the soda smelt. These results were confirmed by Nelson & Kennedy (1956) who demonstrated that $Na_2S$ enhances the explosion of the kraft smelt. These authors claimed that three different RPT types might occur during the water-smelt interaction: instantaneous, short-delayed and delayed.
The superheat theory developed and considered valid for LNG and the other cryogenic fluids cannot be applied here since the smelt temperature (1100 – 1200 K) is much higher than the $T_{sl}$ of pure water (577 K) (Reid, 1983). Shick (1980) proposed a modified superheat theory by supposing that the salt and water concentrations vary at the interface of the two liquids. The mass flow of salt in the water increases the solution concentration and thus its $T_{sl}$. The water flux into the smelt is responsible to delay its solidification due to change in its melting point. The solubility in water depends on the salt type and the water temperature. This theory explains the impossibility to achieve an RPT of molten $Na_2CO_3$ and water, since the solubility of this salt decreases with increasing water temperature.

### 3.5 Water – molten metals

Early and delayed spontaneous RPT might occur under certain circumstances when a molten metal interacts with cold water. In different studies and accidents, RPTs were obtained for molten tin, zinc, lead, aluminum and steel. An extremely large interface area is required to superheat water, i.e. reach its homogeneous nucleation temperature, and then generate an RPT. This is very arduous to achieve with molten metals because their densities are usually much larger than water, hence the interface area between the two fluids is limited. Fragmentation of the molten metal becomes a critical phase in the path toward an RPT for water-molten-metal interaction. A positive feedback between pressure pulse and film-boiling collapse is initiated by a localized overpressure induced by a local film-boiling collapse. Thus, film-boiling collapse is the triggering event of the fragmentation process which propagates through the coarse metal globules. A correlation between the fragmentation degree and the liquid aluminum-water explosion intensity was found by Shen et al. (2020). For the water and molten-metal systems an alternative mechanism to the superheat theory was proposed by Buchanan & Dullforce (1973). Their model starts from the triggering mechanism, which puts the two liquid in contact by collapsing the vapor film with a consequent formation of a vapor bubble (step 1). The bubble then collapses due to condensation in the subcooled liquid generating a jet of coolant toward the hot liquid (step 2). The high-speed coolant jet penetrates the molten metal increasing the interface area and initiating the fragmentation of the hot liquid (step 3). The total heating rate grows as an effect of the increased interface area (step 4). The liquid jet suddenly vaporizes forming a high-pressure bubble due to the temperature increase (step 5). These last four steps are repeated cyclically leading to an RPT under favorable conditions. Obviously, these conditions vary for each of the considered liquid pairs (water-metal). A simplified path, displayed in Figure 2 which derives from the Buchanan and Dullforce model was recognized by different authors when an RPT from molten metals and water is described (Fletcher & Anderson, 1990).

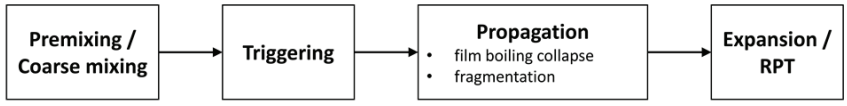


*Figure 2: four steps for the water-molten metal RPT adapted from (Shen et al., 2018).*

An RPT can be initiated with an external trigger for the water-molten metal systems. However, if the interfacial temperature is lower than the metal-melting point, an RPT cannot be achieved even when the vapor film is collapsed by an external pressure pulse (Abe et al., 2002).

#### 3.5.1 Water – molten aluminum

The first molten aluminum water tests were the Alcoa experimental program described by Long (1957). In these experiments 23 kg of molten aluminum was dropped into water, and RPTs were obtained under certain circumstances. A recent study conducted by (Shen et al., 2020) confirmed that the following conditions are

required to achieve an RPT from a water-molten aluminum interaction: (i) the aluminum mass should be heavier than a critical mass, (ii) a long drop path through the air must be avoided to not cool down the metal, (iii) the aluminum temperature must be higher than its solidification point (> 730°C) and (iv) the water temperature must be lower than 33°C. It has also been observed by Shen et al. (2020) that a low melt/water mass ratio (~2) provokes more energetic explosions compared with a higher ratio. The main mechanism for a spontaneous aluminum-water RPT is the impact with the bottom of the water reservoir. Shen et al. (2020) demonstrated that such RPT occurs spontaneously if the inside of the water vessel bottom is composed by a water-wettable surface. For instance, this type of RPT cannot occur if the aluminum impact glass, solid aluminum or organic paint coated surfaces which are non-wettable surfaces. The superheat theory cannot be applied since the temperature of molten aluminum is much higher than the $T_{sl}$ of water. Still, an RPT can be achieved for this pair if an external trigger is applied, such as a strong hammer blow on the external side of the water vessel (Reid, 1983).

## 4. Discussion

In this section, the common aspects of these theories and mechanisms are collected. Firstly, the conditions required to achieve this type of explosion depends mainly on the properties of the two liquids. The geometry arrangement affects the interface area between the fluids, and thus the total heat transfer. For this reason, the multiphase flow together with film boiling are the most important and complex phenomena to simulate in order to estimate the triggering of RPT. Furthermore, the interface area is also influenced by the degree of mixing after the release and the potential fragmentation of one of the fluids after the film boiling collapse. Another fundamental aspect is the determination and quantification of the triggering conditions to understand if and which RPT type (early or delayed, and spontaneous or externally) might occur.

Hydrogen has a very low boiling point (-253°C) and density (70.8 kg $m^{-3}$) at atmospheric pressure (NIST, 2019). Since the boiling points of $LH_2$ and $LN_2$ are both very low, an $LH_2$ RPT could have some similarities compared with an $LN_2$ RPT. Therefore, experimental results on $LN_2$ RPT tests available in the literature can give relevant insights for $LH_2$ RPTs. As for $LN_2$, the $LH_2$ vapor film formed when poured onto water in an initial stratified geometry is not expected to collapse spontaneously due to the large temperature difference between the cryogen and water. The difference in densities of $LH_2$ and $LN_2$ (806 kg/$m^3$ at atmospheric pressure (NIST, 2019)) means that the fluid-flow behaviors are quite different, and this influences the steps preceding an RPT. For instance, only 7% of an $LH_2$ evaporating pool height is submerged in water, while 80% of an $LN_2$ pool is below the water level. It is expected that the mechanisms that trigger an RPT are similar for the two fluids once appropriate conditions are met. Therefore, delayed spontaneous RPT seems very unlikely for $LH_2$ on water. Spreading of cryogenic liquids on a surface after release is generally slower for lighter fluids (Verfondern & Dienhart, 1997), hence the degree of water-cryogen mixing is lower for $LH_2$ than $LN_2$. This indicates that early spontaneous RPT with $LH_2$ is more difficult to achieve than with $LN_2$. Sufficient water-cryogen mixing can be forced by high-momentum injection of $LH_2$ either onto or into water. It should be noted that $LH_2$ $T_{sl}$ (29.5 K), estimated with the method proposed by Reid (1983), is lower than for $LN_2$ (112.3 K). This means that $LH_2$ undergoes homogeneous nucleation for a lower increase in temperature compared with $LN_2$. The $LH_2$ and $LN_2$ properties are collected in Table 1 for a direct comparison. Furthermore, the trigger type and the intensity to collapse the vapor film and initiate the fragmentation process must be properly determined. Finally, flash vaporization is expected to be significant for $LH_2$ (< 30% of the volume in the work by Verfondern & Dienhart (1997)), and must be considered when estimating the released volume.

*Table 1: comparison between $LH_2$ and $LN_2$ properties*

| Substance | Boiling point (°C) | Density (kg $m^{-3}$) | $T_{sl}$ (°C) | Pool penetration in water |
|---|---|---|---|---|
| $LH_2$ | -252.9 (20.3 K) | 70.9 | -243.7 (29.5 K) | 7% |
| $LN_2$ | -195.8 (77.4 K) | 806.1 | -160.9 (112.3 K) | 80% |

## 5. Conclusions

An overview of the RPT theories and mechanisms for different configuration and fluid pairs was provided. The main phenomena and processes which lead to an RPT, and thus form the basis for future modelling activities, were highlighted. The mixing of the fluids, film boiling, triggering and fragmentation are the most critical phenomena and mechanisms involved in the RPT chain of events. Some considerations about $LH_2$-water RPT were given based on the analyzed theories. The formation of a delayed spontaneous RPT seems to be very unlikely while the possibility to provoke an early or delayed RPT by external triggering or an early spontaneous RPT by injecting $LH_2$ into water cannot be excluded. The results of this study will be confirmed by the

experimental tests during the Safe Hydrogen Fuel Handling and Use for Efficient Implementation ($SH_2IFT$) project.

**Acknowledgments**

This work was undertaken as part of the research project Safe Hydrogen Fuel Handling and Use for Efficient Implementation ($SH_2IFT$), and the authors would like to acknowledge the financial support of the Research Council of Norway under the ENERGIX programme (Grant No. 280964).

**References**

Abe, Y., Nariai, H., & Hamada, Y., 2002, The trigger mechanism of vapor explosion, Journal of Nuclear Science and Technology, 39, 845–853.

Anderson, R. P., & Armstrong, D. R., 1972, Experimental Study of Vapor Explosions, LNG-3 Conference. Washington, D.C.

Anderson, R. P., & Armstrong, D. R., 1977, R-22 Vapor Explosions, Annual ASME Winter Meet: Nuclear Reactor Safety Heat Transfer Section.

Archakositt, U., Nilsuwankosit, S., & Sumitra, T., 2004, Effect of Volumetric Ratio and Injection Pressure on Water-Liquid Nitrogen Interaction, Journal of Nuclear Science and Technology, 41, 432–439.

Bang, K. H., & Corradini, M. L., 1991, Vapor explosions in a stratified geometry, Nuclear Science and Engineering, 108, 88–108.

Buchanan, D. J., & Dullforce, T. A., 1973, Mechanism for vapour explosions, Nature, 245, 32–34.

Burgess, D. S., Murphy, J. N., & Zabetakis, M. G., 1970, Hazards associated with the spillage of liquefied natural gas on water - RI7448.

DOE., 2009, Energy requirements for hydrogen gas compression and liquefaction as related to vehicle storage needs.

Fletcher, D. F., & Anderson, R. P., 1990, A review of pressure-induced propagation models of the vapour explosion process, Progress in Nuclear Energy, 23, 137–179.

Goldwire, H., Rodean, H., Cederwall, R., & Kansa, E., 1983, Coyote series data report, LLNL/NWC 1981 LNG spill tests dispersion, vapor burn and rapid phase transition , Vols. 1 and 2, UCID - 19953. Livermore, CA.

Jovanović, A. S., & Baloš, D., 2013, INTeg-Risk project: Concept and first results, Journal of Risk Research, 16, 275–291.

Long, G., 1957, Explosions of molten aluminum in water-cause and prevention, Metal Progress, 71, 107.

Nelson, H. W., & Kennedy, E. H., 1956, What causes Kraft dissolving tank explosions, Paper Trade Journal, 140, 50.

NIST., 2019, NIST Chemistry WebBook. <webbook.nist.gov/> accessed 03/19/2019

Porteous, W. M., & Reid, R., 1976, Light hydrocarbon vapor explosions, Chemical Engineering Progress, 72, 83.

Reid, R., 1976, Superheated Liquids, American Scientist, 64, 146–156.

Reid, R. C., 1983, Rapid Phase Transitions from Liquid to Vapor, Advances in Chemical Engineering, 12, 105–208. Academic Press.

Sallack, J. A., 1955, An investigation of explosions in the soda smelt dissolving operation, Pulp Paper Magazine of Canada, 56, 114.

Salzano, E., Cammarota, F., Di Benedetto, A., Di Sarli, V., & Russo, G., 2013, Combustion-Induced Rapid Phase Transition of CH4/O2/Inert Mixtures, Chemical Engineering Transactions, 31, 883–888.

Shen, P., Zhou, W., Cassiaut-Louis, N., Journeau, C., Piluso, P., & Liao, Y., 2018, Corium behavior and steam explosion risks: A review of experiments, Annals of Nuclear Energy, 121, 162–176.

Shen, Z., Chen, H., Lv, Z., Wang, D., Chen, D., & Huang, F., 2020, Study on large-scale steam explosion of molten aluminum and water, Process Safety Progress, e12149.

Shiang, N. T., Grace, T. M., & Hopenfeld, J. R., 1989, A model to explain composition effects in smelt-water explosions, Chemical Engineering Communications, 79, 175–188.

Shick, P., 1980, Concentration-gradient trigger mechanism for smelt-water explosions. Chicago, IL.

Verfondern, K., & Dienhart, B., 1997, Experimental and theoretical investigation of liquid hydrogen pool spreading and vaporization, International Journal of Hydrogen Energy, 22, 649–660.

Woodward, J. L., & Pitbaldo, R., 2010, LNG Risk Based Safety: Modeling and Consequence Analysis. John Wiley & Sons, Inc., Hoboken, New Jersey.

Zhang, B., Zhang, X. D., & Wu, W. Q., 2017, Experimental Study on Cryogen Injection into Water, Applied Ecology and Environmental Research, 15, 441–456.

Ustolin F, Iannaccone T, Cozzani V, Jafarzadeh S, Paltrinieri N. Time to Failure Estimation of Cryogenic Liquefied Tanks Exposed to a Fire, (Submitted to the 31st European Safety and Reliability Conference – ESREL2021)

This article is awaiting publication and is not included in NTNU Open

This page is intentionally left blank

Ustolin F, Lamb JJ, Burheim OS, Pollet BG. Energy and Safety of Hydrogen Storage. In: Lamb JJ, Pollet Biomass and Bioenergy BGBT-H, editors. Hydrog. Fuel Cells Prim., Academic Press; 2020, p. 133–53. https://doi.org/https://doi.org/10.1016/B978-0-08-102629-8.00008-6.

Stefana E, Paltrinieri N, Ustolin F, A new risk-based framework to integrate occupational and process safety (Submitted to the Journal of Loss prevention in the Process Indutries)

Liu Z, Ustolin F, Spitthoff L, Lamb JJ, Gundersen T, Pollet BG, et al. Liquid Air Energy Storage: Analysis and Prospects. In: Lamb JJ, Pollet BG, editors. Micro-Optics and Energy, Springer, Cham; 2020, p. 115–30. https://doi.org/https://doi.org/10.1007/978-3-030-43676-6_9.

Bairampalli SN, Ustolin F, Ciuonzo D, Rossi PS. Digital Moka: Small-Scale Condition Monitoring in Process Engineering. IEEE Sensors Lett 2021;5:1–4. https://doi.org/10.1109/LSENS.2021.3059850.

Ustolin F, Wan D, Alvaro A, Paltrinieri N. Risk-based inspection planning for hydrogen technologies: review of currents standards and suggestions for modification. IOP Conf. Ser. Mater. Sci. Eng., 2021.

Ustolin F, Åsholt Øygård H, Zdravistch F, Niemi R, Paltrinieri N. Computational Fluid Dynamics Modeling of Liquid Hydrogen Release and Dispersion in Gas Refuelling Stations. Chem Eng Trans 2021;86.

Ustolin F, Hendrick P, Paltrinieri N. Development of Tools Enabling the Deployment and Management of a Multi-Energy Renewable Energy Community with Hybrid Storage. Chem Eng Trans 2021;86.

ISBN 978-82-326-5575-5 (printed ver.)
ISBN 978-82-326-6523-5 (electronic ver.)
ISSN 1503-8181 (printed ver.)
ISSN 2703-8084 (online ver.)





NTNU

Norwegian University of
Science and Technology